AIX-MARSEILLE UNIVERSITE

TITRE:

IMPREGNATION SUPERCRITIQUE POUR L'ELABORATION DE SYSTEMES A LIBERATION PROLONGEE

SUPERCRITICAL FLUID IMPREGNATION FOR THE ELABORATION OF SUSTAINED RELEASE DRUG DELIVERY SYSTEMS

T H E S E

pour obtenir le grade de:

DOCTEUR DE L'UNIVERSITE AIX-MARSEILLE

Faculté des Sciences et Techniques

Discipline: **Génie des Procédés**

Présentée et soutenue publiquement par:

ABIR BOULEDJOUIDJA

Le 29 Janvier 2016

Thèse réalisée sous la direction du Professeur **Elisabeth BADENS**
et du Docteur **Yasmine MASMOUDI**

Ecole doctorale: Sciences de l'Environnement

JURY

Rapporteurs:	
Dr. Stéphane SARRADE	CEA Saclay - Saclay
Dr. Vivek TRIVEDI	Université de Greenwich - Londres
Directrices de thèse:	
Pr. Elisabeth BADENS	Aix-Marseille Université - Marseille
Dr. Yasmine MASMOUDI	Aix-Marseille Université - Marseille
Examinateurs:	
Pr. Abdeslam MENIAI	Université Constantine 3 - Constantine
Pr. Michelle SERGENT	Aix-Marseille Université - Marseille
Membre invité:	
Dr. Olivier FORZANO	Hôpital de la Timone - Marseille

A mes parents

Acknowledgements

Cette thèse a été réalisée dans l'équipe Procédés et Fluides Supercritiques du laboratoire mécanique, modélisation et procédés propres (M2P2), Aix-Marseille université. Ce travail a été financé par le ministère Algérien de l'enseignement supérieur et la recherche scientifique et la région PACA. Je tiens en conséquence à vivement les remercier.

Tout d'abord, je souhaite remercier mes deux directrices de thèse. Merci à Elisabeth Badens pour m'avoir accueillie en thèse dans son équipe. Au cours de ces années de thèse, elle a dirigé mes travaux de recherche et je la remercie pour l'intérêt et la confiance qu'elle a su m'accorder au quotidien. Sans sa disponibilité et ses conseils, ce travail n'aurait pu être réalisé. Un grand merci à Yasmine Masmoudi pour sa patience, sa pédagogie, son enthousiasme, ses encouragements et son humanisme, j'ai énormément appris à ses côtés et je ne saurai la remercier assez pour tout ce qu'elle a fait et continue à faire pour moi.

I would like to express my gratitude to all people who have in any way helped through this research. First of all, I wish to thank the members of jury for accepting to evaluate this work, particularly to Dr. Stéphane Sarrade and Dr. Vivek Trivedi. I would also like to thank Prof. Abdeslam Meniai, Prof. Michelle Sergent and Dr. Olivier Forzano.

Je voudrais également exprimer ma profonde reconnaissance à monsieur Jean-Paul Nisteron, technicien du laboratoire M2P2, de m'avoir aidée pendant les longues heures que j'ai passées au laboratoire. Son appui technique ainsi que ses encouragements permanents ont contribué fortement à la réalisation de ce travail.

Merci à madame Michelle Sergent (LISA, Aix-Marseille université) pour son aide concernant les plans d'expériences. Merci à monsieur Fabio Ziarelli (Spectropole, Aix-Marseille université) pour les analyses RMN des solides.

Je tiens également à remercier monsieur John Tetteh (Greenwich university) et monsieur Daniel Ferry (CINAM, Campus de Luminy) qui ont accepté de réaliser des analyses FTIR-ATR , même si les résultats n'apparaissent pas dans le présent manuscrit.

Je tiens à remercier également Laure Siozade (Institut Fresnel, Aix-Marseille université) pour la caractérisation et la mesure des propriétés optiques des lentilles intraoculaires.

Merci à monsieur Yan-Ping Chen (National Taiwan University) d'avoir accepté de faire des mesures de solubilité des principes actifs dans le CO_2 supercritique.

Je tiens également à remercier Renauld Denoyel et Philip Llewellyn de m'avoir accueilli dans le laboratoire Madirel (Aix-Marseille université) pour faire des tests sur la balance à suspension magnétique.

Un grand merci à monsieur Vivek Trivedi (Greenwich university) pour les analyses DSC, ses remarques pertinentes m'ont été fort utiles.

Je souhaite vivement remercier toutes les personnes du laboratoire M2P2 pour leur accueil et l'intérêt qu'ils ont porté à mon travail et pour tous les moments de convivialité autour d'un café ou du déjeuner. Merci à Camille, Amine, Rania, Salah, Morgane , Marine, Sébastien et "Olivier alias Philippe".

Je tiens à remercier tous mes amis qui m'ont soutenu durant ces années de thèse, plus particulièrement: Assia et Messaoud. Merci à Houda, Fatiha, Kiné-sira, Hyllary, Wuhib, et Garima. Une pensée aussi à Meriem et Abdou mes amis de toujours.

Cette thèse, c'est bien évidemment à mes parents que je la dédie, je n'ai eu de cesse de vouloir les rendre fiers de moi. Merci également à mes frères pour leurs soutiens indéfectibles.

Table of contents

Acknowledgement .....i-ii
Table of contents .....iii-vi
List of abbreviations.....vii
List of figures .....viii-xi
List of tables .....xii-xiii
General introduction 1-5
Chapter I: Drug delivery systems 6-54
I. 1. Introduction.....8
I. 2. Drug delivery systems.....10
I. 3. Distinction between delivery systems.....13
I. 3. 1. Distinction between delivery systems according to their physical state.....13
I. 3. 2. Distinction between delivery systems according to their route of administration..13
I. 3. 2. 1. Oral drug delivery.....13
I. 3. 2. 2. Parenteral drug delivery.....14
I. 3. 2. 3. Transdermal drug delivery.....14
I. 3. 2. 4. Pulmonary drug delivery.....15
I. 3. 2. 5. Nasal drug delivery.....15
I. 3. 2. 6. Ocular drug delivery 16
I. 3. 3. Distinction between drug delivery systems according to their mechanism of drug release.....18
I. 3. 3. 1. Immediate release 18
I. 3. 3. 2. Modified release.....19
I. 3. 3. 2. 1. Delayed release 19
I. 3. 3. 2. 2. Extended-release 20
I. 3. 3. 2. 3. Pulsatile-release 23
I. 4. Novel drug delivery systems.....24
I. 4. 1. Nanomaterials 25
I. 4. 1. 1. Polymeric nanoparticles.....26
I. 4. 1. 2. Dendrimer nanocarriers 28
I. 4. 1. 3. Liposomes.....29
I. 4. 1. 4. Nanoparticles based on solid lipids.....29
I. 4. 1. 5. Microemulsions and nanoemulsions.....30

I. 4. 1. 6. Carbon nanomaterials 30
I. 4. 1. 7. Silica materials 31
I. 4. 2. Ocular medical devices 35
I. 4. 2. 1. Microneedles 35
I. 4. 2. 2. *In-situ* gelling systems 36
I. 4. 2. 3. Implants 36
I. 4. 3. Intraocular lenses 37
I. 4. 3. 1. Hydrophobic acrylic lenses 40
I. 4. 3. 2. Hydrophilic acrylic lenses 41
I. 4. 3. 3. Silicone lenses 41
I. 4. 3. 4. Collamer lenses 42
I. 4. 4. Other systems 42
I. 5. Conclusion 43
References 45
Chapter II: Supercritical impregnation 55-96
II. 1. Introduction 57
II. 2. Supercritical impregnation 59
II. 2. 1. What is a supercritical fluid? 59
II. 2. 2. Impregnation processes 60
II. 3. Polymeric drug delivery systems 63
II. 3. 1. Characterization of the system polymer-drug-CO_2 66
II. 3. 1. 1. Polymer-scCO_2 67
II. 3. 1. 2. Drug-scCO_2 70
II. 3. 1. 3. Polymer-drug 71
II. 3. 2. Bibliographic review 72
II. 4. Ordered mesoporous silica for drug delivery systems 80
II. 5. Conclusion 87
References 89
Chapter III: Supercritical impregnation of intraocular lenses 97-157
III. 1. Introduction 99
III. 2. Materials 99
III. 2. 1. Intraocular lenses 99
III. 2. 2. Active pharmaceutical ingredients 101

III. 2. 3. Solvents 102
III. 2. 4. Solution simulating the aqueous humor 102
III. 3. Methods 102
III. 3. 1. Pretreatment of IOLs 102
III. 3. 2. Influence of pressurization conditions on the properties (aspect) of IOLs 103
III. 3. 3. Experimental design and response surface methodology 103
III. 3. 4. Supercritical impregnation set-up 104
III. 3. 5. Characterizations 106
III. 3. 5. 1. Differential Scanning Calorimeter (DSC) 106
III. 3. 5. 2. Nuclear magnetic resonance (NMR) analysis 106
III. 3. 5. 3. Drug release kinetics studies 106
III. 3. 5. 4. Modeling of drug release kinetics 107
III. 3. 5. 5. Impregnation yields 108
III. 3. 5. 6. Partition coefficients 108
III. 4. Results and discussions 109
III. 4. 1. PMMA IOLs 110
III. 4. 1. 1. Influence of pressurization conditions on the visual aspect of IOLs……110
III. 4. 1. 2. Supercritical impregnation of PMMA IOLs 111
III. 4. 1. 2. 1. Dexamethasone 21-phosphate disodium salt impregnation 112
III. 4. 1. 2. 2. Ciprofloxacin impregnation 131
III. 4. 2. P-HEMA IOLs 134
III. 4. 2. 1. IOLs foaming 134
III. 4. 2. 2. IOLs pretreatment 136
III. 4. 2. 3. Supercritical impregnation of P-HEMA IOLs 137
III. 4. 2. 3. 1. Dexamethasone 21-phosphate disodium salt impregnation 137
III. 4. 2. 3. 2. Ciprofloxacin impregnation 141
III. 4. 3. Comparison between PMMA and P-HEMA IOLs impregnation 150
III. 4. Conclusions 153
References 156
Chapter IV: Impregnation of silica ..... 158 -171
IV. 1. Introduction 160
IV. 2. Materials 160
IV. 2. 1. Silica 160

IV. 2. 2. Fenofibrate 160
IV. 2. 3. Solvent 161
IV. 3. Methods.....161
IV. 3. 1. Impregnation procedures.....161
IV. 3. 1. 1. Impregnation *via* incipient wetness.....161
IV. 3. 1. 2. Supercritical impregnation.....162
IV. 3. 2. Characterization of silica 162
IV. 3. 2. 1. Nitrogen adsorption.....162
IV. 3. 2. 2. Transmission electron microscopy (TEM) 162
IV. 3. 2. 3. X-ray diffraction (XRD) 163
IV. 3. 2. 4. Impregnation yields.....163
IV. 3. 2. 5. Differential scanning calorimetry (DSC).....163
IV. 4. Results and discussions.....163
IV. 4. 1. Characterization of silica before impregnation.....164
IV. 4. 2. Impregnation using incipient wetness.....165
IV. 4. 3. Influence of supercritical treatment on silica structural properties.....165
IV. 4. 4 Supercritical impregnation.....166
IV. 5 Conclusion 170
References 171
Conclusions and perspectives.....172-175
Appendix.....176-183

List of abbreviations

$scCO_2$	Supercritical CO_2
IOL	IntraOcular Lens
PMMA	Poly (Methyl MethAcrylate)
P-HEMA	Poly (2 -HydroxyEthyl MethAcrylate)
OMS	Ordered Mesoporous Silica
DXP	DeXamethasone 21 Phosphate disodium
CIP	CIProfloxacin
API	Active Pharmaceutical Ingredient
PS	PolyStyrene
Ethanol	EtOH
RSM	Response Surface Methodology
ANOVA	ANalysis Of VAriance
Signif.	Significance (%)
ATR-FTIR	Attenuated Total Reflectance Fourier Transform Infra-Red
bi	Coefficient of the model
m_{imp}	Impregnated mass
$m_{CIP\ imp}$	Impregnated mass of CIP
$m_{DXP\ imp}$	Impregnated mass of DXP
Y_{imp}	Impregnation yield
t_{imp}	Impregnation duration
$t_{release}$	Release duration
T_g	Glass transition temperature
M_t	Cumulative amount of drug released at time
DSC	Differential Scanning Calorimeter
TEM	Transmission Electron Microscopy
SEM	Scanning Electron Microscopy
HPLC-UV	High Performance Liquid Chromatography (HPLC) with UV detection
XRD	X-Ray Diffraction
T	Temperature (K)
P	Pressure (MPa)
t	Duration (h or min)
Dep_{rate}	Depressurization rate ($MPa.min^{-1}$)
D	Diopter
K	Kelvin
Å	Ångström
min	Minute
M_∞	Cumulative amount of drug released at infinite time
k	Kinetic constant
n	Release exponent representing release mechanism
m_{0IOL}	Initial mass of dry IOL
y	Solubility (molar fraction of drug in CO_2)
X	Degree of crystallinity
K	Partition coefficient

List of figures

Figure I. 1 Evolution of controlled drug delivery systems. 09
Figure I. 2 Overview of drug delivery development from basic research to clinical applications 10
Figure I. 3 Drug plasma levels after oral administration of a drug from an immediate release dosage form. 11
Figure I. 4 Schematic illustration of the main structure of the eye and the ocular barriers to drug delivery. 17
Figure I. 5 Plasma concentration versus time profile of an immediate and delayed release systems. 20
Figure I. 6 Plasma concentration versus time profile of a sustained-release oral dosage form. 21
Figure I. 7 Example of osmotic pumps [44] 22
Figure I. 8 Plasma concentration versus time profile of a controlled-release dosage form. 22
Figure I. 9 Plasma concentration versus time profile of a pulsatile release. 24
Figure I. 10 Nanoparticle drug delivery systems with relation to other scales [59]. 26
Figure I. 11 Schematization of general structure of polymer-drug conjugate [21]. 27
Figure I. 12 Drug diffusion profile for both (a) monolithic matrix and (b) reservoir systems[21] 27
Figure I. 13 Design of Poly (propylene imine) dendrimer. 28
Figure I. 14 The schematic illustration of the structure of SWCNT, MWCNT and CNH[80]. 31
Figure I. 15 Synthesis of silica mesoporous materials 33
Figure I. 16 The properties that have fuelled the use of ordered mesoporous silica as drug delivery systems [103].. 35
Figure I. 17 IOLs a) PMMA, b) foldable hydrophobic, c) foldable hydrophilic acrylic, d) silicone, and d) collamer [126]. 40
Figure II. 1 Schematic P-T phase diagram of Carbon dioxide [3] 59
Figure II. 2 Supercritical impregnation set-up using two autoclaves: (1) CO_2 cylinder, (2) Cooling bath, (3) High pressure liquid pump, (4) Heating bath, (5) Saturator cell, (6) and (9) Agitators, (7) and (10) Thermostat baths, (8) impregnation cell, (11) and (12) Depressurization valves 61

Figure II. 3 Supercritical impregnation set-up using one autoclave: (1) CO_2 cylinder, (2) Cooling bath, (3) High pressure liquid pump, (4) Heating bath, (5) High pressure cell, (6) Agitator, (7) Thermostat bath, (8) Depressurization valve. 62
Figure II. 4 Interactions governing supercritical impregnation.....66
Figure II. 5 PMMA Tg depression as a function of pressure [45] 68
Figure II. 6 Tg of PMMA–CO_2 mixture as a function of equilibrium mass percentage of CO_2 [46]. 68
Figure II. 7 Pressure dependence of volume expansions of PMMA rods [52].. 69
Figure II. 8 Temperature dependence of volume expansions of PMMA rods [52].. 69
Figure II. 9 Photos of a swollen PMMA sample and diffusion front at 1 hour intervals at 12 MPa and 318 K [52].. 70
Figure II. 10 Schematic representation of the drug loading procedure by incipient wetness [89]……..81
Figure III. 1 Aspect of non treated IOLs made from a) PMMA, b) P-HEMA and their relative skeletal formula c) PMMA, d) P-HEMA. 101
Figure III. 2 Structural formula of a) Ciprfloxacin, b) Dexamethasone 21-phosphate disodium. 102
Figure III. 3 Supercritical impregnation set-up: (1) CO2 cylinder, (2) Cooling bath, (3) High liquid pressure pump, (4) Heating bath, (5) High pressure cell, (6) Support, (7) Magnetic bar, (8) Magnetic stirrer, (9) Thermostat bath, (10) Depressurization valve, (11) Solvent trap. 105
Figure III. 4 Influence of the pressurization flow rate on the visual aspect of some IOLs treated with $scCO_2$ at 20 MPa: a) with a pressurization flow rate of 0.25 $kg.h^{-1}$, b) with a pressurization flow rate of 0.65 $kg.h^{-1}$, c) with a rapid pressurization flow rate of 0.90 $kg.h^{-1}$ 111
Figure III. 5 Schematic representation of mass evolution profiles of IOLs due to sorption/desorption of CO_2.....112
Figure III. 6 Evolution of PMMA IOLs mass due to CO_2 desorption after supercritical treatment (at 20 MPa and 308 K). 112
Figure III. 7 NMR analyses (^{13}C) of an impregnated PMMA IOL with DXP at 8 MPa, 308K, with 5 %mol of ethanol and a) without washing step (red) b) with washing step (black)...114
Figure III. 8 Accumulated drug release mass from PMMA IOLs impregnated at 308 K with an impregnation duration of 2 hours and a depressurization flow rate of 0.2 $MPa.min^{-1}$....115

Figure III. 9 Influence of the temperature on accumulated mass released of IOLs impregnated at 8 MPa. 116
Figure III. 10 Influence of the quantity of co-solvent used on accumulated mass released from IOLs impregnated at 8 MPa and 308 K.....117
Figure III. 11 Influence of the impregnation duration on accumulated mass released from IOLs impregnated 8 MPa and 308 K. 120
Figure III. 12 Influence of the impregnation duration on the impregnation of IOLs at 8 MPa, 308 K, with 5 %mol of ethanol and a depressurization rate of 0.07 MPa.min^{-1}. 120
Figure III. 13 Influence of the impregnation duration on the impregnation of IOLs at 14 MPa and 320.5 K. 121
Figure III. 14 A two-dimensional contour plot and a three-dimensional response surface of impregnated mass illustrating optimal conditions for the supercritical impregnation of PMMA IOLs with DXP. 125
Figure III. 15 Accumulated drug release from IOLs (+21.0 D) impregnated, using experimental design, at 8 MPa, 308 K and with depressurization rate of 0.2 MPa.min^{-1} 127
Figure III. 16 Accumulated drug release from IOLs (+21.0 D) impregnated with a) 2.3 %mol of co-solvent (DXP_ED_1 and 2), b) 5.5 %mol of co-solvent (DXP_ED-5, 9 and 6) and c) 8.7 %mol of co-solvent (DXP_ED_3 and 4).....129
Figure III. 17 Accumulated drug release from impregnated IOLs (DXP_ED_5). 130
Figure III. 18 Accumulated drug release from PMMA IOLs impregnated with CIP (at 308 K and 2 h). 133
Figure III. 19 Influence of the pressurization flow rate on the visual aspect of some IOLs: a) non treated IOL, b) IOL treated with $scCO_2$ at 20 MPa with a pressurization flow rate of 0.65 kg.h^{-1}, c) IOL treated at 20 MPa with a pressurization flow rate of 0.900 kg.h^{-1}. 135
Figure III. 20 Influence of the pressurization flow rate (0.25 kg.h^{-1}) on the visual aspect of IOLs treated with $scCO_2$ at 20 MPa: a) in the presence of ethanol (5 %mol), b) in the absence of co-solvent. 135
Figure III. 21 NMR NMR analyses (13C) of an impregnated P-HEMA IOL with DXP at 20 MPa, 308 K, with 5 %mol of Ethanol and with a) a washing step (black) b) without a washing step (red). 139
Figure III. 22 Accumulated drug release from IOLs (+21.0 D) impregnated at 308 K, pressurization flow rate of 0.25 kg.h^{-1}, impregnation duration of 2 hours and depressurization rate of 0.2 MPa.min^{-1}. 140

Figure III. 23 Accumulated drug release from IOLs (+32.0 D) impregnated at 308 K, pressurization flow rate of 0.25 $kg.h^{-1}$, impregnation duration of 2 hours and depressurization rate of 0.2 $MPa.min^{-1}$. 140
Figure III. 24 Accumulated drug release from IOLs (+5.0 D) impregnated at 308 K with the pressurization flow rate of 0.25 $kg.h^{-1}$, impregnation duration of 2 hours and depressurization rate of 0.2 $MPa.min^{-1}$. 143
Figure III. 25 Accumulated drug release from IOLs (+21.0 D) impregnated at 308 K with the pressurization flow rate of 0.25 $kg.h^{-1}$, impregnation duration of 2 hours and depressurization rate of 0.2 $MPa.min^{-1}$. 144
Figure III. 26 Accumulated drug release from IOLs (+21.0 D) impregnated, using experimental design, at 308 K, pressurization flow rate of 0.25 $kg.h^{-1}$, without co-solvent and depressurization rate of 0.2 $MPa.min^{-1}$. 147
Figure III. 27 Accumulated drug release from IOLs (+21.0 D) impregnated, using experimental design, at a) 14 MPa (experiment CIP_ED_V, IX and VI), b) 18 MPa (experiments CIP_ED_III and IV).. 148
Figure III. 28 A two-dimensional contour plot and a three-dimensional response surface of impregnated mass (mg) illustrating optimal conditions for the supercritical impregnation of P-HEMA IOLs with CIP. 150
Figure IV. 1 Skeletal formula of Fenofibrate 161
Figure IV. 2 XRD pattern of the calcined OMS-L-7 164
Figure IV. 3 TEM picture of the calcined material. 165
Figure IV. 4 N_2 physisorption of the calcined material.....165
Figure IV. 5 N_2 sorption analysis of treated silica with $scCO_2$ and untreated silica. 166
Figure IV. 6 Experimental solubility for Fenofibrate in $scCO_2$ at 308 K [3]. 167
Figure IV. 7 DSC thermograms of impregnated silica.....169

List of tables

Table I. 1 DDS advantages and disadvantages [21]. 12
Table I. 2 Porous structures of ordered mesoporous silica [102]. 34
Table I. 3 Evolution of intraocular lenses [102]. 38
Table I. 4 Classification of IOLs [126]. 39
Table II. 1 Physico-chemical properties of carbon dioxide. 60
Table II. 2 Bibliographical conditions and results of $scCO_2$ impregnation applied for ocular applications. 77
Table II. 3 Ordered mesoporous silica matrices and drugs employed as drug delivery [92]. 85
Table II. 4 Example from literature of the supercritical impregnation of different model drugs in various kind of silica. 86
Table III. 1 Properties of foldable IOLs. 100
Table III. 2 Variables (factors) studied using a central composite design. 104
Table III. 3 Release exponent and corresponding mechanisms of release from a thin film. 108
Table III. 4 Solubilities of DXP and CIP (molar fraction) in $scCO_2$ at 308 K [14] 109
Table III. 5 Influence of the pressure and the use or not of co-solvent (ethanol 5 %mol) on supercritical impregnation. 113
Table III. 6 Influence of the temperature on the supercritical impregnation. 115
Table III. 7 Influence of the quantity of co-solvent on supercritical impregnation at 8 MPa. 117
Table III. 8 Influence of the impregnation duration on supercritical impregnation (0.2 $MPa.min^{-1}$) 118
Table III. 9 Influence of the impregnation duration on the supercritical impregnation (14 MPa and 320.5 K). 119
Table III. 10 Influence of the impregnation duration on supercritical impregnation (0.07 $MPa.min^{-1}$). 119
Table III. 11 Impregnation conditions, results and kinetics parameters of all the preliminary impregnation experiments. 122
Table III. 12 Experimental design conditions for supercritical impregnation (8 MPa, 308 K) of IOLs (+21.0 D). 124
Table III. 13 Tg of PMMA IOLs before and after impregnation. 127

Table III. 14 DXP_ED release kinetic parameters obtained by fitting with equation Eq. (2). 131
Table III. 15 Impregnation rates of PMMA IOLs (at 308 K and 2 hours) determined by drug release studies.....132
Table III. 16 CIP release kinetic parameters obtained by fitting with Eq (2). 134
Table III. 17 Tg of P-HEMA IOLs drying in an oven and with $scCO_2$. 137
Table III. 18 Impregnation rates of IOLs of +21.0 D and +32.0 D diopters (308 K and 2 hours), determined by drug release studies (40 days of release).....138
Table III. 19 DXP release kinetic parameters obtained by fitting with Eq (2).....141
Table III. 20 Influence of the diopter on the drug loading at different conditions.....142
Table III. 21 CIP release kinetic parameters obtained by fitting with Eq (2). 145
Table III. 22 Experimental design conditions for supercritical impregnation of IOLs (+21.0D).....146
Table III. 23 CIP release kinetic parameters obtained by fitting with Eq (2). 149
Table III. 24 Impregnation of PMMA and P-HEMA IOLs with DXP. 151
Table III. 25 Impregnation of PMMA and P-HEMA IOLs with CIP.....152
Table IV. 1 Solubility of Fenofibrate (molar fraction) in $scCO_2$ at 308 K 167
Table IV. 2 Supercritical impregnation of Fenofibrate into silica at 308 K. 168

General introduction

Recent years have seen growth in research and applications of drug delivery systems in the medical and pharmaceutical fields [1]. Controlled drug delivery systems are designed to improve drug bioavailability by preventing premature degradation and enhancing uptake, to maintain drug concentration within the therapeutic window by controlling the drug release rate, to reduce dosing frequency, and in some cases to reduce side effects by targeting the disease site and cells [2], [3].

For most applications, in order to achieve an effective therapy, the drug should be dispersed in a matrix at a molecular level [4]. Indeed, crystallization of the drug could result in a non-controlled dissolution of drug molecules through the matrix. For low water solubility drugs, one of the objectives of drug delivery systems preparation is to enhance drug dissolution rates via dispersion of the drug within a water-soluble matrix. Contrary, for water-soluble and short half-life drugs, prolonged release systems containing an insoluble hydrophobic matrix should be prepared [5], [6].

One route to elaborate such systems is impregnation. Conventional soaking into liquid impregnation process requires the use of organic solvents to dissolve and carry the drug components into the impregnation support. In most cases, conventional methods show several drawbacks, like the residual solvents present in the final materials, drug/solvents dissolution and compatibility issues, undesired drug reactions, drug photochemical and thermal degradation, low incorporation yields and heterogeneous drug incorporation/dispersion [7].

To overcome the above-mentioned limitations, supercritical CO_2 impregnation has proven to be a green alternative process for pharmaceutics [8]. Since the use of organic solvents can be avoided or the quantity used can be reduced [9], [10], and the activity of drug molecules is notably preserved because supercritical carbon dioxide ($scCO_2$) processing is operated at moderate temperatures [11]. An additional advantage of $scCO_2$ is the possibility of adjusting the impregnation efficacy by 'tuning' its properties [12]. When applied to polymers, $scCO_2$ plasticizes and swells the polymeric matrix, increasing the free volume of CO_2-swollen polymers thus enhancing the diffusion of drug molecules in such systems [9].

Drug delivery systems through supercritical impregnation process may be designed for several applications, using different active ingredients (various chemical natures and pharmacological actions) and adequate impregnation supports (polymeric or porous that can be either organic or inorganic). The present work focuses on the elaboration of two different

forms of sustained release drug delivery systems. On the one hand, medical devices for ocular applications were prepared by the impregnation of anti-inflammatory and antibiotic drugs within polymeric intraocular lenses. On the other hand, dosage forms (drug and excipient) for the development of suitable formulation for oral administration of poorly water-soluble drugs were prepared using highly porous and hydrophilic supports (mesoporous silica).

In a first part of this study, supercritical impregnation of commercially available intraocular lenses (IOLs), used for cataract surgery with an anti-inflammatory drug (Dexamethasone 21-phosphate disodium, namely DXP) and an antibiotic (Ciprofloxacin, designed CIP), is studied. Two polymeric IOLs were particularly tested: rigid IOLs made from derivative of Poly (Methyl Methacrylate) (PMMA) and foldable IOLs (hydrated in their original form) made from derivative of Poly (2-Hydroxyethyl Methacrylate) (P-HEMA). A number of parameters such as pressure, temperature, pressurization/depressurization rate, co-solvent requirement and impregnation duration were investigated to achieve optimized drug loading, homogeneous distribution of drugs in IOLs and a controlled drug release. According to the literature, few studies on supercritical impregnation of therapeutic *contact lenses* with various classes of drugs were performed and a prolonged drug delivery was successfully obtained [13-18]. To the best of our knowledge no therapeutic contact lenses have yet been approved or commercialized [13]. As far as we know, this study is the first work dealing with supercritical impregnation of *intraocular lenses* and more practically on commercially available PMMA and P-HEMA IOLs, which makes its originality.

A second part of this work is performed within the framework of a collaboration with Formac pharmaceuticals (Belgium), and deals with the use of mesoporous silica for the improvement of the dissolution kinetics and/or the solubility of poorly water-soluble drugs. Fenofibrate was chosen as an example of a lipophilic drug. According to the literature, few studies on the supercritical impregnation of silica with Fenofibrate were reported [14], [15] where silica supports, with different properties (porous and non porous), were used. One of these works [15] was published the same year as our study [16].

The objective of this work is to achieve a high loading of Fenofibrate with a low degree of a crystallinity, and to compare two loading processes, incipient wetness and supercritical impregnation in terms of impregnation yield, impregnation duration as well as in terms of drug solid state form (degree of crystallinity of the impregnated drug).

The present PhD thesis, begins with a presentation (chapter I) of drug delivery systems. Distinction between these systems has been reported according to their composition/physical

state, their routes of administration or their release mechanisms. A particular focus has been made on polymeric intraocular lenses and mesoporous silica, since they are the impregnation supports used in this PhD work.

The different impregnation processes as well as the corresponding involved mechanisms and influencing parameters are detailed in chapter II.

Chapter III is dedicated to the supercritical impregnations of IOLs (PMMA and P-HEMA) with two kinds of drugs (DXP and CIP). Preliminary impregnation experiments and response surface methodology based on experimental designs have been carried out to study the influence of operating conditions on the resulting impregnated amount and the release profile/duration, in order to determine the optimal conditions of impregnation.

Then, Chapter IV presents impregnation studies of silica with Fenofibrate using two methods: incipient wetness and supercritical impregnation. Both impregnation processes were compared according to the corresponding impregnation yields and durations as well as in term of physical characterization of the drug (degree of crystallinity).

Finally, some overall conclusions are given to underline the advances achieved by this PhD work as well as to bring some relevant elements to improve the understanding and the optimization of the supercritical impregnation for the elaboration of drug delivery systems.

References

[1] Y. Zhang, H. F. Chan, and K. W. Leong, "Advanced materials and processing for drug delivery: The past and the future," *Adv. Drug Deliv. Rev.*, vol. 65, no. 1, pp. 104–120, 2013.

[2] Y. Pierre and T. Rades, *FASTtrack: Pharmaceutics - Drug Delivery and Targeting*, Pharma. P. 2009.

[3] T. Kenakin, *A pharmacology Primer: theory, applications, and methods*, Academic P. 2009.

[4] S. P. Baldwin and W. Mark Saltzman, "Materials for protein delivery in tissue engineering," *Adv. Drug Deliv. Rev.*, vol. 33, no. 1–2, pp. 71–86, Aug. 1998.

[5] A. Frank, S. K. Rath, and S. S. Venkatraman, "Controlled release from bioerodible polymers: effect of drug type and polymer composition.," *J. Control. Release*, vol. 102, no. 2, pp. 333–44, Feb. 2005.

[6] J. Saurina, C. Domingo, S. G. Kazarian, J. M. Andanson, C. a. García-González, a. López-Periago, V. Fernández, and a. Argemí, "Impregnation of a biocompatible polymer aided by supercritical CO2: Evaluation of drug stability and drug–matrix interactions," *J. Supercrit. Fluids*, vol. 48, no. 1, pp. 56–63, Feb. 2009.

[7] V. P. Costa, M. E. M. Braga, C. M. M. Duarte, C. Alvarez-Lorenzo, A. Concheiro, and H. C. Gil, Maria H.de Sousa, "Anti-glaucoma drug-loaded contact lenses prepared using supercritical solvent impregnation," *J. Supercrit. Fluids*, vol. 53, no. 1–3, pp. 165–173, Jun. 2010.

[8] I. Pasquali and R. Bettini, "Are pharmaceutics really going supercritical?," *Int. J. Pharm.*, vol. 364, no. 2, pp. 176–187, 2008.

[9] I. Kikic and F. Vecchione, "Supercritical impregnation of polymers," *Curr. Opin. Solid State Mater. Sci.*, vol. 7, no. 4–5, pp. 399–405, Aug. 2003.

[10] C. Elvira, A. Fanovich, M. Fernández, J. Fraile, J. San Román, and C. Domingo, "Evaluation of drug delivery characteristics of microspheres of PMMA-PCL-cholesterol obtained by supercritical-CO2 impregnation and by dissolution-evaporation techniques.," *J. Control. Release*, vol. 99, no. 2, pp. 231–240, Sep. 2004.

[11] Y. P. Sun, *Supercritical Fluid Technology in Materials Science and Engineering: Syntheses: Properties, and Applications*, Marcel Dek. Clemson, South Carolina, 2002.

[12] M. Lora and I. Kikic, "Polymer Processing with Supercritical Fluids: An Overview, " *Sep. Purif. Rev.*, vol. 28, no. 2, pp. 179–220, 1999.

[13] G. Novack, "Ophthalmic Drug Delivery: Development and Regulatory Considerations," *Clin. Pharmacol. & Ther.*, vol. 85, no. 5, pp. 539–543, 2009.

[14] G. P. Sanganwar and R. B. Gupta, "Dissolution-rate enhancement of fenofibrate by adsorption onto silica using supercritical carbon dioxide.," *Int. J. Pharm.*, vol. 360, no. 1–2, pp. 213–8, Aug. 2008.

[15] R. J. Ahern, J. P. Hanrahan, J. M. Tobin, K. B. Ryan, and A. M. Crean, "European Journal of Pharmaceutical Sciences Comparison of fenofibrate – mesoporous silica

drug-loading processes for enhanced drug delivery," *Eur. J. Pharm. Sci.*, vol. 50, no. 3–4, pp. 400–409, 2013.

[16] Y. Masmoudi, A. Bouledjouidja, M. Van Speybroeck, and E. Badens, "Imprégnation supercritique pour l'élaboration de systèmes à libération contrôlée – Contrôle de la cristallinité du principe actif," in *Cristal 7*, 2013.

CHAPTER **I**

Drug delivery systems

Table of contents

I. 1. Introduction **8**
I. 2. Drug delivery systems **10**
I. 3. Distinction between delivery systems **13**
I. 3. 1. Distinction between delivery systems according to their physical state **13**
I. 3. 2. Distinction between delivery systems according to their route of administration **13**
I. 3. 2. 1. Oral drug delivery 13
I. 3. 2. 2. Parenteral drug delivery 14
I. 3. 2. 3. Transdermal drug delivery 14
I. 3. 2. 4. Pulmonary drug delivery 15
I. 3. 2. 5. Nasal drug delivery 15
I. 3. 2. 6. Ocular drug delivery 16
1. 3. 3. Distinction between drug delivery systems according to their mechanism of drug release **18**
I. 3. 3. 1. Immediate release 18
I. 3. 3. 2. Modified release 19
I. 3. 3. 2. 1. Delayed release 19
I. 3. 3. 2. 2. Extended-release 20
I. 3. 3. 2. 3. Pulsatile-release 23
I. 4. Novel drug delivery systems **24**
I. 4. 1. Nanomaterials **25**
I. 4. 1. 1. Polymeric nanoparticles 26
I. 4. 1. 2. Dendrimer nanocarriers 28
I. 4. 1. 3. Liposomes 29
I. 4. 1. 4. Nanoparticles based on solid lipids 29
I. 4. 1. 5. Microemulsions and nanoemulsions 30
I. 4. 1. 6. Carbon nanomaterials 30
I. 4. 1. 7. Silica materials 31
I. 4. 2. Ocular medical devices **35**
I. 4. 2. 1. Microneedles 35
I. 4. 2. 2. *In-situ* gelling systems 36
I. 4. 2. 3. Implants 36
I. 4. 3. Intraocular lenses **37**
I. 4. 3. 1. Hydrophobic acrylic lenses 40
I. 4. 3. 2. Hydrophilic acrylic lenses 41
I. 4. 3. 3. Silicone lenses 41
I. 4. 3. 4. Collamer lenses 42
I. 4. 4. Other systems **42**
I. 5. Conclusion **43**
References **45**

I. 1. Introduction

The introduction of drugs in the human body can be accomplished by several anatomic routes. In order to achieve the therapeutic purpose, the choice of the most suitable administration route needs is of unquestionable importance. Therefore, several factors must be taken into consideration when administrating a drug; namely its own properties, the disease to be treated and the desired therapeutic time. Drugs can be administrated directly to the target tissue or organ, or can be delivered by systemic routes [1].

Active pharmaceutical ingredients (APIs) are always administered in dosage forms that generally include other substances called excipients. The latter are added to formulations in order to improve the bioavailability and the acceptance of the drug by patients and/or to protect the drug from degradation. Excipients can be of numerous forms such as drug supports, emulsifiers and chemical stabilizers [2]. These substances were initially considered as inert because they do not exert therapeutic action, even if they can modify the biological action of a drug. However, excipients influence the speed and extent of drug absorption, and therefore formulation of these substances affects drug bioavailability [3].

Pharmaceutical treatments were started decades, or even centuries ago, either with solid and liquid oral administration [4], or with injectable active chemical drugs [5]. When either of these methods is applied, drug dose maintenance in the body is achieved by repeated administrations. However, this form of indiscriminate distribution leads to the occurrence of side effects and to the need for high doses of the drug to elicit a satisfactory pharmacological response [2]. During the past two decades, research is being carried out into new formulations that improve the bioavailability of drugs and ensure a greater pharmacological response. That in turn would lead to lower doses as well as frequency of drug taken, and therefore the minimization of side effects. This was the beginning of the so-called drug delivery systems [6].

Drug delivery is a field of vital importance to medicine and healthcare. Controlled drug delivery improves bioavailability by preventing premature degradation and enhancing uptake, maintains drug concentration within the therapeutic window by controlling the drug release rate, and in some cases reduces side effects by targeting disease sites and cells. The first generation of controlled release formulation was introduced by Smith Kline & French in 1952 for 12 hours delivery of dextroamphetamine (Dexedrine) [7]. From that point until the end of 1970s, basic understanding of controlled drug delivery was established, such as the different drug release mechanisms including dissolution, diffusion,

osmosis, and ion exchange-based mechanisms. The technologies developed during the 1st generation were used to develop numerous twice-a-day and once-a-day oral delivery systems and transdermal patches.

For the 2nd generation of controlled drug release, the research efforts were focused on developing zero-order delivery systems. It was thought that delivery systems with zero-order release kinetics would be superior because they maintain a steady drug concentration in the blood. Nevertheless, for some drugs, such as nitroglycerin and hormones or insulin, a constant blood level may not even be desired. It took a decade to understand this simple and intuitive fact, but it allowed increased flexibility in the design of future drug delivery systems [8].

During the 2nd generation, the "smart" polymers [9] and hydrogels [10] were developed to make delivery systems that are triggered by changes in environmental factors, such as pH, temperature, or glucose levels. Biodegradable microparticles, solid implants [11], and *in-situ* gel-forming implants were used to deliver peptides and proteins over month-long periods. The last decade of the 2nd generation was dedicated to the development of nanotechnology-based drug delivery systems [12]–[15].

The 3rd generation of drug delivery is yet to be established, and thus, the technologies listed in Figure I. 1 are predictions. The 3rd generation of drug delivery should address and overcome the hurdles associated with the current drug delivery systems listed in Figure I. 1 [8].

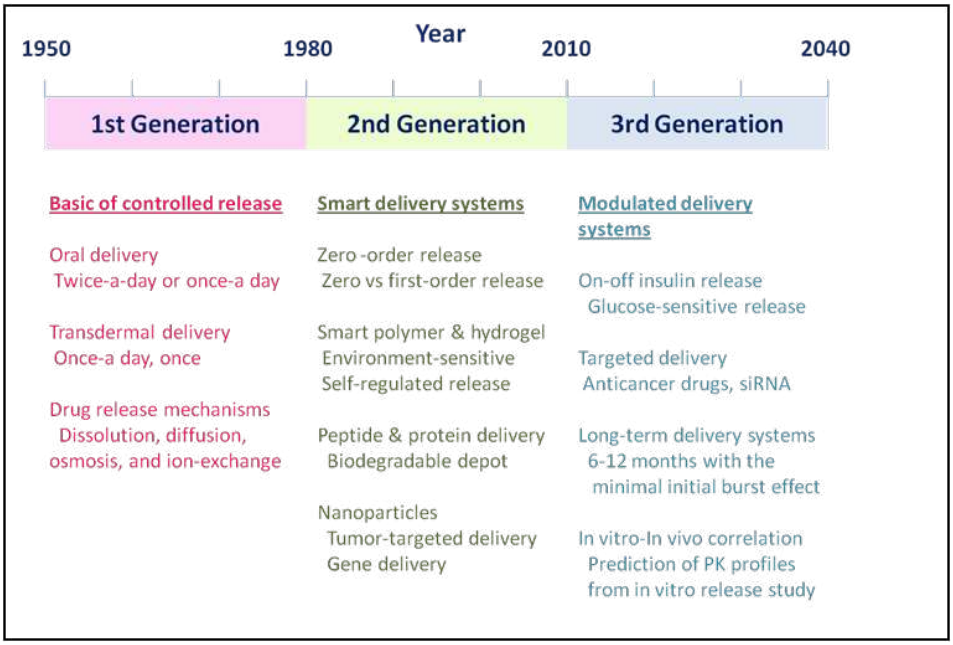

Figure I. 1 Evolution of controlled drug delivery systems [8].

The fundamental objective of drug delivery research is to develop formulations that can be used in clinical applications to treat different diseases. As shown in Figure I. 2, development of drug delivery systems requires simultaneous consideration of multiple factors, and their interdependence has to be taken into account. For example, after the drug selection, an appropriate delivery system has to be selected while taking into account simultaneously the delivery route as well as the drug release mechanism and kinetic.

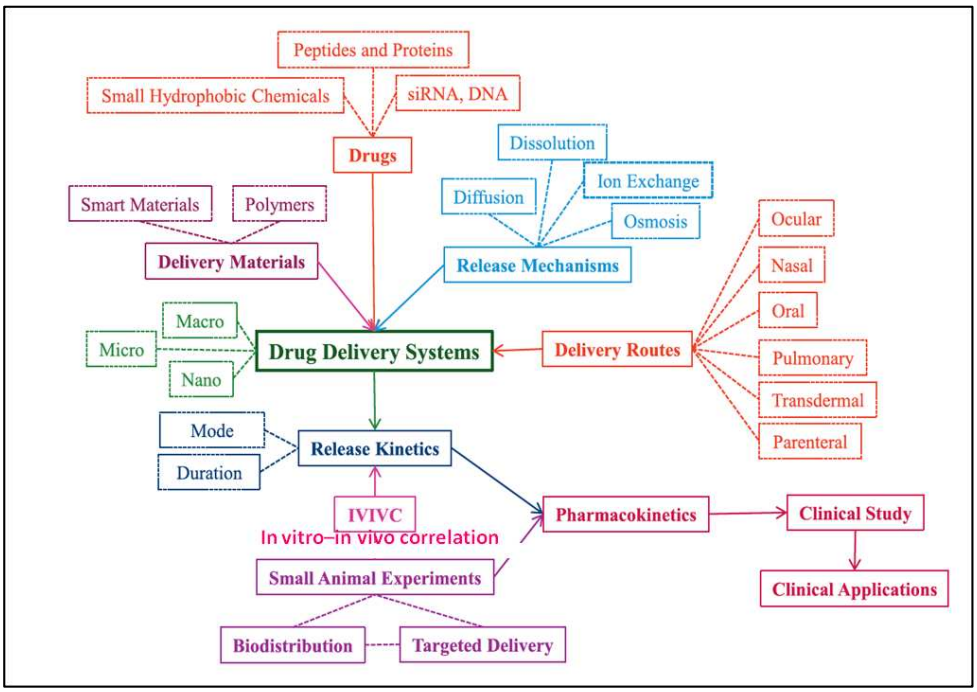

Figure I. 2 Overview of drug delivery development from basic research to clinical applications [8].

The main components of drug delivery systems and processes are shown in a bold-face and solid box, and subsection of each component are shown in a dashed box in Figure I. 2.

I. 2. Drug delivery systems

Since the first Food and Drug Administration (FDA) approval in 1990 of drug delivery system (DDS), liposomal amphotericin B and several DDS are now commercially available to treat diverse diseases ranging from cancer to fungal infection and muscular degeneration [16]. They have also changed the economics of drug development [17]. Packaging an existing drug into controlled release formulations may not only improve its performance but also extend its patent life as a new product [18].

Controlled release drug delivery systems are those dosage formulations designed to release an active ingredient at rates, which differ significantly from their corresponding conventional dosage forms. The controlled release drug delivery systems allow to control the rate of drug delivery, sustain the duration of therapeutic activity and/or target the delivery of the drug to a tissue. Drug release from these systems should be at a desired rate, predictable and reproducible. The ideal drug delivery system should be inert, biocompatible, mechanically strong and comfortable for the patient.

The drug concentration at the appropriate site should be above the minimal effective concentration (MEC) and below the minimal toxic concentration (MTC) [19], otherwise known as 'the therapeutic window'. The concept is illustrated in Figure I. 3 showing the drug plasma levels after oral administration of a drug from an immediate-release dosage form [20].

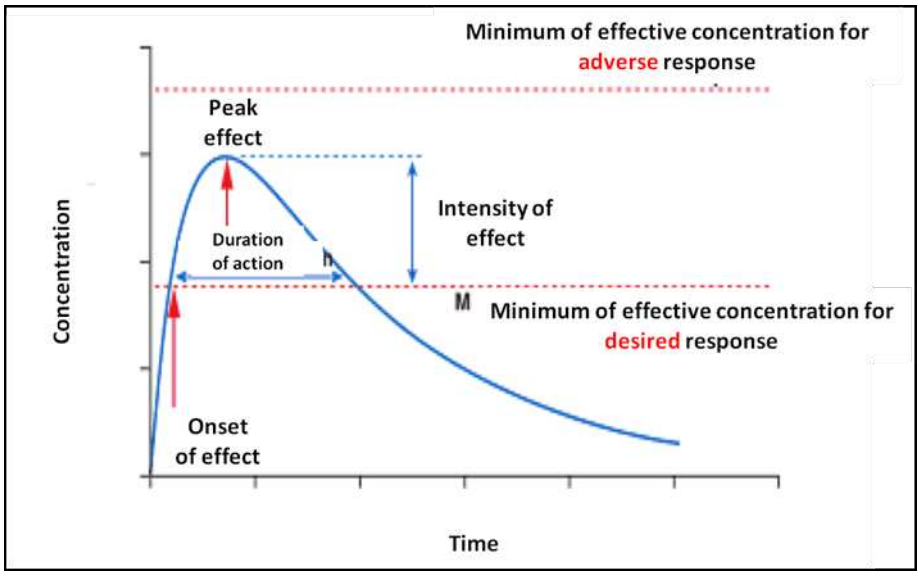

Figure I. 3 Drug plasma levels after oral administration of a drug from an immediate release dosage form [20].

DDS presents several advantages including the improvement of the drug bioavailability and the patient compliance. Nevertheless, DDS disadvantages are also well known. DDS main advantages and disadvantages are summarized in Table I. 1.

Table I. 1 DDS advantages and disadvantages [21].

DDS advantages:

- Maintenance of optimum therapeutic drug concentration in the blood with minimum fluctuations (of the drug levels within a desired range),
- Predictable and reproducible release rates for extended duration,
- Enhancement of therapeutic activity duration for drugs having short biological half-life,
- Elimination of side effects, frequent dosing and wastage of drugs,
- Better patient compliance,
- To mask the unpleasant taste and odor of drugs,
- Prevention of drug degradation (due to light, oxidation …),
- Alteration of site of absorption,
- Elimination of incompatibilities among the drugs.

DDS disadvantages:

- Possibility of toxicity of the materials,
- Harmful degradation products,
- Necessity of surgical intervention for certain systems either on application or removal (such as some implants or scaffolds),
- Patients discomfort with some DDS device,
- High cost of final product.

In recent years, controlled drug delivery formulations used have become much more sophisticated, with the ability to do more than simply extend the effective release period for a particular drug. For example, current controlled-release systems can respond to changes in the biological environment (for example, a pH change), and deliver or cease to deliver drugs based on these changes. In addition, new materials have been developed and should lead to targeted delivery systems, in which a particular formulation can be directed to the specific cell, tissue or site where the drug it contains is to be delivered. While much of this work is still in its early stages, emerging technologies offer possibilities that scientists have only begun to explore.

I. 3. Distinction between delivery systems

Drug delivery can be classified in three ways according to its physical state, the route of administration or the mechanism of drug release.

I. 3. 1. Distinction between delivery systems according to their physical state

Pharmaceutical dosages are available in different forms; solid (*e.g,*. powders, granules, tablets and capsules), liquid (*e.g,*. syrup) and gaseous (*e.g,*. anesthetics). There are also semi solid dosage forms (*e.g,*. creams, ointments, gels and pastes). Numerous dosage forms contain several phases that can be of the same state; for example, emulsions that contain two liquid phases (oil and water) or of different states such as suspensions of solid phases in liquids.

I. 3. 2. Distinction between delivery systems according to their route of administration

The administration routes refer to the methods of getting drugs into the body. They mainly include oral and parenteral routes. Furthermore, alternative routes such as transdermal, pulmonary nasal or ocular administrations are assuming greater importance in drug delivery [3].

I. 3. 2. 1. Oral drug delivery

The oral administration is the most used and preferred route, being convenient and controlled by the patient without requiring skilled medical intervention. It is estimated that 90 % of all medicines usage is in oral forms [19]. Nevertheless, some limitations should be considered when looking for administrating drugs through this route such as:

- First pass effect where the concentration of a drug is considerably reduced or inactivated in the gut wall or the liver before it reaches the systemic circulation,
- Drug absorption rates are variable and may be unpredictable because the pH conditions in the gastrointestinal tract vary considerably from a low pH in the stomach (1.5-2 in the fasted state to around 5 in the fed state) to a higher pH in the small and large intestine (which can reach 7.5),
- Many macromolecules and polar compounds cannot effectively cross the cells of the epithelial membrane in the small intestines to reach the blood stream,
- Many drugs become insoluble at the low pH levels encountered in the digestive tract,

- Some drugs irritate the gastrointestinal tract which can be partially counteracted by coating.

Despite disadvantages, the oral route remains the preferred route of drug delivery. Several improvements have taken place in the formulation of drugs for oral delivery for improving their action [6].

I. 3. 2. 2. Parenteral drug delivery

The parenteral route can refer to any administration route allowing the avoidance of the gastrointestinal tract and therefore the first-pass effect of drugs. Nevertheless, common usage more closely associates the term parenteral as being synonymous with "injectable."

The main clinical role of parenteral therapy is to administer drugs that cannot be given by the oral route, either because of their poor absorption properties or propensity to degrade in the gastrointestinal tract. The major routes of parenteral administration are intravenous, intramuscular and subcutaneous. These three routes satisfy to a large extent the four principal reasons for administering parenteral: therapy (definitive or palliative), prevention, diagnosis, and temporarily altering tissue function(s) to facilitate other forms of therapy [22]. It is estimated that 40% of all drugs administered in hospitals are in the form of an intravenous injection, since this route allows a rapid drug effect.

Additional parenteral routes can also be utilized under special circumstances such as intrathecal, subconjunctival, intraocular or intra-articular routes.

I. 3. 2. 3. Transdermal drug delivery

Transdermal delivery represents an attractive approach used to deliver drugs across the skin for systemic distribution. It involves drug transport to viable epidermal and or dermal tissue of the skin through local application. A major fraction of drug is then transported into the systemic blood circulation.

Transdermal application is a non-invasive method convenient for a variety of clinical indications [23]. It presents many advantages over the conventional oral route such as the avoidance of the first pass metabolism and a better patient compliance [24]. Nevertheless, the protective barrier nature of the skin limits the absorption of most drugs. Variety of strategies can be adopted for the enhancement of drug absorptions such as the use of penetration enhancers or drug carrier (*e.g.*, nanoparticules) which penetrates through the skin more easily [23].

I. 3. 2. 4. Pulmonary drug delivery

Pulmonary route of drug delivery is gaining much importance in the present day research field as it enables to target the drug delivery directly to lung for local and systemic treatment [25]. For local applications, it allows a direct access for the treatment of respiratory diseases with a rapid onset of drug action, and consequently, reduced side effects can be achieved [26][27]. Furthermore, it provides an enormous surface area and a controlled environment for systemic absorption of medications.

However, pulmonary administration presents also some drawbacks. Indeed, since the lungs are a major port of entry to the body, several barriers are present to avoid the invasion of unwanted airborne particles and to control their sterility. As a consequence, they also limit the therapeutic effectiveness of inhaled medications. The drug efficacy may therefore be affected by the delivered dose but also by the location where it is deposited in the respiratory tract. Furthermore, because of the relatively short duration of drug action, multiple daily inhalation maneuvers, ranging up to 9 times a day, can be required [5].

I. 3. 2. 5. Nasal drug delivery

The nasal route is generally used for local diseases treatment such as nasal allergy, congestion or infections [23]. Recent years have shown that the nasal route can also be exploited for the systemic delivery of drugs. In general, among the primary targets for intranasal administration are pharmacologically active compounds with poor stability in gastrointestinal fluids, poor intestinal absorption and/or extensive hepatic first-pass elimination such as polar drugs, peptides or proteins [28].

The main advantage of the nasal route arises from the particular anatomical, physiological and histological characteristics of the nasal cavity, which provides potential for rapid drug absorption and quick onset of action. In addition, intranasal absorption avoids the gastrointestinal and hepatic presystemic metabolism, enhancing drug bioavailability in comparison with that obtained after gastrointestinal absorption [29].

Nasal administration, nevertheless, presents some disadvantages that must be considered during therapy. In addition to physicochemical properties of drugs, a variety of physiological and pathological conditions related to nasal mucosa may also influence the extent of nasal drug absorption and therapy efficacy [30]. Furthermore, the low volume of nasal cavity restricts the amount of drug formulation administrated to about 100-150 µL

[31]. If nasal delivery of high doses of poorly water-soluble drugs is necessary, particular problems may appear such as irritation of mucosa.

I. 3. 2. 6. Ocular drug delivery

Ocular drug delivery has remained as one of the most challenging task for pharmaceuticals scientists. The unique structure of the eye restricts the admission of drug molecules [32] and hinders reaching optimal drug concentration at the required site of action [33].
Conventionally, the drug can be delivered to the ocular tissues by different modes such as topical application, systemic application, intravitreal injections and periocular injections.

Topical application of ocular drug has remained the most preferred method due to the ease of administration and its low cost. Upon topical utilization, drugs are absorbed either by corneal route (the drug passes through the cornea to reach the aqueous humor and later the intraocular tissues) or non-corneal route (the drug crosses the conjunctiva to achieve the sclera and subsequently reach the choroid/retinal pigment epithelium (RPE)). The preferred route depends mainly on the corneal permeability of drug molecules [34].
Generally, topical application is useful in the treatment of disorders affecting the anterior segment of the eye [32]. Indeed, anatomical and physiological barriers hinder drugs reaching the posterior segment of eye mainly at choroid and retina (Figure I. 4). Even for anterior segment treatments, major fraction of drug following topical administration is lost by lacrimation, tear dilution, nasolacrimal drainage and tear turnover. Such precorneal losses result in very low ocular bioavailability. Typically, less than 5 % of the total administered dose reaches the aqueous humor [35]. Therefore in order to maintain minimum concentrations, frequent dosage are required resulting in poor patient compliance.
Classically, topical ocular drug administration is accomplished by eye drops but they have only a short contact time on the eye surface. The contact, and thereby duration of drug action, can be prolonged by formulation design (*e.g,.* gels, gelifying formulations, ointments, and inserts).

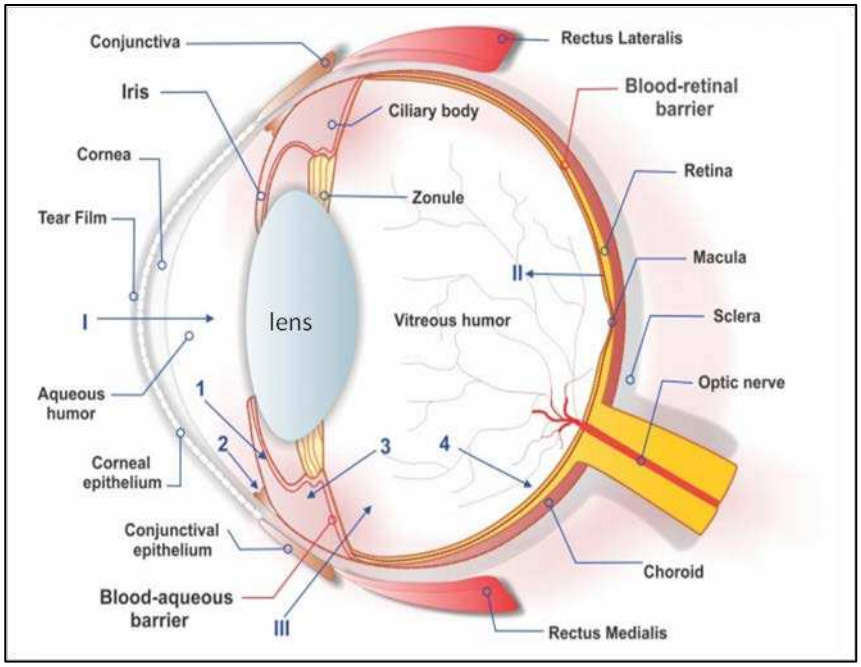

Figure I. 4 Schematic illustration of the main structure of the eye and the ocular barriers to drug delivery [36].

The primary physiologic blockage against instilled drugs is the tear film. Cornea is the main route for drug transport to the anterior chamber (I). The retinal pigment epithelium and the retinal capillary endothelium are the main barriers for systemically administered drugs (II). Intravitreal injection is an invasive strategy to reach the vitreous (III). The administered drugs can be carried from the anterior chamber away either by venous blood flow after diffusing across the iris surface (1) or by the aqueous humor outflow (2). Drugs can be removed from the vitreous away through diffusion into the anterior chamber (3), or by the blood–retinal barrier (4) (Figure I. 4).

Unlike topical administration, systemic dosing helps in the treatment of diseases affecting posterior segment of the eye. A major drawback associated with systemic administration is only 1–2 % of administered drug reaches to vitreous cavity [32].

Lack of adequate bioavailability and failure to deliver therapeutic amounts of drugs to the retina, choroid and intraocular tissues through topical and systemic routes prompted ophthalmologists to search for alternative routes of administration.

Over the past decade, intravitreal injections have drawn significant attention from researchers. Introducing drugs into the eye by direct injection through the pars plana is the most efficient mode of drug delivery to the posterior segment. It is however also the most

invasive route that leads to serious complications [37][38] such as retinal detachment, endophthalmitis and intravitreal hemorrhages [39].

Periocular administration has also been considered as an efficient route for drug delivery to the posterior segment. The periocular administration includes peribulbar, retrobulbar, subtenon, and subconjunctival routes. This method is less invasive than the intravitreal even if anterior segment complications have been observed in some patients [40].

Given the different challenges regarding ocular drug delivery routes, several innovative DDS will be developed in section 1. 4. 2.

1. 3. 3. Distinction between drug delivery systems according to their mechanism of drug release

Another classification that can be used to distinguish the different drug delivery systems is according to the way the drug is released. Generally, they can be distinguished as follows:

- Immediate release: drug is released immediately after administration.
- Modified release: drug release occurs a while after administration, or for a prolonged period of time, or to a specific target in the body. Modified release systems can be further classified as:

    a- Delayed release: drug is released a certain time after the initial administration.

    b- Extended release: prolongs the release to reduce dosing frequency [19].

    c- Pulsatile drug release system, where the drug is released after two or more of lag-time.

I. 3. 3. 1. Immediate release

Immediate release is designed to release the drug as quickly as possible after administration (Figure I. 5). This is useful if a fast onset of action is required for therapeutic reasons. For example, a tablet containing a painkiller should disintegrate quickly in the gastrointestinal tract to allow a fast uptake into the body [19].

Immediate release dosage forms are those for which more than 85% of labeled amount dissolves within 30 min. For immediate release of solid oral dosage forms, the only 'barrier' to drug release is disintegration or erosion stage, which is generally accomplished in less than one hour [41]. For the intravenous injections, the onset of action is very fast and the pharmacological effect may be seen in a matter of seconds after administration

since the drug is already in solution and is directly administered into the body. So no time is lost due to the drug permeation through the gastrointestinal tract, skin or mucosal membranes, before the target organs can be reached [20].

Immediate releases have some advantages such as: enhancement of compliance/added convenience, stability improvement, high drug absorption, ability to provide advantages of liquid medication in the form of solid preparation, and cost-effectiveness.

The duration of action of a drug is known as its half-life. This is the period of time required for the concentration or amount of drug in the body to be reduced by one-half. However, the high drug concentration does not necessarily involve increased drug half-life. To reduce the frequency of drug administration it is often not possible simply to increase the dose of an immediate-release dosage form, as the peak plasma concentration may be too high and lead to unacceptable side effects (such as irritation).

I. 3. 3. 2. Modified release

Modified release drug delivery systems are developed to modulate the apparent absorption and/or alter the site of release of drugs, in order to achieve specific clinical objectives that cannot be attained with immediate release dosage forms. Possible therapeutics benefits of a modified release product include improved efficacy and reduced adverse events, increased convenience and patient compliance, optimized performance, a greater selectivity of activity, or new indications [42]. According to the US food and drug administration, modified release dosage forms include delayed, extended, and pulsatile release products [43].

I. 3. 3. 2. 1. Delayed release

Delayed-release dosage forms can be defined as systems which are formulated to release the active ingredient at a time other than immediately after administration (Figure I. 5). In this case, the therapeutic action of the drug is not extended.

These formulations are used for some drugs that are unstable in certain environments, such as in acidic conditions. Therefore, the active ingredient is protected with coating, generally sensitive to pH in order to optimize the drug therapeutic action. Usually, these formulations present a coating that protects the active ingredient from the acidity of the stomach. They are stable at the highly acidic pH but breaks down rapidly at a less acidic pH. Therefore, the dosage forms are able to travel from the low-pH environment of the

stomach to the higher-pH environment of the small intestine where the coating material dissolves and the drug can be released.

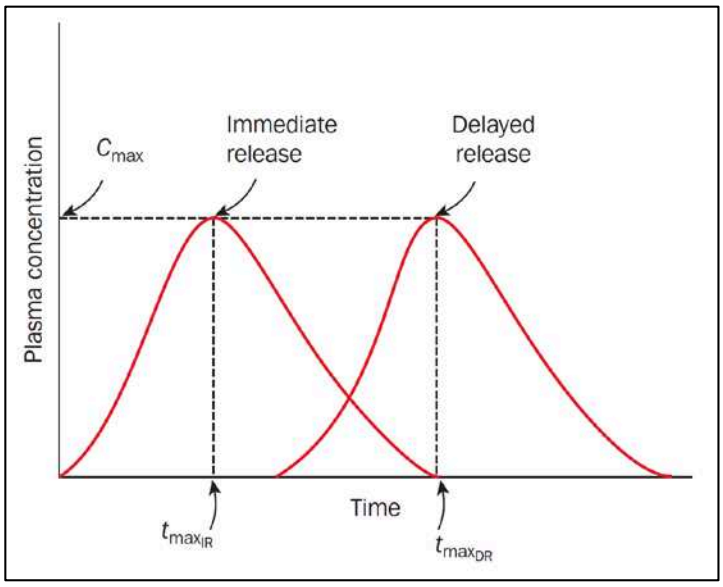

Figure I. 5 Plasma concentration versus time profile of an immediate and delayed release systems [19].

These formulations are interesting for drugs that show poor bioavailability and are rapidly metabolized and eliminated from the body after administration and thus presenting a short half-life, or those with a narrow therapeutic window. These formulations present, however, some disadvantages: a lack of reproducibility and unpredictability *in-vitro*/*in-vivo* correlations.

I. 3. 3. 2. 2. Extended-release

Extended-release systems allow the drug release over prolonged time periods. By extending the release profile, the frequency of dosing can be reduced. The majority of modern extended release technologies are based on polymeric systems and fall into one of three categories: matrix, reservoir (or membrane controlled), and osmotic systems. Drug release from these delivery systems generally presents one or more of the following mechanisms: drug diffusion, system swelling or erosion and dissolution, or osmotic pressure-induced release [19]. Extended-release systems can be further classified as sustained and controlled release.

a. Sustained release

These systems maintain the rate of drug release over a sustained period; the active substance is gradually released and the therapeutic effect is sustained over a long period of time (Figure I. 6). The pharmaceutical formulations corresponding to this type of system are for example osmotic pumps, these devices are generally a semi permeable polymer containing an aqueous solution of drug (Figure I. 7). Those systems control the outflow of drug solutions through osmotic potential gradients across semi permeable polymer barriers. The pressurized chambers contain the aqueous solution of the drug and the polymeric osmotic system. Upon immersion in water, the osmotic system is hydrated and swollen, thus causing an increase in pressure, which is relieved by the flow of the solution out of the delivery device through an orifice in the upper part [44].

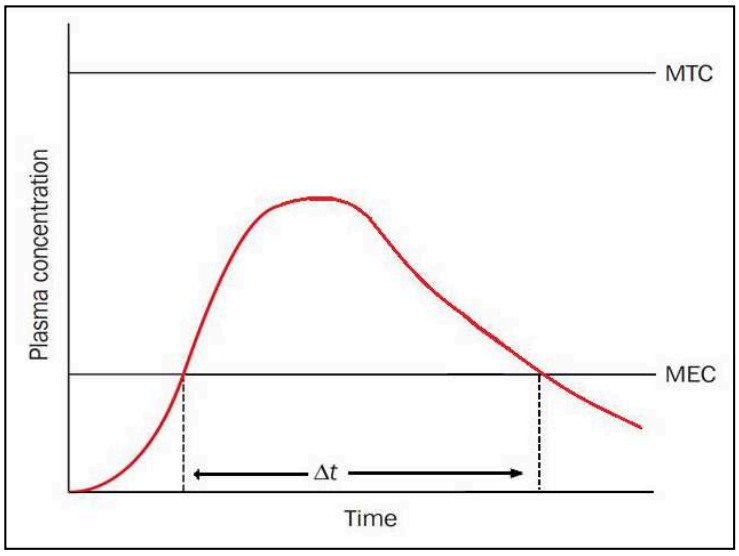

Figure I. 6 Plasma concentration versus time profile of a sustained-release oral dosage form.

Drug delivery through osmotic systems is affected by a number of factors such as solubility, osmotic pressure, size of the delivery orifice and membrane type and characteristics.

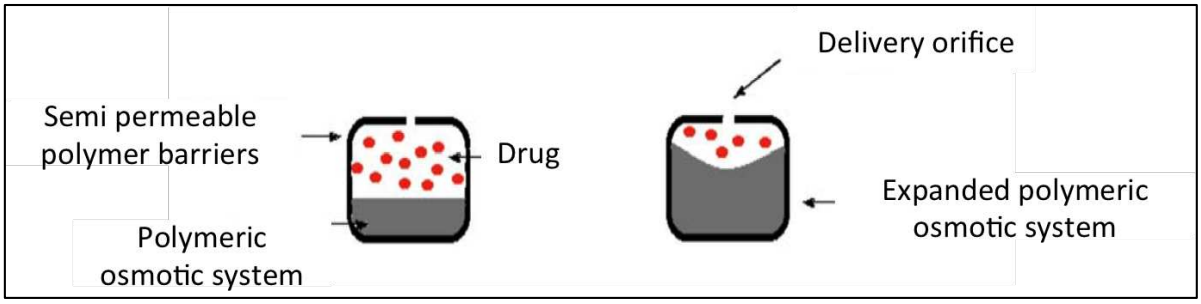

Figure I. 7 Example of osmotic pumps [44].

b. Controlled release

Controlled release allows drug delivery at a specific constant rate (release kinetics of order-zero) for a definite period of time independent of the local environments (Figure I. 8). The periods of delivery are usually much longer than in the case of sustained release and vary from days to years [6]. Another difference between sustained-and controlled-release dosage forms is that the former are basically restricted to oral dosage forms whilst controlled-release systems are used in variety of administration routes, including transdermal, oral and vaginal administration [19].

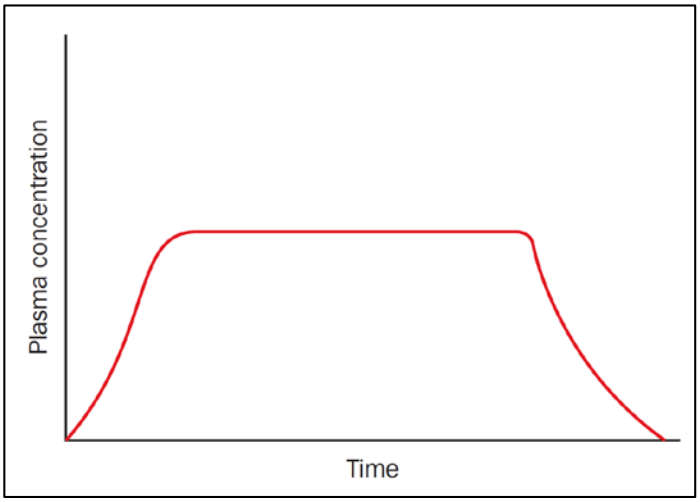

Figure I. 8 Plasma concentration versus time profile of a controlled-release dosage form.

Controlling release offers numerous advantages over immediate dosage forms. This approach increases the therapeutic activity and decreases side effects, thus reducing the number of drug dosages required during treatment. Many different kinds of drugs can benefit from distribution or time-controlled delivery, such as anti-inflammatory agents [45], antibiotics [46], chemotherapeutic drugs [47], immunosuppressants [48], anesthetics [49]

and vaccines [50].

Ideally, the release rate from the dosage form should be the rate-determining step for the absorption of the drug and for the drug concentration in the plasma and target site. However, controlled release systems are not necessarily target-specific, which means that they do not exclusively deliver the drug to the target organ. This may be achieved by so called targeted delivery systems which aim to exploit the characteristics of the drug carrier and the drug target to control the biodistribution of the drug.

Drug targeting aims to control the distribution of the drug within the body such that the majority of the dose selectively interacts with the target tissue at a cellular or subcellular level. By doing so, it is possible to enhance the activity and specificity of the drug and to reduce its toxicity and side effects. Drug targeting can be achieved by designing systems that passively target sites by exploiting the naturel conditions of the target organ or tissue to direct the drug to the target site (active targeting). Alternatively drugs and certain delivery systems can be actively targeted using targeting groups such as antibodies to bind to specific receptors on cells [19]. The challenge has been on three fronts: identifying the proper target for a particular disease state, finding a drug that effectively treats this disease, and finding a means of carrying the drug in a stable form to specific sites while avoiding the immunogenic and nonspecific interactions that efficiently clear foreign material from the body [51].

I. 3. 3. 2. 3. Pulsatile-release

Pulsatile delivery systems usually refer to immediate release of the entire dose in two or more portions separated by predetermined lag times as illustrated in Figure I. 9. In particular, oral pulsatile drug release pertains to the burst delivery of drugs following a programmed pattern from the time of oral administration. For example, Ritalin, is a pulsatile delivery product that provides immediate release of 50% of the total dose upon oral ingestion followed by a burst release of the remaining drug after four hours [52].

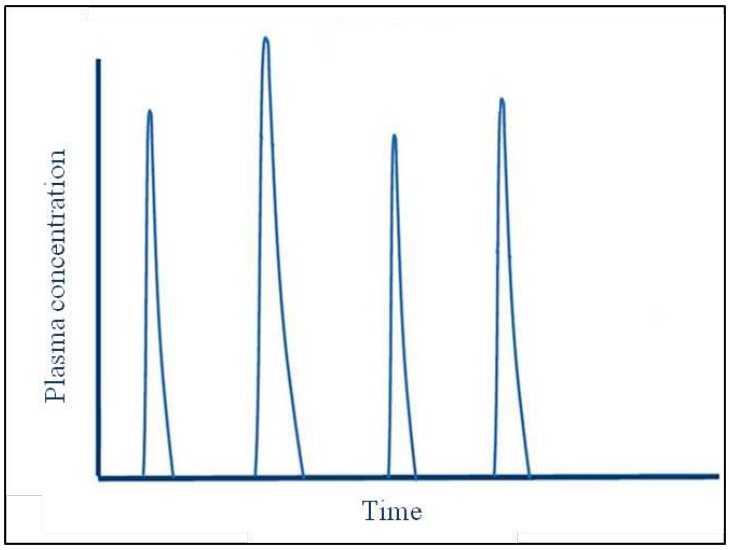

Figure I. 9 Plasma concentration versus time profile of a pulsatile release.

In the field of modified release, these types of non-monotonic and multi-cargo release profiles have been proven to offer clinical benefits in optimizing chronotherapy, mimicking natural patterns of endogenous secretion or multiple dosing regimen, and providing optimal therapy for tolerance inducing drugs where constant levels lead to receptor down-regulation. There are numerous advantages of pulsatile drug delivery systems such as short gastric residence time, bioavailability improvement, stability and patient comfort, adverse effects reduction and tolerability improvement, local irritation risk reduction, and avoidance of dose dumping.

These pulsatile drug release systems present also some drawbacks such as: low drug loading capacity and a possibility of incomplete release of drug, large number of process variables, multiple formulations steps, need of advanced technology, lack manufacturing reproducibility and efficacy, and higher cost of production [53].

From immediate and delayed release to extended and controlled release, the resulting plasma concentration versus time curves have become more and more flatter; prolonging the time of drug release in the therapeutic range after a single administration of the dosage form. This has led to the popular slogan: 'The flatter the better'. However, for some diseases pulsatile release systems may be more advantageous to have varying release of the drug depending on the needs of the patient or circadian rhythms in the body.

I. 4. Novel drug delivery systems

The slow progress in the efficacy of the treatment of certain diseases and particularly

severe diseases, has led to a growing need for a multidisciplinary approach to the delivery of therapeutics in tissues. New ideas for controlling the pharmacokinetics, pharmacodynamics, non-specific toxicity, immunogenicity, and efficacy of drugs were generated based on composition/physical state, mechanism, and route of administration of drug delivery systems. These new strategies, often called novel drug delivery systems, are based on interdisciplinary approaches that combine polymer science, pharmaceutics, bioconjugate chemistry, molecular biology and chemical engineering.

Novel drug delivery systems can include those approaches based on physical mechanisms and others based on biochemical mechanisms. Physical mechanisms include osmosis, diffusion, erosion and dissolution transport. Biochemical mechanisms include monoclonal antibodies, gene therapy, and vector systems like polymer drug conjugates or liposomes or even inactivated viruses. Therapeutic benefits of new drug delivery systems include optimization of drug action duration while decreasing dosage frequency, controlling the site of release and maintaining constant drug levels [54]. Some novel drug delivery systems are presented in the following section.

I. 4. 1. Nanomaterials

Recent developments in nanotechnology have shown that nanomaterials have a great potential as drug carriers. According to the definition from NNI (National Nanotechnology Initiative), nanoparticles are structures of sizes ranging from 1 to 100 nm in at least one dimension. Due to their small sizes, the nanostructures exhibit unique physicochemical and biological properties (*e.g.*, a high reactive area as well as an ability to cross cell and tissue barriers) that make them a favorable material for biomedical application.

Porous structures with pore size of less than 100 nm can be subdivided in three categories according to IUPAC (International Union of Pure and Applied Chemistry): microporous (0.2-2 nm), mesoporous (2-50 nm) and macroporous materials (50-1000 nm). Advances in nanofabrication have made it possible to precisely control the pore size, pore distribution, porosity, and chemical properties of pores in materials.

Porous materials are useful especially for the delivery of macromolecular and biopharmaceutical drugs (peptides, proteins, antibodies, *etc.*). These drugs could lose their biological activity prior to arrival at the target organs and cells due to the very low absorption rate and the degradation by enzymes inside the body. Once nanoporous materials are employed in a target position, the diffusion-based release through

nanochannels provides a safe route to deliver the drugs. In addition, a nanosized pathway enables the long-term release of the drugs by preventing initial burst release; and thus, the release rate of the drugs can be tuned by controlling the porosity of the nanomaterials.

Nanotechnology has been adopted in several fields such as drug/gene delivery [55], [56], imaging [57] and diagnostics [58]. As an example of nanocarriers that have been used as drug delivery systems, we can cite liposomes, polymeric nanoparticles, dendrimers, carbon materials and silica (Figure I. 10).

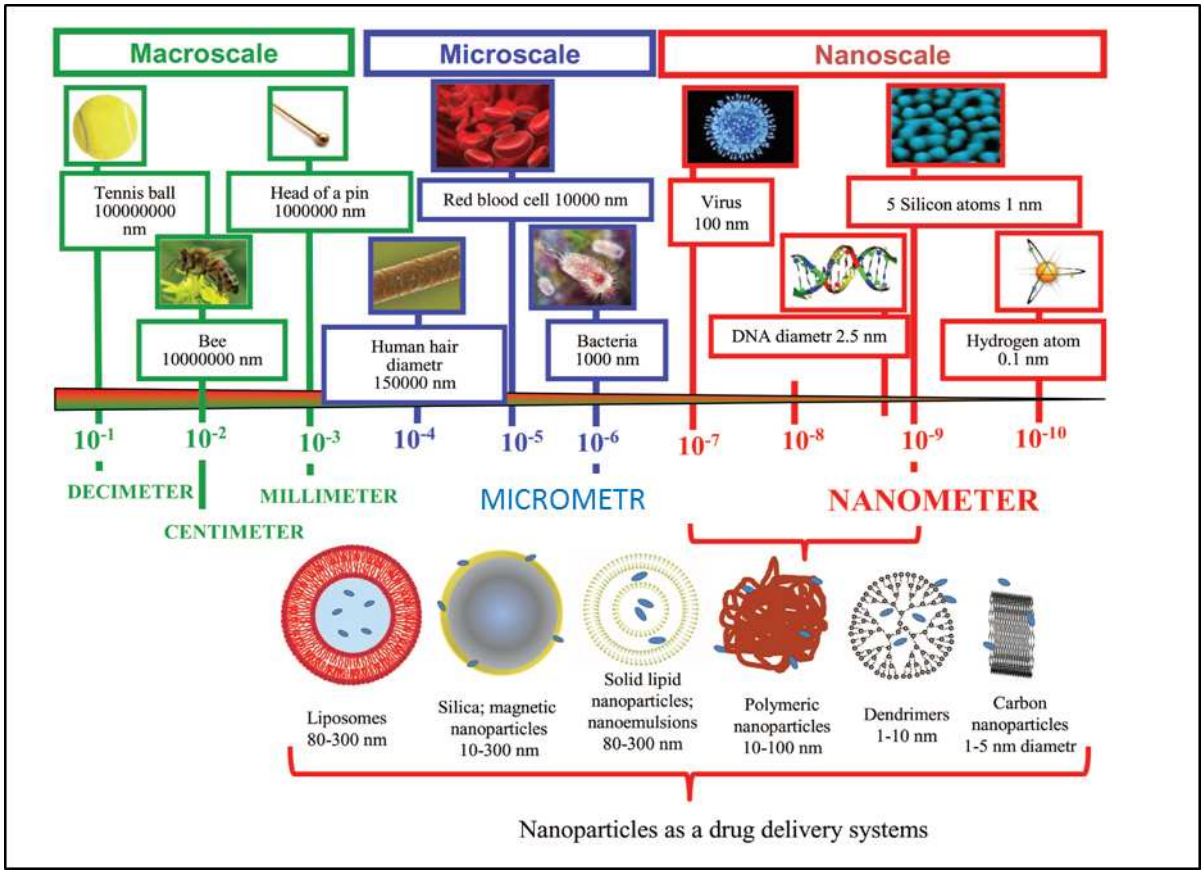

Figure I. 10 Nanoparticle drug delivery systems with relation to other scales [59].

I. 4. 1. 1. Polymeric nanoparticles

The polymeric nanoparticles (PNPs) are prepared most of the time from biocompatible and biodegradable polymers in sizes between 10-100 nm where the drug is dispersed, entrapped, encapsulated or attached to a nanoparticle matrix [60]. Thus, polymer drug delivery systems can broadly be classified into three types of systems: polymer-drug conjugate systems, reservoir-based systems and monolithic matrix systems.

In polymer-drug conjugate systems (Figure I. 11), drugs are delivered in the form of covalent conjugates with water-soluble and biodegradable polymers. This has the potential

to enhance the solubility of poorly soluble drugs and the bioavailability of rapidly degraded therapeutics [61].

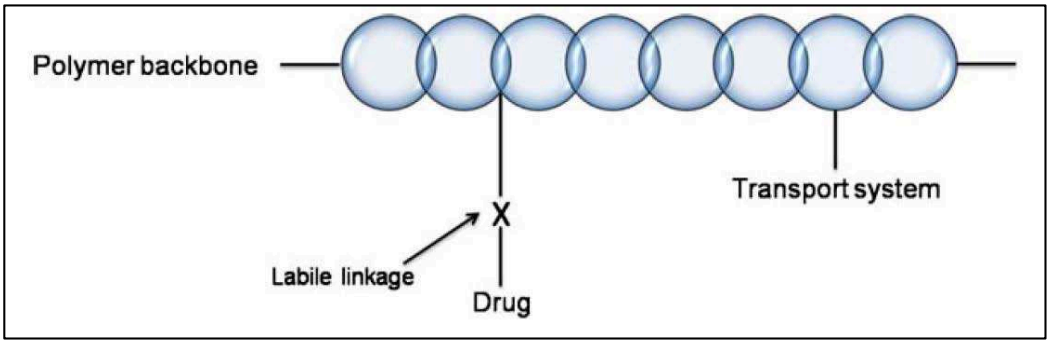

Figure I. 11 Schematization of general structure of polymer-drug conjugate [21].

In reservoir-based systems (Figure I. 12, b), the drug is enclosed within polymer coatings. The drug releases through the rate-controlling porous polymeric membrane. Monolithilc matrix systems (Figure I. 12, a) are similar to reservoir-based systems, but in this case, the drug is dispersed within the polymer matrix. In both reservoir-based and monolithic matrix systems, drugs are noncovalently embedded or dispersed within the polymer matrices [61][62].

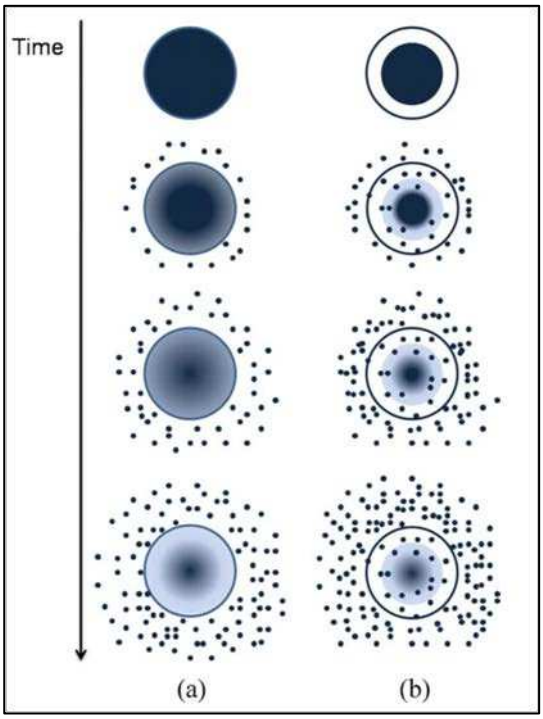

Figure I. 12 Drug diffusion profile for both (a) monolithic matrix and (b) reservoir systems [21].

The PNPs are obtained from synthetic polymers such as poly-ε-caprolactone,

polyacrylamide or polyacrylate; or from natural polymers like chitosan or gelatin. Based on *in-vivo* behavior, PNPs may be classified as biodegradable (like poly (L-lactide) (PLA) or polyglycolide (PGA)) and non-biodegradable (like polyurethane) [59]. PNPs are promising vehicles for the preparation of drug delivery to specific target, which improves the drug safety and their nanometer size promotes an effective drug permeation through cell membranes and stability in the blood stream.

I. 4. 1. 2. Dendrimer nanocarriers

Dendrimers are artificial macromolecules which have a tree-like structure. They are globular and nano-scaled macromolecules with a particular architecture constituted of three distinct domains: a central core which is either a single atom or an atomic group having at least two identical chemical functions, branches emanating from the core, constituted of repeat units having at least one branch junction, whose repetition is organized in a geometrical progression that results in a series of radially concentric layers called generations, and many terminal functional groups, generally located in the exterior of the macromolecule, which play a key role on the dendrimer properties [63]. For example, a design of Poly (propylene imine) dendrimer is presented in the Figure I. 13.

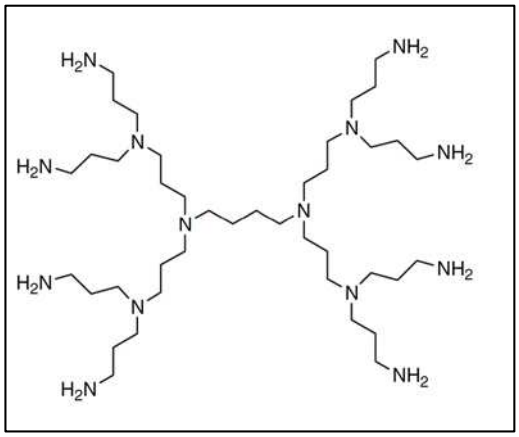

Figure I. 13 Design of Poly (propylene imine) dendrimer.

Attractive features like nanoscopic size (1-100 nm), narrow polydispersity index, excellent control over molecular structure, availability of multiple functional groups at the periphery and cavities in the interior distinguishes them from the available polymers [64]. Dendrimers have been successfully proved as useful additives in different routes of drug administration because they can enhance water-solubility, bioavailability, and biocompatibility of drug formulation. Terminal functionalities provide a platform for conjugation of the drug and targeting moieties. In addition, these peripheral functional

groups can be employed to tailor-make the properties of dendrimers, enhancing their versatility [65].

I. 4. 1. 3. Liposomes

Liposomes are nano/micro-particular or colloidal carriers, usually with 80–300 nm size range [66]. They are most often composed of phospholipids, but my also include other lipids. Phospholipids are amphiphilic molecules, where one part of the molecule is polar (hydrophilic head) and the other non-polar (hydrophobic tail). When phospholipids are placed in contact with water, the unfavorable interactions of the hydrophobic segments of the molecule with the solvent result in the self-assembly of lipids, forming then a spherical vesicles having at least one lipid bilayer, so called liposomes [67].

Liposomes have been reported to increase the drug dissolution kinetic and improve their pharmacokinetic properties, such as the reduction of harmful side effects and increase of *in-vitro* and *in-vivo* anticancer activity. Drug distribution is then controlled primarily by properties of the carrier and no longer by physico-chemical characteristics of the drug substance only [68].

Lipids forming liposomes may be natural or synthetic; and liposome constituents are not exclusive of lipids, new generation liposomes can also be formed from polymers (sometimes referred to polymersomes). Whether composed of natural or synthetic lipids or polymers, liposomes are biocompatible and biodegradable which makes them suitable for biomedical research.

I. 4. 1. 4. Nanoparticles based on solid lipids

Solid lipid particles are composed of lipids and stabilizers in most cases surfactants, co-surfactants and coating materials. The ability to incorporate drugs into solid lipid nanoparticles offers a new prototype in drug delivery that could be used for secondary and tertiary levels of drug targeting. Hence, solid lipid nanoparticles hold great promise for reaching the goal of controlled and site specific drug delivery.

Those formulation ingredients are safe and under the generally recognized as safe (GRAS) status issued by the FDA [69]. Solid lipid particulate systems such as solid lipid nanoparticles (SLN), lipid microparticles (LM), nanostructured lipid carriers (NLC), lipospheres and lipid drug conjugates (LDC) have been sought as alternative carriers for therapeutic peptides, proteins and antigens due to their properties [69].

SLNs are produced by replacing the liquid lipid (oil) of an oil/water emulsion by a solid lipid or a blend of solid lipids [12]. SLNs offer unique properties such as smaller size, larger surface area, interaction of phases at the interfaces; and these properties are attractive for their ability to improve performance of nutraceuticals, pharmaceuticals and other materials [70]. SLNs present several advantages such as good biocompatibility, low toxicity, physical stability and a good delivery of lipophilic drugs. Important peptides such as cyclosporine A, insulin, calcitonin and somatostatin have been incorporated into solid lipid particles and are currently under investigation. This is one of the most popular approaches to improve oral bioavailability of poorly water soluble drugs [71].

I. 4. 1. 5. Microemulsions and nanoemulsions

Microemulsions (ME) and nanoemulsions (NE) are lipid based nanocarrier systems wherein the dispersed phase could be as small as 20 nm [72]. ME and NE are isotropic mixtures of oil/water stabilized by surfactants frequently in combination with co-surfactants [3,4,41]. They have shown good dissolution properties and thermodynamic stability. The stabilizers prevent particle agglomeration and/or drug leakage. Permeation of the drug formulations is enhanced which can be exploited in transdermal delivery [41]. The capacity of ME and NE to dissolve large quantities of low soluble drugs along with their biocompatibility and ability to protect the drugs from hydrolysis and enzymatic degradation makes them ideal drug delivery vectors [73]. The major advantages of NE as drug delivery carriers include increased drug loading, enhanced drug solubility and bioavailability, reduced patient variability, controlled drug release, and protection from enzymatic degradation [74].

ME and NE have found wide applications in bioavailability enhancement and delivery through various administration routes, namely oral [75], parenteral [76], nasal [77], transdermal [78] or also ocular [79].

I. 4. 1. 6. Carbon nanomaterials

Carbon nanocarriers used in DDS are differentiated into nanotubes (CNTs) and nanohorns (CNHs).

CNTs have a cylindrical structure with a diameter of only several nanometers composed of sheets of linked hexagonal rings of carbon atoms. CNTs consisting of a single sheet are called single walled carbon nanotubes (SWCNTs) and those formed by rolling up more

than one sheet are called multi-walled CNTs (MWCNTs) (Figure I. 14). In the medical field, three main attributes of CNTs have been exploited [14]: their small size, their high surface to volume ratio and their ability to contain chemicals.

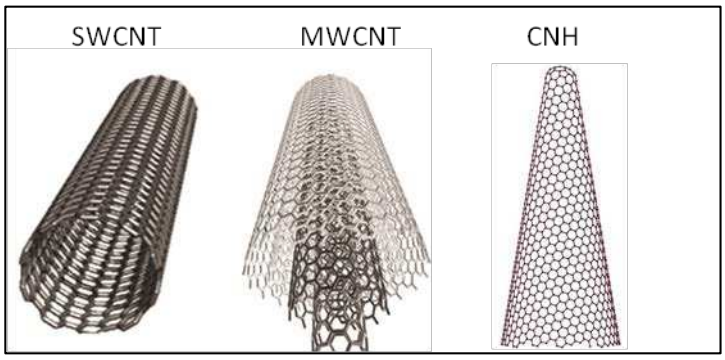

Figure I. 14 The schematic illustration of the structure of SWCNT, MWCNT and CNH [80].

CNHs (Figure I. 14) are spherical aggregates of SWCNTs with a diameter of 80 to 100 nm. They are particularly suitable as drug carriers to the tumor tissue because their size fulfills the condition for achieving enhanced permeability and retention effect. They can permeate through the damaged vessels in tumor tissue and remain there because of little lymphatic drainage. In addition to an extensive surface area, carbon nanohorns have tubes at the end of spherical aggregates with diameter 2-5 nm. Holes can be generated at the tips of the tubes and can be exploited to insert different therapeutic agents into their empty space [81]. Functionalized carbon nanohorns have been proposed for controlled drug release of anti-inflammatory and anticancer agents including dexamethasone, doxorubicin, and cisplatin [80].

I. 4. 1. 7. Silica materials

Silica is widespread in living nature from single celled organisms to higher plants and can be used for various purposes [82]. The active surface property of amorphous silica allows developing silica particles with various surface properties through surface functionalization with different molecules, which consequently allows targeted delivery of different types of therapeutic agents. Due to their strong Si–O bonds, silica particles are stable to external *stimuli* such as mechanical stress and degradation eliminating the need for any additional stabilisation such as covalent linkers used in other delivery systems like dendrimers [83]

[84]. The abundant presence of silanol groups in silica can also have an affinity to phospholipids, which can be actively taken up by the cells [85].

Silica materials used in controlled drug delivery systems are classified as natural silica materials *e.g,*. diatoms [86], fumed silica nanoparticles [87], silica-based xerogels and aerogels [88]–[91], and ordered mesoporous silica based materials [92]. They exhibit several advantages as carrier systems including biocompatibility, an ease in terms of functionalization and ability to present highly porous framework [93]. Among inorganic nanoparticles, silica materials are the carriers which are most often chosen for biological purposes [94].

Biosilica with complex 3-dimensional porous structures [86] are found in the nature; they are formed following biologically based self-assembly synthetic routes [86]. The most outstanding example is diatom, single cell photosynthetic algae with distinct silica cell walls called frustules and consisting of highly ordered pore structures, species characteristic patterns and hierarchical pore organization with unique mechanical, molecular transport, optical and photonic properties [95]. The structures of diatom frustules with hollow and large inner space, microscale and nanoscale porosity, high surface area, excellent biocompatibility, amorphous silica state, modifiable surface chemistry, high permeability, low density, non-toxicity and low cost make diatom silica a promising biomaterial for drug delivery applications [96].

Fumed silica is an extremely small non porous particle with high surface area and purity. Fumed silica is formed by injecting chlorosilanes, such as silicon tetrachloride, into a flame of hydrogen and air. Fumed silica nanoparticles have been used as a solid carrier for the preparation of dry emulsions. Dry emulsions have the ability to increase the dissolution rates and bioavailability of poorly water-soluble drug compounds, protect the drug against light or oxidation, and eliminate the shortcomings of conventional liquid emulsions in particular physical instability [87].

Silica xerogels and aerogels possess an amorphous structure with high porosity (up to 99% of the whole volume) and enormous surface area which make them interesting carriers for drugs. The porous structure (shape and pore dimensions) depends on the synthesis parameters and the drying process [97]. The synthesis of these systems is carried out through the sol-gel technique leading in a first step to the formation of a gel presented as a solid interconnected porous structure in an equilibrium with a liquid phase within the pores. According to the drying process, a xerogel is obtained through an evaporative drying

process and an aerogel through a supercritical drying process. DDS based on aerogels and xerogels base can be obtained either by introducing the active ingredient during the sol-gel process or through an ulterior impregnation step [98].

Since a part of our experimental research work was carried out on the formulation of drug delivery systems based on mesoporous ordered silica, the materials will be detailed in the following section and the methods of the elaboration of drug mesoporous-silica systems will be presented in chapter II.

Ordered mesoporous silica for drug delivery systems

Since the discovery of ordered mesoporous silica materials in 1990s, synthesis and applications of mesoporous solids have received impressive consideration due to their highly ordered structures, large pore size and high surface area. In the past decade, mesoporous materials have found a lot of applications in separation, catalysis, sensors and devices [99], [100].

Ordered mesoporous silica, which were prepared using surfactants as structure-directing agents, were produced with hexagonal and cubic symmetries and pore sizes ranging from 2 to 10 nm. Basically, silica synthesis requires the addition of one silica source (from an inorganic source as sodium silicate solution or from an organic source as tetraethyl orthosilicate (TEOS)) with the surfactant template. In the scheme below we see the procedure to synthesize mesoporous materials (Figure I. 15).

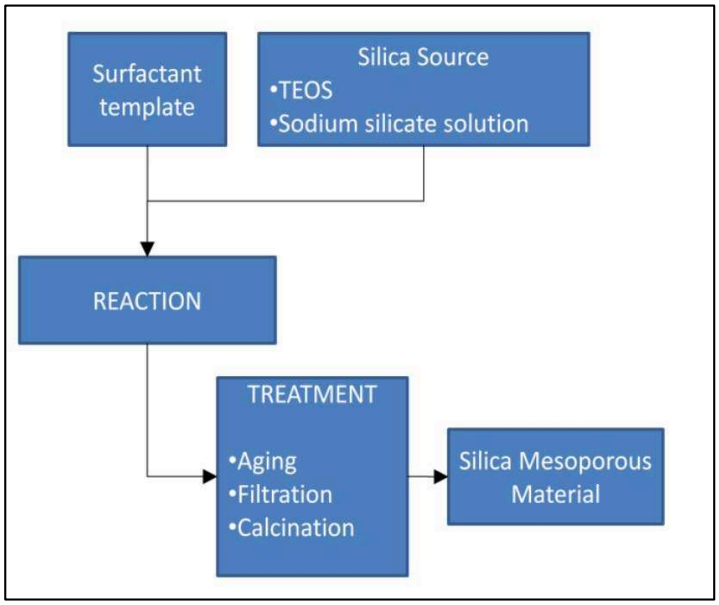

Figure I. 15 Synthesis of silica mesoporous materials.

Since the work carried out by Vallet-Regi *et al.* in 2001 using MCM-41 as a new drug delivery system [101], a lot of investigations have been done in this area developing different types of mesoporous materials with varying porous structures and functionalities for sustained drug release and *stimuli*-responsive release.

Table I. 2 presents the different porous structures of some ordered mesoporous silica, which have been employed for drug delivery.

Table I. 2 Porous structures of ordered mesoporous silica [102].

Mesoporous solid	Pore diameter nm	Structure
MCM-41	2-5	Hexagonal 1D chanel
MCM-48	2-5	Bicontinuous 3D
SBA-15	5-10	Hexagonal 1 D chanel
SBA-16	Min 1-6; max 4-9	Body center arrangement of cages
SBA-1	2-4	Cubic 3D
SBA-3	2-4	2D hexagonal
MSU	2-5	2D hexagonal
HMS	2-5	Hexagonal

Due to stable structure and well-defined surface properties, ordered mesoporous materials seem ideal for encapsulation of pharmaceutical drug, proteins and other biogenic molecules. It has been shown that both small and large molecular size drugs can be entrapped within the mesopores by an impregnation process and liberated via a diffusion-controlled mechanism. The reasons for the high impact of these materials in the field of biotechnological research is based on their properties of (Figure I. 16):

- An ordered pore network, which is very homogeneous in size and allows fine control of the drug release kinetics,
- A high pore volume to host the required amount of pharmaceuticals,
- A high surface area, which implies high potential for drug adsorption,
- A silanol-containing surface that can be functionalized to allow better control over drug loading and release.

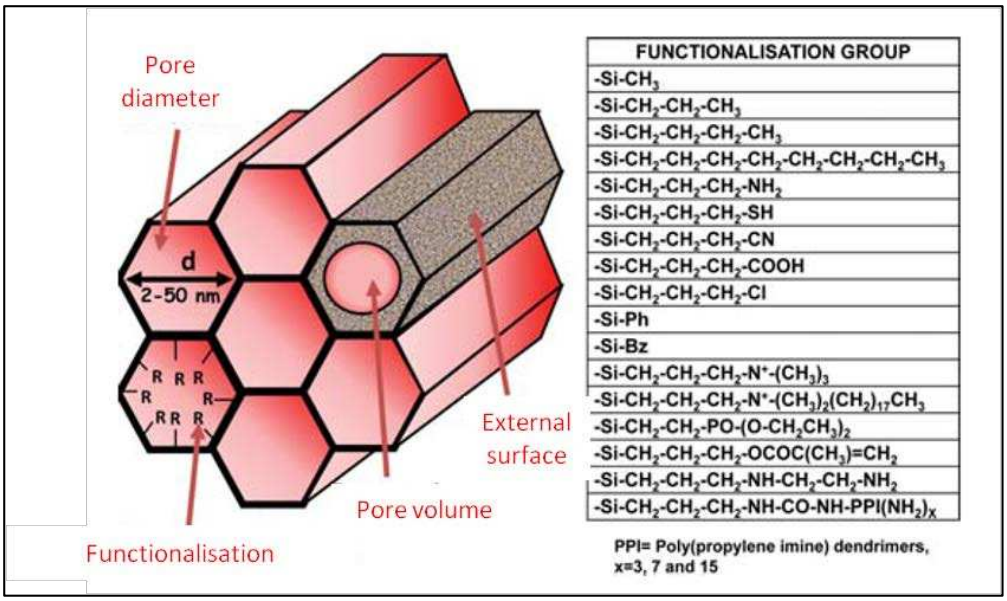

Figure I. 16 The properties that have fuelled the use of ordered mesoporous silica as drug delivery systems [103].

I. 4. 2. Ocular medical devices

Anatomy and physiology of the eye makes it a highly protected organ, which restricts the admission of drug molecules and hinders reaching optimal drug concentration at the required site of action [32], [104]. As mentioned above (section I. 3. 2. 6), conventional delivery systems such as: eye drops, suspensions, ointments and local injections can not be considered optimal. Indeed, these formulations do not offer adequate bioavailability due to the washing off of the drugs from the eye or structural and physiological barriers which limit the penetration of administered actives into the ocular tissues.

Some of the newer methods for administrating ocular drugs, microneedles, in-situ gelling systems, implants and intraocular lenses, are bravely discussed hereafter. Since a part of our experimental research work was carried out on the preparation of drug delivery systems based on intraocular lenses, this last part will be detailed separately in the section I. 4. 3.

I. 4. 2. 1. Microneedles

Microneedle based technique is an emerging and minimally invasive mode of drug delivery to posterior ocular tissues [105]. This technique can provide more localized and targeted delivery of ophthalmic drugs than traditional drug delivery methods, with minimal

drug loss and tissue damage. Microneedles are solid or hollow needles of micrometric dimension and were designed to create micron-size pores in the tissue. This would enable delivery of free drug or drug encapsulated within nanoparticles or microparticles for controlled release over time within the sclera [106]. Drug could then diffuse from the sclera to neighboring choroidal and retinal tissues to treate diseases of the posterior segment of the eye [107]. Microneedles are custom designed to penetrate only hundreds of microns into sclera thus avoiding damage of deeper ocular tissues [105].

This new microneedle based administration strategy may reduce the risks and complications associated with intravitreal injections such as retinal detachment, hemorrhage, cataract, and endophthalmitis. Moreover, this strategy may help to circumvent blood retinal barrier and deliver therapeutic drug levels to retina/choroid.

I. 4. 2. 2. *In-situ* gelling systems

In-situ forming hydrogels refer to polymer solution which can be administered as liquid upon instillation and undergo phase transition in the ocular *cul-de-sac* to form viscoelastic gel. *In-situ* hydrogel formation provides a response to environmental changes since gelation can be triggered by variations in temperature or pH [105], [108]. It is widely accepted that increasing the viscosity of a drug formulation in the precorneal region will lead to increased bioavailability due to slower drainage rate from the cornea. Moreover, the efficacy of ophthalmic hydrogels is mostly based on an increase in ocular residence time via enhanced viscosity and mucoadhesive properties [108].

Different polymers are used for this in-situ gelling system according to their sensitivity. We can cite, among other polymers; poloxamers, multiblock copolymers made of polycaprolactone, polyethylene glycol, poly (lactide), poly (glycolide), poly (Nisopropylacrylamide) and chitosan [109].

I. 4. 2. 3. Implants

Drug loaded ocular implants are one dose systems of drug and polymeric materials, which can release the drug at controlled rate without interfering with the vision. Implants can be localized within the anterior or posterior segments, through a simple surgical implantation. Compared to traditional methods of drug administration to the eye, ocular implants have many advantages, including enhancing drug bioavailability and sustaining the drug delivery in controlled therapeutic levels directly to the site of action and bypassing the

blood-brain barrier [105], [110] as well as improving patient compliance.

In general, subconjunctival implantation is used for anterior-segment diseases, whereas intravitreal and suprachoroidal methods are typically used to treat posterior-segment diseases. Intrasceral implants can be used for either. A significant amount of crossover can occur, and a drug may be delivered to both segments regardless of placement [111].

The structures of polymeric devices for controlled and sustained release are classified as non-biodegradable and biodegradable. Non-biodegradable implants have the advantage of steady, controlled release of a drug during potentially long periods of time (years) and the disadvantage of difficulty of removal and/or replacement when the drug is depleted. Biodegradable implants have the advantage of being able to be fashioned into many shapes, they do not require removal and they increase the half-life of the drug [111]. Several implants are undergoing clinical trials while a few are already commercialized [112].

I. 4. 3. Intraocular lenses

Contact lenses were initially successfully used as drug delivery systems [113]. Currently, several approaches are under study to endow intraocular lenses (IOLs) with the ability to host drugs and to prolong its release in order to treat various ocular diseases.

Among other diseases, cataract is the most common cause of blindness and severe visual impairment worldwide. The number of patients with cataract is continuously increasing [114]. Currently, about 2 million people have their cataractous lens removed and replaced with an intraocular lens (IOL) each year [115].

The surgery involves implantation of an artificial intraocular lens to replace opacified (damaged) natural crystalline lens [114]. It is generally considered as safe, however, postoperative endophthalmitis [116], [117], a rare but potentially devastating infection, and posterior capsular opacification, a less serious but much more common postoperative complication [118]–[121], may occur.

To prevent short- and long-term complications, a concentrated solution of anti-inflammatory or antibiotic drugs is injected (subconjunctival, topical, intracameral or intravitreal) in the eye after cataract surgery [116]. The efficacy of this treatment is limited either due to poor drug bioavailability across the blood-ocular barriers [122] or serious side effects [115].

Significant advances have been made in developing new treatments for the prevention of ocular risks following cataract surgery. The advent of new technologies opens the door to

new controlled drug delivery systems to prevent postoperative complications. The drug-IOL combination may be the result of loading commercially available IOLs with specific drugs or of design of IOLs with particular composition in order to improve drug loading and to achieve efficient control of release [123].

Different types of IOLs are used for the treatment of cataract. From the time of Ridley's first lens implantation (IOL without drug) (1949/1950) [124], the evolution of IOLs in form, composition and use is divided into six generations as referred in Table I. 3.

Table I. 3 Evolution of intraocular lenses [125].

Generation	Dates and types (approximate)
I	1949-1954 Original Rideley posterior chamber. PMMA IOL manufactured by Rayner, LTD., U.K.
II	1952-1962 Early anterior chamber lens.
III	1953-1973 Iris-supported, including iridocapsular IOL implanted after extracapsular cataract extraction (ECCE).
IV	1963-1992 Transition towards modern anterior chamber IOLs.
V	1977-1992 Transition to and maturation of posterior chamber lenses.
VI	1992-2000 Modern posterior chamber IOLs.

Several types of IOLs are currently available. IOLs can be differentiated in different ways. The most important of these classifications are shown in Table I. 4.

Table I. 4 Classification of IOLs [126].

Implantation site/type	Capsular bag, ciliary sulcus, scleral fixation, iris fixation, angle supported
Overall design	1 piece /3 pieces*
Optic materials	Rigid (PMMA), foldable (hydrophobic acrylic, hydrophilic acrylic), flexible (silicone), collamer
Refraction index	1.42–1.55
Optics shape	Biconvex, plano-convex, meniscus
Overall length	10–13 mm
Optics diameter	5–7 mm
Optics design	Spherical, aspheric, toric multifocal, multifocal toric
Optics color	Transparent, tinted
Haptics properties	1 piece/3 pieces (PMMA, PVDF, polyamide, 2, 3, 4, 6 haptics)
Type of implantation	Injectable, not injectable
Type of packaging	Pre-loaded, not pre-loaded

* IOL consist of small optics with side structures, called haptics, which can be prepared from the same material (1 piece) or different materials (3 pieces).

Generally, IOL materials fall into three groups, acrylate/methacrylate polymers, silicone elastomer and collamer [127] as illustrated in Figure I. 17

.

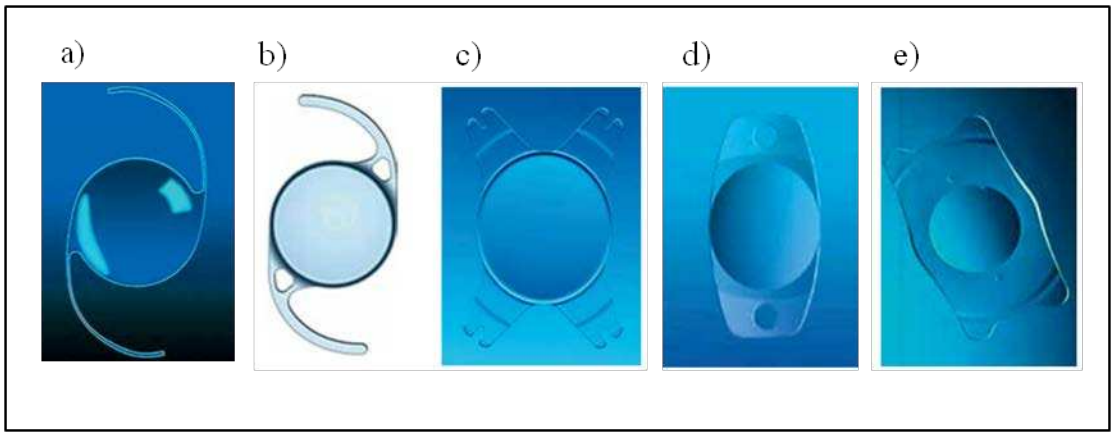

Figure I. 17 IOLs a) PMMA, b) foldable hydrophobic, c) foldable hydrophilic acrylic, d) silicone, and d) collamer [126].

I. 4. 3. 1. Hydrophobic acrylic lenses

- **Poly (methyl methacrylate) lenses**

The first hard or rigid polymeric lenses were those manufactured by Kevin Tuohey in 1948 from PMMA. PMMA lenses (Figure I. 17, a) are prepared from rods or buttons of PMMA obtained by bulk free-radical polymerization of methyl methacrylate. It is a rigid and non foldable hydrophobic material (water content <1%). The refractive index is 1.49, and the usual optic diameter is 5-7 mm. PMMA is rather hydrophobic but becomes slightly more hydrophilic after contact with water as indicated by a decrease in contact angle [128].

PMMA IOLs present good optical properties, are light in weight, and have acceptable surface wettability and exceptional durability. However, the low oxygen permeability of this material limits the long-term wear of these lenses.

As already mentioned, acrylic PMMA polymer was used in the first implantation of IOL performed by Harold Ridley in 1949. It is still a popular material for IOL optic and remains the standard against which other materials are compared [129]. PMMA lenses are usually thin as the rigidity of the material balances the low refraction index. However, because of the required large incision, PMMA IOLs are seldom preferred today. They are still currently used in developing countries because of the low cost, and in children treatment given the proven long life in implanted eyes [130].

– **Foldable hydrophobic acrylic lenses**

Hydrophobic foldable acrylic materials are a series of copolymers of acrylate and methacrylate derived from rigid PMMA. The typical wetting contact angle with water is 73° [131]. Hydrophobic foldable acrylic lenses can be folded, pushed and pulled; always regaining their original shape in a matter of seconds [132]. Hydrophobic acrylic IOLs are available in 3 piece or 1 piece designs (the last design is presented in the Figure I. 17, b), optic diameter between 5.5 and 7.0 mm, and overall length between 12 and 13 mm [126]. These acrylic polymers are synthesized from esters of acrylic or methacrylic acid and they are foldable under room temperature. This facilitates folding and insertion through a smaller incision. The materials have very low water content and higher refractive index (1.55) than PMMA or silicone, making them among the thinnest of available lenses. Furthermore, their hardness is temperature dependent and the lens is rigid like PMMA at temperatures lower than room temperature [133].

I. 4. 3. 2. Hydrophilic acrylic lenses

Hydrophilic acrylic materials (Figure I. 17, c) are composed of a mixture of hydroxyethylmethacrylate (poly-HEMA) and hydrophilic acrylic monomer [134]. These lenses are cut in the dehydrated state and then hydrated and stored in solution. The water content between IOLs varies widely and can be as high as 38% [133]. Hydrophilic acrylic lenses are soft, somewhat compressible, and have excellent biocompatibility because of their hydrophilic surface. The wetting contact angle with water is lower than 50°. Most IOLs are single piece and designed for capsular bag implantation with few exceptions. Hydrophilic acrylic material is the easiest to handle and can be implanted through a very small incision (2 mm).

I. 4. 3. 3. Silicone lenses

Silicone was the first material available for foldable IOLs. It is composed of polymers with a dialkyl or diaryl siloxane functional groups, and the simplest is polydimethylsiloxane [116]. Silicone (Figure I. 17 d) is hydrophobic with a contact angle with water of 99°, higher than that of hydrophobic acrylic materials. The refractive index is usually between 1.41 and 1.46, and the optic diameter is ranges from 5.5–6.5 mm [133]. Current models are 3 pieces with PMMA, polyvinyl difluoride (PVDF) or polyamide haptics. Because of the

low refractive index, the optics is rather thick, requiring incisions larger than 3.2 mm to implant higher power lenses. These IOLs are no longer used nowadays [126].

I. 4. 3. 4. Collamer lenses

Collamer is the name of the material used exclusively by STAAR® surgical company. The name comes from the combination of 'collagen' and 'polymer'. These IOLs (Figure I. 17, e) are composed of a hydrophilic porcine collagen (<0.1%)/hydroxyethyl methacrylate copolymer with an ultraviolet-absorbing chromophore [23]. IOLs made from collamer are highly biocompatible, and easy to implant because of the softness of the material [135]. Indeed, water content is very high, at about 40%, which makes this material very soft [136].

Several methods of preparations of drug delivery systems, according to the type of IOLs presented above, were used in the literature. The preparation of drug delivery systems based on PMMA and P-HEMA IOLs was the core of our work. Those kinds of drug delivery systems have not been yet commercialized; the different past or ongoing research works dealing with the loading of IOLs will be detailed in chapter II.

I. 4. 4. Other systems

Some other novel drug delivery systems such as microsponges, cyclodextrins, viruses and immunoconjugates are briefly presented in the following section.

Microsponge delivery system is highly cross-linked porous polymeric microspheres that can entrap wide range of active ingredients and then release them onto the skin over a time and in response to trigger [137]. Microsponges are biologically safe and offer unique advantages of programmable release. This technology is believed to contribute towards reduced side effects, improved stability and enhanced formulation flexibility [138]–[140]. This technology is being used for topical formulations and also for oral administration [141].

Cyclodextrins (CDs), with lipophilic inner cavities and hydrophilic outer surfaces, are capable of interacting with a large variety of guest molecules to form noncovalent inclusion complexes [142]. They are widely used as "molecular cages" in different industries such as agrochemicals, foods, pharmaceuticals and cosmetics. In pharmaceutical industry they are used as complexing agents to increase the aqueous solubility of poorly

soluble drugs and to increase their bioavailability and stability [143]. In addition, cyclodextrins can be used to reduce gastrointestinal drug irritation, convert liquid drugs into microcrystalline or amorphous powder, and prevent drug–drug and drug–excipient interactions.

Virus particles typically consist of several hundreds to thousands of protein molecules, which self-assemble to form a hollow scaffold packaging the viral nucleic acid. Viruses are potential vehicles for drug and gene therapies due to their natural ability to infect specific cells and transport genomic materials to the nucleus. As an emerging and important nanocarrier platform, virus-like particles offer the great advantages of morphological uniformity, biocompatibility, and easy functionalization.

Immunoconjugates consist of three separate components: a monoclonal antibody that binds to a cancer cell antigen with high specificity, an effector molecule that has a high capacity to kill the cancer cell (drug), and a linker that will ensure the effector does not separate from the antibody during transit and will reliably release the effector to the cancer cell or tumour stroma [144]. The idea behind this technology is to target potent drugs to the specific site by using the specificity of monoclonal antibodies thus avoiding non-targeted organs toxicity [145]. These immunoconjugates can be used across a wide spectrum of diseases by selecting the appropriate molecular domains [146].

I. 5. Conclusion

The sustained release drug delivery systems should be at a desired, predictable and reproducible rate. The ideal drug delivery system should be inert, biocompatible, mechanically strong and comfortable for the patient.

Several drug delivery systems were presented in this chapter and efficacy of drugs were generated based on composition/physical state, mechanism, and route of administration of a drug delivery system. A bibliographic review of the state of the art in drug delivery systems was also presented in order to give the technical basis for the rest of the discussion in the other chapters.

In this PhD work, we are interested in the elaboration of two different drug delivery systems through supercritical impregnation process. Polymeric supports were used for the elaboration of ocular medical devices applied to cataract surgery and mesoporous silica was used as support for the elaboration of dosage forms for oral administration of poorly water-soluble drugs. Thereafter, the impregnation processes for the formulation of both

systems as well as the characterization and the parameters influencing impregnation will be detailed in the chapter II. The impregnation results of both systems will be presented and discussed in the chapter III and IV respectively.

References

[1] D. Golan, A. Tashjian, E. Armstrong, J. Galanter, A. Armstrong, R. Arnaout, and H. Rose, *Principles of pharmacology: the pathophysiological basis of drug therapy*, Lippincott. 2008.

[2] G. Vilar, J. Tulla-Puche, and F. Albericio, "Polymers and drug delivery systems," *Curr. Drug Deliv.*, vol. 9, no. 4, pp. 367–94, 2012.

[3] A. Hillery, A. LLoyd, and J. Swarbrick, *Drug delivery and targeting for pharmacists and pharmaceutical scientists*, Taylor & F. 2001.

[4] E. J. Wood, "Aspirin: the remarkable story of a wonder drug. Dairmuid Jeffreys, Bloomsbury, London, 2005, 335 pp., ISBN 0-7475-7083-3 and 1-5823-4600-3 (in U.S.A.), $15.92," *Biochem. Mol. Biol. Educ.*, vol. 34, no. 6, pp. 459–460, 2006.

[5] P. Magalhães, A. Lopes, P. Mazzola, C. Rangel-Yagui, T. Penna, and A. Pessoa, "Methods of endotoxin removal from biological preparations: A review," *J. Pharm. Pharm. Sci.*, vol. 10, no. 3, pp. 388–404, 2007.

[6] K. Jain, "Drug Delivery Systems – An Overview," *Drug Deliv. Syst.*, vol. 437, pp. 1–50, 2008.

[7] R. Mahato and A. Narang, *Pharmaceutical Dosage Forms and Drug Delivery*, CRC Press . 2010.

[8] K. Park, "Controlled drug delivery systems: Past forward and future back.," *J. Control. Release*, vol. 190, pp. 3–8, 2014.

[9] S. Kankane, S. Bhanu, a. K. Bajpai, and S. K. Shukla, "Responsive polymers in controlled drug delivery," *Prog. Polym. Sci.*, vol. 33, no. 11, pp. 1088–1118, Nov. 2008.

[10] S. J. Buwalda, K. W. M. Boere, P. J. Dijkstra, J. Feijen, T. Vermonden, and W. E. Hennink, "Hydrogels in a historical perspective: From simple networks to smart materials.," *J. Control. Release*, vol. 190, pp. 254–273, 2014.

[11] V. Ranade, "Drug Delivery Systems in Drug Delivery," pp. 871–889, 1990.

[12] R. Nair, K. S. A. Kumar, K. V. Priya, and M. Sevukarajan, "Recent Advances in Solid Lipid Nanoparticle Based Drug Delivery Systems," vol. 3, no. 2, pp. 368–384, 2011.

[13] M. Cagdas, A. Sezer, and S. Bucak, *Nanotechnology and Nanomaterials: Application of nanotechnology in drug delivery*. 2014.

[14] W. H. De Jong and P. J. a Borm, "Drug delivery and nanoparticles:applications and hazards.," *Int. J. Nanomedicine*, vol. 3, no. 2, pp. 133–149, 2008.

[15] J. Safari and Z. Zarnegar, "Advanced drug delivery systems: Nanotechnology of health design A review," *J. Saudi Chem. Soc.*, vol. 18, no. 2, pp. 85–99, Apr. 2014.

[16] T. Allen and P. Cullis, "Drug delivery systems: entering the mainstream," *Science (80-.).*, vol. 303, no. 5665, pp. 1818–1822, 2004.

[17] Y. Zhang, H. F. Chan, and K. W. Leong, "Advanced materials and processing for drug delivery: The past and the future," *Adv. Drug Deliv. Rev.*, vol. 65, no. 1, pp.

104–120, 2013.

[18] Y. Zhang, H. F. Chan, and K. W. Leong, "Advanced materials and processing for drug delivery: The past and the future," *Adv. Drug Deliv. Rev.*, vol. 65, no. 1, pp. 104–120, 2013.

[19] Y. Pierre and T. Rades, *FASTtrack: Pharmaceutics - Drug Delivery and Targeting*, Pharma. P. 2009.

[20] T. Kenakin, *A pharmacology Primer: theory, applications, and methods*, Academic P. 2009.

[21] J. F. Coelho, P. C. Ferreira, P. Alves, R. Cordeiro, A. C. Fonseca, J. R. Góis, and M. H. Gil, "Drug delivery systems: Advanced technologies potentially applicable in personalized treatments," *EPMA J.*, pp. 1–46, 2010.

[22] H. Bhattacharjee and L. Thoma, "Parenteral drug administration: routes of administration and devices," no. Im.

[23] C. J. Mbah, P. F. Uzor, and E. O. Omeje, "Perspectives on transdermal drug delivery," *J. Chem. Pharm. Res.*, vol. 3, no. 3, pp. 680–700, 2011.

[24] V. Yadav, S. A. B. M, Y. Mamatha, and V. V Prasanth, "TRANSDERMAL DRUG DELIVERY : A TECHNICAL WRITEUP," vol. 1, no. 1, pp. 5–12, 2012.

[25] J. Patil and S. Sarasija, "Pulmonary drug delivery strategies: A concise, systematic review," *Lung India*, vol. 29, no. 1, 2012.

[26] D. A. Groneberg, C. Witt, U. Wagner, K. F. Chung, and A. Fischer, "Fundamentals of pulmonary drug delivery," *Respir. Med.*, vol. 97, no. 4, pp. 382–387, Apr. 2003.

[27] T. Gessler, M. Beck-Broichsitter, T. Schmehl, and W. Seeger, "Evaluating the controlled release properties of inhaled nanoparticles using isolated, perfused, and ventilated lung models," *J. Nanomater.*, vol. 2011, 2011.

[28] A. Pires, A. Fortuna, G. Alves, and A. Falcão, "Intranasal drug delivery: How, why and what for?," *Journal of Pharmacy and Pharmaceutical Sciences*, vol. 12, no. 3. pp. 288–311, 2009.

[29] S. Turker, E. Onur, and Y. Ozer, "Nasal route and drug delivery systems," *Int. joutnal cliical Pharm.*, vol. 38, no. 2, pp. 35–37, 2004.

[30] L. Illum, "Nasal drug delivery: new developments and strategies," *Drug Discov. Today*, vol. 7, no. 23, pp. 1184–1189, Dec. 2002.

[31] H. R. Costantino, L. Illum, G. Brandt, P. H. Johnson, and S. C. Quay, "Intranasal delivery: physicochemical and therapeutic aspects.," *Int. J. Pharm.*, vol. 337, no. 1–2, pp. 1–24, Jun. 2007.

[32] H. Vincent, J. Robinson, and L. Robinson, "Topical ocular drug delivery: recent developments and future challenge," *J. Ocul. Pharmacol. Ther.*, vol. 2, no. 1, pp. 67–108, 1986.

[33] J. C. Lang, "Ocular drug delivery conventional ocular formulations," *Adv. Drug Deliv. Rev.*, vol. 16, no. 1, pp. 39–43, Aug. 1995.

[34] I. Ahmed and T. F. Patron, "Importance of the Noncorneol Absorption Route in Topicol Ophthalmic Drug Delivery," *Invest. Ophthalmol. Vis. Sci.*, vol. 26, no. April,

pp. 584–587, 1985.

[35] P. M. Hughes, O. Olejnik, J.-E. Chang-Lin, and C. G. Wilson, "Topical and systemic drug delivery to the posterior segments.," *Adv. Drug Deliv. Rev.*, vol. 57, no. 14, pp. 2010–32, Dec. 2005.

[36] A. Nakhlband and J. Barar, "Impacts of nanomedicines in ocular pharmacotherapy," *BioImpacts*, vol. 1, no. 1, pp. 7–22, 2011.

[37] A. Westfall, A. Osborn, D. Kuhl, M. Benz, and W. Mieler, "Acute endophthalmitis incidence: intravitreal triamcinolone," *Arch Opkthalmol*, vol. 123, no. 8, pp. 1075–1077, 2005.

[38] D. M. Moshfeghi, P. K. Kaiser, I. U. Scott, J. E. Sears, M. Benz, J. P. Sinesterra, R. S. Kaiser, S. J. Bakri, R. K. Maturi, J. Belmont, P. M. Beer, T. G. Murray, H. Quiroz-Mercado, and W. F. Mieler, "Acute endophthalmitis following intravitreal triamcinolone acetonide injection," *Am. J. Ophthalmol.*, vol. 136, no. 5, pp. 791–796, 2003.

[39] S. K. Akula, P. E. Ma, G. a Peyman, M. H. Rahimy, N. E. Hyslop, a Janney, and P. Ashton, "Treatment of cytomegalovirus retinitis with intravitreal injection of liposome encapsulated ganciclovir in a patient with AIDS.," *Br. J. Ophthalmol.*, vol. 78, no. 9, pp. 677–680, 1994.

[40] A. Castellarin and D. J. Pieramici, "Anterior segment complications following periocular and intraocular injections," *Ophthalmol. Clin.*, vol. 17, no. 4, pp. 583–590, Aug. 2015.

[41] V. G. Rathod, V. Kadam, S. B. Jadhav, and V. B. Bharkad, "IMMEDIATE RELEASE DRUG DELIVERY SYSTEM : A REVIEW," vol. 3, no. 6, pp. 545–558, 2014.

[42] Y. Qiu, Y. Chen, G. Zhang, L. Liu, and W. Porter, *Developing Solid Oral Dosage Forms: Pharmaceutical Theory & Practice*. 2008.

[43] FDA, "Guidance for Industry Guidance for Industry, Chemistry, Manufacturing, and Controls; In vitro Dissolution Testing and In vivo Bioequivalence Documentation. US Department of Health and Human Services, Food and Drug Administration, Center for Drug Evaluatio," *In Vitro*, no. September, 1997.

[44] S. Vermaa, RK Mishrab, B Garga, "Osmotically Controlled Oral Drug Delivery," *Drug Dev. Ind. Pharm.*, vol. 26, no. 7, 2000.

[45] B. Wagenaar and B. Müller, "Piroxicam release from spray-dried biodegradable microspheres," *Biomaterials*, vol. 15, no. 1, 1994.

[46] J. M. Schierholz, H. Steinhauser, A. F. E. Rump, R. Berkels, and G. Pulverer, "Controlled release of antibiotics from biomedical polyurethanes: morphological and structural features," *Biomaterials*, vol. 18, no. 12, pp. 839–844, Jan. 1997.

[47] K. Walter, R. Tamargo, A. Olivi, P. Burger, and H. Brem, "Intratumoral chemotherapy.," *Neurosurgery*, vol. 37, no. 6, pp. 1128–45, 1995.

[48] N. Katayama, R. Tanaka, Y. Ohno, C. Ueda, T. Houjou, and K. Takada, "Implantable slow release cyclosporin A (CYA) delivery system to thoracic lymph duct," *Int. J. Pharm*, vol. 115, pp. 87–93, 1995.

[49] C. F. Weiniger, L. Golovanevski, a. J. Domb, and D. Ickowicz, "Extended release formulations for local anaesthetic agents," *Anaesthesia*, vol. 67, no. 8, pp. 906–916, 2012.

[50] D. O'Hagan, H. Jeffery, M. Roberts, J. McGee, and S. Davis, "Controlled release microparticles for vaccine development," *Vaccine*, vol. 9, no. 10, pp. 768–71, 1991.

[51] T. M. Fahmy, P. M. Fong, A. Goyal, and W. M. Saltzman, "Targeted for drug delivery," *Mater. Today*, vol. 8, no. 8, pp. 18–26, Aug. 2005.

[52] J. Ravi Kumar Reddy, M. Veera Jyothsna, T. S. Mohamed Saleem, and C. Madhu Sudhana Chetty, "Review on: Pulsatile drug delivery systems," *J. Pharm. Sci. Res.*, vol. 1, no. 4, pp. 109–115, 2009.

[53] N. G. R. Rao, P. Soumya, K. Revathi, and B. S. Nayak, "International research journal of pharmacy," vol. 4, no. 3, pp. 31–44, 2013.

[54] R. Article, M. Rangasamy, and K. G. Parthiban, "Recent advances in novel drug delivery systems," vol. 1, no. 2, pp. 316–326, 2010.

[55] W. Geldenhuysa, T. Mbimbaa, T. Buia, K. Harrisona, and V. Sutariya, "Brain-Targeted Delivery of Paclitaxel Using Glutathione-Coated Nanoparticles for Brain Cancers," *J. Drug Target.*, vol. 19, no. 9, 2011.

[56] O. Taratula, O. B. Garbuzenko, P. Kirkpatrick, I. Pandya, R. Savla, V. P. Pozharov, H. He, and T. Minko, "Surface-engineered targeted PPI dendrimer for efficient intracellular and intratumoral siRNA delivery.," *J. Control. Release*, vol. 140, no. 3, pp. 284–93, Dec. 2009.

[57] V. Mody, R. Siwale, A. Singh, and H. Mody, "Introduction to Metallic Nanoparticles," *J Pharm Bioallied Sci*, vol. 2, no. 4, pp. 282–9, 2010.

[58] D. Brambilla, B. Le Droumaguet, J. Nicolas, S. H. Hashemi, L.-P. Wu, S. M. Moghimi, P. Couvreur, and K. Andrieux, "Nanotechnologies for Alzheimer's disease: diagnosis, therapy, and safety issues.," *Nanomedicine*, vol. 7, no. 5, pp. 521–40, Oct. 2011.

[59] A. Z. Wilczewska, K. Niemirowicz, K. H. Markiewicz, and H. Car, "Nanoparticles as drug delivery systems," *Pharmacol. Reports*, vol. 64, no. 5, pp. 1020–1037, 2012.

[60] K. S. Soppimath, T. M. Aminabhavi, A. R. Kulkarni, and W. E. Rudzinski, "Biodegradable polymeric nanoparticles as drug delivery devices," *J. Control. Release*, vol. 70, no. 1–2, pp. 1–20, 2001.

[61] W. R. Gombotz and D. K. Pettit, "Biodegradable Polymers for Protein and Peptide Drug Delivery," *Bioconjug. Chem.*, vol. 6, no. 4, pp. 332–351, Jul. 1995.

[62] R. Langer, "New methods of drug delivery," *Sci.* , vol. 249 , no. 4976 , pp. 1527–1533, Sep. 1990.

[63] a Patidar and D. S. Thakur, "Dendrimers : Potential Carriers for Drug Delivery," pp. 1383–1389, 2011.

[64] M. J. Taylor, S. Tanna, and T. Sahota, "In vivo study of a polymeric glucose-sensitive insulin delivery system using a rat model.," *J. Pharm. Sci.*, vol. 99, no. 10, pp. 4215–4227, 2010.

[65] P. Kesharwani, K. Jain, and N. K. Jain, "Dendrimer as nanocarrier for drug delivery," *Prog. Polym. Sci.*, vol. 39, no. 2, pp. 268–307, Feb. 2014.

[66] C. Sunderland, M. Steiert, J. Talmadge, A. Derfus, and S. Barry, "Targeted nanoparticles for detecting and treating Cancer," *Drug Dev. Res.*, vol. 67, pp. 70–93, 2006.

[67] R. Silva, H. Ferreira, and A. Cavaco-Paulo, "Sonoproduction of liposomes and protein particles as templates for delivery purposes," *Biomacromolecules*, vol. 12, no. 10, pp. 3353–3368, 2011.

[68] T. M. Allen and P. R. Cullis, "Liposomal drug delivery systems: from concept to clinical applications.," *Adv. Drug Deliv. Rev.*, vol. 65, no. 1, pp. 36–48, Jan. 2013.

[69] A. J. Almeida and E. Souto, "Solid lipid nanoparticles as a drug delivery system for peptides and proteins.," *Adv. Drug Deliv. Rev.*, vol. 59, no. 6, pp. 478–90, Jul. 2007.

[70] J. Pardeike, A. Hommoss, and R. H. Müller, "Lipid nanoparticles (SLN, NLC) in cosmetic and pharmaceutical dermal products," *Int. J. Pharm.*, vol. 366, no. 1–2, pp. 170–184, 2009.

[71] a S. Waghmare, N. D. Grampurohit, M. V Gadhave, D. D. Gaikwad, and S. L. Jadhav, "Issn 2230 – 8407 Solid Lipid Nanoparticles : a Promising Drug Delivery System," vol. 3, no. 4, pp. 100–107, 2012.

[72] R. RAZDAN and P. V. DEVARAJAN, "Microemulsions: A review," *Indian drugs*, vol. 40, no. 3, pp. 139–146.

[73] R. Prakash U and P. Thiagarajan, "Nanoemulsions for drug delivery through different routes," *Res. Biotechnol.*, vol. 2, no. 3, pp. 1–13, 2011.

[74] S. Kotta, A. W. Khan, K. Pramod, S. H. Ansari, R. K. Sharma, and J. Ali, "Exploring oral nanoemulsions for bioavailability enhancement of poorly water-soluble drugs," *Expert Opin. Drug Deliv.*, vol. 9, no. 5, pp. 585–598, Mar. 2012.

[75] J. Sarciaux, "Using microemulsion formulations for oral drug delivery of therapeutic peptides," *Int. J. Pharm.*, vol. 120, no. 2, pp. 127–136, Jun. 1995.

[76] S. R. Hwang, S.-J. Lim, J.-S. Park, and C.-K. Kim, "Phospholipid-based microemulsion formulation of all-trans-retinoic acid for parenteral administration.," *Int. J. Pharm.*, vol. 276, no. 1–2, pp. 175–83, May 2004.

[77] L. Li, I. Nandi, and K. H. Kim, "Development of an ethyl laurate-based microemulsion for rapid-onset intranasal delivery of diazepam," *Int. J. Pharm.*, vol. 237, no. 1–2, pp. 77–85, Apr. 2002.

[78] X. Zhao, J. P. Liu, X. Zhang, and Y. Li, "Enhancement of transdermal delivery of theophylline using microemulsion vehicle.," *Int. J. Pharm.*, vol. 327, no. 1–2, pp. 58–64, Dec. 2006.

[79] Y. Kapoor and A. Chauhan, "Ophthalmic delivery of Cyclosporine A from Brij-97 microemulsion and surfactant-laden p-HEMA hydrogels.," *Int. J. Pharm.*, vol. 361, no. 1–2, pp. 222–9, Sep. 2008.

[80] M. Guldi and N. Martin, *Carbon Nanotubes and Related Structures: Synthesis, Characterization*. 2010.

[81] K. Ajima, M. Yudasaka, T. Murakami, A. Maigné, K. Shiba, and S. Iijima, "Carbon nanohorns as anticancer drug carriers," *Mol. Pharm.*, vol. 2, no. 6, pp. 475–480, 2005.

[82] L. Brannon-Peppas, "Recent advances on the use of biodegradable microparticles and nanoparticles in controlled drug delivery," *Int. J. Pharm.*, vol. 116, no. 1, pp. 1–9, Mar. 1995.

[83] A. Kumar, H. Mansour, A. Friedman, and E. Blough, *Nanomedicine and drug delivery*. 2013.

[84] S. Kwon, R. K. Singh, R. a Perez, E. a Abou Neel, H.-W. Kim, and W. Chrzanowski, "Silica-based mesoporous nanoparticles for controlled drug delivery.," *J. Tissue Eng.*, vol. 4, no. 0, p. 2041731413503357, 2013.

[85] M. Liong, J. Lu, M. Kovochich, T. Xia, S. G. Ruehm, A. E. Nel, F. Tamanoi, and J. I. Zink, "Multifunctional inorganic nanoparticles for imaging, targeting, and drug delivery," *ACS Nano*, vol. 2, no. 5, pp. 889–896, 2008.

[86] R. Gordon, D. Losic, M. A. Tiffany, S. S. Nagy, and F. A. S. Sterrenburg, "The Glass Menagerie: diatoms for novel applications in nanotechnology.," *Trends Biotechnol.*, vol. 27, no. 2, pp. 116–27, Feb. 2009.

[87] R. Changa, M. Leonziob, M. Hussainb, and M. Hussainc, "Effect of colloidal silicon dioxide on flowing and tableting properties of an experimental crosslinked polyalkylammonium polymer," *Pharm. Dev. Technol.*, vol. 4, no. 2, pp. 285–289, 1999.

[88] S. B. Nicoll, S. Radin, E. M. Santos, R. S. Tuan, and P. Ducheyne, "In vitro release kinetics of biologically active transforming growth factor-β1 from a novel porous glass carrier," *Biomaterials*, vol. 18, no. 12, pp. 853–859, Jan. 1997.

[89] Y. Jiang, Z. Wu, L. You, and H. Xiang, "Bis(trimethoxysilylpropyl)amine and tetraethoxysilane derived gels as effective controlled release carriers for water-soluble drugs of small molecules.," *Colloids Surf. B. Biointerfaces*, vol. 49, no. 1, pp. 55–9, Apr. 2006.

[90] M. Vallet-Regí, F. Balas, M. Colilla, and M. Manzano, "Bone-regenerative bioceramic implants with drug and protein controlled delivery capability," *Prog. Solid State Chem.*, vol. 36, no. 3, pp. 163–191, Aug. 2008.

[91] W. Zeng, X.-F. Qian, J. Yin, and Z.-K. Zhu, "The drug delivery system of MCM-41 materials via co-condensation synthesis," *Mater. Chem. Phys.*, vol. 97, no. 2–3, pp. 437–441, Jun. 2006.

[92] C. T. Kresge, M. E. Leonowicz, W. J. Roth, J. C. Vartuli, and J. S. Beck, "Ordered mesoporous molecular sieves synthesized by a liquid-crystal template mechanism," *Nature*, vol. 359, no. 6397. pp. 710–712, 1992.

[93] G. Amato, "Silica-encapsulated efficient and stable Si quantum dots with high biocompatibility," *Nanoscale Res. Lett.*, vol. 5, no. 7, pp. 1156–1160, 2010.

[94] I. I. Slowing, B. G. Trewyn, S. Giri, and V. S. Y. Lin, "Mesoporous Silica Nanoparticles for Drug Delivery and Biosensing Applications," *Adv. Funct. Mater.*, vol. 17, no. 8, pp. 1225–1236, 2007.

[95] R. Gordon, D. Losic, M. A. Tiffany, S. S. Nagy, and F. a S. Sterrenburg, "The Glass Menagerie: diatoms for novel applications in nanotechnology," *Trends Biotechnol.*, vol. 27, no. 2, pp. 116–127, 2009.

[96] M. Bariana, M. S. Aw, and D. Losic, "Tailoring morphological and interfacial properties of diatom silica microparticles for drug delivery applications," *Adv. Powder Technol.*, vol. 24, no. 4, pp. 757–763, Jul. 2013.

[97] J. C. Echeverría, J. Estella, V. Barbería, J. Musgo, and J. J. Garrido, "Synthesis and characterization of ultramicroporous silica xerogels," *J. Non. Cryst. Solids*, vol. 356, no. 6–8, pp. 378–382, Mar. 2010.

[98] I. Smirnova, "Synthesis of silica aerogels and their application as a drug delivery system," 2002.

[99] A. Taguchi and F. Schüth, "Ordered mesoporous materials in catalysis," *Microporous Mesoporous Mater.*, vol. 77, no. 1, pp. 1–45, Jan. 2005.

[100] Z.-Z. Li, L.-X. Wen, L. Shao, and J.-F. Chen, "Fabrication of porous hollow silica nanoparticles and their applications in drug release control.," *J. Control. Release*, vol. 98, no. 2, pp. 245–54, Aug. 2004.

[101] M. Vallet-Regí, "Ceramics for medical applications," *J. Chem. Soc. Dalt. Trans.*, no. 2, pp. 97–108, 2001.

[102] S. Wang, "Ordered mesoporous materials for drug delivery," *Microporous Mesoporous Mater.*, vol. 117, no. 1–2, pp. 1–9, 2009.

[103] M. Manzano and M. Vallet-Regí, "New developments in ordered mesoporous materials for drug delivery," *J. Mater. Chem.*, vol. 20, no. 27, p. 5593, 2010.

[104] R. Gaudana, J. Jwala, S. H. S. Boddu, and A. K. Mitra, "Recent perspectives in ocular drug delivery," *Pharm. Res.*, vol. 26, no. 5, pp. 1197–1216, 2009.

[105] A. Patel, K. Cholkar, V. Agrahari, and A. Mitra, "Ocular drug delivery systems: An overview," *World J. Pharmacol.*, vol. 2, no. 2, p. 47, 2013.

[106] J. Jiang, J. S. Moore, H. F. Edelhauser, and M. R. Prausnitz, "Intrascleral Drug Delivery to the Eye Using Hollow Microneedles," *Pharm. Res.*, vol. 26, no. 2, pp. 395–403, Feb. 2009.

[107] N. Jiang, "OCULAR DRUG DELIVERY USING MICRONEEDLES," 2006.

[108] G. Rajoria and A. Gupta, "In-Situ Gelling System : A Novel Approach for Ocular Drug Delivery," *Cornea*, vol. 2, no. May, 2012.

[109] D. Kumar, N. Jain, N. Gulati, and U. Nagaich, "Nanoparticles laden in situ gelling system for ocular drug targeting," *J. Adv. Pharm. Technol. Res.*, vol. 4, no. 1, pp. 9–17, 2013.

[110] R. Kesarwani, S. Harikumar, A. Rana, C. Kashyap, K. Amanpreet, and N. Steh, "A novel Approach to ocular drug delivery review," *J. drug Formul. Res. Ocul. Implant.*, vol. 2, no. 5, 2011.

[111] B. G. Short, "Safety evaluation of ocular drug delivery formulations: techniques and practical considerations.," *Toxicol. Pathol.*, vol. 36, no. 1, pp. 49–62, 2008.

[112] J. L. Bourges, C. Bloquel, A. Thomas, F. Froussart, A. Bochot, F. Azan, R. Gurny,

D. BenEzra, and F. Behar-Cohen, “Intraocular implants for extended drug delivery: therapeutic applications.,” *Adv. Drug Deliv. Rev.*, vol. 58, no. 11, pp. 1182–202, Nov. 2006.

[113] V. P. Costa, M. E. M. Braga, J. P. Guerra, A. R. C. Duarte, C. M. M. Duarte, E. O. B. Leite, M. H. Gil, and H. C. de Sousa, “Development of therapeutic contact lenses using a supercritical solvent impregnation method,” *J. Supercrit. Fluids*, vol. 52, no. 3, pp. 306–316, Apr. 2010.

[114] S. Eperon, M. Rodriguez-Aller, K. Balaskas, R. Gurny, and Y. Guex-Crosier, “A new drug delivery system inhibits uveitis in an animal model after cataract surgery,” *Int. J. Pharm.*, vol. 443, no. 1–2, pp. 254–261, 2013.

[115] S. Eperon, L. Bossy-Nobs, I. K. Petropoulos, R. Gurny, and Y. Guex-Crosier, “A biodegradable drug delivery system for the treatment of postoperative inflammation,” *Int. J. Pharm.*, vol. 352, no. 1–2, pp. 240–247, 2008.

[116] C. Parsons, D. S. Jones, and S. P. Gorman, “The intraocular lens : challenges in the prevention and therapy of infectious endophthalmitis and posterior capsular opacification,” pp. 161–173, 2005.

[117] P. Barry, D. V Seal, G. Gettinby, F. Lees, M. Peterson, and C. W. Revie, “ESCRS study of prophylaxis of postoperative endophthalmitis after cataract surgery: Preliminary report of principal results from a European multicenter study.,” *J. Cataract Refract. Surg.*, vol. 32, no. 3, pp. 407–10, Mar. 2006.

[118] P. . Wright, C. . Wilkinson, H. . Balyeat, J. Popham, and M. Reinke, “Angiographic cystoid macular edema after posterior chamber lens implantation,” *Arch. Ophtalmol*, no. 106, pp. 740–744, 1988.

[119] K. Miyake, K. Masuda, S. Shirato, T. Oshika, K. Eguchi, H. Hoshi, Y. Majima, W. Kimura, and F. Hayashi, “Comparison of diclofenac and fluorometholone in preventing cystoid macular edema after small incision cataract surgery: A multicentered prospective trial,” *Jpn. J. Ophthalmol.*, vol. 44, no. 1, pp. 58–67, 2000.

[120] J. Simone and M. Whitacre, “Effects of anti-inflammatory drugs following cataract extraction,” *Curr Opin Ophthalmol*, vol. 1, no. 12, pp. 63–67, 2001.

[121] T. Yorio, A. F. Clark, and M. . Wax, *Ocular Therapeutics, Eye on new discoveries*. 2008.

[122] C. N. J. McGhee, S. Dean, and H. Danesh-Meyer, “Locally administered ocular corticosteroids: benefits and risks.,” *Drug Saf.*, vol. 25, no. 1, pp. 33–55, 2002.

[123] G. D. Novack, “Ophthalmic drug delivery: development and regulatory considerations.,” *Clin. Pharmacol. Ther.*, vol. 85, no. 5, pp. 539–543, 2009.

[124] H. Ridley, “Intra-ocular acrylic lenses* 10 Years’ development,” *Brit. J. Ophthal*, vol. 44, pp. 705–712, 1960.

[125] “Evolution of Cataract Surgery and Intraocular Lenses (IOLs),” *Surv. Ophthalmol.*, vol. 45, pp. S53–S69, Nov. 2000.

[126] R. Bellucci, “An Introduction to Intraocular Lenses : Material , Optics , Haptics , Design and Aberration,” vol. 3, pp. 38–43, 2013.

[127] T. Kohnen, “the variety of foldable intraocular lens materials,” *J. Cataract Refract*,

vol. 22, no. S2, pp. 1255–1258, 1996.

[128] A. Bettencourt and A. J. Almeida, "Poly(methyl methacrylate) particulate carriers in drug delivery," *J. Microencapsul.*, vol. 29, no. 4, pp. 353–367, 2012.

[129] A. W. Lloyd, R. G. A. Faragher, and S. P. Denyer, "Ocular biomaterials and implants," *Biomaterials*, vol. 22, no. 8, pp. 769–785, Apr. 2001.

[130] J. Ram, N. Gupta, J. S. Sukhija, M. Chaudhary, N. Verma, S. Kumar, and S. Severia, "Outcome of cataract surgery with primary intraocular lens implantation in children.," *Br. J. Ophthalmol.*, vol. 95, no. 8, pp. 1086–1090, 2011.

[131] C. M. Cunanan, M. Ghazizadeh, S. Y. Buchen, and P. M. Knight, "Contact-angle analysis of intraocular lenses," *J. Cataract Refract. Surg.*, vol. 24, no. 3, pp. 341–351, Sep. 2015.

[132] T. Oshika and Y. Shiokawa, "Effect of folding on the optical quality of soft acrylic intraocular lenses," *J Cataract Refract Surg*, vol. 22, no. 2, 1996.

[133] D. M. Colvard, "Achieving Excellence in Cataract Surgery A Step-by-Step Approach."

[134] M. Chehade and M. J. Elder, "Intraocular lens materials and styles: a review.," *Aust. N. Z. J. Ophthalmol.*, vol. 25, no. 4, pp. 255–263, 1997.

[135] D. C. Brown and S. L. Ziémba, "Collamer intraocular lens: clinical results from the U.S. FDA core study," *J. Cataract Refract. Surg.*, vol. 27, no. 6, pp. 833–840, Jun. 2001.

[136] P. Fernandes, J. M. González-Méijome, D. Madrid-Costa, T. Ferrer-Blasco, J. Jorge, and R. Montés-Micó, "Implantable Collamer Posterior Chamber Intraocular Lenses: A Review of Potential Complications," *J. Refract. Surg.*, vol. 27, no. 10, pp. 765–776, 2011.

[137] B. N. Parikh, G. D. Gothi, T. D. Patel, H. V. Chavda, and C. N. Patel, "Microsponge as novel topical drug delivery system," *J. Glob. Pharma Technol.*, vol. 2, no. 1, pp. 17–29, 2010.

[138] R. A. M. Osmani, N. H. Aloorkar, D. J. Ingale, P. K. Kulkarni, U. Hani, R. R. Bhosale, and D. Jayachandra Dev, "Microsponges based novel drug delivery system for augmented arthritis therapy," *Saudi Pharm. J.*, Mar. 2015.

[139] N. Jadhav, V. Patel, S. Mungekar, G. Bhamare, and M. Karpe, "Microsponge Delivery System : An updated review , current status and future prospects," vol. 2, no. 6, pp. 1097–1110, 2013.

[140] M. S. Charde, P. B. Ghanawat, A. S. Welankiwar, J. Kumar, and R. D. Chakole, "Microsponge A Novel New Drug Delivery System : A Review * Correspondence Info : Keywords :," vol. 2, no. 6, 2013.

[141] N. H. Aloorkar, a S. Kulkarni, D. J. Ingale, and R. a Patil, "Microsponges as Innovative Drug Delivery Systems," vol. 5, no. 1, pp. 1597–1606, 2012.

[142] R. Challa, A. Ahuja, J. Ali, and R. K. Khar, "Cyclodextrins in drug delivery: an updated review.," *AAPS PharmSciTech*, vol. 6, no. 2, pp. E329–E357, 2005.

[143] T. Loftsson and D. Duchêne, "Cyclodextrins and their pharmaceutical applications.,"

Int. J. Pharm., vol. 329, no. 1–2, pp. 1–11, Feb. 2007.

[144] P. Trail, "Antibody Drug Conjugates as Cancer Therapeutics," *Antibodies*, vol. 2, pp. 113–129, 2013.

[145] A. M. Wu and P. D. Senter, "Arming antibodies: prospects and challenges for immunoconjugates," *Nat Biotech*, vol. 23, no. 9, pp. 1137–1146, Sep. 2005.

[146] A. L. Nelson, "Antibody fragments: Hope and hype," *MAbs*, vol. 2, no. 1, pp. 77–83, Nov. 2010.

CHAPTER **II**

Supercritical impregnation

Table of contents

II. 1. Introduction ... 57
II. 2. Supercritical impregnation ... 59
II. 2. 1. What is a supercritical fluid? ... 59
II. 2. 2. Impregnation processes ... 60
II. 3. Polymeric drug delivery systems ... 63
II. 3. 1. Characterization of the system polymer-drug-CO_2 ... 66
II. 3. 1. 1. Polymer-$scCO_2$ ... 67
II. 3. 1. 2. Drug-$scCO_2$ ... 70
II. 3. 1. 3. Polymer-drug ... 71
II. 3. 2. Bibliographic review ... 72
II. 4. Ordered mesoporous silica for drug delivery systems ... 80
II. 5. Conclusion ... 87
References ... 89

II. 1. Introduction

Advanced drug delivery systems present indubitable benefits for drug administration. Drug delivery systems are designed to release the active ingredients in a controlled manner, optimizing thus their bioavailability and decreasing potential side effects, as well as to target a specific site in the body. For most applications, in order to achieve an effective therapy, the drug should be dispersed in a matrix at a molecular level. One route to elaborate such systems is impregnation which can be conducted in liquid or in supercritical media.

Impregnation by soaking into liquid consists in putting in contact over a given duration a solution containing the solute to be impregnated, with an impregnation support. Referring to the literature, two types of impregnation supports were used in most cases for the elaboration of drug delivery systems: organic compounds such as polymers or inorganic compounds such as mesoporous silica. Different solutes are used in literature according to the relative application such us active ingredients for pharmaceutics and cosmetics, dyes for textile, fungicides for wood industry, aroma and food coloring for food industry, *etc.*

The standard way for such preparations involves the following steps:

- Dissolution of the solute to be impregnated in an appropriate solvent;
- Partition of the solute between the solvent-rich phase and the impregnation support,
- Elimination of the solvent.

This relatively simple method is only adequate for drugs that possess affinity with the impregnation support and that, consequently, can be up-taken and retained within. In addition to the match of the chemical groups of the drug and the impregnation support, several other factors (*e.g.*, drug concentration in the impregnation medium, impregnation duration, pH of the solution, temperature, *etc.*) are involved in the determination of the drug loading yield.

Residual solvents in pharmaceuticals are defined as volatile organic chemicals (VOC). Since they can be toxic, all residual solvents should be removed to the highest possible extent possible to meet product specifications, good manufacturing practices, or other quality-based requirements. Solvents are classified by the European Medicines Agency as [1], [2]:

- Class I: solvents to be avoided (known human carcinogens, strongly suspected human carcinogens and environmental hazard),
- Class II: solvents to be limited (non-genotoxic animal carcinogens or possible causative agents of other irreversible toxicity such as neurotoxicity or teratogenicity),
- Class III: solvents with low toxic potential (solvents with low toxic potential to man;

no health-based exposure limit is needed).

Despite the step of removing solvent on conventional impregnation, the impregnated support is not totally free of solvent and traces may induce a certain toxicity of the drug formulation. The presence of significant amounts of residual organic solvents into matrices impregnated in liquid media remains one of the main drawbacks of the soaking into liquid method.
Alternatively, a solute may be loaded into a support using supercritical fluid impregnation. This technique has successfully proved its applicability to the preparation of drug delivery systems. The interest of supercritical impregnation relies mainly on the opportunity to utilize the specific supercritical fluid properties (high density, low viscosity, diffusivity higher than the ones of liquids, low interfacial tension, *etc.*). Thanks to those properties, the solute to be impregnated may be easily and rapidly transferred inside the solid support of impregnation. Moreover, if carbon dioxide is used, the process of impregnation can be performed at rather moderate temperatures in comparison with soaking into liquid method. Furthermore, CO_2 is released spontaneously from the final product upon depressurization at the end of the process, reducing thus the number of unitary operations often used in conventional processes for products purification. Lastly, it may be then possible to improve efficiency of drug loading and release compared to those achievable by conventional preparation technique, while using a more environment friendly technology.

In this PhD study, we are interested in the elaboration of two different forms of sustained released drug delivery systems through supercritical impregnation of pharmaceutical active ingredients in two types of supports, polymeric intraocular lenses used in cataract surgery for the elaboration of ocular medical devices and mesoporous silica for the elaboration of suitable dosage forms for oral administration of poorly water soluble drugs.
In this chapter, generalities about supercritical fluids and their properties are first presented. Then, supercritical impregnation process principle and modes are presented. A bibliographic review of the state of the art of supercritical impregnation of polymers focusing on ocular lenses as well as of mesoporous silica are then detailed in two separate subsections. Characterizations of each system, involved mechanisms and parameters influencing supercritical impregnation are presented.

II. 2. Supercritical impregnation

II. 2. 1. What is a supercritical fluid?

Supercritical fluids (SCFs) have received a great interest within the research community over the last decades because of their unique properties which are midway between those of liquids and gases. A supercritical fluid is defined as a substance for which both pressure and temperature are above the critical values (Figure II. 1). Above this critical point, a single phase is present with unique properties such as liquid-like density, gas-like viscosity, low interfacial tension and higher diffusivity than liquids. As an example, Table II. 1 gives the physico-chemical properties of carbon dioxide, the most used fluid for supercritical applications. In particular, carbon dioxide (CO_2) has many properties that make it an attractive solvent, including not flammable and not toxic, and environmentally benign nature when compared to organic solvents. CO_2 present mild critical conditions especially in term of temperature (P_c = 7.38 MPa and T_c = 304.06 K).

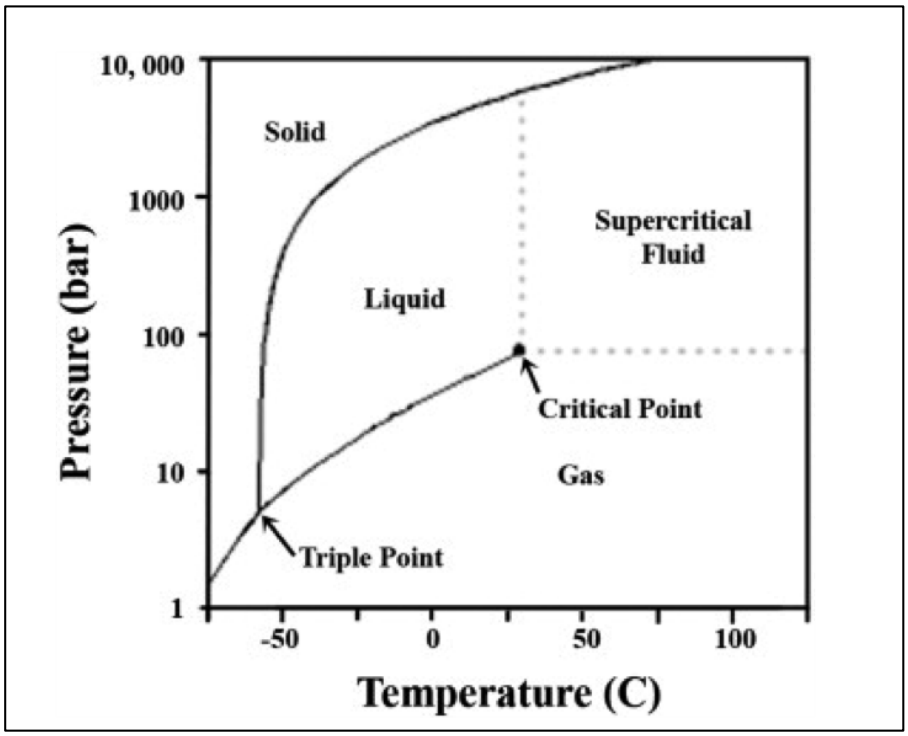

Figure II. 1 Schematic P-T phase diagram of Carbon dioxide [3].

CO_2 has been proposed as a “green” alternative to traditional liquid organic solvent because it is neither regulated as a VOC nor restricted in food or pharmaceutical applications [4], exhibiting tunable solvent power in most applications. The main interest of supercritical fluids is related to their adjustable properties, that can be changed easily by monitoring pressure and

temperature within the supercritical region [5]. The experimental conditions can be therefore adjusted according to the targeted specifications.

Table II. 1 Physico-chemical properties of carbon dioxide.

Temperature K	Pressure MPa	Fluid nature	Density [6] $kg.m^{-3}$	Diffusivity [7] $m^2.s^{-1}$	Viscosity [8] Pa.s
313	0.1	Gas	1.7	5.1×10^{-6}	1.6×10^{-5}
313	10	Supercritical fluid	631.7	1.4×10^{-8}	4.8×10^{-5}
300	50	Liquid	1028.9	$8.7\ 10^{-9}$	1.33×10^{-4}

SCFs are involved in numerous industrial processes and have potentially wide fields of applications. Current applications include extraction and fractionation, cleaning of electronic and optical devices, chemical reaction (such as: polymerization and oxidation), waste treatment and recycling, soil remediation, aerogels elaboration, crystallization and particle generation, nanomaterials preparation, coating and impregnation.

II. 2. 2. Impregnation processes

SCF technology is an attractive alternative for the formulation of pharmaceuticals systems. Supercritical fluids are the first choice vectors because they possess a rather good solvent power and their specific properties as detailed above, allow the diffusion of the supercritical fluid phase deeply into the impregnation solid support.

Supercritical processes enable to obtain a more homogeneous impregnated matrix with shorter processing duration compared to conventional soaking into liquid technologies. When the impregnation is performed with $scCO_2$ and without the addition of a co-solvent, the impregnated support is then totally free of traces of residual solvent.

In general, the principle of supercritical impregnation consists in solubilizing the solute of interest in the supercritical phase which carries it within the impregnation support through diffusion phenomena. During the contact duration, the solute molecules are partitioned between the fluid phase and the impregnation support. At the end of the process, during the depressurization step CO_2 is released and the solute is entrapped within the impregnation support.

The supercritical impregnation process can be carried out either in a batch or in a semi-continuous mode; using one or two autoclaves. In the latter case, a first high pressure cell, called extractor or saturator, generally equipped with a stirring system is used to solubilize the compound of interest in the supercritical phase. The impregnating support is placed in a second high pressure cell, called impregnation cell. When operating in a dynamic mode (semi-continuous process), a continuous flow of the supercritical fluid sweeps across the extractor and the cell of impregnation for a given time (Figure II. 2).

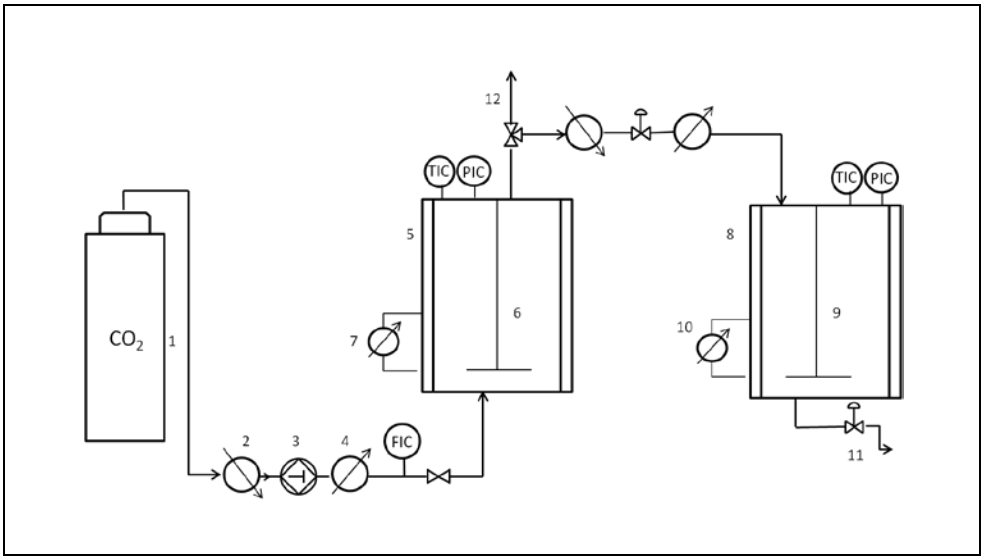

Figure II. 2 Supercritical impregnation set-up using two autoclaves: (1) CO_2 cylinder, (2) Cooling bath, (3) High pressure liquid pump, (4) Heating bath, (5) Saturator cell, (6) and (9) Agitators, (7) and (10) Thermostat baths, (8) impregnation cell, (11) and (12) Depressurization valves.

In a batch mode, a process based on a single high pressure cell is generally used (Figure II. 3). In that case, the solute and the impregnation support are initially placed together in the autoclave. The high pressure cell is heated to reach the desired temperature and the fluid is introduced into the cell until the working condition of pressure is reached. The system is then left for a given time corresponding to the fixed impregnation duration.

Once the impregnation phase is finished, The system is then depressurized at a depressurization rate which must be controlled to avoid an eventual desorption of the impregnated solute [9].

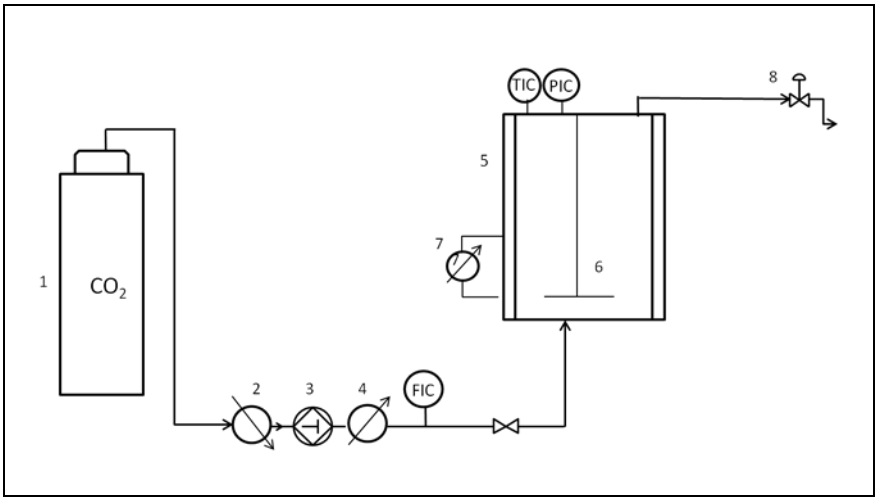

Figure II. 3 Supercritical impregnation set-up using one autoclave: (1) CO_2 cylinder, (2) Cooling bath, (3) High pressure liquid pump, (4) Heating bath, (5) High pressure cell, (6) Agitator, (7) Thermostat bath, (8) Depressurization valve.

When impregnation is carried out using a co-solvent, a supplementary washing step is performed to avoid the condensation (or precipitation) of the co-solvent in the autoclave during depressurization. This step consists in washing the high pressure cell with pure flow rate of CO_2 or with an inert gas, so as to remove the co-solvent while avoiding extracting the impregnated solute.

The performance of the impregnation process depends on the solubility of the solute of interest in the fluid phase but also on its 'affinity' with the impregnation matrix. The balance between these two phenomena can be characterized through the partition coefficient *K*, which corresponds to the ratio of the equilibrium concentrations of solute in the impregnation matrix ($C_{\text{solute-support}}$) to that in the $scCO_2$ phase ($C_{\text{solute-CO2}}$).

$$K = \frac{C_{solute-support}}{C_{solute-CO_2}} \qquad Eq.1$$

To apply successfully the supercritical impregnation, the drug to be impregnated should be soluble in the fluid phase and the partition coefficient of the drug should be favorable enough towards the impregnation support to enable sufficient impregnation amounts.

Several applications of supercritical impregnation have been reported in literature during the last twenty years. Objectives may be different from one application to another. The target can be to elaborate sustained release systems, like in this work, but it also can be to protect a

support or change some properties of a matrix (like for example dying). Different works are reported in literature describing the impregnation of biocides into wood and wood composites [10], the polymer composite preparation by monomer impregnation in polymer followed by *in-situ* polymerization [11], carbon-carbon or ceramic precursors for improving the oxidation resistance of carbon [12], paper impregnation for a deacidification and reinforcement process for damaged books [13], and the impregnation for drug delivery [14]. Another process for online impregnation after extraction, especially attractive for natural products, processing as one sole operation leads directly to the usable product [15].

In this work we are interested in the preparation of sustained release drug delivery systems, since they can provide lower and sustained dosages through a drug release in the affected site by diffusion or surface erosion, increasing thus its therapeutic effect and improving the patient compliance. Those systems have also proven to be more effective and safe compared to conventional immediate release dosage (Chapter I). Different carriers can be used for the elaboration of drug delivery systems and the impregnation phenomena are dependent on the considered system. As previously mentioned, this study focuses on the elaboration of sustained release delivery systems through supercritical impregnation of different APIs in two different impregnation supports: polymeric supports used as ocular medical devices and mesoporous support used as excipient for the elaboration oral dosage form.

Supercritical impregnation mechanisms are different according to the studied support. Indeed, unlike in silica, dissolution of supercritical CO_2 within polymers (CO_2 absorption) occurs during the impregnation process, resulting in polymers swelling and plasticization.

For this purpose, the characterization of each impregnation system (based on polymeric support and mesoporous silica) and the corresponding involved mechanisms and parameters influencing impregnation are presented in two different subsections.

II. 3. Polymeric drug delivery systems

Polymers used for controlled drug release are often called therapeutic polymers. However, these systems do not have specific therapeutic activity and are considered as excipients in pharmaceutical formulations. Polymers occupy an outstanding position due to the versatility of the synthesis routes, their possible biocompability (and sometimes biodegradability) and the possibility of tuning their features and performances to fulfill the needs of every particular application. Controlled drug delivery occurs when a polymer, whether natural or synthetic, is

judiciously combined with a drug or other active agents in such a way that the active ingredient is released from the material in a predesigned manner. Moreover, polymers can finely regulate the site and the rate at which the drug is released from the formulation, improve drug solubility, contribute to the stability in the physiological environment, mask the unpleasant taste of a drug and help the drug to overcome the cellular barriers.

Several chemical natures of polymers have been tested as potential drug delivery systems, including: Poly (2-hydroxy ethyl methacrylate), Poly (2-hydroxy methyl methacrylate), Poly (N-vinyl pyrrolidone), Poly (methyl methacrylate), Poly (vinyl alcohol), Poly (acrylic acid), Polyacrylamide, Poly (ethylene-co-vinyl acetate), Poly (ethylene glycol) and Poly (methacrylic acid). However, in recent years, additional polymers designed primarily for medical applications have entered the area of controlled release. Many of these materials are designed to degrade within the body, few of them among these include: Polylactides (PLA), Polyglycolides (PGA), Poly (lactide-co-glycolides) (PLGA), Polyanhydrides, Polyorthoesters.

An extensive part of this work focuses on the impregnation of two kinds of polymeric intraocular lenses (PMMA and P-HEMA) used for cataract surgery (Chapter I, section I. 4. 3). The development of drug incorporated in IOLs allows the combination of the cataract surgery and postoperative treatment in a single procedure [16]. It can provide a prolonged intraocular release of anti-inflammatory and antibiotic agents after surgery leading to improved efficacy, reduced toxicity, and better patient compliance [17].

The classical solvent method (soaking into liquid) used initially and widely for the impregnation of contact lenses [18]–[22], consists in dispersing the drug in a polymer matrix. First, the drug is dissolved in an organic solvent and the polymer is put in contact with the solvent containing the drug, then the drug can diffuse inside the polymer. Diffusion phenomena can be enhanced if the polymeric network is swollen in the presence of the considered impregnation solvent. At the end of impregnation, the organic solvent is removed.

The same method was used for the impregnation of IOLs with ophthalmic drug. Heyrrman et *al.* in 1989 [23] have studied *in-vitro* and *in-vivo* uptake and release of Chloramphenicol, Dexamethasone, Epinephrine, Pilocarpine, and bovine serum albumin by P-HEMA IOLs with that of the intact crystalline lens of humans and rabbits. Experiments shows that the P-HEMA absorbs drugs in a similar manner than the natural crystalline eyes. The authors conclude that the IOLs studied cannot behave as significant reserves of drugs in the eye.

The study of Chapman et *al.* [24] have completed the previous study (Hyerman *et al.*) on drug

interactions with P-HEMA IOLs, considering other polymers (PMMA, Acrysof, and two types of silicone lenses) and other drug (Gentamicin). The impregnated amounts obtained were low (few ng/mg lens) and the P-HEMA lenses presents the higher uptake and release compared to the others lenses. Despite the greater uptake and release of P-HEMA IOLs, the maximum drug uptake would only provide one-tenth of the greatest aqueous humor concentration that occurs after topical drug administration. This researchers concludes that the IOL can not provide sufficient quantities of drugs in the eye.

El Meski *et al.* [25] proposed a method for incorporating a drug solution (water/ethanol at 57 w/w % of ethanol saturated in drug) in a polymer involving a drying step at the end of impregnation to evacuate the solvent vehicle. Aiache *et al.* [26] have completed the research of El Meski *et al* and they have patented a method for impregnation by soaking into liquid of IOLs from different natures (PMMA, P-HEMA and Silicone) with different drugs (Diclofenac, Indomethacine and Dexamethasone). The impregnation was performed on commercialized IOLs and in blanks shaped discs or pallets of polymers (which will be cut and machined in the shape of IOLs at the end of impregnation) in drug solution (water/ethanol at 57 w/w % of ethanol saturated in drug). Impregnations were followed by a drying step at the end of process in order to evacuate the solvent mixtures. The inventors have demonstrated that if drugs are sufficiently soluble in a solvent to diffuse into the polymer, impregnation was significant (*e.g,*. can reach 333 µg/ml in the release solution for the impregnation of P-HEMA with Diclofenac).

The inventors have implanted impregnated IOLs (PMMA and P-HEMA) in the anterior chamber of the one eye of rabbits. Samples of aqueous humor and plasma were taken at random intervals and analyzed by high-performance liquid chromatography. Clinical examination showed that the inflammatory reactions had disappeared by the tenth day from implantation. It can therefore be concluded that the clinical results are satisfactory and that this impregnated IOLs emphasizes the benefit of localizing the distribution of drug to the immediate vicinity of the action sites, in order to limit the doses of drug delivered into the eye and to avoid the drug having any unwanted action in other parts of the body.

One of the main drawbacks of this classical impregnation technique is the drying step. Actually, it is practically impossible to remove completely the solvent and the residual solvent may induce a certain toxicity effect for patients. Several other manufacturing processes have been developed to produce drug delivery based on contact lenses such as molecular

imprinting [27], [28], miscellaneous [29], ion ligands binding [30], [31] or particular-laden contact lenses [32], [33]. Nevertheless, these conventional techniques have some disadvantages such as: high processing temperatures that can deteriorate thermosensitive active pharmaceutical ingredients, or the use of organic solvents that must be removed through numerous purification steps to meet EMA's requirements [34].

To overcome the above-mentioned limitations, the supercritical impregnation process has been proved to be an alternative green process for pharmaceuticals [35]. The activity of the drug molecules is preserved notably because supercritical carbon dioxide ($scCO_2$) processing can be operated at moderate temperatures [36].

The preparation of controlled polymeric drug delivery products with supercritical impregnation for ophthalmic application has received attention in the last years. The use of supercritical fluids especially supercritical carbon dioxide ($scCO_2$) can take advantage of their high diffusivity in polymers, in combination with solubility and plasticizing action. Consequently, compressed CO_2 can be used as a vector to carry the drug into biocompatible polymers.

II. 3. 1. Characterization of the system polymer-drug-CO_2

The supercritical CO_2 impregnation process involves three components: CO_2 as an impregnation vector, the API as a product to be impregnated and the polymer matrix as an impregnation support. Different interactions are involved in $scCO_2$ impregnation process as presented in Figure II. 4.

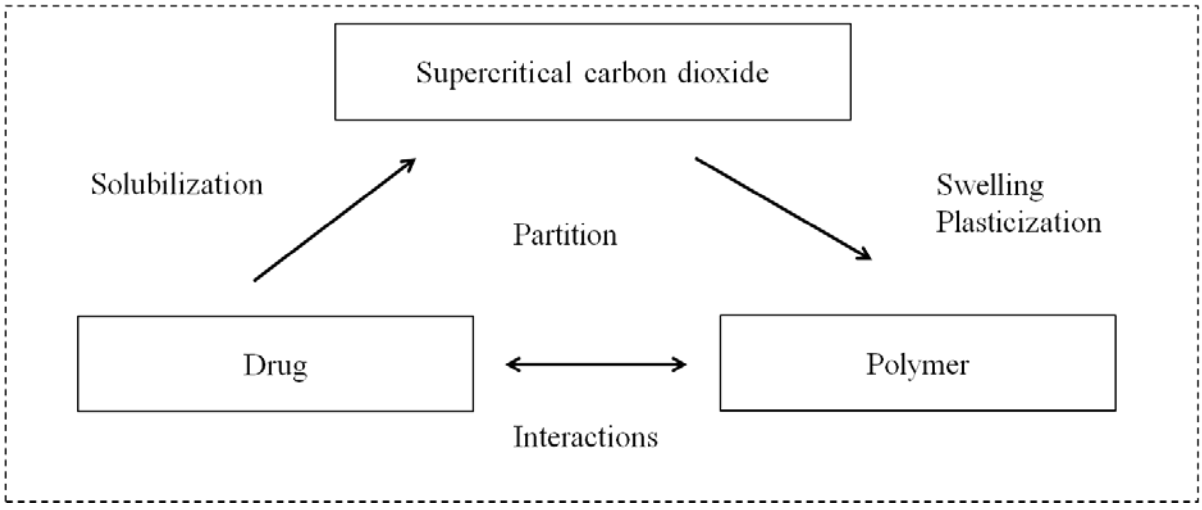

Figure II. 4 Interactions governing supercritical impregnation.

II. 3. 1. 1. Polymer-scCO$_2$

The supercritical impregnation can take advantage from the absorption of scCO$_2$ in polymers leading to their swelling and plasticization [37]. It is possible to tune the degree of polymer swelling by modifying the sorption degree while varying scCO$_2$ density. The process of diffusion of the drug within CO$_2$-swollen polymer can therefore be controlled to obtain desired amount of drug into the polymer support [38].

The absorption of scCO$_2$ into polymers results in their swelling and changes the mechanical and physical properties of the polymers. The most important effect is the reduction of the glass transition temperature (Tg) of glassy polymer subjected to scCO$_2$, often simply called plasticization.

The plasticization of polymer results from the ability of CO$_2$ to interact with the basic sites in polymer molecules [39]. As for example, we can cite the interaction between CO$_2$ and the carbonyl group in PMMA, which has been suggested to be of the Lewis acid-base type [40]. Such interactions result in enhanced segmental and chain mobility and an increase in interchain distances [41]. Thus, increased mobility of the ester groups in PMMA was observed at 313 K when a PMMA film was subjected to scCO$_2$ at a pressure of 10 MPa. In the absence of CO$_2$, mobility of the ester group is only observed when the PMMA is heated above its glass transition temperature (378 K). This example demonstrates how the effect of scCO$_2$ mimics the effect of heating the polymer [42].

One well-known effect of CO$_2$ is then to reduce the Tg for many glassy polymers (from 5 to 28 K/MPa) according to the considered system [43]. When the interactions between scCO$_2$ and polymer are stronger, the Tg reduction is more important (such as in the case of PMMA, Figure II. 5). Handa *et al.* [44] have demonstrated that the Tg decrease of PMMA (12 K/MPa) was higher than that of PS (9 K/MPa) in the same conditions. An explanation could be that in the case of PMMA, the presence of oxygen atoms promotes the interactions with scCO$_2$.

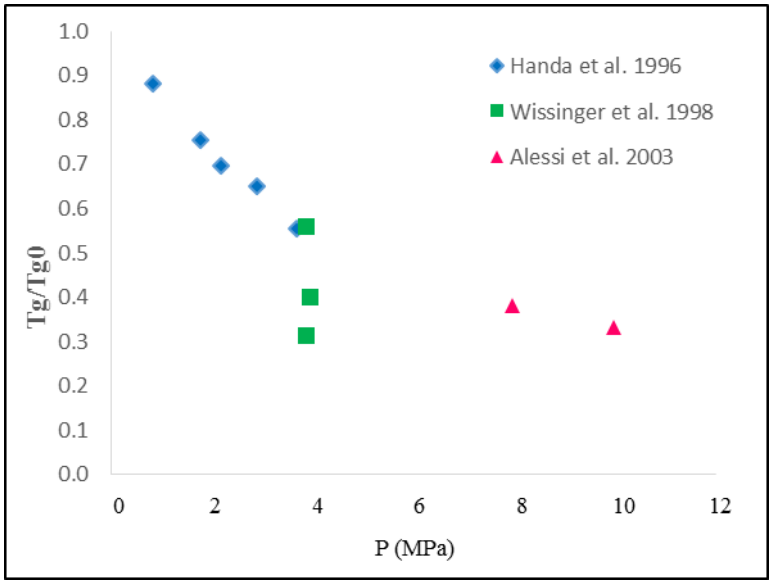

Figure II. 5 PMMA Tg depression as a function of pressure [45].

Guo *et al* have studied [46] the glass transition temperature (T_g) of PMMA-CO_2 as a function of equilibrium mass percentage of absorbed CO_2 in the polymer. As shown in the Figure II. 6, T_g reduces from 376 to 260.5 K when 39.3 % CO_2 is absorbed into PMMA.

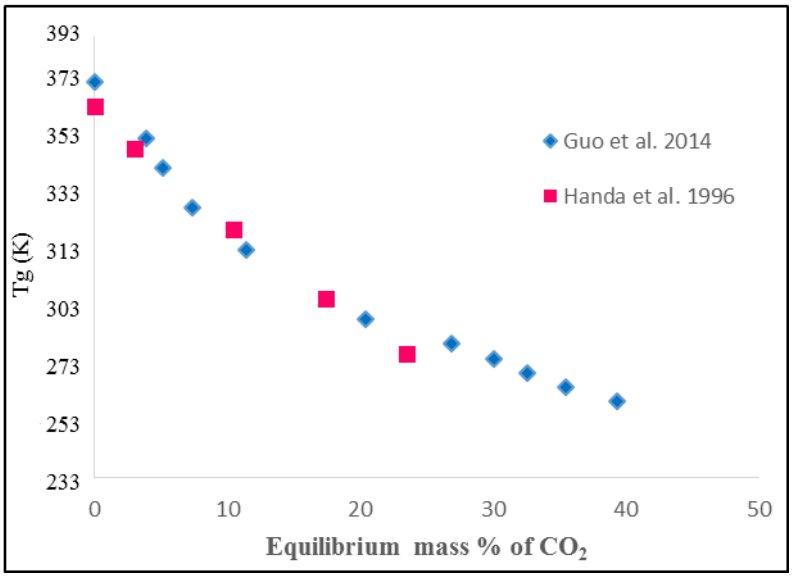

Figure II. 6 T_g of PMMA–CO_2 mixture as a function of equilibrium mass percentage of CO_2 [46].

The swelling of PMMA in CO_2 has been widely investigated with different methods of measurement [47]–[57]. While polymers with low polarity are CO_2-phylic, PMMA is CO_2-philic because of the carbonyl oxygen. Üzer *et al* [52] have demonstrated that the volume

expansions of swollen PMMA were between 9 and 25 %. Volume increases with pressure (Figure II. 7) but decreases as temperature increases (Figure II. 8). Thus, there is a linear correlation of volume increase with density; higher densities causing higher volume expansions.

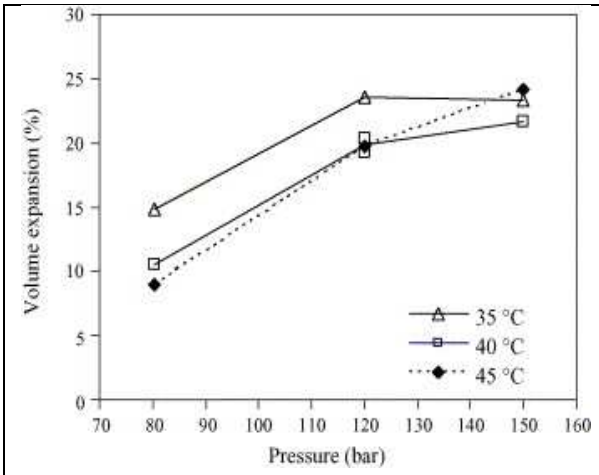

Figure II. 7 Pressure dependence of volume expansions of PMMA rods [52].

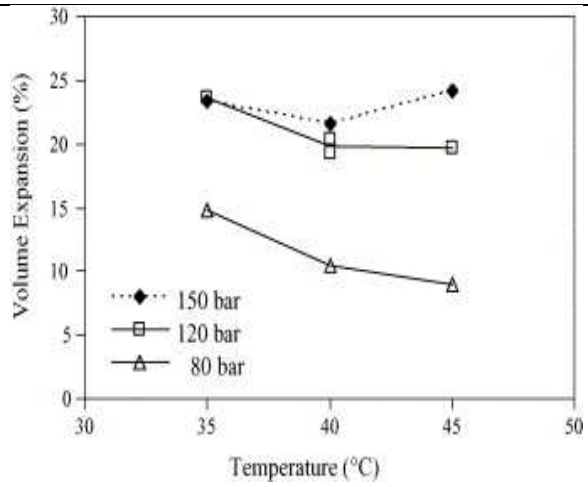

Figure II. 8 Temperature dependence of volume expansions of PMMA rods [52].

These same workers have observed the appearance of a diffusion front propagating inside the PMMA rods with dimensions of 3.5 mm × 3.5 mm × 20 mm. At 12 MPa and 318 K, this diffusion front became apparent after the first few minutes and propagated slowly in all directions. The diffusion front is visible from the first, second to the third hour of contact with $scCO_2$, then disappears in the fourth hour (Figure II. 9).

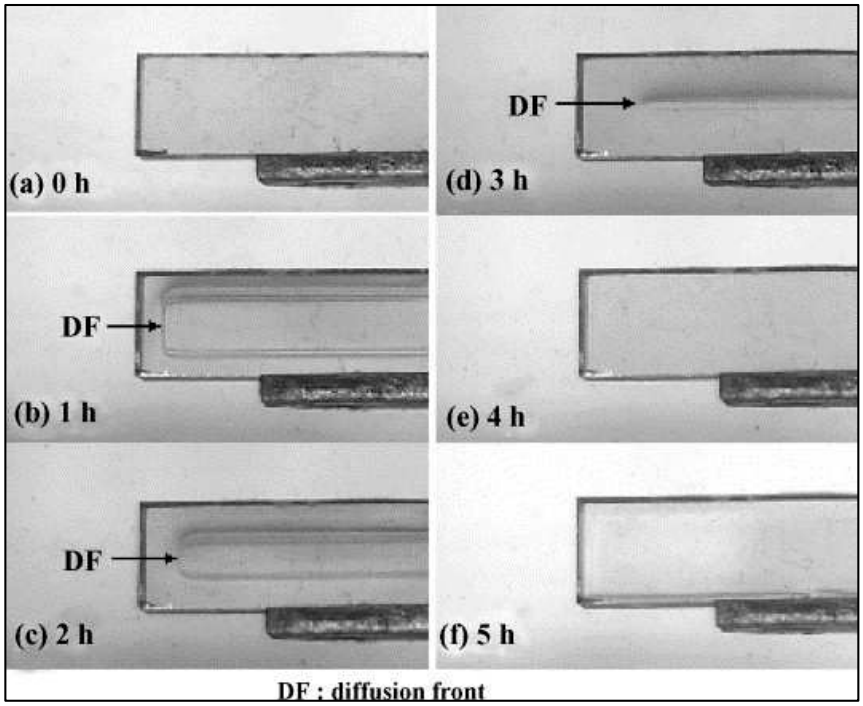

Figure II. 9 Photos of a swollen PMMA sample and diffusion front at 1 hour intervals at 12 MPa and 318 K [52].

Nikitin *et al.* [47] detected also the same boundary and stated that the diffusion front was an interface between glassy and plasticized regions of the polymer. This interface moved to the center until it reached the interface propagating from the opposite side.

Kazarian and workers [42] [58] showed that the CO_2 acts as a kind of 'molecular lubricant', making it easier for polymeric chains to slip over one another, thus accelerating the solute diffusion.

II. 3. 1. 2. Drug-scCO_2

The solubility controls the amount of drug component that can be carried by the fluid phase within the polymeric matrix. Solutes with high solubility in scCO_2 can be easily delivered to the impregnation support. Meanwhile, studies show that the impregnation of low CO_2-philic API could also be achieved if it has a strong affinity for the polymer leading to favorable partitioning toward the polymer matrix [59]. Furthermore, higher drug inclusion can be achieved by the addition of small quantities of polar co-solvent to the scCO_2 phase to increase the solubility of solid compound in media.

The solubility of different components in scCO_2 has been widely reviewed in the literature. Chim *et al* [60] have measured the solubility of Dexamethasone in scCO_2 using a static

method at 308.2, 318.2, and 328.2 K in the pressure range of 15.1 to 35.7 MPa. The solubility in $scCO_2$ was found to be of 1.25 10^{-6} at 308.2 K and 15.1 MPa and of 2.81 10^{-6} at 328.2 K and 34.8 MPa in terms of mole fraction. The obtained results describe the temperature dependence and the solubility increase for higher pressure.

II. 3. 1. 3. Polymer-drug

A strong affinity between the polymer and the drug favors the impregnation and the molecular dispersion of the drug into the polymeric matrix [61]. The high partition coefficients are based on the strong affinity of API molecules for the polymer matrix.

Kazarian *et al.* [61], [62] and Kikic *et al.* [63] propose two main mechanisms of drug impregnation into polymers in supercritical media.

The mechanism based upon the partition coefficient of the solute between the fluid phase and the polymer relies on the affinity of the solute toward the polymer due to specific interactions (*e.g.* van der Waals interactions). This approach can explain the impregnation of compounds with low solubility in $scCO_2$ [59]. In this mechanism, the solute is believed to be molecularly dispersed within the polymer and the process is expected to be complete when an equilibrium concentration is achieved in the matrix [62]. This mechanism is usually named impregnation with molecular dispersion.

The second mechanism involves deposition of a solute into the polymeric matrix when the CO_2 leaves the swollen polymer during depressurization. This deposition approach was initially introduced by Berens *et al.* [64]. During the impregnation process, the $scCO_2$ solubilizes the drug and swells the polymer; the fluid phase containing the drug is allowed to diffuse inside the matrix for a predetermined period followed by the depressurization step. When the high-pressure vessel is depressurized, the solubility of the solute in $scCO_2$ suddenly decreases and simultaneous CO_2 expulsion from the polymer results in the solute entrapment inside the matrix. This approach is especially effective for solutes which are highly soluble in $scCO_2$ [62], [63].

One of the major advantages of supercritical impregnation is the possibility of adjusting the impregnation efficacy by ‘tuning’ the properties of $scCO_2$. Different operating parameters of the process can be varied such as the pressure, temperature, impregnation duration, the process mode (batch or semi-continuous), CO_2 flow rate in a semi-continuous mode, solute concentration in the supercritical phase, the use/ratio and nature of a co-solvent as well as the depressurization rate. Thus, several parameters are available to modulate the impregnation

amount whereas with the traditional processes of impregnation in liquid solutions, only the concentration of the solute, the nature of the solvent phase and the temperature have a significant effect.

The effect of the variation of the operating pressure is a bit more complex since different mechanisms involved in the impregnation process can be influenced and the effect of pressure on impregnation differs from one study to another [65], [66].

Opposite effects of temperature on drug loading were reported. The impregnation efficiency was found either to increase [66]–[70], decrease [71], [72], be constant [9], or first decrease and then increase [73] with temperature under isobaric conditions depending on the studied system.

The supercritical process mode influences impregnation performance. Compared to semi-continuous mode, batch process could lead to higher impregnation yields in shorter durations since it allows a higher contact time between polymer and the fluid phase containing the drug [74]. Drug diffusion into the polymeric matrix are therefore promoted, leading also to a more homogeneous impregnation.

.

The impregnation duration has been demonstrated to influence significantly the process efficiency; longer contact time between the supercritical fluid and polymer leads to higher impregnation yields [65], [75].

The chemical nature of the polymeric matrix and drug influence significantly the impregnation efficiency. The use of an appropriate co-solvent may favor significantly the supercritical impregnation by increasing the polarity of the fluid phase and therefore enhancing the solubility of a polar drug in this mobile phase as well as by increasing the swelling/plasticizing of the polymer.

II. 3. 2. Literature review

The supercritical impregnation for ocular applications in order to enhance drug loading and to achieve more controlled delivery has been reported in the scientific literature. Table II. 2 reviews the conditions and the results of the few publications that have investigated $scCO_2$ impregnation applied for the development of polymer-based therapeutic ophthalmic articles.

A global research project has been performed in Portugal to develop the $scCO_2$ impregnation process of contact lenses. This research led to the deposition of the patent EP 1 611877 Al1 [76] that deals with the possibility of using such a process for ophthalmic articles.

Braga *et al.* [77] studied the supercritical impregnation of chitosane derivatives (N-carboxymethyl chitosan (CMC), N-carboxybutyl chitosan (CBC and N-succinyl (SCC)) with Flurbiprofen (an anti-inflammatory drug) and Timolol maleate (an anti-glaucoma drug) in the presence of co-solvent (ethanol) in order to develop hydrogel type ophthalmic drug delivery systems. The impregnations were performed at pressures from 9 to 14 MPa and at temperatures ranging from 303 to 323 K. The CMC impregnation rates showed that the predominant effect in the impregnation process was the solubility of drug in CO_2 and CO_2 + EtOH as well as the swelling and plasticizing effect of CO_2 and ethanol on the polymer. Finally, the supercritical impregnation was shown to be more efficient and tunable than the conventional method.

Duarte *et al.* [74] have proposed P(MMA-EHA-EGDMA) as a promising matrix to be used for intraocular delivery of anti-inflammatory drug used in eye surgery. They studied the effect of the solubility of flurbiprofen in $scCO_2$, as well as the sorption degree of the polymeric matrix on the supercritical impregnation of P(MMA-EHA-EGDMA) with Flurbiprofen. For this purpose, different experimental conditions of pressure (10, 15 and 18 MPa), temperature (308 and 313 K), impregnation duration (3 and 5 hours) and the impregnation mode (semi-continuous or batch) were investigated. The impregnation yield of the semi continuous process for 5 hours was lower than that obtained in a batch process with a shorter impregnation period of 3 hours. Moreover, more homogeneously dispersed drug within the polymer for the batch mode was obtained. The results obtained for semi-continuous mode suggest that the best impregnation conditions are low temperature (308 K) and pressure (10 MPa), which at the same time correspond to a lower solubility of the drug in $scCO_2$ and a weaker swelling of the polymer.

Natu *et al.* [78] have performed the impregnation of Poly (ε-caprolactone) blends with timolol maleate. The effects of operational conditions; pressure (11 and 20 MPa), chemical natures and compositions of blends of Poly (3-caprolactone), as well as the nature of the co-solvents (water and ethanol in a molar ratio of 10 %mol) on the supercritical impregnation were studied. The results show that the best impregnation conditions were obtained when a co-solvent was used and when specific drug-polymer interactions occurred. Higher pressures were either a favorable factor when there is enough drug affinity for the polymers, or an unfavorable factor when weaker bending is involved. *In-vitro* drug release kinetics studies results show that a sustained drug release can be obtained by changing the operating conditions of impregnation and by modulating the compositions of blends. Moreover, the

profile of release (*in-vitro*) showed that a burst release occurs and then the drug is progressively released during one month.

The effect of operational conditions on the impregnation of several commercial soft contact lenses, Nelifecon A, Hilafilcon B, Methafilcon A and Omafilcon A, with two ophthalmic drugs, Flurbiprofen (a nonsteroidal anti-inflammatory drug (NSAID), hydrophobic) and Timolol maleate (an anti-glaucoma drug, hydrophilic), was studied by Costa *et al.* [65]. They studied the effect of operational pressure from 9 up to 16 MPa and impregnation duration from 30 up to 180 min on the impregnation at 313 K. For the employed drugs, and for all performed experiments, the amounts of released drugs were inside their corresponding therapeutic windows. The impregnated IOLs were transparent and did not contain harmful solvent residues. Supercritical impregnation shows much higher released drug amount compared to conventional soaking in concentrated physiological solutions of Flurbiprofen. Moreover, the supercritical impregnations were carried out in much shorter durations than the conventional impregnation (just for 2 hours compared to 48 hours and 1 week).

Costa *et al.* [75] have also studied the supercritical impregnation of Balaficon A contact lenses with two anti-glaucoma drugs (hydrophobic Acetazolamide (ACZ) and hydrophilic Timolol maleate,). Pressure (17 MPa) and temperature (313 K) as well as the impregnation duration (90 min) and the depressurization rate (0.06 $MPa.min^{-1}$) were kept constant while the influence of nature of co-solvents (ethanol and water) and their concentrations (5, 10 and 15 %mol) were studied. The authors demonstrated that modifying the co-solvent nature and/or its concentration leads to different impregnation yields, which could be helpful for tuning the amount of hydrophobic / hydrophilic drug loaded in the contact lenses. Additionally, the supercritical impregnation did not modify the O_2 permeability and T_g of contact lenses.

Braga *et al.* [9] have pursued the research of Costa *et al.* [65] on the preparation of therapeutic soft contact lenses (Balaficon A). The supercritical impregnation of ACZ in commercially available silicone based contact lenses (Balaficon A) was carried out in the presence of a co-solvent (5 %mol, ethanol). The influence of the variation of some experimental conditions such as the pressure (15-20 MPa), the temperature (313 and 323 K), the impregnation duration (1, 2 and 3 hours) and the depressurization rate (from 0.06 up to 0.15 $MPa.min^{-1}$) was investigated. It was shown that it is possible to control ACZ loaded amounts by changing the different operational conditions investigated, which will allow to adjust the final ACZ release levels into the desired therapeutic limit, and without modifying some of their most thermos-mechanical and optical properties.

As preliminary studies for this Ph.D. work, Masmoudi *et al.* [70] have impregnated rigid intraocular lenses (PMMA) with Cefuroxime sodium in order to obtain ophthalmic drug release systems dedicated to the prevention of postoperative complications following cataract surgery. The influence of pressure (8-20 MPa), the temperature (308 and 333 K), impregnation duration (1-5 hours), the addition of a co-solvent (5 %mol of ethanol) as well as the depressurization rate (slow and rapid) has been studied. At rapid depressurization rates (few minutes), the impregnation yields obtained varied between (0.2 and 6.3 wt%). Nevertheless, a non-desired foaming phenomenon was observed for the most favorable conditions. Foaming was avoided by carrying out slow depressurization (0.2 $MPa.min^{-1}$). However, the impregnation process was less efficient (the impregnation yields were too much low to be quantified gravimetrically).

Yañez *et al.* [79] developed a supercritical fluid assisted molecular imprinting method consisting in the application of several consecutive processing cycles of impregnation/extraction, producing a specific nano-range structural changes in contact lenses with the goal to create specific and high affinity 'cavities' for a template drug. In particularly, the authors focused on improving the Flurbiprofen load / release capacity on Halafilcon B commercial contact lenses. The impregnations were conducted at 12 MPa and 313 K, while $scCO_2$ extraction were carried out at 20 MPa and 313 K. Processing with $scCO_2$ did not change some of the critical functional properties of contact lenses such as: glass transition temperature, transmittance, oxygen permeability and contact angle. Moreover, this imprinting method offers the advantage of controlling the loaded/released amounts of drug in much shorter process duration than those using conventional aqueous-based molecular imprinting methods.

González-Chomón *et al.* [19] have carried out a complete study dedicated to the comparison between two impregnation processes: aqueous soaking and supercritical impregnation. They were interested in the impregnation of acrylic hydrogel, combining 2-hydroxyethyl methacrylate (HEMA) and 2-butoxyethyl methacrylate (BEM) at various ratios, with Norfloxacin, an antibiotic. The supercritical impregnation was carried out at pressures of 15 and 30 MPa, a temperature of 313 K, and an impregnation duration of 14 hours. The amount of loaded Norfloxacin was significantly higher through supercritical impregnation compared to that achieved by soaking in aqueous solution. The blend prepared with HEMA/BEM 20:80 vol/vol and impregnated with $scCO_2$ combines adequate mechanical properties, biocompatibility and Norfloxacin loading.

Yokozaki *et al.* [80] used $scCO_2$ for the impregnation of Hilaficon B contact lenses with Salicylic acid; inexpensive model compound compared with anti-inflammatory and ophthalmic drugs. The impregnation was conducted at pressures ranging between 9 to 15 MPa, temperatures of 303, 313 and 318 K. The loaded amount of Salicylic acid increases with the decrease in temperature and when pressure increases, which can be explained from the strong correlation between its solubility in the $scCO_2$. The lowest depressurization rate leads to the highest impregnation yields (release rates) of the Salicylic acid from contact lenses.

Table II. 2 Bibliographical conditions and results of $scCO_2$ impregnation applied for ocular applications.

Author	Polymer	API	P (MPa)	T (K)	Co-solvent	t_{imp} (hour)	Dep_{rate}* (MPa.min^{-1})	Mode**	Drug loading (wt%)
Braga 2008 [77]	Chitosane derivatives (CMC, BC and SCC)	Flurbiprofen	9-13	303, 313 and 323	5 %mol EtOH	1	0.6	B	1.7-14.7
		Timolol maleate	9-14	303, 313 and 323		1	1.2	B	8.6-85
Duarte, 2008 [74]	P(MMA-EHA-EGDMA)	Flurbiprofen	10-18	308-313	/	3-5	Slowly	S-C and B	0.18-0.82
Natu, 2008 [78]	PCL and PCL /POE and PCL/PEVA blends	Timolol maleate	11-20	313	With/without water and ethanol	2	0.5	B	0-3.3
Costa, 2010 [65]	Acrylic-based hydrogel (Nelifecon A, Hilafilcon B, Methafilcon A and Omafilcon	Timolol maleate	9-16	313	Without or with EtOH (2-5 %mol) Without or	1	0.01-0.02	B	0.3-1.3

	A)	Flurobiprofen	9-16	313	with EtOH (2-5 %mol)	1	0.01-0.02	B	1-6
Costa, 2010 [75]	Silicon based hydrogel (Balaficon A)	Timolol maleate	17	313	EtOH and water at 5; 10 and 15 %mol	1.5	0.06	B	1.04-1.81
		Acetazolamide	17	313		1.5	0.06	B	0.15
Masmoudi, 2011 [70]	PMMA	Cefuroxim sodium	8-20	308-333	Without or with EtOH (5 %mol)	2	0.2	B	0.2-6.3
Yañez, 2011 [79]	Acrylic based hydrogel P(HEMA/BEM)	Flurbiprofen	12	313	Water-swollen hydrogel	14 5	Slow	B S-C	1-55
Braga, 2011 [9]	Silicon based hydrogel (Balaficon)	Acetazolamide	15-20	313-323	EtOH 5 %mol Soft commercialized contact lens	1	0.06-0.15	B	0.52-1.97
Gnozález-Chomón, 2012 [19]	Acrylic based hydrogel P(HEMA/BEM)	Norfloxacin	15-30	313	Water-swollen gel	14	0.1	B	0.01-0.16

Yokozaki, 2015 [80]	Acrylic-based hydrogel (Hilaficon B)	Salicylic acid	9-15	303, 313 and 318	Water	2	0.006	B	29.6-54.5

*Dep $_{rate}$: depressurization rate (MPa.min^{-1}).

** B: Batch; S-C: Semi-continuous.

II. 4. Ordered mesoporous silica for drug delivery systems

Drug solubility as well as dissolution kinetics are determinant for its oral bioavailability [81]. Good bioavailability of many new compounds in drug development presents a challenge for the development of a suitable formulation for oral administration. Common solid formulation approaches to overcome these difficulties and improve dissolution rates of these drugs have been used, including decreasing crystallinity and/or increasing specific surface area by decreasing particle size, adsorption onto porous supports [82], co-precipitation with an excipient [83], [84].

It has long been established that increasing the specific surface area of a poorly water-soluble drug is one of the most efficient methods for improving drug dissolution kinetics [85]. This can be achieved by loading drugs onto a porous support. Quite recently, a silica mesoporous support has been proposed for the development of formulations for oral therapy [86] in order to improve dissolution rate and oral bioavailability of poorly water-soluble molecules [85]. Indeed, mesoporous silica has several attractive features for these formulations such as: stable uniform mesoporous structures, high specific surface areas, tunable pore sizes with narrow distributions, and well defined surface properties [87], which allow molecules access to large internal surfaces and cavities. Furthermore, the surface of silica presents free hydroxyl groups which are easily accessible for specific interactions with molecules likely to make hydrogen bonds [88]. It has been shown that both small and large molecular drugs can be entrapped within the mesopores through an impregnation process and liberated via a diffusion-controlled mechanism [87].

Several methods have been studied to load drugs into mesoporous silica such as incipient wetness method, solvent method and melt method. For the incipient wetness the host material (silica) should be placed into a concentrated solution of the drug to be adsorbed, and stirring should be applied to favor the diffusion of the drug molecules into the mesopores (Figure II. 10). The employed solvent should be removed by evaporation. Concerning the solvent method, physical mixture of drug and silica were prepared and subsequently added to the solvent under stirring. At the end of impregnation duration, the used solvent was evaporated.

According to the study of Mellaerts *et al*. [86] the incipient wetness favors the positioning of drug molecules in the micropores, while the solvent method favors their positioning on mesopore walls. For this, incipient wetness was one of the methods used in our experimental work for the preparation of silica-drug formulations.

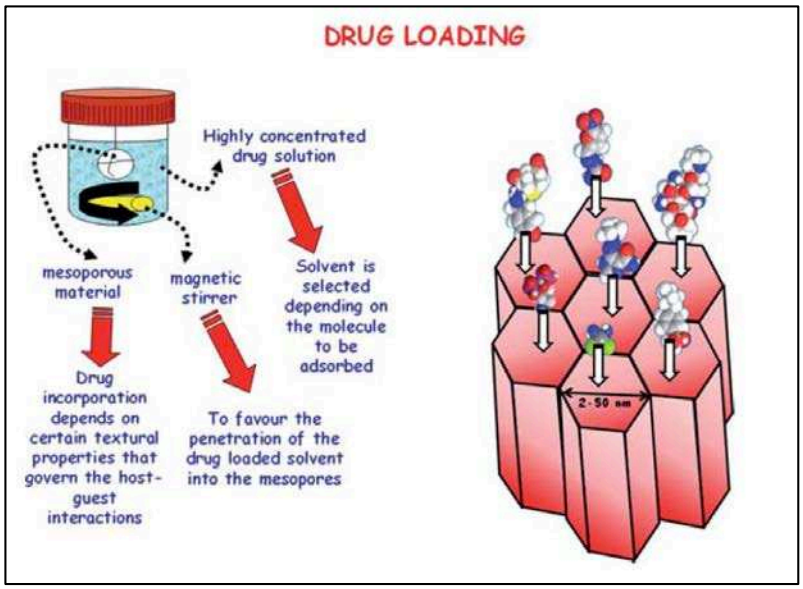

Figure II. 10 Schematic representation of the drug loading procedure by incipient wetness [89].

Silica loading can also be carried by the melt method, physical mixture of drug and silica should be prepared and heated above the drug's melting temperature for a certain duration [85], [86], [90], [91].

Table II. 3 presents some silica–drug systems reported in the literature as well as the drug loading for these systems. The impregnated systems presents different properties (Surface area and pore diameter) and are prepared with several methods. The drug loading is confirmed and quantified through different characterization techniques.

Table II. 3 Ordered mesoporous silica matrices and drugs employed as drug delivery [92].

Mesoporous solid	Surface area ($m^2.g^{-1}$)	Pore diameter (nm)	Drug	Loading (wt%)	Reference
MCM-41	1157	3.6	Ibuprofen	34	[93]
AlSi-MCM41	1124	4.3	Diflunisal	8.7	[94]
AlSi-MCM41	1124	4.3	Naproxen	7.3	[94]
AlSi-MCM41	1124	4.3	Ibuprofen	6.4	[94]
AlSi-MCM41	1124	4.3	Ibuprofen Na salt	6.9	[94]
Si-MCM41	1210	2.8	Captopril	32.5	[95]
Si-MCM41-A	1157	2.5	Ibuprofen	2.9	[96]
Si-MCM41-A	1024	3.6	Aspirin	3.88	[97]
Si-SBA-15	787	6.1	Gentamicin	20.0	[98]
Si-SBA-15	787	8.8	Erythromycin	34	[99]
Si-SBA-15-C8T	559	8.2	Erythromycin	13	[99]
Si-SBA-15-C18ACE	71	5.4	Erythromycin	15	[99]
Si-SBA-15	602	8.6	Ibuprofen	14.6	[100]
Si-SBA-15-APTMS-O	571	8.6	Ibuprofen	16.9	[100]
Si-SBA-15-APTMS-P	473	7.8	Ibuprofen	20.6	[100]
Si-SBA-15	602	8.6	Bovine serum albumin	9.9	[100]
Si-SBA-15-APTMS-O	571	8.6	Bovine serum albumin	28.5	[100]
Si-SBA-15-APTMS-P	473	7.8	Bovine serum albumin	1.1	[100]
Si-SBA-15	602	4.9	Amoxicillin	24	[101]
HMS	1152	-	Ibuprofen	35.9	[102]

MCM-41	1210	2.7	Ibuprofen	74.4	[102]
HMS	1244	2.7	Ibuprofen	96.9	[103]
HMS-N-TES	1083	2.5	Ibuprofen	76.8	[103]
HMS-NN-TES	1036	2.4	Ibuprofen	74.2	[103]
HMS-NNN-TES	990	2.5	Ibuprofen	70.9	[103]
Si-MSU	1200	4.2	Pentapeptide	-	[104]
MCM-41	1200	3.3	Ibuprofen	41	[105]
SBA-3	1000	2.6	Ibuprofen	33	[105]
SBA-1	1000	1.8	Ibuprofen	25	[105]
SBA-16	490	8.5	ZnNIA	14.3	[106]
SB-16	490	8.5	AnPCB	18.3	[106]
MCM-48	1166	3.6	Ibuprofen	28.7	[107]
LP-la3d	857	5.7	Ibuprofen	20.1	[107]
MCM-48	1166	3.6	Erythromycin	28.0	[107]
LP-la3d	857	5.7	Erythromycin	28.0	[107]
MCM-41	835	2.4	α-tocopheryl acetate	0.95	[108]
Hypersil	228	9.0	α-tocopheryl acetate	0.49	[108]
SBA-15	461	8.4	Itravonazole	0.29	[86]
SBA-15	461	8.4	Ibuprofen	0.30	[86]

Those conventional impregnation methods present limitations for drugs formulation because of the presence of residual solvent traces, often toxic, and/or the use of high temperatures. These drawbacks can be overcome through the use of supercritical fluids as impregnation vectors. The principle of supercritical impregnation was presented in the section II. 2. 2. The supercritical impregnation was also used in our experimental work for the preparation of silica-drug formulations.

The drug loading can be confirmed and quantified through different characterization techniques. Generally; the first step should be to check that the characteristics of mesostructures are maintained after the loading process. This is normally confirmed by

carrying out small angle XRD patterns before and after loading the drug. Furthermore, nitrogen adsorption analysis could be employed to compare the pore size distribution and the pore volume of the materials before and after the loading process. The specific surface area as well as the available pore volume commonly decrease after the loading process, indicating that drug molecules are partially filling the mesopores. The amount of drug confined in the pores can be quantified using different thermal techniques, such as thermogravimetry and elemental analysis or through dissolution tests.

Up until now, several bibliographical studies aimed to enhance the dissolution kinetics of several drugs by their adsorption using $scCO_2$ on silica material; such as fumed silica, silica aerogels and ordered mesoporous silica using $scCO_2$ [82], [85], [108]–[110]. The operating conditions and drug loadings obtained by the different authors are given in Table II. 4.

Smirnova *et al.* [109] studied the supercritical impregnation of six model drugs, Ketoprofen, Miconazole, Terenadine, Dithranol, Niclosamid and Griseofulvin, in different hydrophilic and hydrophobic silica aerogels. The supercritical impregnation was carried out through a batch mode, under a pressure of 18 MPa and a temperature of 313 K for contact durations varying from 24 to 72 hours. The maximum drug loading was obtained for Miconazole (600 mg/g aerogel). *In-vitro* drug release was studied for both drugs; Ketoprofen and Griseofulvin.

The supercritical impregnation of Fenofibrate in non porous fumed silica was studied by Sanganwar *et al*. [82] through a batch mode at a pressure of 17.05 MPa and a temperature of 313 or 323 K for an impregnation duration of 2.5 hours . Loadings up to 379 mg/g of drug onto silica were obtained. *in-vitro* drug release studies have shown a significant increase in drug dissolution rate (about 80 % of the drug is released in 20 minutes) compared to micronized Fenofibrate (about 20 % of the drug is released in 20 minutes), which can be attributed on the one hand to the increase in the specific surface area and on the other hand to the decrease in drug crystallinity after adsorption onto silica [82].

Belhadj-Ahmed *et al*. [108] used a dynamic process to study the supercritical impregnation of α-tocopheryl acetate (vitamine E acetate) with two kinds of silica; a commercial silica (Hypersil) and MCM-41-type mesoporous silica. The experimental domain investigated was:pressure from 8 to 15 MPa, at 313 K and carbon dioxide flow rates varying from 60 to 120 g h^{-1}. The results showed that the drug loading is more than twice as much for the MCM-

41 (1140 mg/g of adsorbent) than for a Hypersil (475 mg/g of adsorbent). Those results are not surprising since the specific surface area of the MCM-41 is significantly higher than that the Hypersil. The drug loading obtained using supercritical impregnation (for an impregnation duration of 1 hour) was similar those obtained using liquid impregnation (for an impregnation duration of 4 hour) using hexane as solvent.

Wang *et al*. [110] studied the supercritical impregnation of Ibuprofen in a MCM-41-type mesoporous silica through a batch mode, at a pressure from 20 to 30 MPa, at 313 K and with a treatment duration of 2 hours. The loading of Ibuprofen could reach 386 mg/g of silica and is higher than that obtained by the solution immersion method. The authors studied the delivery profile of Ibuprofen and found that the sustained-effect of Ibuprofen impregnated by the supercritical method was 50 % in 15 minutes and 90 % in 60 minutes. It was longer than that impregnated by the solution immersion method due to a deeper impregnation in supercritical impregnated supports.

Finally, Ahern *et al.* [85] carried out a complete study dedicated to comparing several loading processes. A drug model, Fenofibrate, was loaded into mesoporous silica SBA-15 using physical mixing, melt impregnation, solvent impregnation, sub-critical (27.58 MPa, 298 K) and supercritical impregnation (27.58 MPa, 313 K). Physical mixing produced a heterogeneous drug loading unlike any other impregnation methods used. Liquid and supercritical impregnation gave the best impregnation yield for a treatment duration of only 30 minutes: 184 mg/g silica.

Table II. 4 Example from literature of the supercritical impregnation of different model drugs in various kind of silica.

Authors	Surface area ($m^2.g^{-1}$)	Drug	Silica	Pressure/temperature	Solute or drug loading
Smirnova *et al.* [109]	587	Miconazole Ketoprofen Terenadine Dithranol Niclosamid Griseofulvin	Silica aerogels	18 MPa 313 K	600 mg/g aerogel 310 mg/g aerogel 240 mg/g aerogel 60 mg/g aerogel 40 mg/g aerogel 10mg/g aerogel
Sanganwar *et al.* [82]	200	Fenofibrate	Fumed silica	17.05 MPa 313-323 K	379 mg/g silica
Belhadj-Ahmed *et al.* [108]	835 228	α-tocopheryl acetate	-commercial silica (Hypersil) -MCM-41 mesoporous silica	8-15 MPa 313 K	1140 mg/g silica 475 mg/g silica
Wang *et al.* [110]	346-265	Ibuprofen	MCM-41 mesoporous silica	20-30 MPa 313 K	314-386 mg/g silica
Ahern *et al.* [85]	-	Fenofibrate	Silica SBA-15	27.58 MPa 313 K	184 mg/g silica

II. 5. Conclusion

Supercritical impregnation has drawn an increasing interest as a green alternative to conventional processes and has been successfully applied these last twenty years to the elaboration of drug delivery systems. In these applications, supercritical fluid, generally carbon dioxide is used as an impregnation vehicle of the drug within the matrix that can be either polymeric (biocompatible and sometimes biodegradable) or a high porosity support.

For different studied bibliographical systems, more homogeneous impregnated matrices with shorter processing duration have been obtained compared to conventional soaking into liquid technologies. This stems from the specific properties of supercritical fluids (high density, low viscosity, diffusivity higher than the ones of liquids, low interfacial tension, *etc.*). When carbon dioxide is used as supercritical fluid, the impregnation process is generally performed at moderate temperatures while limiting or avoiding the use of organic solvents. Furthermore, spontaneous separation of CO_2 from the final product upon depressurization leads to a more compact process comparing to conventional methods. Moreover, the supercritical process is inherently sterile and is therefore suitable for pharmaceutical application.

This PhD study focuses on the preparation of two different sustained release drug delivery systems forms: ocular medical devices based on polymeric support (intraocular support) used for cataract surgery and dosage forms based on mesoporous support (mesoporous silica) used for the development of suitable formulation for oral administration.

We have studied the elaboration of these two systems based either on polymeric supports or mesoporous silica using supercritical carbon dioxide impregnation. Unlike silica, physicochemical properties of polymers can be modified by the supercritical treatment. Indeed, the absorption of supercritical CO_2 in polymers results in their swelling and plasticization.

Concerning the application of supercritical impregnation on polymeric matrixes for ophthalmic delivery lenses, a few studies have been reported in the bibliography and were mostly carried out by the same research team (Portugal) in the framework of a global research project focusing on contact lenses. Different chemical natures of polymeric lenses with various classes of drugs were studied. Results were promising concerning the potential of supercritical technologies for the development of such systems and led to the deposition of a patent EP1611877Al1 [76] that deals with the possibility of using such a process for ophthalmic articles. To the best of our knowledge no therapeutic contact lenses have been yet approved or commercialized [111]. Regarding the elaboration of loaded intraocular lenses, as

far as we know, only few results are reported in literature and are only based on conventional techniques. A patent dealing with soaking into liquid process of IOLs has been deposited and recently published by Aiache *et al.* (2008). Despite the low impregnation amounts obtained, the inventors have implanted the loaded IOLs in the eye of rabbits and clinical examinations showed that the inflammatory reactions had disappeared after ten days of implantation. However, one of the limitations of this patented route is the use of organic solvents (Ethanol, Dichloromethane, *etc.*) in the loading solutions.

As far as we know, this Ph.D. work is the first study dealing with the supercritical impregnation of *polymeric commercially available intraocular lenses* with ocular drugs, which makes its originality. The objective of this work is to achieve optimized drug loading, homogeneous distribution of drugs in IOLs and a sustained drug release.

In a second part of this Ph.D. study, we are interested in loading ordered mesoporous silica with Fenofibrate (poorly water-soluble drug), to enhance its dissolution kinetics. In literature, silica supports with different properties (surface areas and pore sizes) were loaded with various classes of drugs and several impregnation methods were studied such as incipient wetness impregnation and melt method requiring the use of organic solvents, often toxic, and/or high temperatures. Supercritical impregnation for the preparation of loaded silica have been as alternative to the conventional techniques. Few studies in the literature reports the loading of drug molecules on silica material using $scCO_2$. Several drugs have been loaded on silica based supports: fumed silica, silica aerogels and ordered mesoporous silica. According to the literature, two works on the supercritical impregnation of silica supports with Fenofibrate were reported [82], [85] and one of these works [85] was published the same year than our study [112].

The impregnation results of polymeric intraocular lenses and ordered mesoporous silica for the elaboration of drug delivery systems are presented and discussed in the chapter III and IV respectively.

References

[1] European Medicines Agency, “Impurities: Guideline for residual solvents,” 2013.

[2] E. Kiran, P. Debenedetti, and C. Peters, “Supercritical fluids:Fundamentals and Applications,” NATO Scien., Series E: Applied Sciences- Vol. 366, Ed. 1994.

[3] N. Budisa and D. Schulze-makuch, “Supercritical Carbon Dioxide and Its Potential as a Life-Sustaining Solvent in a Planetary Environment,” *Life*, vol. 4, pp. 331–340, 2014.

[4] E. J. Beckman, “Supercritical and near-critical CO2 in green chemical synthesis and processing,” *J. Supercrit. Fluids*, vol. 28, no. 2–3, pp. 121–191, Mar. 2004.

[5] S. P. Nalawade, F. Picchioni, and L. P. B. M. Janssen, “Supercritical carbon dioxide as a green solvent for processing polymer melts: Processing aspects and applications,” *Prog. Polym. Sci.*, vol. 31, no. 1, pp. 19–43, 2006.

[6] “Nist Chemistry WebBook, http://webbook.nist.gov/chemistry/ (accessed Octobre 28, 2013).” .

[7] A. . Clifford and S. . Coleby, “Diffusion of a Solute in Dilute Solution in a Supercritical Fluid,” *Proc. R. Coc. Math. Phys. Eng. Sci*, vol. 433, pp. 63–79, 1991.

[8] V. Vesovic, J. . Sengers, J. T. . Watson, and J. Millat, “The transport propeties of Carbon Dioxide,” *J. Phys. Chem*, vol. 19, no. 3, 1990.

[9] M. E. M. Braga, V. P. Costa, M. J. T. Pereira, P. T. Fiadeiro, A. P. a R. Gomes, C. M. M. Duarte, and H. C. De Sousa, “Effects of operational conditions on the supercritical solvent impregnation of acetazolamide in Balafilcon A commercial contact lenses,” *Int. J. Pharm.*, vol. 420, no. 2, pp. 231–243, 2011.

[10] A. W. Kjellow and O. Henriksen, “Supercritical wood impregnation,” *J. Supercrit. Fluids*, vol. 50, no. 3, pp. 297–304, Oct. 2009.

[11] Q. Xu, Y. Chang, J. He, B. Han, and Y. Liu, “Supercritical CO2-assisted synthesis of poly(acrylic acid)/nylon6 and polystyrene/nylon6 blends,” *Polymer (Guildf).*, vol. 44, no. 18, pp. 5449–5454, Aug. 2003.

[12] P. Berneburg and V. Krukonis, “Processing of carbon/carbon composites using supercritical fluid technology,” US5035921 A, 1991.

[13] M. Perrut, E. Francais, and J. Theobald, “Procedure and equipement for processing paper documents using supercritical pressure fluid,” W09739190, 1997.

[14] P. J. Ginty, M. J. Whitaker, K. M. Shakesheff, and S. M. Howdle, “Drug delivery goes supercritical,” *Mater. Today*, vol. 8, no. 8, pp. 42–48, Aug. 2005.

[15] M. Perrut and W. Majewski, “Method and instalation for setting in adsorbed state on a porous support active compounds contained in a product,” US6709595B1, 2004.

[16] E. M. Anderson, M. L. Noble, S. Garty, H. Ma, J. D. Bryers, T. T. Shen, and B. D. Ratner, “Sustained release of antibiotic from poly(2-hydroxyethyl methacrylate) to prevent blinding infections after cataract surgery,” *Biomaterials*, vol. 30, no. 29, pp. 5675–5681, 2009.

[17] K. E. Uhrich, K. E. Uhrich, S. M. Cannizzaro, S. M. Cannizzaro, R. S. Langer, R. S. Langer, K. M. Shakesheff, and K. M. Shakesheff, “Polymeric systems for controlled

drug release," *Chem. Rev.*, vol. 99, no. 11, pp. 3181–3198, 1999.

[18] J. Kim, C.-C. Peng, and A. Chauhan, "Extended release of dexamethasone from silicone-hydrogel contact lenses containing vitamin E.," *J. Control. Release*, vol. 148, no. 1, pp. 110–116, Nov. 2010.

[19] C. González-Chomón, M. E. M. Braga, H. C. De Sousa, A. Concheiro, and C. Alvarez-Lorenzo, "Antifouling foldable acrylic IOLs loaded with norfloxacin by aqueous soaking and by supercritical carbon dioxide technology," *Eur. J. Pharm. Biopharm.*, vol. 82, no. 2, pp. 383–391, Oct. 2012.

[20] J. Kim and A. Chauhan, "Dexamethasone transport and ocular delivery from poly(hydroxyethyl methacrylate) gels.," *Int. J. Pharm.*, vol. 353, no. 1–2, pp. 205–222, Apr. 2008.

[21] C. Gupta and A. Chauhan, "Drug transport in HEMA conjunctival inserts containing precipitated drug particles.," *J. Colloid Interface Sci.*, vol. 347, no. 1, pp. 31–42, Jul. 2010.

[22] C. C. S. Karlgard, N. S. Wong, L. W. Jones, and C. Moresoli, "In vitro uptake and release studies of ocular pharmaceutical agents by silicon-containing and p-HEMA hydrogel contact lens materials.," *Int. J. Pharm.*, vol. 257, no. 1–2, pp. 141–151, May 2003.

[23] T. Heyrman, M. McDermott, J. Ubels, and H. Edelhauser, "Drug uptake and release by a hudrogel intraocular lens and the human crystalline lens," *J. Cataract Refract. Surg.*, vol. 1, no. 2, pp. 169–75, 1989.

[24] J. Chapman, L. Cheeks, and K. Green, "Drug Interaction with intraocular Lenses of Different Materials," *J Cataract Refract Surg*, vol. 18, no. 5, 1992.

[25] S. El Meski, A. Beyssac, and J. Aiache, "Use of polymethylmethacrylate (PMMA) as a Drug Support.," in *1st World Meeting APGI/APV Budapest*, 1995.

[26] J. Aiache, S. Meski, G. Serpin, and P. Tourrette, "Intraocular lens containing releasable medication," 2008.

[27] C. Alvarez-Lorenzo and A. Concheiro, "Molecularly imprinted polymers for drug delivery," *J. Chromatogr. B Anal. Technol. Biomed. Life Sci.*, vol. 804, no. 1, pp. 231–245, 2004.

[28] S. Venkatesh, S. P. Sizemore, and M. E. Byrne, "Biomimetic hydrogels for enhanced loading and extended release of ocular therapeutics," *Biomaterials*, vol. 28, no. 4, pp. 717–724, 2007.

[29] C.-C. Li, M. Abrahamson, Y. Kapoor, and A. Chauhan, "Timolol transport from microemulsions trapped in HEMA gels.," *J. Colloid Interface Sci.*, vol. 315, no. 1, pp. 297–306, Nov. 2007.

[30] R. Uchida, T. Sato, H. Tanigawa, and K. Uno, "Azulene incorporation and release by hydrogel containing methacrylamide propyltrimenthylammonium chloride, and its application to soft contact lens," *J. Control. Release*, vol. 92, no. 3, pp. 259–264, 2003.

[31] T. Sato, R. Uchida, H. Tanigawa, K. Uno, and A. Murakami, "Application of polymer gels containing side-chain phosphate groups to drug-delivery contact lenses," *J. Appl. Polym. Sci.*, vol. 98, no. 2, pp. 731–735, 2005.

[32] A. Danion, H. Brochu, Y. Martin, and P. Vermette, “Fabrication and characterization of contact lenses bearing surface-immobilized layers of intact liposome,” *J. Biomed. Mater. Res. A*, vol. 81, no. 4, pp. 771–780, 2007.

[33] A. Danion, C. J. Doillon, C. J. Giasson, S. Djouahra, P. Sauvageau, R. Paradis, and P. Vermette, “Biocompatibility and light transmission of liposomal lenses.,” *Optom. Vis. Sci.*, vol. 84, no. 10, pp. 954–961, 2007.

[34] M. Champeau, J.-M. Thomassin, T. Tassaing, and C. Jérôme, “Drug Loading of Polymer Implants by Supercritical CO2 Assisted Impregnation: a Review,” *J. Control. Release*, vol. 209, pp. 248–259, 2015.

[35] I. Pasquali and R. Bettini, “Are pharmaceutics really going supercritical?,” *Int. J. Pharm.*, vol. 364, no. 2, pp. 176–187, 2008.

[36] Y. P. Sun, *Supercritical Fluid Technology in Materials Science and Engineering: Syntheses: Properties, and Applications*, Marcel Dek. Clemson, South Carolina, 2002.

[37] I. Kikic and F. Vecchione, “Supercritical impregnation of polymers,” *Curr. Opin. Solid State Mater. Sci.*, vol. 7, no. 4–5, pp. 399–405, Aug. 2003.

[38] S. G. Kazarian, M. F. Vincent, B. L. West, and C. A. Eckert, “Partitioning of solutes and cosolvents between supercritical CO and polymer phases,” vol. 13, pp. 107–112, 1998.

[39] S. G. Kazarian, “Polymer Processing with Supercritical Fluids,” *Polym. Sci.*, vol. 42, no. 2, pp. 78–101220, 2000.

[40] S. G. Kazarian, M. F. Vincent, F. V. Bright, C. L. Liotta, and C. a. Eckert, “Specific Intermolecular Interaction of Carbon Dioxide with Polymers,” *J. Am. Chem. Soc.*, vol. 118, no. 7, pp. 1729–1736, 1996.

[41] S. G. Kazarian and G. G. Martirosyan, “Spectroscopy of polymer/drug formulations processed with supercritical fluids: In situ ATR-IR and Raman study of impregnation of ibuprofen into PVP,” *Int. J. Pharm.*, vol. 232, no. 1–2, pp. 81–90, 2002.

[42] S. G. Kazarian, N. H. Brantley, B. L. West, M. F. Vincent, and C. A. Eckert, “In Situ Spectroscopy of Polymers Subjected to Supercritical CO 2 : Plasticization and Dye Impregnation,” vol. 51, no. 4, pp. 491–494, 1997.

[43] D. L. Tomasko, H. B. Li, D. H. Liu, X. M. Han, M. J. Wingert, L. J. Lee, and K. W. Koelling, “A review of CO(2) applications in the processing of polymers,” *Ind. Eng. Chem. Res.*, vol. 42, no. 25, pp. 6431–6456, 2003.

[44] Y. Handa, P. Kruus, and M. O’neill, “High-pressure calorimetric study of plasticization of poly(methyl methacrylate) by methane, Ethylenen and Carbon dioxide,” *J. Polym. Sci. Part B Polym. Phys.*, vol. 34, pp. 2635–2639, 1996.

[45] P. Alessi, A. Cortesi, I. Kikic, and F. Vecchione, “Plasticization of polymers with supercritical carbon dioxide: Experimental determination of glass-transition temperatures,” *J. Appl. Polym. Sci.*, vol. 88, no. 9, pp. 2189–2193, 2003.

[46] H. Guo and V. Kumar, “Solid-state poly(methyl methacrylate) (PMMA) nanofoams. Part I: Low-temperature CO2 sorption, diffusion, and the depression in PMMA glass transition,” *Polymer (Guildf).*, vol. 57, pp. 157–163, Jan. 2015.

[47] L. N. Nikitin, E. E. Said-galiyev, R. A. Vinokur, and A. R. Khokhlov, “Poly (methyl

methacrylate) and Poly (butyl methacrylate) Swelling in Supercritical Carbon Dioxide," pp. 934–940, 2002.

[48] M. Pantoula, J. von Schnitzler, R. Eggers, and C. Panayiotou, "Sorption and swelling in glassy polymer/carbon dioxide systems," *J. Supercrit. Fluids*, vol. 39, no. 3, pp. 426–434, Jan. 2007.

[49] Y. Zhang, K. K. Gangwani, and R. M. Lemert, "Sorption and swelling of block copolymers in the presence of supercritical fluid carbon dioxide," *J. Supercrit. Fluids*, vol. 11, no. 1–2, pp. 115–134, Oct. 1997.

[50] S.-H. Chang, S.-C. Park, and J.-J. Shim, "Phase equilibria of supercritical fluid–polymer systems," *J. Supercrit. Fluids*, vol. 13, no. 1–3, pp. 113–119, Jun. 1998.

[51] U. Fehrenbacher, T. Jakob, T. Berger, W. Knoll, and M. Ballauff, "Refractive index and swelling of thin PMMA films in CO2/MMA mixtures at elevated pressures," *Fluid Phase Equilib.*, vol. 200, no. 1, pp. 147–160, Jul. 2002.

[52] S. Üzer, U. Akman, and Ö. Hortaçsu, "Polymer swelling and impregnation using supercritical CO2: A model-component study towards producing controlled-release drugs," *J. Supercrit. Fluids*, vol. 38, no. 1, pp. 119–128, Aug. 2006.

[53] S. M. Sirard, K. J. Ziegler, I. C. Sanchez, P. F. Green, and K. P. Johnston, "Anomalous properties of poly(methyl methaerylate) thin films in supercritical carbon dioxide," *Macromolecules*, vol. 35, no. 5, pp. 1928–1935, 2002.

[54] T. Koga, Y. S. Seo, K. Shin, Y. Zhang, M. H. Rafailovich, J. C. Sokolov, B. Chu, and S. K. Satija, "The role of elasticity in the anomalous swelling of polymer thin films in density fluctuating supercritical fluids," *Macromolecules*, vol. 36, no. 14, pp. 5236–5243, 2003.

[55] R. Eggers, J. von Schnitzler, M. Pantoula, and C. Panayiotou, "Sorption and swelling in glassy polymer/carbon dioxide systems," *J. Supercrit. Fluids*, vol. 39, no. 3, pp. 426–434, Apr. 2007.

[56] T. Shinkai, K. Ito, and H. Yokoyama, "Swelling measurement of polymers in high pressure carbon dioxide using a spectroscopic reflectometer," *J. Supercrit. Fluids*, vol. 95, pp. 553–559, 2014.

[57] S. R. Academy and S. A. N. Nesmeyan, "Poly (methyl methacrylate) and Poly (butyl methacrylate) Swelling in Supercritical Carbon Dioxide and the Formation of a Porous Structure Poly (methyl methacrylate) and Poly (butyl methacrylate) Swelling in Supercritical Carbon Dioxide and the For," no. September 2015, 2002.

[58] S. . Kazarian, N. H. Brantley, and C. A. Eckert, "Dyeing to be clean: use supercritical carbon dioxide," *Chemetech*, vol. 29, pp. 36–41, 1999.

[59] S. G. Kazarian, M. F. Vincent, B. L. West, and C. A. Eckert, "Partitioning of solutes and cosolvents between supercritical CO2 and polymer phases," *J. Supercrit. Fluids*, vol. 13, no. 1–3, pp. 107–112, Jun. 1998.

[60] R. B. Chim, M. B. C. de Matos, M. E. M. Braga, a. M. a. Dias, and H. C. de Sousa, "Solubility of Dexamethasone in Supercritical Carbon Dioxide," *J. Chem. Eng. Data*, vol. 57, no. 12, pp. 3756–3760, Dec. 2012.

[61] S. G. Kazarian and G. G. Martirosyan, "Spectroscopy of polymer/drug formulations

processed with supercritical fluids: in situ ATR-IR and Raman study of impregnation of ibuprofen into PVP.," *Int. J. Pharm.*, vol. 232, no. 1–2, pp. 81–90, 2002.

[62] S. G. Kazarian, "Supercritical Fluid Impregnation of Polymers for Drug Delivery, Supercritical Fluid Technology for Drug Product Development, Marcel Dekker, Inc.," vol. 138, 2004.

[63] M. Lora and I. Kikic, "Polymer Processing with Supercritical Fluids: An Overview," *Sep. Purif. Rev.*, vol. 28, no. 2, pp. 179–220, 1999.

[64] A. R. Berens, G. S. Huvard, R. W. Korsmeyer, and F. W. Kunig, "Application of compressed carbon dioxide in the incorporation of additives into polymers," *J. Appl. Polym. Sci.*, vol. 46, no. 2, pp. 231–242, 1992.

[65] V. P. Costa, M. E. M. Braga, J. P. Guerra, A. R. C. Duarte, C. M. M. Duarte, E. O. B. Leite, M. H. Gil, and H. C. de Sousa, "Development of therapeutic contact lenses using a supercritical solvent impregnation method," *J. Supercrit. Fluids*, vol. 52, no. 3, pp. 306–316, Apr. 2010.

[66] R. Y. and R. M. and N. R. Foster, "Impregnation of Ibuprofen into Polycaprolactone using supercritical carbon dioxide," *J. Phys. Conf. Ser.*, vol. 215, no. 1, p. 12087, 2010.

[67] O. Guney and A. Akgerman, "Synthesis of controlled-release products in supercritical medium," *AIChE J.*, vol. 48, no. 4, pp. 856–866, 2002.

[68] K. Sugiura, S. Ogawa, I. Tabata, and T. Hori, "Impregnation of Tranilast to the Poly(lactic acid) Fiber with Supercritical Carbon Dioxide and the Release Behavior of Tranilast," *Fiber*, vol. 61, no. 6, pp. 159–165, 2005.

[69] C. S. Grant and Y. a. Hussain, "Ibuprofen impregnation into submicron polymeric films in supercritical carbon dioxide," *J. Supercrit. Fluids*, vol. 71, pp. 127–135, Nov. 2012.

[70] Y. Masmoudi, L. Ben Azzouk, O. Forzano, J.-M. Andre, and E. Badens, "Supercritical impregnation of intraocular lenses," *J. Supercrit. Fluids*, vol. 60, pp. 98–105, Dec. 2011.

[71] A. R. C. Duarte, J. F. Mano, and R. L. Reis, "Dexamethasone-loaded scaffolds prepared by supercritical-assisted phase inversion," *Acta Biomater.*, vol. 5, no. 6, pp. 2054–2062, 2009.

[72] R. D. Weinstein, K. R. Muske, S. Martin, and D. D. Schaeber, "Liquid and Supercritical Carbon Dioxide-Assisted Implantation of Ketoprofen into Biodegradable Sutures," pp. 7281–7286, 2010.

[73] J. Yu, Y. Guan, S. Yao, and Z. Zhu, "Preparation of Roxithromycin-Loaded Poly (l - lactic Acid) Films with Supercritical Solution Impregnation," pp. 13813–13818, 2011.

[74] A. R. C. Duarte, A. L. Simplicio, A. Vega-Gonzalez, P. S. Paternault, P. Coimbra, M. H. Gil, H. C. De Sousa, and C. M. M. Duarte, "Impregnation of an Intraocular Lens for Ophthalmic Drug Delivery," *Curr. Drug Deliv.*, vol. 5, pp. 102–107, 2008.

[75] V. P. Costa, M. E. M. Braga, C. M. M. Duarte, C. Alvarez-Lorenzo, A. Concheiro, and H. C. Gil, Maria H.de Sousa, "Anti-glaucoma drug-loaded contact lenses prepared using supercritical solvent impregnation," *J. Supercrit. Fluids*, vol. 53, no. 1–3, pp. 165–173, Jun. 2010.

[76] H. De Sousa, M. . Gil, C. Duuarte, E. Leite, and A. Duarte, "Method for preparing therapeutic ophthalmic articles using compressed fluids," US20060008506 A1, 2006.

[77] M. E. M. Braga, H. S. R. C. Silva, M. H. Gil, M. T. V. Pato, E. I. Ferreira, C. M. M. Duarte, and H. C. de Sousa, "Supercritical solvent impregnation of ophthalmic drugs on chitosan derivatives," *J. Supercrit. Fluids*, vol. 44, no. 2, pp. 245–257, Mar. 2008.

[78] M. V. Natu, M. H. Gil, and H. C. de Sousa, "Supercritical solvent impregnation of poly(ε-caprolactone)/poly(oxyethylene-b-oxypropylene-b-oxyethylene) and poly(ε-caprolactone)/poly(ethylene-vinyl acetate) blends for controlled release applications," *J. Supercrit. Fluids*, vol. 47, no. 1, pp. 93–102, Nov. 2008.

[79] F. Yañez, L. Martikainen, M. E. M. Braga, C. Alvarez-Lorenzo, A. Concheiro, C. M. M. Duarte, M. H. Gil, and H. C. de Sousa, "Supercritical fluid-assisted preparation of imprinted contact lenses for drug delivery.," *Acta Biomater.*, vol. 7, no. 3, pp. 1019–1030, Mar. 2011.

[80] Y. Yokozaki, J. Sakabe, B. Ng, and Y. Shimoyama, "Effect of temperature, pressure and depressurization rate on release profile of salicylic acid from contact lenses prepared by supercritical carbon dioxide impregnation," *Chem. Eng. Res. Des.*, vol. 100, pp. 89–94, 2015.

[81] C. Leuner and J. Dressman, "Improving drug solubility for oral delivery using solid dispersions.," *Eur. J. Pharm. Biopharm.*, vol. 50, no. 1, pp. 47–60, Jul. 2000.

[82] G. P. Sanganwar and R. B. Gupta, "Dissolution-rate enhancement of fenofibrate by adsorption onto silica using supercritical carbon dioxide.," *Int. J. Pharm.*, vol. 360, no. 1–2, pp. 213–8, Aug. 2008.

[83] E. Badens, V. Majerik, G. Horváth, L. Szokonya, N. Bosc, E. Teillaud, and G. Charbit, "Comparison of solid dispersions produced by supercritical antisolvent and spray-freezing technologies," *Int. J. Pharm.*, vol. 377, no. 1–2, pp. 25–34, 2009.

[84] Y. Fei, E. S. Kostewicz, M.-T. Sheu, and J. B. Dressman, "Analysis of the enhanced oral bioavailability of fenofibrate lipid formulations in fasted humans using an in vitro-in silico-in vivo approach.," *Eur. J. Pharm. Biopharm.*, vol. 85, no. 3 Pt B, pp. 1274–84, Nov. 2013.

[85] R. J. Ahern, J. P. Hanrahan, J. M. Tobin, K. B. Ryan, and A. M. Crean, "European Journal of Pharmaceutical Sciences Comparison of fenofibrate – mesoporous silica drug-loading processes for enhanced drug delivery," *Eur. J. Pharm. Sci.*, vol. 50, no. 3–4, pp. 400–409, 2013.

[86] R. Mellaerts, J. a G. Jammaer, M. Van Speybroeck, H. Chen, J. Van Humbeeck, P. Augustijns, G. Van den Mooter, and J. a Martens, "Physical state of poorly water soluble therapeutic molecules loaded into SBA-15 ordered mesoporous silica carriers: a case study with itraconazole and ibuprofen.," *Langmuir*, vol. 24, no. 16, pp. 8651–9, Aug. 2008.

[87] S.-W. Song, K. Hidajat, and S. Kawi, "Functionalized SBA-15 materials as carriers for controlled drug delivery: influence of surface properties on matrix-drug interactions.," *Langmuir*, vol. 21, no. 21, pp. 9568–75, Oct. 2005.

[88] V. Ambrogi, L. Perioli, C. Pagano, F. Marmottini, M. Moretti, F. Mizzi, and C. Rossi, "Econazole nitrate-loaded MCM-41 for an antifungal topical powder formulation.," *J.*

Pharm. Sci., vol. 99, no. 11, pp. 4738–45, Nov. 2010.

[89] M. Manzano and M. Vallet-Regí, "New developments in ordered mesoporous materials for drug delivery," *J. Mater. Chem.*, vol. 20, no. 27, p. 5593, 2010.

[90] S.-C. Shen, W. K. Ng, L. Chia, Y.-C. Dong, and R. B. H. Tan, "Stabilized amorphous state of ibuprofen by co-spray drying with mesoporous SBA-15 to enhance dissolution properties.," *J. Pharm. Sci.*, vol. 99, no. 4, pp. 1997–2007, Apr. 2010.

[91] C. a Aerts, E. Verraedt, a Depla, L. Follens, L. Froyen, J. Van Humbeeck, P. Augustijns, G. Van den Mooter, R. Mellaerts, and J. a Martens, "Potential of amorphous microporous silica for ibuprofen controlled release.," *Int. J. Pharm.*, vol. 397, no. 1–2, pp. 84–91, Sep. 2010.

[92] S. Wang, "Ordered mesoporous materials for drug delivery," *Microporous Mesoporous Mater.*, vol. 117, no. 1–2, pp. 1–9, 2009.

[93] M. Vallet-Regi, a. Rámila, R. P. Del Real, and J. Pérez-Pariente, "A new property of MCM-41: Drug delivery system," *Chem. Mater.*, vol. 13, no. 2, pp. 308–311, 2001.

[94] G. Cavallaro, P. Pierro, F. Palumbo, F. Testa, L. Pasqua, and R. Aiello, "Drug delivery devices based on mesoporous silicate," *Drug Deliv.*, vol. 11, no. 1, pp. 6–41, 2004.

[95] F. Qu, G. Zhu, S. Huang, S. Li, and S. Qiu, "Effective controlled release of captopril by silylation of mesoporous MCM-41," *ChemPhysChem*, vol. 7, no. 2, pp. 400–406, 2006.

[96] B. Muñoz, a. Rámila, J. Pérez-Pariente, I. Díaz, and M. Vallet-Regí, "MCM-41 organic modification as drug delivery rate regulator," *Chem. Mater.*, vol. 15, no. 2, pp. 500–503, 2003.

[97] W. Zeng, X.-F. Qian, Y.-B. Zhang, J. Yin, and Z.-K. Zhu, "Organic modified mesoporous MCM-41 through solvothermal process as drug delivery system," *Mater. Res. Bull.*, vol. 40, no. 5, pp. 766–772, May 2005.

[98] A. L. Doadrio, E. M. B. Sousa, J. C. Doadrio, J. Pérez Pariente, I. Izquierdo-Barba, and M. Vallet-Regí, "Mesoporous SBA-15 HPLC evaluation for controlled gentamicin drug delivery.," *J. Control. Release*, vol. 97, no. 1, pp. 125–32, May 2004.

[99] J. C. Doadrio, E. M. B. Sousa, I. Izquierdo-Barba, A. L. Doadrio, J. Perez-Pariente, and M. Vallet-Regí, "Functionalization of mesoporous materials with long alkyl chains as a strategy for controlling drug delivery pattern," *J. Mater. Chem.*, vol. 16, no. 5, p. 462, 2006.

[100] S. W. Song, K. Hidajat, and S. Kawi, "Functionalized SBA-15 Materials as Carriers for Controlled Drug Delivery: Influence of Surface Properties on Matrix− Drug Interactions," *Langmuir*, vol. 21, no. 21, pp. 9568–9575, 2005.

[101] M. VALLETREGI, "Hexagonal ordered mesoporous material as a matrix for the controlled release of amoxicillin," *Solid State Ionics*, vol. 172, no. 1–4, pp. 435–439, Aug. 2004.

[102] Y. Zhu, J. Shi, H. Chen, W. Shen, and X. Dong, "A facile method to synthesize novel hollow mesoporous silica spheres and advanced storage property," *Microporous Mesoporous Mater.*, vol. 84, no. 1–3, pp. 218–222, Sep. 2005.

[103] Y. Z. and J. S. and W. S. and H. C. and X. D. and M. Ruan, "Preparation of novel hollow mesoporous silica spheres and their sustained-release property,"

Nanotechnology, vol. 16, no. 11, p. 2633, 2005.

[104] C. Tourne, C. Charnay, L. Nicole, and S. Be, "The Potential of Ordered Mesoporous Silica for the Storage of Drugs : The Example of a Pentapeptide Encapsulated in a," pp. 281–286, 2003.

[105] M. L. Jenny Andersson, Jessica Rosenholm, Sami Areva, "Influences of material characteristics on ibuprofendrug loading and release profiles from ordered micro-and mesoporous silica matrices," *Chem. Mater.*, vol. 16, no. 21, pp. 4160–4167, 2004.

[106] V. Zeleňák, V. Hornebecq, and P. Llewellyn, "Zinc(II)-benzoato complexes immobilised in mesoporous silica host," *Microporous Mesoporous Mater.*, vol. 83, no. 1–3, pp. 125–135, 2005.

[107] I. Izquierdo-Barba, A. Martinez, A. L. Doadrio, J. Pérez-Pariente, and M. Vallet-Regí, "Release evaluation of drugs from ordered three-dimensional silica structures.," *Eur. J. Pharm. Sci.*, vol. 26, no. 5, pp. 365–73, Dec. 2005.

[108] F. Belhadj-Ahmed, E. Badens, P. Llewellyn, R. Denoyel, and G. Charbit, "Impregnation of vitamin E acetate on silica mesoporous phases using supercritical carbon dioxide," *J. Supercrit. Fluids*, vol. 51, no. 2, pp. 278–286, Dec. 2009.

[109] I. Smirnova, S. Suttiruengwong, and W. Arlt, "Feasibility study of hydrophilic and hydrophobic silica aerogels as drug delivery systems," *J. Non. Cryst. Solids*, vol. 350, pp. 54–60, 2004.

[110] W. Li-hong, C. Xin, X. Hui, Z. Li-li, H. Jing, Z. Mei-juan, L. Jie, L. Yi, L. Jin-wen, Z. Wei, and C. Gang, "A novel strategy to design sustained-release poorly water-soluble drug mesoporous silica microparticles based on supercritical fluid technique," *Int. J. Pharm.*, vol. 454, no. 1, pp. 135–142, Sep. 2013.

[111] G. Novack, "Ophthalmic Drug Delivery: Development and Regulatory Considerations," *Clin. Pharmacol. & Ther.*, vol. 85, no. 5, pp. 539–543, 2009.

[112] Y. Masmoudi, A. Bouledjouidja, M. Van Speybroeck, and E. Badens, "Imprégnation supercritique pour l'élaboration de systèmes à libération contrôlée – Contrôle de la cristallinité du principe actif," in *Cristal 7*, 2013.

CHAPTER III

Supercritical impregnation of intraocular lenses

Table of contents

III. 1. Introduction 99
III. 2. Materials 99
III. 2. 1. Intraocular lenses 99
III. 2. 2. Active pharmaceutical ingredients 101
III. 2. 3. Solvents 102
III. 2. 4. Solution simulating the aqueous humor 102
III. 3. Methods 102
III. 3. 1. Pretreatment of IOLs 102
III. 3. 2. Influence of pressurization conditions on the properties (aspect) of IOLs 103
III. 3. 3. Experimental design and response surface methodology 103
III. 3. 4. Supercritical impregnation set-up 104
III. 3. 5. Characterizations 106
III. 3. 5. 1. Differential Scanning Calorimeter (DSC) 106
III. 3. 5. 2. Nuclear magnetic resonance (NMR) analysis 106
III. 3. 5. 3. Drug release kinetics studies 106
III. 3. 5. 4. Modeling of drug release kinetics 107
III. 3. 5. 5. Impregnation yields 108
III. 3. 5. 6. Partition coefficients 108
III. 4. Results and discussions 109
III. 4. 1. PMMA IOLs 110
III. 4. 1. 1. Influence of pressurization conditions on the visual aspect of IOLs 110
III. 4. 1. 2. Supercritical impregnation of PMMA IOLs 111
III. 4. 1. 2. 1. Dexamethasone 21-phosphate disodium salt impregnation 112
III. 4. 1. 2. 2. Ciprofloxacin impregnation 131
III. 4. 2. P-HEMA IOLs 134
III. 4. 2. 1. IOLs foaming 134
III. 4. 2. 2. IOLs pretreatment 136
III. 4. 2. 3. Supercritical impregnation of P-HEMA IOLs 137
III. 4. 2. 3. 1. Dexamethasone 21-phosphate disodium salt impregnation 137
III. 4. 2. 3. 2. Ciprofloxacin impregnation 141
III. 4. 3. Comparison between PMMA and P-HEMA IOLs impregnation 150
III. 4. Conclusions 153
References 156

III. 1. Introduction

The aim of this chapter is to study the supercritical impregnation of commercially available intraocular lenses with anti-inflammatory and antibiotic drugs in order to combine cataract surgery and post-operative treatment in a single step. Globally, the use rate of intraocular lenses for cataract surgery in the world is equally shared at 50 % between rigid and foldable lenses, even if only foldable lenses will be used in long-term because they require a small incision during surgery (only 2-3 mm incision in comparison to 10-12 mm for nonfoldable lenses) [1]. Consequently, in this work, we were interested in polymeric IOLs from both kinds: rigid IOLs made from derivative of Poly (Methyl Methacrylate) and foldable IOLs made from derivative of Poly (2-Hydroxyethyl Methacrylate).

The impregnation of IOLs was performed with drugs currently used in post-operative treatment of cataract, an anti-inflammatory drug (Dexamethasone 21-phosphate disodium, namely DXP) and an antibiotic (Ciprofloxacin, designed CIP).

This part of PhD work and the choice of the corresponding systems was carried out in collaboration with the Service of Ophthalmology at Hospital « La Timône » (Marseille, France).

For both types of IOLs, supercritical impregnations were carried out in a batch mode and the impregnation yields were determined through drug release kinetics studies. In order to determine the parameters worth studying and to delimit the experimental domain, preliminary experiments were carried out as a first step for each type of IOL. A response surface methodology based on experimental designs was used thereafter to determine the influence of the operating conditions on supercritical impregnation.

III. 2. Materials

All the materials used for the supercritical impregnation of intraocular lenses are presented in the following sections.

III. 2. 1. Intraocular lenses

Supercritical impregnation was performed on two types of commercially available IOLs supplied by “the Fred Hollows Intraocular Lens” (Nepal):

- Rigid IOLs made from derivative of Poly (methyl methacrylate) (PMMA): hydrophobic and rigid IOLs at ambient temperature. IOLs with a diopter of +21.0 D were used,
- Foldable IOLs made from derivative of Poly (2-hydroxyethyl methacrylate) (P-HEMA): IOLs are initially conditioned in a soaking physiological solution. IOLs with three different diopters were used (+5.0D, +21.0D and 32.0D).

The properties of both IOLs as reported by the supplier are summarized in Table III. 1 and photographs of the IOLs as well as the chemical formula of the polymers are represented in Figure III. 1.

Table III. 1 Properties of foldable IOLs.

	PMMA	P-HEMA		
Model	FH106	FLEX		
Dioptric power (D)	+21.0	+5.0D	+21.0D	+32.0D
Optical diameter (mm)	6	6	5.9	5.8
Overall diameter (mm)	13	13.5	13	12.5
Convexity	Biconvex	Biconvex	Biconvex	Biconvex

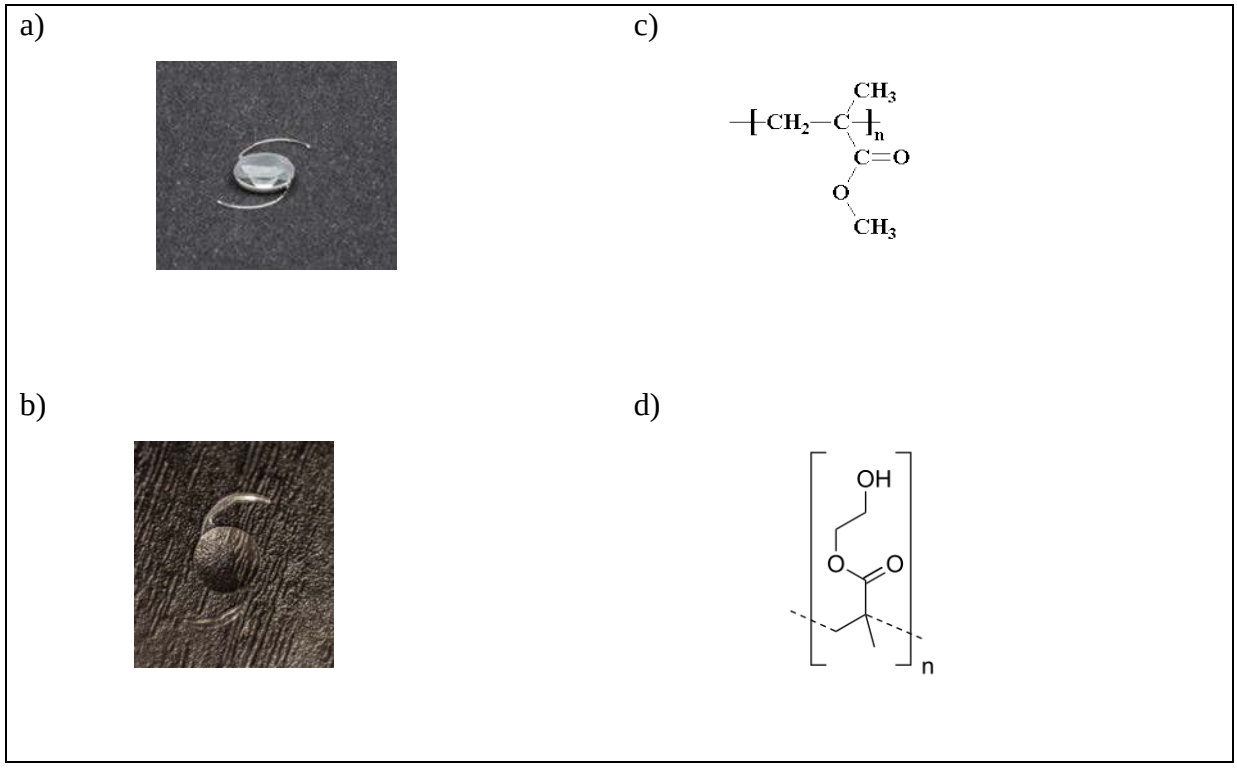

Figure III. 1 Aspect of non treated IOLs made from a) PMMA, b) P-HEMA and their relative skeletal formula c) PMMA, d) P-HEMA.

III. 2. 2. Active pharmaceutical ingredients

Ciprofloxacin (CIP) and Dexamethasone 21-phospahte disodium (DXP) are amongst the most commonly used ophthalmic drugs in postoperative cataract treatment. Both drugs were supplied by Sigma-Aldrich (France).

Dexamethasone 21-phospahte disodium salt ($C_{22}H_{28}FNa_2O_8P$), a synthetic adrenal corticosteroid with potent anti-inflammatory properties, is used in eye, ear and systemic formulations. It is a white crystalline powder hygroscopic with a molar mass of 0.516 $kg.mol^{-1}$ and a melting temperature of 513 K.

Ciprofloxacin ($C_{17}H_{18}FN_3O_3$) is a synthetic antibiotic of second-generation fluoroquinolone, largely used to treat eye infections caused by bacteria and ulcers in the cornea of the eye [2]. It is solid under ambient conditions with a molar mass of 0.331 $kg.mol^{-1}$ and a melting temperature of 545 K. The chemical structure of CIP and DXP is presented in Figure III. 1.

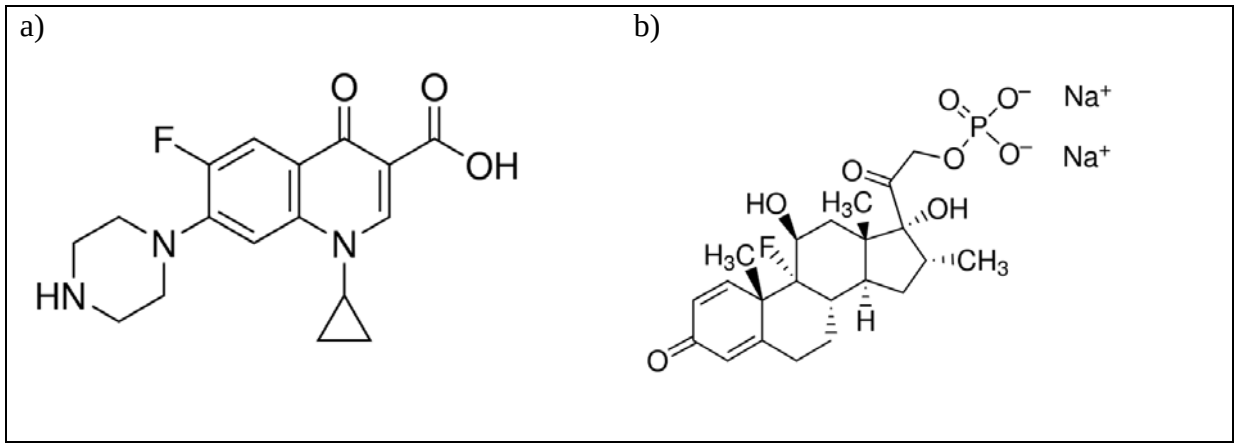

Figure III. 2 Structural formula of a) Ciprfloxacin, b) Dexamethasone 21-phosphate disodium.

III. 2. 3. Solvents

The solvents employed in this work were carbon dioxide (99.7 % purity) from Air Liquide, France and ethanol (≥99.8 % purity) supplied by Groupe MERIDIS, France.

III. 2. 4. Solution simulating the aqueous humor

In-vitro drug release studies were carried out in simulated aqueous humor (pH of 7.2). It was prepared by mixing 9.08 $g.L^{-1}$ of a monobasic potassium phosphate (KH_2PO_4) solution and 9.47 $g.L^{-1}$ of a disodium hydrogenophosphate (Na_2HPO_4) solutions in a volume ratio of 0.285/0.715 respectively [3].

Both KH_2PO_4 (molar mass of 136.09 $g.mol^{-1}$) and the Na_2HPO_4 (molar mass of 136.09 $g.mol^{-1}$) were supplied by Sigma-Aldrich (purity >99.0%).

III. 3. Methods

III. 3. 1. Pretreatment of IOLs

P-HEMA IOLs are supplied pre-soaked in a physiological solution. They therefore absorb a certain quantity of this solution, which makes them flexible under ambient conditions.

The P-HEMA IOLs were dried to have a reproducible initial state (removal of water) for impregnation in contrast with the already dried PMMA which does not require drying step.

These wet P-HEMA IOLs were dried using two different methods: in an oven and using supercritical CO_2. The drying in the oven was performed at two temperatures (313 and 363 K) for long durations (10 days or more).

The drying of IOLs with $scCO_2$ was carried out in a batch mode under 8 and 20 MPa and for different durations. A temperature of 308 K, a carbon dioxide flow rate of 0.25 $kg.h^{-1}$ for the pressurization and a depressurization rate of 0.2 $MPa.min^{-1}$ were kept constants for these experiments.

III. 3. 2. Influence of pressurization conditions on the properties (aspect) of IOLs

Preliminary studies were conducted in order to determine the influence of the supercritical treatment on both types of IOLs (PMMA and P-HEMA) under various pressurization and depressurization conditions. These studies were carried out at 20 MPa (the highest pressure used for impregnation) and 308 K using three different carbon dioxide flow rates during the pressurization phase: slow (0.25 $kg.h^{-1}$), intermediate (0.65 $kg.h^{-1}$) and rapid pressurization (> 0.90 $kg.h^{-1}$). Contact duration between the high-pressure fluid phase and the IOLs of 2 hours was maintained before depressurization. Based on previous studies on rigid PMMA IOLs, the depressurization phase was carried out under a controlled rate of 0.2 $MPa.min^{-1}$ [3].

III. 3. 3. Experimental design and response surface methodology

Response surface methodology (RSM) consists of a group of mathematical and statistical techniques that can be used to define the relationships between the response and independent input variables. In RSM, an empirical mathematical model is postulated and a suitable experimental design is performed to estimate required coefficients. This model, once validated can be used to predict the response in the whole experimental domain with good precision [4].

In a first step, a series of preliminary supercritical impregnation was carried out in order to delimit the experimental operating domain by varying different parameters. Based on the obtained results, two different experimental designs have been elaborated for each type of IOLs, considering two factors in a central composite design with 9 individual design points in a spherical domain. The two input variables were the amount of co-solvent (in %mol, x_{1PMMA}) and the impregnation duration (in min, x_{2PMMA}) for PMMA IOLs. For P-HEMA IOLs, the input variables were the pressure (in MPa, $x_{1P\text{-}HEMA}$) and the impregnation duration (in min, $x_{2P\text{-}HEMA}$) (Table III. 2). Other variables of the process: temperature (308 K) and depressurization rate (0.2 $MPa.min^{-1}$) were kept constant. Response or dependent output variable studied was the impregnated amount quantified through release studies (Y_1).

Table III. 2 Variables (factors) studied using a central composite design.

Input variables	Symbols	levels		
		-1	0	+1
PMMA				
% mol co-solvent	x_{1PMMA}	1	5.5	10
t_{imp} (min)	x_{2PMMA}	30	135	240
P-HEMA				
P (MPa)	$X_{1P\text{-}HEMA}$	8	14	20
t_{imp} (min)	$X_{2P\text{-}HEMA}$	30	135	240

A second order polynomial model as presented in Eq. 1 was postulated to capture the possible nonlinear effects and curvatures in the studied domain:

$$y = b_0 + \sum_{i=1}^{k} b_i x_i + \sum_{j=1}^{k} b_{ii}\, x_i^2 + \sum\sum_{i<j} b_{ij} x_i x_j \qquad Eq.1$$

Where x_j (j=1, 2,… k) is the variables and b_0 , b_i, b_{ii} and b_{ij} are regression coefficient for intercept, linear, quadratic and synergic respectively. The coefficients were estimated using multilinear regression from the results of studied responses. The calculations were performed with the Nemrod-W software (LPRAI, Marseille, France) developed for building and processing experimental design.

For validation of the model suitability, several techniques were used *i.e.* residual analysis, ANOVA (ANalysis Of VAriance) and prediction error sum of squares residuals (especially the coefficient of determination, R^2). After validation, this model was used to calculate the response all over the domain. The visualization of the predicted response was obtained by the response surface plot (3D response) and contour plot (2D response).

III. 3. 4. Supercritical impregnation set-up

A schematic diagram of the experimental high-pressure set-up is shown in Figure III. 3. It is mainly composed of a 125 mL high-pressure cell (Top Industrie S. A., France) withstanding pressures up to 35 MPa and temperature up to 523 K as well as a high-pressure liquid CO_2 pump (Milton Roy, France). The autoclave is positioned on a magnetic stirrer to enhance the

kinetics of the API solubilization and immersed in a thermostat bath to regulate its temperature.

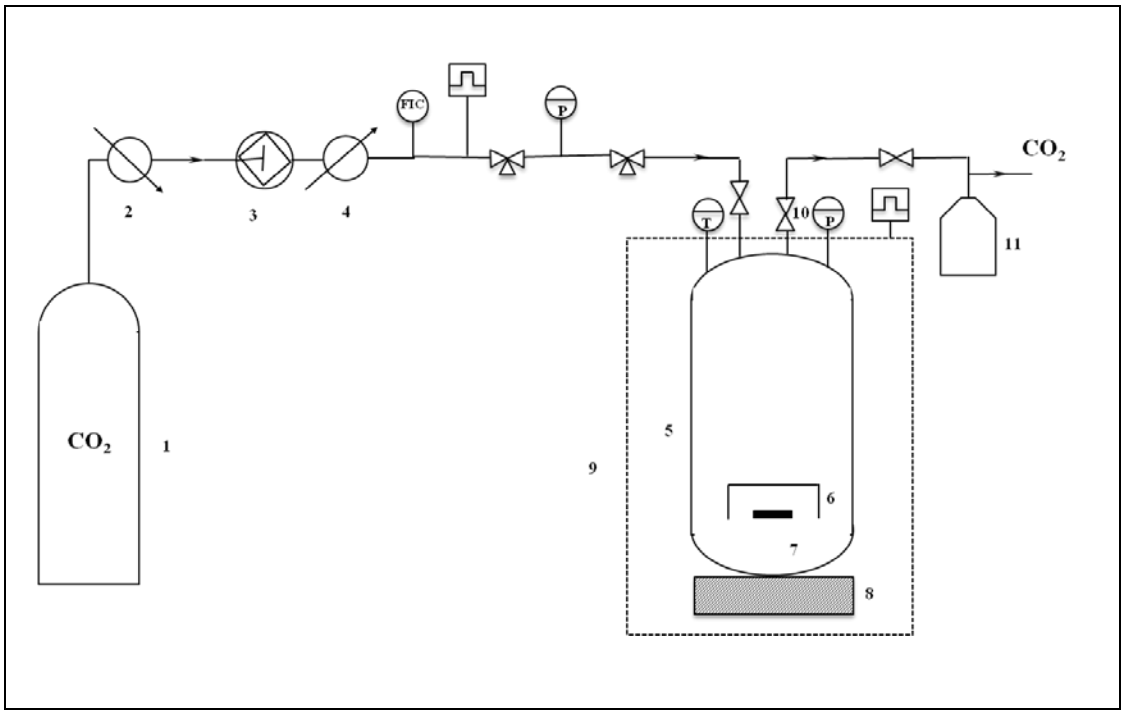

Figure III. 3 Supercritical impregnation set-up: (1) CO_2 cylinder, (2) Cooling bath, (3) High pressure liquid pump, (4) Heating bath, (5) High pressure cell, (6) Support, (7) Magnetic bar, (8) Magnetic stirrer, (9) Thermostat bath, (10) Depressurization valve, (11) Solvent trap.

Supercritical impregnations were carried out in a batch mode where IOLs (2 per batch) were placed on an aluminum support inside the high-pressure cell to separate them from the stirrer bar. A known quantity of the API was introduced in the autoclave and was protected by a frit filter to prevent any contamination of the IOLs surface. For the impregnation with a co-solvent, a predefined quantity of ethanol was first placed in the bottom of the autoclave and IOLs support was positioned carefully to prevent any contact with the lenses. The high-pressure vessel was closed and heated to 308 K and then filled with CO_2. For this purpose, CO_2 was first liquefied through a cooling unit and then pressurized and supplied to the system after heating until desired pressure was reached. The fluid phase containing API was allowed to diffuse within the IOLs for a pre-determined impregnation duration. The system was then slowly depressurized (0.2 $MPa.min^{-1}$) in order not to damage the IOLs and to avoid foaming [3].

For impregnations carried out using a co-solvent, a supplementary CO_2 washing step (1 hour) was carried out before depressurization to remove ethanol and avoid its condensation inside the autoclave.

III. 3. 5. Characterizations

III. 3. 5. 1. Differential Scanning Calorimeter (DSC)

Thermal analyses of various pretreated and impregnated IOLs were performed in a TA Q2000 DSC. Samples were accurately weighed (18-21 mg) into aluminum pans and thermograms were obtained over a temperature range of 323 to 573 K. Each sample was exposed to heat-cool-heat cycle with a heating or cooling rate of 10 $K.min^{-1}$. DSC analysis was performed on samples before and after pretreatment and drug impregnation to identify possible changes in the thermal properties of IOLs.

III. 3. 5. 2. Nuclear magnetic resonance (NMR) analysis

Solid-state NMR spectroscopy was used for quantifying residual solvent content in the impregnated IOLs. ^{13}C NMR spectra were obtained using a Bruker Avance 400 MHz spectrometer consisting Bruker double-channel probe operating at a resonance frequency of 106 MHz. 20 mg of each sample was placed into zirconium dioxide rotors with 4 mm outer diameter. The rotors were equipped with two PTFE spacers and spun at a Magic Angle Spinning rate of 10 kHz. The cross polarization (CP) technique [5] was applied with a ramped 1H-pulse starting at 100 % and decreasing until 50 % during the contact time of 2 ms to circumvent Hartmann-Hahn mismatches [6], [7]. A dipolar decoupling GT8 pulse sequence [8] was applied during the acquisition time to improve the resolution. In order to obtain a good signal-to-noise ratio in the ^{13}C CPMAS experiment, 8K scans were accumulated at room temperature using a delay of 3 s. The ^{13}C chemical shifts were referenced to tetramethylsilane and calibrated with the glycine carbonyl signal set at 176.5 ppm.

III. 3. 5. 3. Drug release kinetics studies

In-vitro drug release kinetics studies were carried out in simulated aqueous humor [3]. Prior to release studies, IOLs were washed in 5 ml of simulated aqueous humor for 3 min under stirring to remove any drug deposited at the surface. The rinsing solution was analyzed spectrophotometrically for determining the CIP and DXP content at 248 and 277 nm

respectively using an apparatus Jenway 6715 UV/Vis (appendix A). Drug concentrations in washing solution were found to be too low for UV-Vis analysis.

Release studies were then conducted by immersing impregnated IOLs in 5 ml of simulated aqueous humor (pH of 7.2) under stirring in a closed vessel at 310 K. An aliquot of 0.4 mL was collected every day for 60 days and CIP or DXP release was quantified at 248 nm or 277 nm respectively (Jenway 6715 UV/Vis). Aliquots were then returned to the release vessel to maintain the initial volume. The drug release from both IOLs impregnated in the same batch was studied separately in order to verify the impregnation homogeneity among the different treated IOLs.

At the end of the release studies, IOLs were placed again in temperature-controlled stirred glass vials containing 5 mL of fresh simulated aqueous humor for few days in order to check if there was any further presence of residual API in IOLs.

III. 3. 5. 4. Modeling of drug release kinetics

There are a large number of articles on drug release kinetics modeling from matrix systems starting from the pioneering work of Higuchi [9] to recent detailed models of Galdi [10]. Peppas *et al*. [11] suggested a simple empirical equation which can be used to analyze drug release (below 60 % of the whole accumulated released mass) from non-swellable polymeric delivery systems:

$$\frac{M_t}{M_\infty} = k\ t^n \qquad Eq.2$$

Where M_t and M_∞ represent the cumulative drug released at times t and infinity respectively. k is a kinetic constant that incorporates structural /geometric characteristics of a delivery system (polymer + drug) and n is designated as an exponent representing the release mechanism.

The Eq. 2 can also be used for the analysis of controlled release systems based on moderately swelling polymers (*e.g.*, systems based on hydroxypropyl methyl cellulose, poly (vinyl alcohol), poly (2-hydroxyethyl methacrylate), *etc.*) [11]. Therefore, this equation was used to model drug release from IOLs as overall swelling of these systems was less than 25 %. In this work, the release constant k and release exponent parameter n were fitted using the Eq. 2 to the first 60 % release of the impregnated drugs from IOLs.

To describe drug release mechanism, Ritger *et al.* [12] have distinguished a Fickian diffusion configuration (case I) from a solute release behavior and swelling-controlled release systems (Case-II). An anomalous (non Fickian) release molecular mechanism can be used to describe the coupling of diffusion and swelling phenomena. Table III. 3 summarizes the diffusional exponents and corresponding drug release mechanisms from a thin film [12].

Table III. 3 Release exponent and corresponding mechanisms of release from a thin film.

Diffusional exponent, n	Drug release mechanism
0.5	Fickian diffusion
0.5 < n <1.0	Anomalous (non-Fickian) transport
1.0	Swelling-controlled diffusion (case-II transport)

III. 3. 5. 5. Impregnation yields

The impregnated amounts were determined through release studies and defined as cumulative mass of the released drug after reaching a constant value. The impregnation yield was calculated according to the following equation (Eq. 3):

$$Y_{imp} = \frac{m_{imp}}{m_{0\,IOL}} \qquad Eq.3$$

Where, m_{imp} is the mass of impregnated API (corresponding to m_∞ during release) and m_{0IOL} is the initial mass of dry IOL.

III. 3. 5. 6. Partition coefficients

The affinity between the drug and the polymer can be determined through partitioning coefficient (K), which is the ratio of the mass fractions of the drug in impregnation matrix to that in $scCO_2$ phase.

$$K = \frac{y_{drug-polymer}}{y_{drug-CO_2}} \qquad Eq.4$$

Where $y_{drug\text{-}polymer}$ and $y_{drug\text{-}CO2}$ are the mass fractions of the drug in the impregnation matrix and in the fluid phase respectively.

III. 4. Results and discussions

In this work, we are interested in the impregnation of drugs into PMMA and P-HEMA IOLs. For each kind of IOL, the results were discussed first for DXP and then for CIP. The factors governing supercritical impregnation are complex because they involve different parameters which influence the impregnation process, such as solubility of drug in $scCO_2$, swelling/plasticizing of polymer and affinity between the drug and the polymer.

The phase behavior of the mixture of drug and $scCO_2$ is very important for the choice of experimental conditions of impregnation as well as for the understanding of impregnation results. A semi-flow type apparatus [13] was used to measure the solubilities of both drugs (DXP and CIP) in CO_2 without the use of a co-solvent. The solubilities of drugs were measured by varying the pressure from 8 to 20 MPa at 308 K [14]. The corresponding experimental conditions (pressure and CO_2 densities) and drugs solubilities are summarized in the Table III. 4.

Table III. 4 Solubilities of DXP and CIP (molar fraction) in $scCO_2$ at 308 K [14].

P (MPa)	CO_2 density ($kg.m^{-3}$)	y_{drug}	
		DXP	CIP
8	419.09	$1.22\ 10^{-7}$	$1.83\ 10^{-7}$
14	801.41	-	$3.11\ 10^{-7}$
20	865.72	$2.15\ 10^{-7}$	$4.51\ 10^{-7}$

The solubilities of both DXP and CIP in $scCO_2$ were low, with higher values obtained for CIP. An increase in the pressure (from 8 to 20 MPa) leads to an enhancement in drug solubility in $scCO_2$ ($1.22\ 10^{-7}$ to $2.15\ 10^{-7}$ for DXP and $1.83\ 10^{-7}$ to $4.51\ 10^{-7}$ for CIP in molar fraction).

This behavior is due to enhanced drug-CO_2 specific interactions that occur when the CO_2 density increases and that reduce the intermolecular mean distance of the involved molecules.

A previous work in literature presented the solubility of Dexamethasone in the same conditions and the values were higher (from $1.25\ 10^{-6}$ to $1.27\ 10^{-6}$) [15] than the obtained values for DXP (Dexamethasone 21-phosphate disodium) in this work. Since CO_2 is non polar and since DXP is an ionic compound, it is not surprising that the solubility of the salt is

lower than the one of Dexamethasone. To our knowledge experimental data of DXP and CIP in $scCO_2$ is presented for the first time in this work.

III. 4. 1. PMMA IOLs

The influence of pressurization conditions as well as the operating conditions on supercritical impregnation of PMMA IOLs with both drugs (DXP and CIP) are presented in the following sections.

III. 4. 1. 1. Influence of pressurization conditions on the visual aspect of IOLs

Foaming resulting from the sorption of $scCO_2$ by a polymeric matrix is very common [16]. Hence, it was important to carry out experiments in pressurization and depressurization conditions that do not alter the optical properties of PMMA IOLs. For that purpose, supercritical treatment was carried out in a batch mode at 20 MPa (the highest pressure used for impregnation), 308 K and during 2 hours in the absence of API. Based on previous studies on rigid PMMA IOLs, the depressurization was carried out under a controlled rate of 0.2 $MPa.min^{-1}$ [3]. Three pressurization rates were carried out with three different carbon dioxide flow rates corresponding to slow (0.25 $kg.h^{-1}$), intermediate (0.65 $kg.h^{-1}$) and fast pressurization (> 0.90 $kg.h^{-1}$).

Transparent IOLs (without foaming) were obtained for the IOLs treated at the different pressurization rates (Figure III. 4) and present therefore comparable visual aspects to non-treated ones.

Similar transparent IOLs were obtained for samples treated at lower pressure (8 MPa) and slower depressurization rates (0.07 $MPa.min^{-1}$) with or without co-solvent, which is suitable for the intended application.

a) b) c)

.

Figure III. 4 Influence of the pressurization flow rate on the visual aspect of some IOLs treated with $scCO_2$ at 20 MPa: a) with a pressurization flow rate of 0.25 $kg.h^{-1}$, b) with a pressurization flow rate of 0.65 $kg.h^{-1}$, c) with a rapid pressurization flow rate of 0.90 $kg.h^{-1}$.

All the following supercritical impregnation experiments in this work were performed at a CO_2 flow rate of 0.25 $kg.h^{-1}$ for pressurization.

III. 4. 1. 2. Supercritical impregnation of PMMA IOLs

At first and before the supercritical impregnation, some PMMA IOLs were treated with $scCO_2$ in the absence of the API at pressure of 20 MPa, temperature of 308 K, duration of supercritical treatment of 2 hours and a depressurization flow rate of 0.2 $MPa.min^{-1}$ in order to verify if the $scCO_2$ extract some impurities from IOLs and if it induces a mass variation of the IOL after treatment.

The mass of samples during the supercritical treatment experiments, *i.e.* while in the high pressure cell in presence of $scCO_2$, were not measured. However, a representation of the expected mass increase due to CO_2 sorption within the polymer is depicted in Figure III. 5. After the experiment, CO_2 desorption (in open-air) results in a mass reduction. The evolution of the IOLs mass (measured by weighing) for the swollen samples (after experiments) is illustrated in Figure III. 6. These measurements correspond to the 30 days observation zone depicted in Figure III. 5.

PMMA IOLs treated with $scCO_2$ in the absence of API regain their initial mass after 15 days of CO_2 desorption. Actually, the final mass can even be lower than the initial one since some residual compounds (solvent, water, monomers or oligomers, *etc.*) may have been extracted by $scCO_2$.

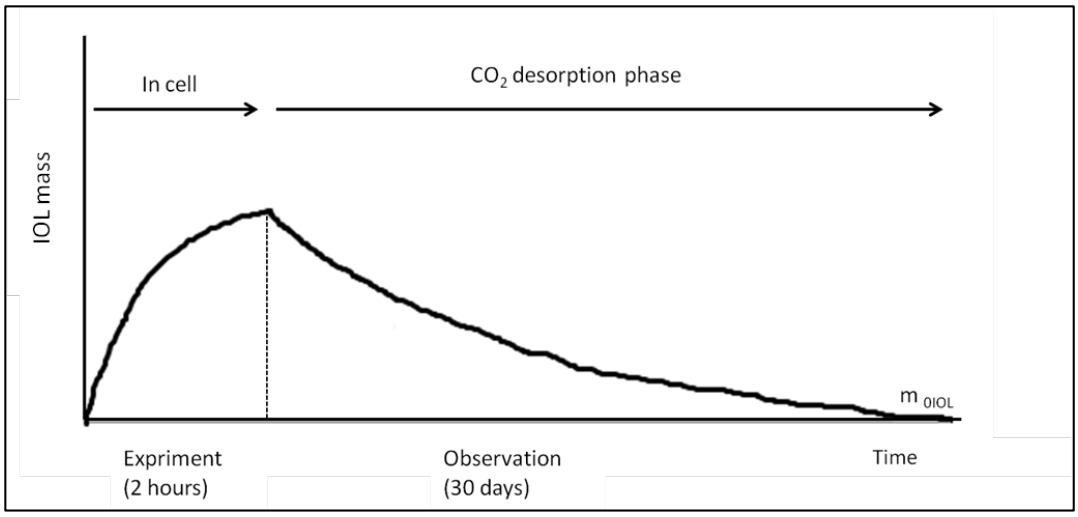

Figure III. 5 Schematic representation of mass evolution profiles of IOLs due to sorption/desorption of CO_2.

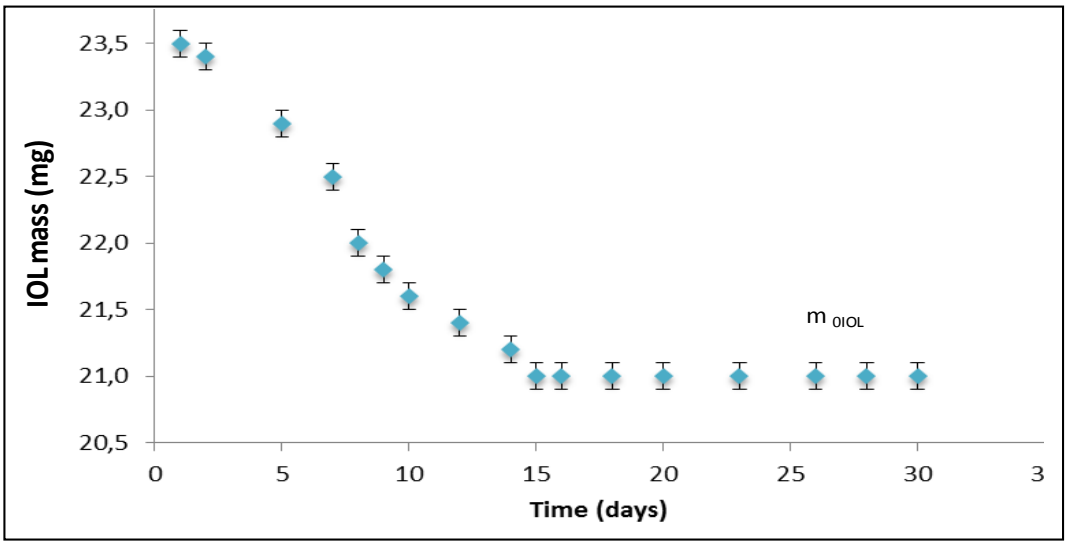

Figure III. 6 Evolution of PMMA IOLs mass due to CO_2 desorption after supercritical treatment (at 20 MPa and 308 K).

III. 4. 1. 2. 1. Dexamethasone 21-phosphate disodium salt impregnation

a. Preliminary impregnation

In the first part of this study, supercritical impregnations were performed with or without using a co-solvent at 8 and 20 MPa on IOLs with a diopter of +21.0 D. The influence of temperature, impregnation duration and the quantity of co-solvent used was also studied, while respecting a pressurization flow rate of 0.25 $kg.h^{-1}$.

The impregnation results were discussed in terms of impregnated amounts or impregnation yields and drug release (release duration and profile). The results of all the preliminary impregnation experiments are summarized in Table III. 11.

Initially, supercritical impregnations were performed without using a co-solvent or using ethanol (5 %mol) at 8 and 20 MPa on IOLs with a diopter of +21. 0 D. The temperature was kept constant at 308 K, the impregnation duration at 2 hours and the depressurization flow rate to 0.2 MPa.min^{-1}.

The impregnation results presented in Table III. 5 are expressed in term of the impregnated mass of DXP in IOLs ($m_{DXP\ imp}$), the impregnation yields (Y_{imp}) and the release duration ($t_{release}$). Reproducibility of results was verified (Appendix B).

Table III. 5 Influence of the pressure and the use or not of co-solvent (ethanol 5 %mol) on supercritical impregnation.

N°	m_{0IOL} (*)	Pressure	$m_{DXP\ imp}$	Y_{imp}	$t_{release}$
	mg±0.2	MPa	µg	µg $_{drug}$/mg $_{IOL}$	days
Without co-solvent					
DXP_1	18.9	8	159 ± 24	8.4 ± 1.3	≈ 40
DXP_2	19.0	20	165 ±		

pressure of 20 MPa which can be explained by a drug partition becoming more favorable towards the supercritical phase.

Interestingly, impregnation yields were improved at low pressure in the presence of co-solvent. Hence, all DXP loadings later in this work were performed at 8 MPa and in the presence of co-solvent.

NMR analyses were carried out on DXP impregnated PMMA IOLs at 8 MPa in the presence of co-solvent (DXP_3) without and with carrying out a CO_2 washing step phase (1 hour) before depressurization. As it can be observed in Figure III. 7, ethanol peaks disappear when the washing phase is carried out indicating an efficient removal of ethanol (residual ethanol lower than 0.01 wt %) which is suitable for the intended application.

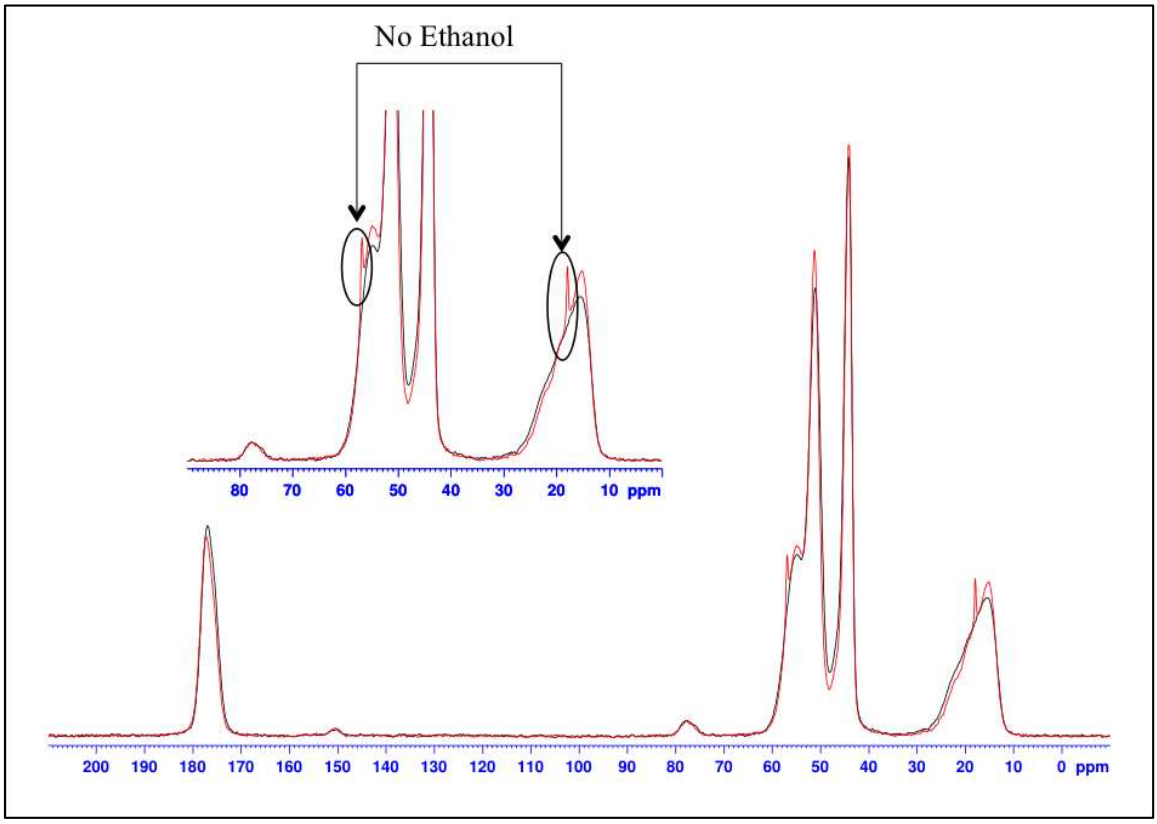

Figure III. 7 NMR analyses (^{13}C) of an impregnated PMMA IOL with DXP at 8 MPa, 308 K, with 5 %mol of ethanol and a) without washing step (red) b) with washing step (black).

In-vitro kinetics studies of drug release from impregnated IOLs were conducted for 60 days on all impregnated IOLs. The release kinetics from DXP loaded IOLs is illustrated in Figure III. 8. The release durations ($t_{release}$) were determined when accumulated drug released mass became constant in time and are presented in Table III. 5.

Drug release from all the studied conditions exhibited a sustained release profile without an initial burst release which suggests deep impregnation of the drug in IOLs and an absence of drug deposition onto the IOL surface.

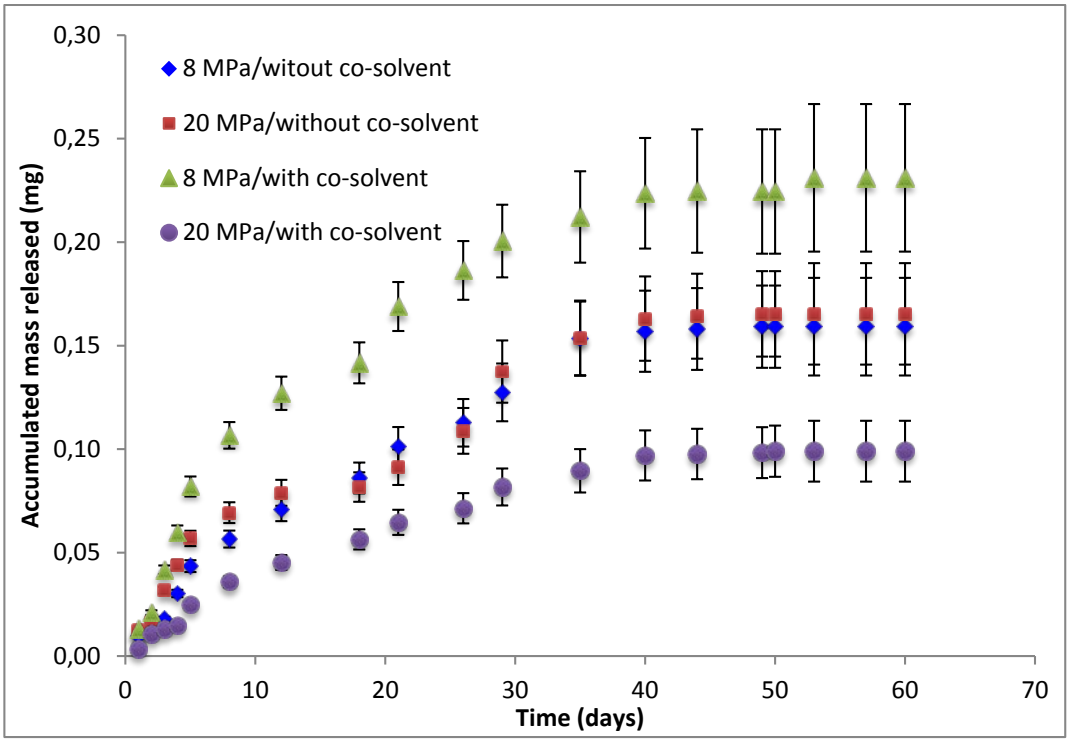

Figure III. 8 Accumulated drug release mass from PMMA IOLs impregnated at 308 K with an impregnation duration of 2 hours and a depressurization flow rate of 0.2 MPa.min^{-1}.

For the experiments (DXP_1, 2, 3 and 4), the release duration was almost the same (about 40 days) for different impregnation conditions presenting different impregnation yields, which suggests a deep and homogenous impregnation.

The influence of the temperature on the supercritical impregnation was studied at 8 MPa in the presence of co-solvent (5 %mol of ethanol), during 2 hours and with depressurization rate of 0.2 MPa.min^{-1}. The obtained results are shown in Table III. 6.

Table III. 6 Influence of the temperature on the supercritical impregnation.

N°	m_{0IOL}	Temperature	$m_{DXP\ imp}$	Y_{imp}	$t_{release}$
	mg±0.2	K	µg	µg $_{drug}$/mg $_{IOL}$	days
DXP_3	20.0	308	240 ± 36	12.0 ± 1.8	≈ 44
DXP_5	20.1	320.5	157 ± 16	7.8 ± 0.8	≈ 35
DXP_6	20.2	333	123 ±12	6.1 ± 0.6	≈ 40

As we can observe in Table III. 6, increasing the temperature was unfavorable for impregnation. This could be attributed to a decrease in CO_2 density resulting in a reduction of DXP solubility in the fluid phase (well-known retrograde behavior). Furthermore, decreasing CO_2 density leads to a lesser PMMA swelling. Üzer *et al* [18] showed that volume expansions of CO_2 swollen PMMA between 9 and 25 % increased with pressure but decreased with temperature augmentation.

The highest impregnation yield (12.0 $\mu g_{drug}/mg_{IOL}$) was obtained at the lowest studied temperature (308 K). Therefore, all the impregnation experiments later in this work were carried out at 308 K.

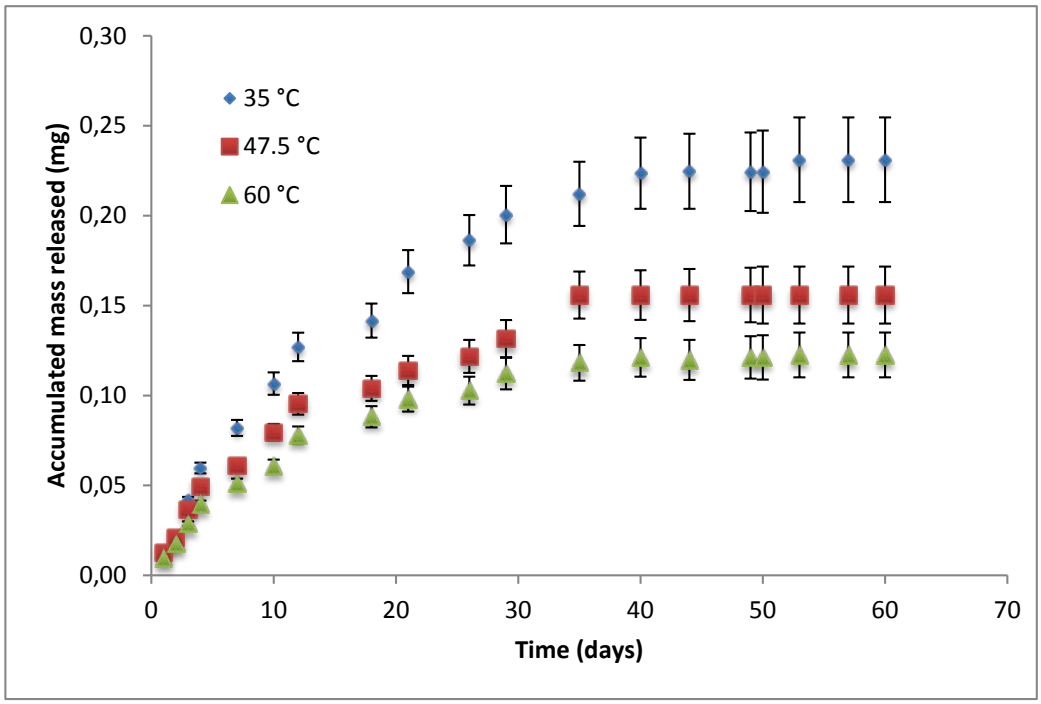

Figure III. 9 Influence of the temperature on accumulated mass released of IOLs impregnated at 8 MPa.

Once again, *in-vitro* drug release from impregnated IOLs were performed for 60 days on all IOLs. The release kinetics from DXP loaded IOLs is represented in Figure III. 9. The release duration ($t_{release}$) was determined when accumulated drug became constant in time and are presented in Table III. 6. Drug release from IOLs exhibited a sustained release profile during about 40 days for the experiments (DXP_3, 5 and 6), which suggests once again deep and homogenous impregnation of the drug in IOLs.

The influence of the quantity of co-solvent on the impregnation was also studied at 8 MPa and 308 K with an impregnation duration of 2 hours and a depressurization rate of 0.2 MPa.min^{-1}. Impregnation conditions as well as the obtained results are shown in the Table III. 7.

Table III. 7 Influence of the quantity of co-solvent on supercritical impregnation at 8 MPa.

N°	m_{0IOL}	Co-solvent	$m_{DXP\ imp}$	Y_{imp}	$t_{release}$
	mg±0.2	%mol	µg	µg $_{drug}$/mg $_{IOL}$	Days
DXP_7	20.0	2	127 ± 13	6.3 ± 0.7	≈ 40
DXP_3	20.0	5	240 ± 36	12.0 ± 1.8	≈ 44
DXP_8	21.0	10	224 ± 23	10.7 ± 1.2	≈ 40

A significant increase in the impregnation yields (6.3 to 12.0 µg $_{drug}$/mg $_{IOL}$) was observed when increasing the amount of the used co-solvent from 2 to 5 %mol which can be explained by an increase in the fluid phase polarity enhancing thus DXP solubility in this–phase. Increasing the polarity of the fluid phase may also enhance impregnation by promoting PMMA swelling.

However, supplementary increase in the amount of ethanol to 10 %mol does not further improve impregnation, similar impregnation yields were obtained for 5 and 10 %mol (12.0 and 10.7 µg $_{drug}$/mg $_{IOL}$ respectively) indicating similar partition coefficients even if such an increase in the co-solvent ratio should further enhance DXP solubility in the fluid phase.

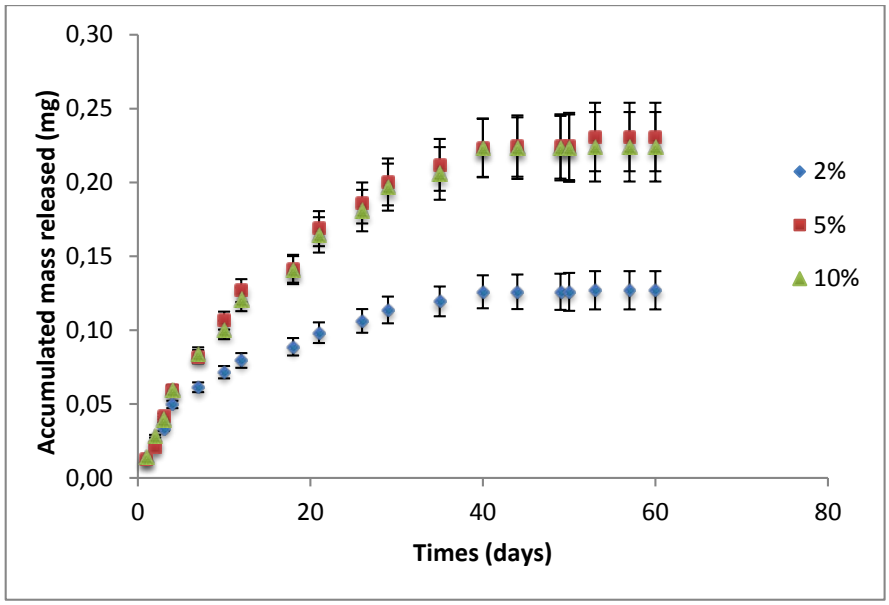

Figure III. 10 Influence of the quantity of co-solvent used on accumulated mass released from IOLs impregnated at 8 MPa and 308 K.

Once again, drug release from IOLs exhibited a sustained profile (Figure III. 10) during about 40 days for the experiments (DXP_7, 3 and 8), which suggests once more deep and homogenous impregnation of the drug in IOLs.

The influence of the impregnation duration was then studied at 8 MPa and 308 K, in presence of 5 %mol of ethanol (the higher impregnation yield was obtained with 5 %mol of ethanol), and with a depressurization rate of 0.2 MPa.min^{-1}. The obtained results are presented in Table III. 8.

Table III. 8 Influence of the impregnation duration on supercritical impregnation (0.2 MPa.min^{-1}).

N°	m_{0IOL}	Impregnation duration	$m_{DXP\ imp}$	Y_{imp}	$t_{release}$
	mg±0.2	h	µg	µg $_{drug}$/mg $_{IOL}$	days
DXP_3	20.0	2	240 ± 36	12.0 ± 1.8	≈ 44
DXP_9	18.9	4.5	156 ± 12	8.2 ± 0.7	≈ 40
DXP_10	19.0	10.5	89 ± 7	4.7 ± 0.4	≈ 30

As we can observe in Table III. 8, the impregnation yields decrease significantly (from 12 to 4.7 µg $_{drug}$/mg $_{IOL}$) by increasing the impregnation duration (from 2 to 10.5 hours). These unexpected results suggest that short impregnation durations are favorable to increase the quantity of DXP in the IOLs. When the impregnation duration is increased, it is expected to enhance the quantity of drug solubilized in the CO_2 rich phase (if the equilibrium is not reached) as well as to improve the swelling/relaxation of polymer, assisting thus the fluid phase penetration within the polymeric matrix during impregnation.

Referring to literature and as discussed in chapter II, the sorption of CO_2 requires a certain duration which depends on the operating conditions, the chemical nature and the geometric characteristics of the polymeric sample (shape, dimensions, ect.). Indeed, some works reported figures about the kinetics of diffusion front inside polymeric matrices. This suggests that for a duration of 2 hours, the swelling of IOLs is probably less important than for longer durations.

Since we have obtained lowest impregnation yields for longer durations, the results may be explained by a facilitated drug release from more swollen polymeric matrices during the depressurization after longer durations.

The tendency was confirmed at a different pressure of 14 MPa and a temperature of 320.5 K. The impregnation experiments were carried out with 5 %mol of ethanol and with a depressurization rate of 0.2 MPa.min^{-1}. The results are shown in the Table III. 9.

Table III. 9 Influence of the impregnation duration on the supercritical impregnation (14 MPa and 320.5 K).

N°	m_{0IOL}	Impregnation duration	$m_{DXP\ imp}$	Y_{imp}	$t_{release}$
	mg±0.2	h	µg	µg $_{drug}$/mg $_{IOL}$	days
DXP_15	18.6	1	172 ± 7	9.2 ± 0.4	≈ 40
DXP_16	19.0	14	89 ± 13	4.7 ± 0.8	≈ 35

Similar evolution of the impregnation yields at 8 MPa were observed while varying the impregnation duration at a lower depressurization yield of 0.07 MPa.min^{-1} (Table III. 10) supporting the hypothesis of the API being dragged out during the depressurization phase. Furthermore, similar impregnation yields to those obtained at 0.2 MPa.min^{-1} indicate that decreasing the depressurization rate does not influence impregnation.

Table III. 10 Influence of the impregnation duration on supercritical impregnation (0.07 MPa.min^{-1}).

N°	m_{0IOL}	Impregnation duration	$m_{DXP\ imp}$	Y_{imp}	$t_{release}$
	mg±0.2	h	µg	µg $_{drug}$/mg $_{IOL}$	Days
DXP_11	18.5	2	233 ± 24	12.6 ± 1.3	≈ 35
DXP_12	18.6	6	129 ± 50	6.9 ± 2.7	≈ 40
DXP_13	19.0	12	76 ± 8	4.0 ± 0.4	≈ 18
DXP_14	20.0	16	89 ± 9	4.4 ± 0.5	≈ 21

Drug release profiles from IOLs are sustained for about 40 days for experiments DXP_3 and 9 while, a shorter release of only 30 days was obtained for a longer impregnation duration of 10.5 hours (DXP_10), (Figure III. 11 and Table III. 8). Drug release profiles exhibit a more sustained release for shorter impregnation durations (40 days for the experiments DXP_11 and 12 compared to 18 and 21 days for experiments DXP_13 and 14, Figure III. 12).

According to these results, at 8 MPa and in the presence of ethanol, moderate impregnation durations (lower than 6 hours) allow deeper impregnation of DXP drug in PMMA IOLs.

At 14 MPa and 320.5 K, while increasing the impregnation duration to 14 hours, the release was only slightly decreased to almost 35 days compared to 40 days of release for 1 hour of impregnation (Figure III. 13). Nevertheless, higher yields obtained for 1 hour of impregnation favoring shorter impregnation durations.

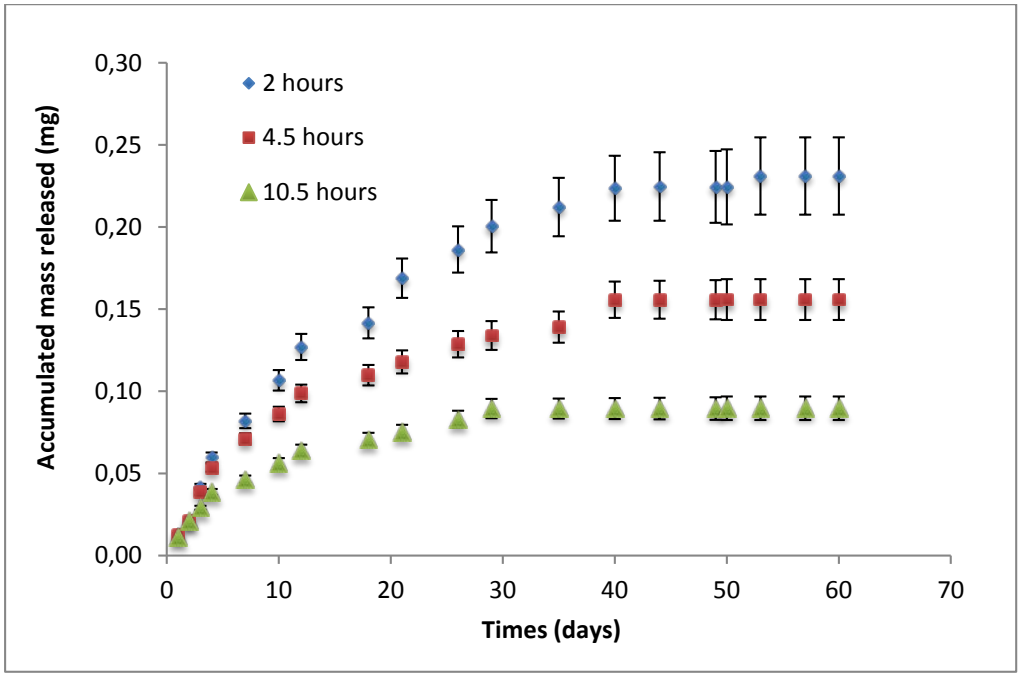

Figure III. 11 Influence of the impregnation duration on accumulated mass released from IOLs impregnated at 8 MPa and 308 K.

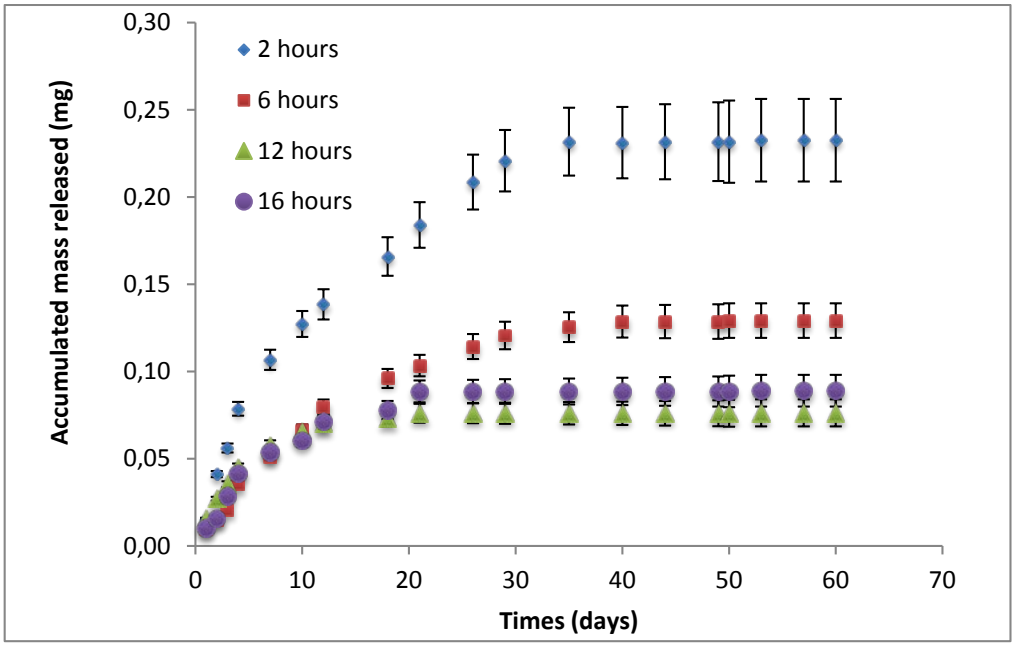

Figure III. 12 Influence of the impregnation duration on the impregnation of IOLs at 8 MPa, 308 K, with 5 %mol of ethanol and a depressurization rate of 0.07 MPa.min^{-1}.

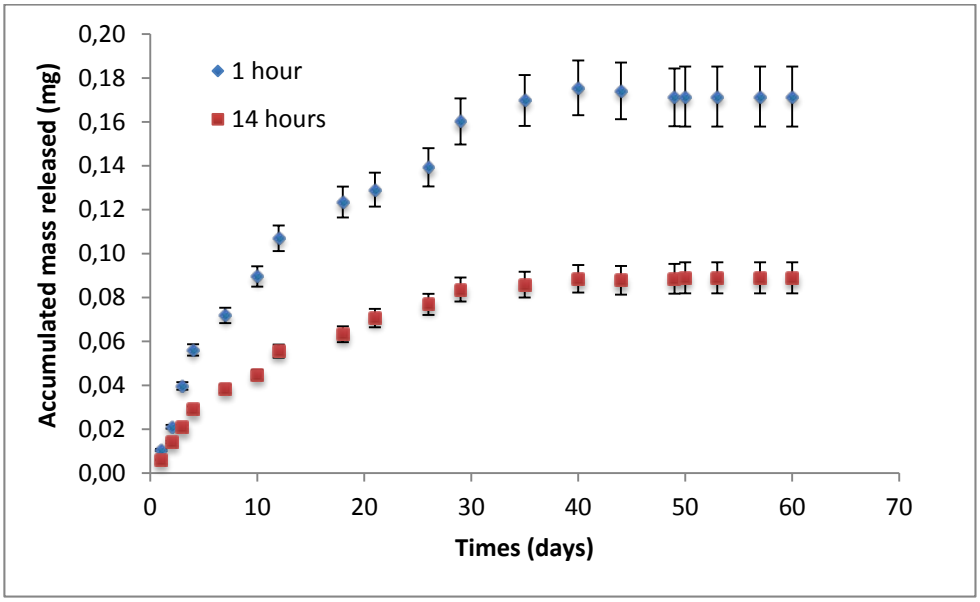

Figure III. 13 Influence of the impregnation duration on the impregnation of IOLs at 14 MPa and 320.5 K.

Release profiles for all the preliminary experiments discussed above were fitted with equation Eq. (2) and the fitting parameters obtained are summarized in Table III. 11. For all the preliminary experiments of PMMA IOLs with DXP (DXP_1 to 16), a regression coefficient higher than 91.9 % was obtained indicating that the model used fits well with the experimental data. Release exponent values for all the impregnated IOLs, in the different tested conditions are lower or equal to 0.5 suggesting that for impregnated IOLs, drug release occurred by Fickian diffusion mechanism [12][11].

Following these results, we can conclude that the impregnation duration does not favor the impregnation of DXP in PMMA IOLs in the studied conditions. The increase in the impregnation duration improves the swelling and the relaxation of chain of PMMA polymer which not only facilitates the diffusion of the fluid phase containing the drug but also assists the drug in leaving the polymer during the depressurization phase. For this reason, all the impregnation experiments later in this work did not exceed impregnation duration of 4 hours.

Table III. 11 Impregnation conditions, results and kinetics parameters of all the preliminary impregnation experiments.

Samples	Pressure (MPa)	Temperature (K)	Co-solvent (%mol)	Impregnation duration (h)	Depressurization rate ($MPa.min^{-1}$)	$m_{DXP\ imp}$ (μg)	Y_{imp} $\mu g_{drug}/mg_{IOL}$	$t_{release}$ (days)	Kinetics parameters (fitting)		
									n	k	R^2
DXP_1	8	308	/	2	0.2	**159 ± 24**	**8.4 ± 1.3**	≈ **40**	0.535	0.116	0.999
DXP _2	20	308	/	2	0.2	**165 ±**					

b. Experimental design

Following the results of the first series of experiments, drug loadings were shown to be significantly influenced by the presence and the amount of the co-solvent. In the presence of ethanol, increasing the pressure from 8 to 20 MPa at 308 K was unfavorable to impregnation. At 8 MPa and in the presence of ethanol, increasing the temperature led to lower impregnation yields. Furthermore, long impregnation durations were also shown to be unfavorable to impregnation.

Therefore, according to these first results, a response surface methodology based on experimental designs was used to study the influence of the amount of the co-solvent as well as the impregnation duration on impregnation of IOLs with diopter +21. 0 D. 5 levels for each of these two entry parameters were considered: amount of co-solvent (1 to 10 %mol) and impregnation duration (30 to 240 min). The pressure was kept at 8 MPa, the temperature at 308 K, the CO_2 flow rate at 0.25 kg. h^{-1} during the pressurization and the depressurization rate at 0.2 MPa.min^{-1}.

The impregnation results were also discussed in terms of impregnated amounts or impregnation yields along with drug release (duration and release profile).

The operational conditions and the impregnated amounts by drug release studies are summarized in Table III. 12. Experiment in the middle of domain was repeated three times (Appendix B).

Table III. 12 Experimental design conditions for supercritical impregnation (8 MPa, 308 K) of IOLs (+21.0 D).

N°	m_{0IOL}	Amount of co-solvent	t_{imp}	$m_{DXP\ imp}$	Y_{imp}	$t_{release}$
	mg±0.2	%mol	min	µg	$\mu g_{drug}/mg_{IOL}$	days
DXP_ED*_1	20.2	2.3	60	**259 ± 26**	**12.8 ± 1.3**	**≈ 40**
DXP_ED_2	18.9	2.3	210	**171 ± 26**	**9.0 ± 1.4**	**≈ 40**
DXP _ED_3	20.5	8.7	60	**144 ± 56**	**7.0 ± 2.8**	**≈ 40**
DXP_ED_4	21.1	8.7	210	**151 ± 19**	**7.2 ± 0.9**	**≈42**
DXP_ED_5	21.2	5.5	30	**398 ± 16**	**18.3 ± 0.8**	**≈44**
DXP_ED_6	21.0	5.5	240	**122 ± 21**	**5.8 ± 1.0**	**≈ 40**
DXP_ED_7	20.9	1	240	**118 ± 30**	**5.6 ± 1.5**	**≈ 40**
DXP_ED_8	19.0	10	135	**279 ± 29**	**14.7 ± 1.6**	**≈ 40**
DXP_ED_9	19.0	5.5	135	**184 ± 19**	**9.4 ± 1.0**	**≈ 41**
DXP_ED_9**	20.1	5.5	135	**215 ± 22**	**10.7 ± 1.1**	**≈ 40**

* ED: Experimental design.

** For this drug release experiment, a single sample was collected at the end of release to quantify the drug release.

For the different experimental conditions, the amount of impregnated drug varies between 118 and 398 µg which suggests that the studied factors influence the surface response.

The experimental results (impregnated amounts) were used to calculate an impregnation model by multilinear regression *via* Nemrod-W software (LPRAI, Marseille, France). The model coefficients are presented in Eq. 4 with a value of R^2 of 0.496 (Appendix C). This low value of the regression coefficient, essentially resulting from the experiments DXP_ED_5 and 8 which present a relatively high value of impregnated drug quantity compared to other experiments of the plan design, as illustrated by the high amount of residue in these two points (Appendix C). The model can hardly explain these high values.

Despite the rather weak value of R^2, the regression model is still significant because it provides a good estimation of the values of a majority of the experimental points. So, the

regression models can be considered as reliable for the prediction of the changes of the impregnated amounts in the range of operating conditions tested.

$$y = 0.204 - 0.051\,x_1 + 0.011\,x_2 + 0.011x_{11}^2 - 0.016\,x_{22}^2 + 0.040x_{12} \qquad Eq.3$$

Figure III. 14 shows the impregnated amount and impregnation yields evolution respectively predicted by the RSM model in terms of amount of co-solvent and impregnation duration.
The response surface is the theoretical three-dimensional plot showing the relationship between the response and the independent variables. The two-dimensional display of the surface plot is called contour plot where lines of constant response are drawn in the plane of the independent variables [4].

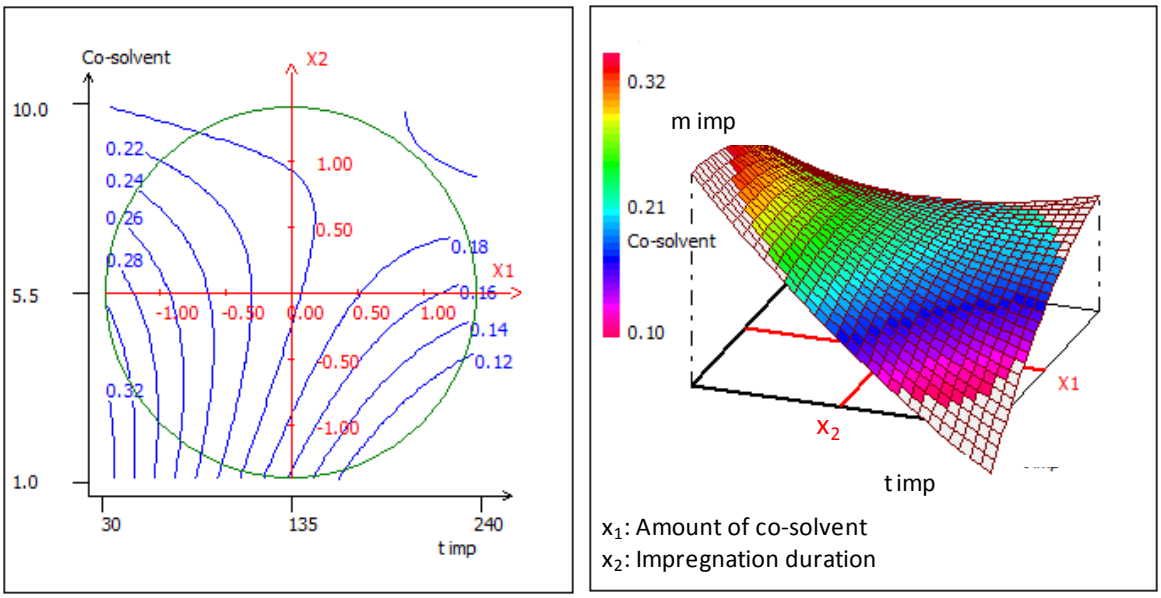

Figure III. 14 A two-dimensional contour plot and a three-dimensional response surface of impregnated mass illustrating optimal conditions for the supercritical impregnation of PMMA IOLs with DXP.

According to the response surface presented in Figure III. 14, the predominant effect is the impregnation duration. Indeed, the response variations are significant, particularly for low quantities of co-solvents (lower than 5.5 %mol). The most advantageous conditions of impregnation are short duration with low amount of co-solvent (5.5 %mol).

Increasing the impregnation duration can lead to higher amounts of dissolved DXP in the fluid phase and/or an enhancement in the polymer swelling if the thermodynamic equilibrium conditions are not reached. Even if the diffusion of the fluid phase is richer in DXP in the more swelled polymeric matrix, longer impregnation durations are shown to be unfavorable for impregnation suggesting that enhancing the swelling and the relaxation of polymer during the contact phase with the fluid phase enables an easier drag out of the drug from the polymer during the depressurization phase. This result is in good agreement with the tendency observed for a higher variation of impregnation duration (from 1 to 16 hours) in the preliminary experiments DXP_3 and DXP_9 to 14.

The variation in the amount of co-solvent, has a small but complex influence on impregnation. Indeed, increasing the amount of co-solvent has little effect for short impregnation durations and becomes even unfavorable when short impregnation durations and amounts of co-solvent greater than 5.5 %mol are applied. Increasing the amount of the co-solvent for impregnation durations higher than 135 min, becomes slightly favorable to impregnation. It is important to point out that the experiment DXP 8 (using 10 %mol of co-solvent for an impregnation duration of 135 min), gives a higher impregnated amount compared to the estimated one by the proposed model resulting in a high residue value. The corresponding yield is also significantly increased compared to 5.5 %mol ethanol for the same duration (9.4 and 14.7 $\mu g_{drug}/mg_{IOL}$ respectively). Several parameters are involved in impregnation and vary with the quantity of the co-solvent such as the drug solubility in the fluid phase, the swelling of the polymer as well as the diffusivity of the fluid phase within the polymer. Furthermore, the variation of the contact time plays an important role on the evolution of the diffusion front within the polymer but also on the quantity of the dissolved drug and the swelling of the polymer by CO_2 sorption. All these concurrent phenomena interfere and can explain the result obtained for the highest amount of 10 %mol of ethanol. Supplementary experiments are required in order to further investigate the influence of varying the impregnation duration at amount of co-solvent higher than 10 %mol. Nevertheless, considering the given application, the quantity of the co-solvent used should be reduced.

According to the result obtained, the response surface shows short impregnation duration as the key factor for efficient drug impregnation in IOLs. The highest impregnation yields in our experimental domain are reached for short impregnations (30 min) with amount of co-solvent ranging between 1 and 5.5 %mol.

DSC analysis were carried out on the impregnate PMMA IOLs DXP_ED_9 (8 MPa, 5.5 %mol of ethanol and 135 min). The thermograph shows a Tg of 390 K (Table III. 13), which is the same as that obtained for non-treated PMMA IOL (before impregnation). The DXP melting peak was not observed in the thermograph. This could be either due to the quantity of the impregnated DXP being below the sensitivity limit of DSC or due to molecular dispersion of DXP within the IOLs.

Table III. 13 Tg of PMMA IOLs before and after impregnation.

IOLs	Tg (K)
Non-treated IOL	391
IOL DXP_ED_9 (impregnated at 8 MPa with 5.5 %mol of ethanol for 135 min)	390

Drug release studies were conducted on all impregnated IOLs prepared at different conditions for 60 days. The evolution of the accumulated drug release mass is illustrated in Figure III. 15.

Drug release curves exhibited quite similar profiles with sustained drug release. For all the samples DXP_ED_1- 9, a sustained release of almost 40 days was obtained.

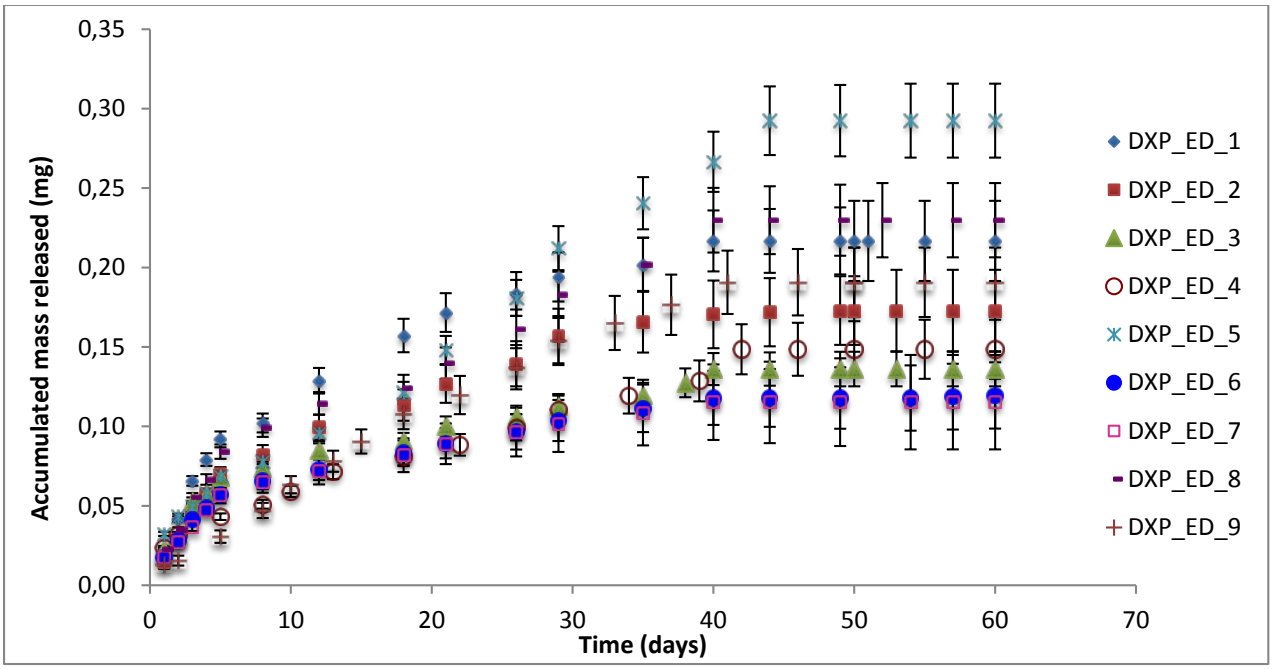

Figure III. 15 Accumulated drug release from IOLs (+21.0 D) impregnated, using experimental design, at 8 MPa, 308 K and with depressurization rate of 0.2 MPa.min^{-1}.

Figure III. 16 presents the effect of the impregnation duration (from 60 to 210 min, from 30 to 240 min and from 60 to 210 min respectively) on drug release from samples prepared with a different amount of co-solvent (2.3, 5.5 and 8.7 %mol respectively) according to conditions fixed in the experimental design (Table III.12).

It is interesting to note that release curves exhibit almost the same slope and the same release duration (about 40 days) for samples processed at different impregnation durations.

As we can observe in the Figure III. 16 a and b, the amount of co-solvent of 2.3 or 5.5 %mol decrease the impregnated amounts with the increase of the impregnation duration while for a higher amount of 8.7 %mol the impregnation duration does not influence the impregnated drug (Figure III. 16c).

a)

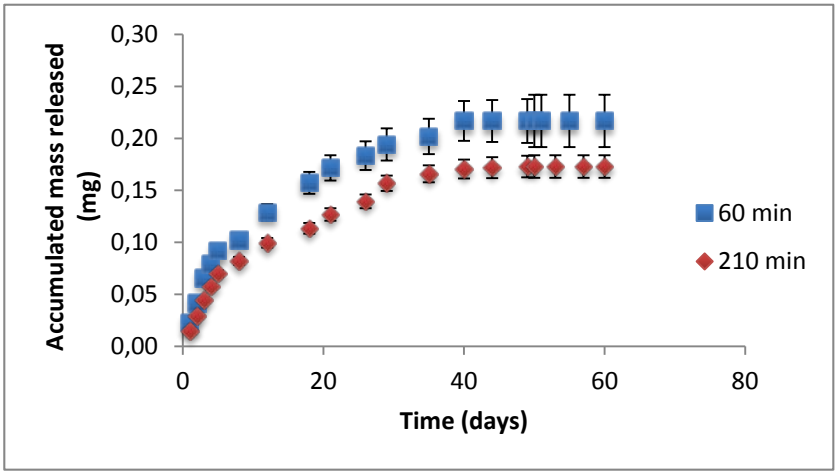

b)

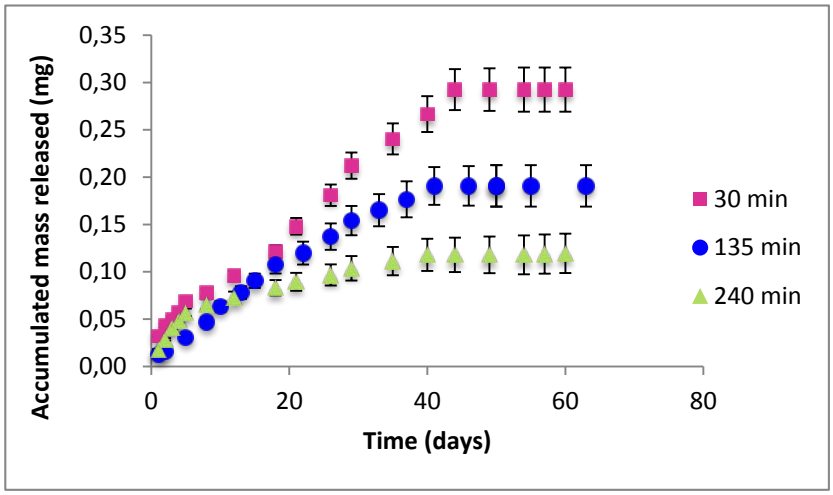

c)

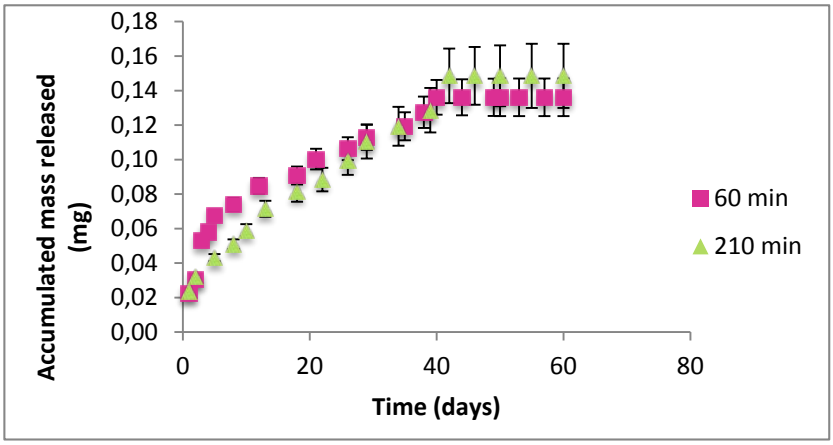

Figure III. 16 Accumulated drug release from IOLs (+21.0 D) impregnated with a) 2.3 %mol of co-solvent (DXP_ED_1 and 2), b) 5.5 %mol of co-solvent (DXP_ED-5, 9 and 6) and c) 8.7 %mol of co-solvent (DXP_ED_3 and 4).

Drug release from PMMA IOLs impregnated with 5.5 %mol of ethanol and during 30 min (which presents the highest experimental impregnation yield, DXP_ED_5) showed a sustained and without an initial burst (inset Figure III. 17) release which suggests in-depth and homogeneous impregnation of the drug in IOLs.

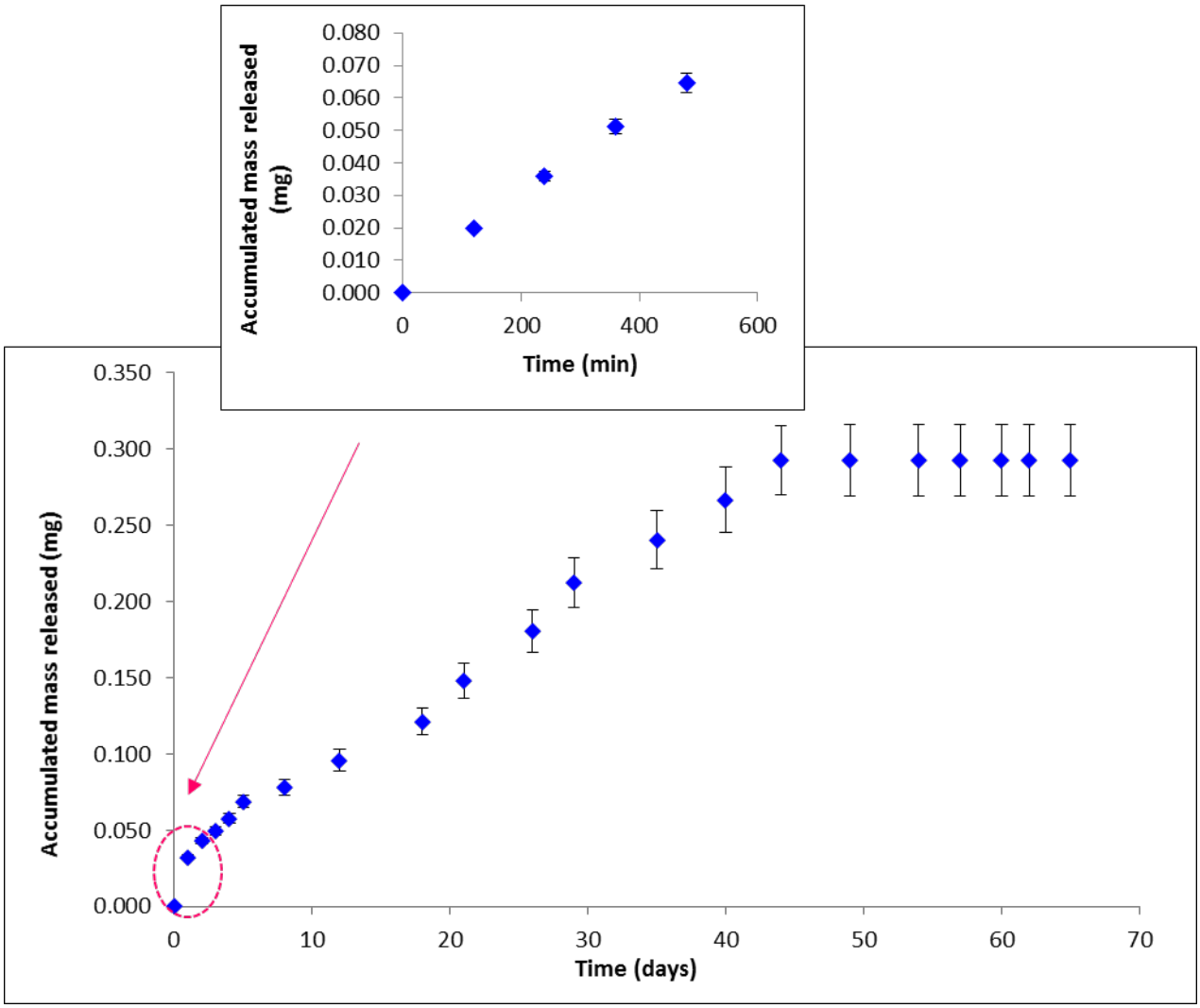

Figure III. 17 Accumulated drug release from impregnated IOLs (DXP_ED_5).

Release profiles were fitted to equation Eq. (2) and the fitting parameters obtained for IOL samples are summarized in Table III. 14. The release exponents for impregnated IOLs were similar to those obtained for the preliminary experiments. The release exponents were lower than 0.5 for all the experiments confirming drug release to occur through a Fickian diffusion configuration (case I). For all the impregnation experiments of PMMA IOLs with DXP, a

regression coefficient higher than 92.7 % was obtained indicating that the model used fits well with the experimental data.

Table III. 14 DXP_ED release kinetic parameters obtained by fitting with equation Eq. (2).

	Kinetics parameters		
	+21.0 D		
Samples	n	k	R^2
DXP_ED_1	0.454	0.191	0.970
DXP_ED_2	0.204	0.055	0.985
DXP_ED_3	0.262	0.028	0.995
DXP_ED_4	0.376	0.024	0.994
DXP_ED_5	0.409	0.032	0.996
DXP_ED_6	0.400	0.231	0.956
DXP_ED_7	0.419	0.239	0.927
DXP_ED_9	0.446	0.161	0.941
DXP_ED_9	0.411	0.172	0.900

III. 4. 1. 2. 2. Ciprofloxacin impregnation

Supercritical impregnation of CIP in PMMA IOLs was carried out at various conditions, the influence of pressure (8 and 20 MPa) and use of a co-solvent (5 %mol ethanol) on drug impregnation was studied for diopter +21.0 D. Other parameters i.e. temperature (308 K), impregnation duration (2 hours), pressurization flow rate (0.25 $kg.h^{-1}$) and depressurization rates (0.2 $MPa.min^{-1}$) were kept constant for all experiments.

The experimental conditions and impregnation yields for CIP loading are summarized in Table III. 15. The CIP impregnation studies were performed at 8 and 20 MPa without the use of a co-solvent or with ethanol as co-solvent.

Table III. 15 Impregnation rates of PMMA IOLs (at 308 K and 2 hours) determined by drug release studies.

N°	m_{0IOL}	Pressure	$m_{CIP\ imp}$	Y_{imp}	$t_{release}$
	mg	MPa	µg	µg $_{drug}$/mg $_{IOL}$	days
Without co-solvent					
CIP_1	19.0	8	**16 ± 1**	**0.8 ± 0.1**	**≈ 12**
CIP_2	19.6	20	**48 ±4**	**2.4 ± 0.2**	**≈ 40**
With co-solvent					
CIP_3	19.9	8	**55 ± 5**	**2.8 ± 0.0**	**≈ 40**
CIP_4	20.5	20	**57 ± 5**	**2.8 ± 0.2**	**≈ 40**

In the absence of co-solvent, the increase in pressure from 8 to 20 MPa improved significantly the impregnated yields (from 0.8 to 2.4 µg $_{drug}$/mg $_{IOL}$). This could be attributed to the concurrent increase in the solubility of the drug (from 1.83 10^{-7} to 4.51 10^{-7} respectively), CO_2 sorption in the matrix and the polymer swelling. Addition of ethanol as co-solvent in the procedure resulted in a further increase in drug impregnation yield (from 0.8 to 2.8 µg $_{drug}$/mg $_{IOL}$ at 8 MPa). It is well known that co-solvent such as ethanol promotes the solubilization of polar drugs in CO_2 by enhancing the overall polarity of the fluid phase. Furthermore, the CO_2 sorption and swelling/plasticizing can also be enhanced with the addition of a co-solvent if polymer /fluid phase (CO_2/co-solvent) interactions are favored [17] [3].

However, in the presence of ethanol, the increase in pressure (from 8 to 20 MPa) did not affect the drug loading. This could be either due to the saturation of IOLs with drug or no further improvement in polymer/drug interactions at higher pressures.

Impregnation yields were quite similar on comparison with those obtained in the presence of a co-solvent (CIP_3 and CIP_4) and those obtained at 20 MPa without using a co-solvent (experiment CIP_2). These results led us to dispense with the use of co-solvent for drug impregnation which is also preferable for the intended application.

In-vitro drug release from impregnated IOLs were performed for 60 days on all impregnated IOLs. The release kinetics from CIP loaded IOLs is illustrated in Figure III. 18. The release durations ($t_{release}$) were determined when accumulated drug release became constant in time and are presented in Table III. 15.

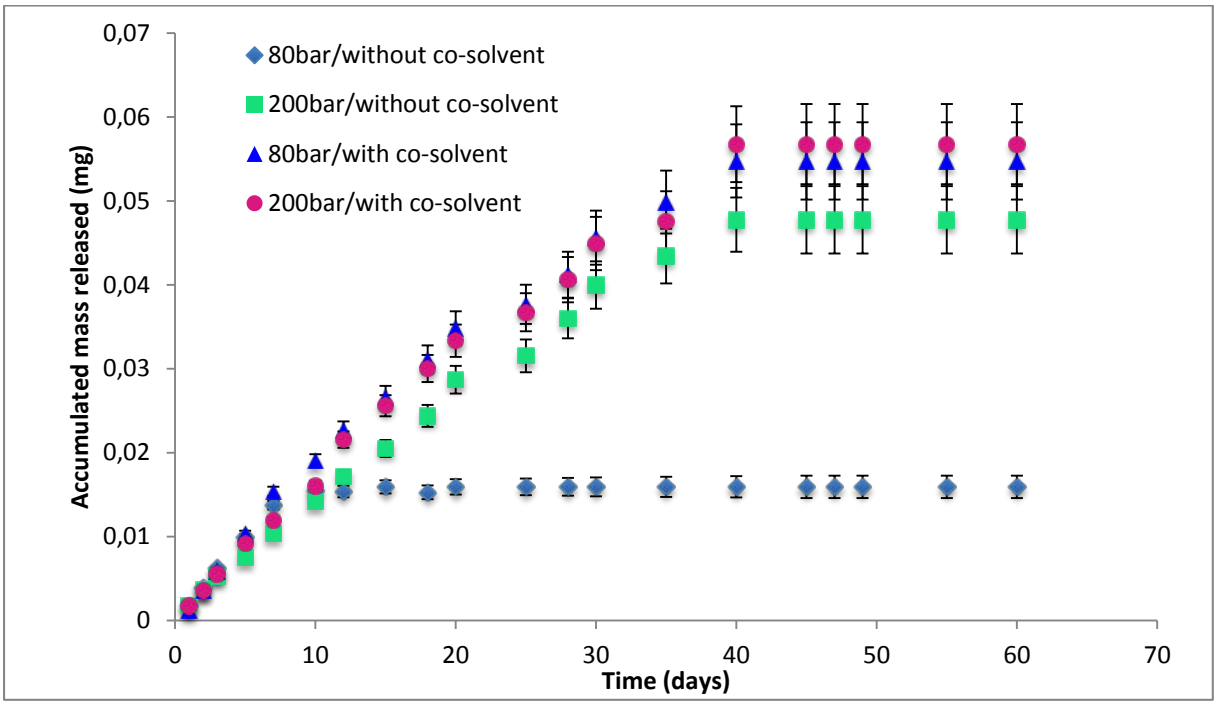

Figure III. 18 Accumulated drug release from PMMA IOLs impregnated with CIP (at 308 K and 2 hours).

Drug release from IOLs exhibited a sustained release profile with the same slope for all the experiments. For the IOLs impregnated at 8 MPa without co-solvent (CIP_1), a sustained release for 12 days was obtained while for the other three samples (CIP_2, 3 and 4) the release duration was significantly more important (40 days) indicating a more in-depth and homogeneous impregnation.

Release profiles discussed above were fitted with equation Eq. (2) with a regression coefficient higher than 93% was obtained indicating that the model used fits well with the experimental release profiles. The obtained fitting parameters are summarized in Table III. 16. Exponent values were lower than 0.5 for all tested conditions of supercritical impregnation, confirming drug release to occur by a Fickian diffusion configuration (case I) [11], [12].

Table III. 16 CIP release kinetic parameters obtained by fitting with Eq (2).

	Kinetics parameters		
	+21.0 D		
Samples	n	k	R^2
DXP_1	0.404	0.197	0.979
DXP _2	0.422	0.249	0.932
DXP _3	0.434	0.159	0.977
DXP _4	0.418	0.175	0.935

III. 4. 2. P-HEMA IOLs

The influence of pressurization conditions and the conditions/results of the supercritical impregnation of P-HEMA IOLs with both drugs (DXP and CIP) were discussed in the following sections.

III. 4. 2. 1. IOLs foaming

In our experimental conditions, the pressurization flow rate was observed to be a significantly important factor in controlling the visual aspect (transparence) of P-HEMA IOLs. In order to elucidate this phenomenon, the influence of the pressurization with CO_2 at three different flow rates: slow (0.25 $kg.h^{-1}$), intermediate (0.65 $kg.h^{-1}$) and fast conditions (> 0.90 $kg.h^{-1}$), was studied in a batch mode at fixed pressure (20 MPa), temperature (308 K) and duration (2 hours). Based on previous studies on rigid PMMA IOLs, the depressurization was carried out under controlled rate of 0.2 $MPa.min^{-1}$ [3].

The $scCO_2$ treatment of IOLs with pressurization flow rates of 0.65 and 0.90 $kg.h^{-1}$ resulted in foaming and therefore loss in the optical properties of the IOLs as illustrated in Figure III. 19. Similar loss in optical properties was observed for samples treated at a lower pressure (8 MPa) and slower depressurization rate (0.07 $MPa.min^{-1}$) with or without a co-solvent for pressurization flow rates of 0.65 and 0.90 $kg.h^{-1}$.

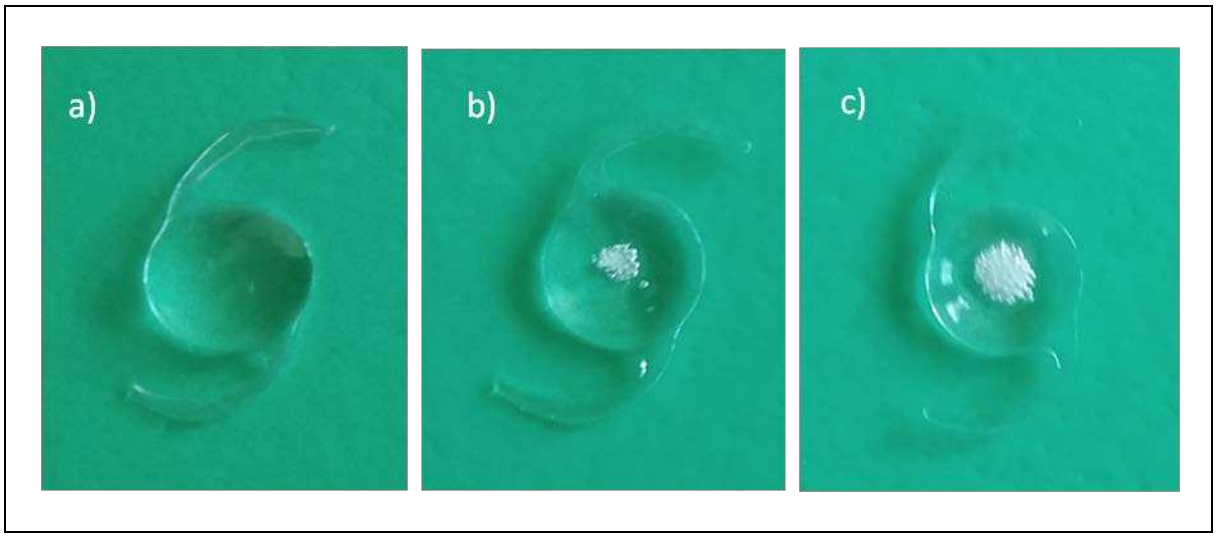

Figure III. 19 Influence of the pressurization flow rate on the visual aspect of some IOLs: a) non treated IOL, b) IOL treated with $scCO_2$ at 20 MPa with a pressurization flow rate of 0.65 $kg.h^{-1}$, c) IOL treated at 20 MPa with a pressurization flow rate of 0.900 $kg.h^{-1}$.

Due to the application of IOLs, foaming even with few bubbles had to be imperatively avoided. This was achieved by a controlled pressurization CO_2 flow rate of 0.25 $kg.h^{-1}$ coupled with a depressurization rate of 0.2 $MPa.min^{-1}$. Samples treated at abovementioned conditions resulted in transparent IOLs at both 8 and 20 MPa and in the presence or absence of a co-solvent (Figure III. 20).

Figure III. 20 Influence of the pressurization flow rate (0.25 $kg.h^{-1}$) on the visual aspect of IOLs treated with $scCO_2$ at 20 MPa: a) in the presence of ethanol (5 %mol), b) in the absence of co-solvent.

In the literature, foaming in polymers is generally reported to occur following certain conditions of depressurization. This is due to the quick desorption of a gaseous phase from a matrix during rapid depressurization. The rapid decrease in pressure leads to a decrease in the CO_2 sorption capacity of the polymer, inducing then a high supersaturation of CO_2 in the polymer. When the depressurization rate is high, the CO_2 cannot be completely released from the polymeric matrix. Nucleation and growth of bubbles of CO_2 occur until the pressure reaches to a point where foamed structure freezes [19]. The number and size of the created bubbles depend on the pressure, temperature and impregnation duration in addition to the depressurization rate [16], [20], [21].

In our work, even in slow depressurization conditions, foaming was observed for rapid pressurization phases suggesting that a brisk CO_2 sorption in P-HEMA lenses promotes sudden swelling and subsequent deformation. All $scCO_2$ treatments of P-HEMA IOLs (pre-treatments as well as impregnations) were performed at a CO_2 flow rate of 0.25 $kg.h^{-1}$ from hereon to avoid foaming and loss of optical properties during processing.

III. 4. 2. 2. IOLs pretreatment

Since the hydrophilic P-HEMA IOLs were supplied pre-conditioned in a physiological solution, a preliminary drying step was necessary to extract absorbed water and to obtain reproducible initial conditions for impregnation. At first, the influence of the drying mode (oven and $scCO_2$) was studied to understand the suitability of these methods and to determine required conditions for efficient drying.

The IOLs were dried in an oven at two temperatures (313 and 363 K) and DSC analyses were performed to determine the Tg of IOLs after this procedure. DSC analyses of the IOLs dried in an oven at 313 and 363 K showed a Tg of 386 and 394 K respectively (Table III. 17). This can be attributed to the efficient removal of water from IOLs at 363 K. Absorbed water in a polymeric matrix acts as a plasticizer which leads to a decrease in Tg as for samples dried at 313 K. The temperature of 363 K was efficient for the complete removal of water from P-HEMA IOLs.

DSC analyses of the IOLs dried with $scCO_2$ at (8 MPa, 30 min) and (14 MPa, 135 min) show a Tg of respectively 386 and 394 K (Table III. 17). Once again, the increase of Tg with increase in pressure and drying time can be explained by the efficient removal of water from P-HEMA IOLs.

Table III. 17 Tg of P-HEMA IOLs drying in an oven and with $scCO_2$.

Drying mode	Drying conditions	Tg (K)
Oven	313 K	386
Oven	363 K	394
$ScCO_2$	8 MPa and 308 K, 30 min	392
$ScCO_2$	14 MPa and 308 K, 135 min	394

A Tg of 394 K for IOLs dried by both oven (363 K) and $scCO_2$ (14 MPa, 308 K for 135 min) methods along with the same weight loss (0.21 g_{water} / $g_{dried\ IOL}$) indicated efficient removal the water at these conditions.

III. 4. 2. 3. Supercritical impregnation of P-HEMA IOLs

The supercritical impregnations of P-HEMA IOLs were carried out with both drugs: DXP and CIP in different operating conditions. The obtained results were presented in the following sections.

III. 4. 2. 3. 1. Dexamethasone 21-phosphate disodium salt impregnation

It is well known that the efficiency of the supercritical impregnation is not only dependent on the employed operating conditions but also on the physicochemical interactions between all involved substances in the process. The supercritical impregnation of DXP on P-HEMA IOLs was carried out at various conditions. The influence of pressure (8 and 20 MPa) and use of a co-solvent (5 %mol ethanol) on drug impregnation was studied for diopters +21.0 and +32.0 D. Other parameters i.e. temperature (308 K), impregnation duration (2 hours), pressurization (0.25 $kg.h^{-1}$) and depressurization rates (0.2 $MPa.min^{-1}$) were kept constant for all experiments.

The experimental conditions and impregnation yields for DXP loading are summarized in Table III. 18.

Table III. 18 Impregnation rates of IOLs of +21.0 D and +32.0 D diopters (at 308 K and 2 hours), determined by drug release studies (**40 days** of release).

		+21.0 D			+32.0 D		
N°	P	m_{0IOL}	m_{DXPimp}	Y_{imp}	m_{0IOL}	m_{DXPimp}	Y_{imp}
	MPa	mg	µg	$\mu g_{drug}/mg_{IOL}$	mg	µg	$\mu g_{drug}/mg_{IOL}$
Without co-solvent							
DXP_I	8	19.4	**165 ± 25**	**8.5 ± 1.3**	20.1	**171 ± 25**	**8.5 ± 1.3**
DXP_II	20	20.0	**182 ± 27**	**9.1 ± 1.4**	20.5	**191 ± 28**	**9.3 ± 1.4**
With co-solvent							
DXP_III	8	19.0	**247 ± 37**	**13.1 ± 2.0**	20.2	**266 ± 39**	**13.2 ± 2.0**
DXP_IV	20	19.5	**270 ± 40**	**13.8 ± 2.10**	20.3	**295 ± 43**	**14.5 ± 2.2**

Impregnation yields obtained at the different experimental conditions were comparable and reproducible for both diopters. The increase in pressure from 8 to 20 MPa had no significant effect on the amount of DXP impregnated in IOLs. However, higher impregnation yields were obtained upon the addition of ethanol in the processing media. The increase in pressure for samples processed with co-solvent did not show significant improvement in the drug loading. These results suggest that the use of co-solvent is favorable towards DXP impregnation. However, residual solvent can be a concern for ocular implants. Hence, NMR analyses were carried out on DXP impregnated IOLs to determine the presence of ethanol. Figure III. 21 compares NMR spectra of IOLs impregnated in the presence of a co-solvent with and without the washing step before depressurization. As it can be observed, ethanol peaks disappear when a supplementary CO_2 washing step is performed indicating a residual solvent content to be lower than 0.01 wt% of ethanol in the IOLs.

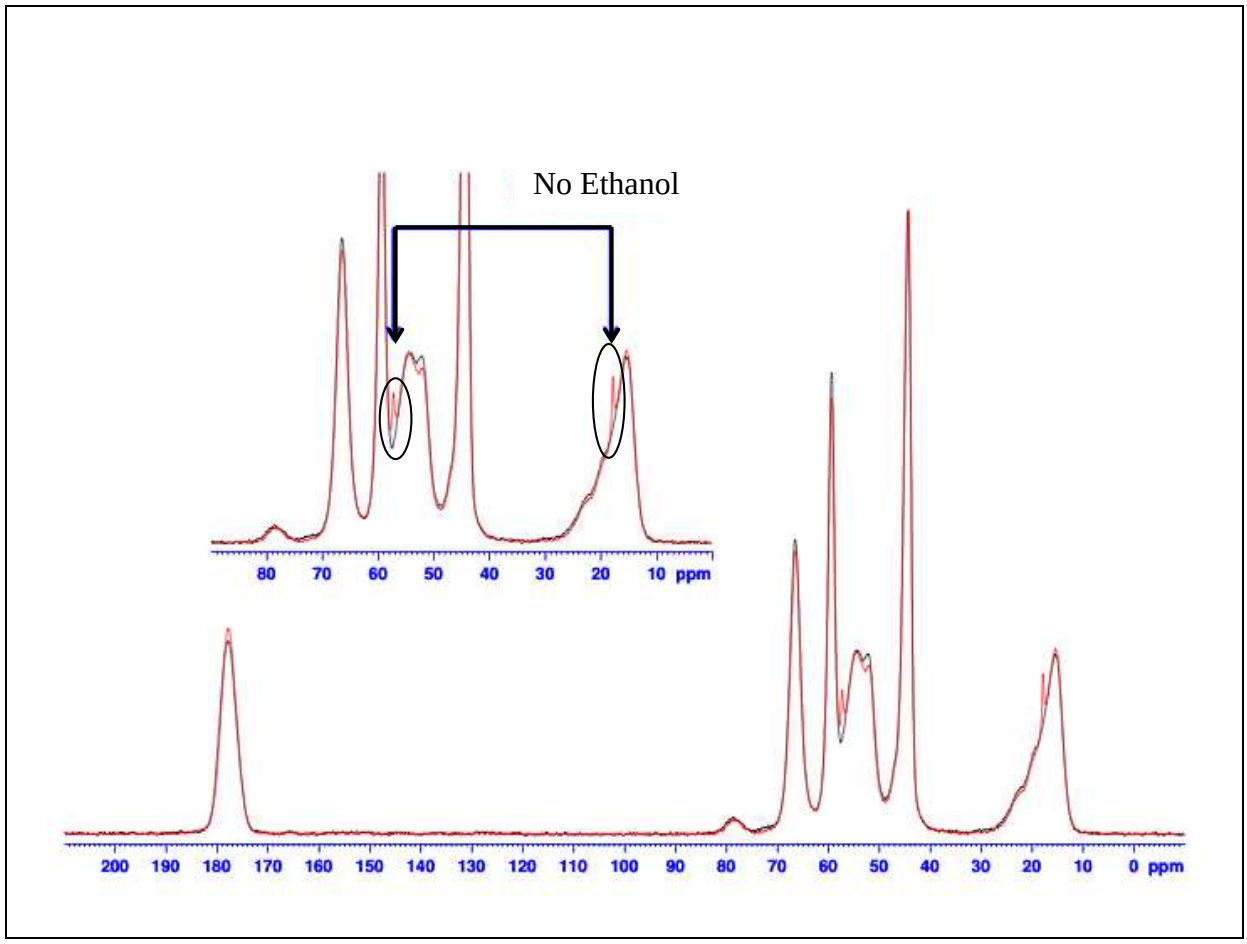

Figure III. 21 NMR analyses (13C) of an impregnated P-HEMA IOL with DXP at 20 MPa, 308 K, with 5 %mol of Ethanol and with a) a washing step (black) b) without a washing step (red).

The DXP release from impregnated IOLs is presented in Figure III. 22 and Figure III. 23 for both +21.0 and +32.0 D diopters. Samples prepared at both pressures, with or without co-solvent exhibited same release profile without any burst release. This indicates in-depth and homogenous impregnation of DXP within P-HEMA IOLs.

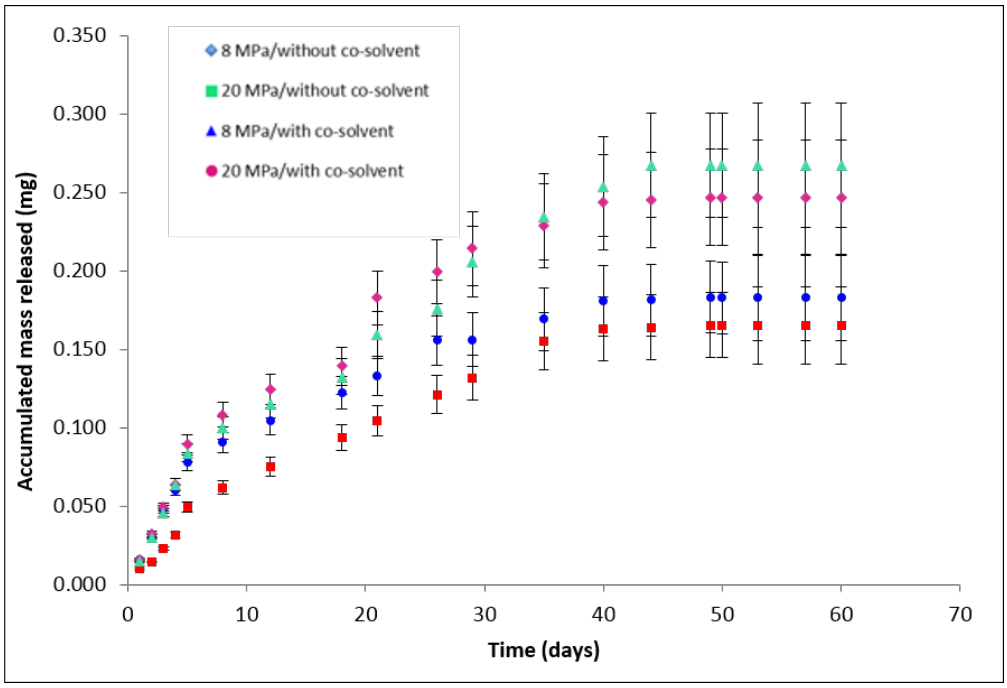

Figure III. 22 Accumulated drug release from IOLs (+21.0 D) impregnated at 308 K, pressurization flow rate of 0.25 kg.h^{-1}, impregnation duration of 2 hours and depressurization rate of 0.2 MPa.min^{-1}.

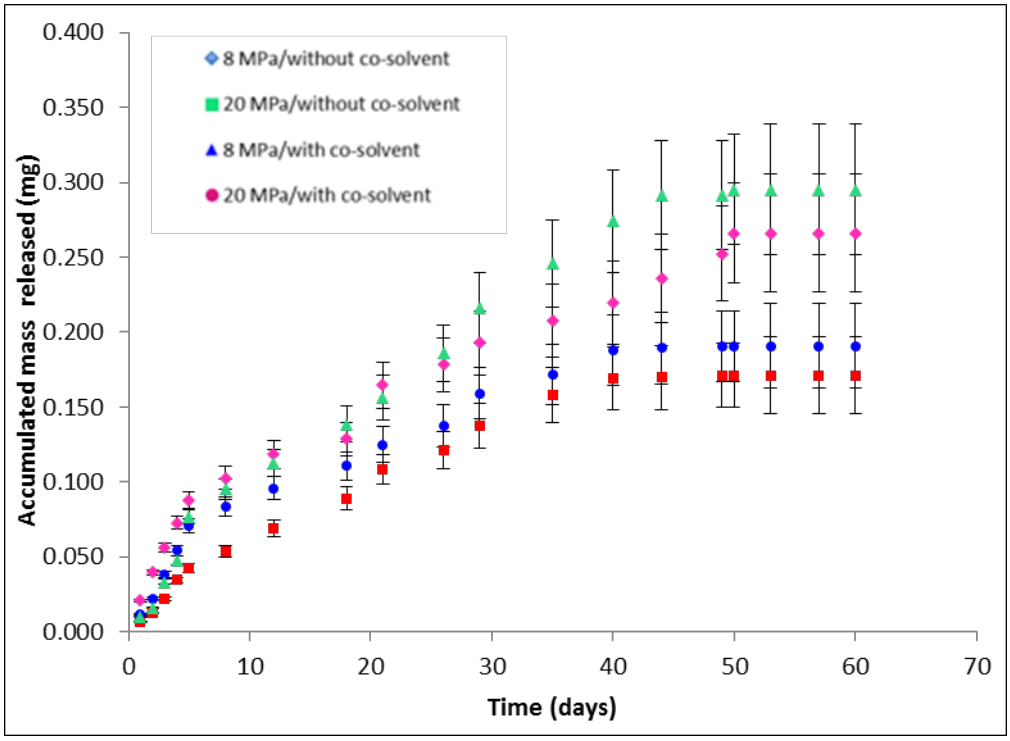

Figure III. 23 Accumulated drug release from IOLs (+32.0 D) impregnated at 308 K, pressurization flow rate of 0.25 kg.h^{-1}, impregnation duration of 2 hours and depressurization rate of 0.2 MPa.min^{-1}.

Release profiles of DXP were fitted with equation Eq. (2) and the release parameters are presented in Table III. 19.

Table III. 19 DXP release kinetic parameters obtained by fitting with Eq (2).

Experiments	Kinetics parameters					
	+21.0 D			+32.0 D		
	n	k	R^2	n	k	R^2
DXP_I	0.842	0.058	0.967	0.919	0.044	0.962
DXP_II	0.781	0.099	0.954	0.790	0.077	0.931
DXP_III	0.763	0.080	0.942	0.791	0.098	0.934
DXP_IV	0.733	0.072	0.946	0.929	0.038	0.944

Regression coefficients of more than 93% were obtained for both diopters prepared at discussed conditions. Furthermore, similar release exponents for the impregnated IOLs suggest DXP release to also occur by an anomalous transport type (*i.e.* the superimposition of Fickian controlled and swelling controlled release) [12][11]. This result is expected since the P-HEMA IOLs are hydrophilic and they plasticize in the presence of water.

III. 4. 2. 3. 2. Ciprofloxacin impregnation

a. Preliminary impregnations

IOLs were dried at 363 K in an oven before preliminary impregnation experiments. The drug impregnations were performed with and without co-solvent at 8 and 20 MPa on IOLs with two different diopters (+5.0 D and +21.0 D).

The impregnation results presented in Table III. 20 are expressed in term of the impregnated mass of ciprofloxacin in one IOL ($m_{cip\ imp}$) and the impregnation yield (Y_{imp}).

Table III. 20 Influence of the diopter on the drug loading at different conditions.

		+5.0 D				+21.0 D			
N°	P	m_{0IOL} (*)	$m_{CIP\ imp}$	Y_{imp}	$t_{release}$	m_{0IOL} (*)	$m_{CIP\ imp}$	Y_{imp}	$t_{release}$
	MPa	mg	µg	$\mu g_{drug}/mg_{IOL}$	days	mg	µg	$\mu g_{drug}/mg_{IOL}$	days
Without co-solvent									
CIP_I	8	11.9	**11 ± 0.2**	**0.9 ±** 0.1	**20**	20.1	**20 ±0.2**	**0.9 ± 0.1**	**≈ 20**
CIP_II	20	11.3	**39 ± 0.5**	**3.4 ±** 0.5	**40**	20.6	**59 ± 0.5**	**2.9 ± 0.3**	**≈ 40**
With co-solvent									
CIP_III	8	11.5	**44 ± 0.6**	**3.8 ±** 0.6	**40**	20.5	**61±0.5**	**3.0 ± 0.3**	**≈ 40**
CIP_IV	20	11.4	**47 ± 0.6**	**4.1 ±** 0.6	**40**	20.3	**65 ± 0.5**	**3.2 ± 0.3**	**≈ 40**

* Initial mass of the dry IOL before impregnation

In the absence of co-solvent, a pressure increase from 8 to 20 MPa led to improve CIP impregnation. The drug impregnation for diopter +5.0 D increased from 0.9 to 3.4 $\mu g_{drug}/mg_{IOL}$. Similarly, an increase from 0.9 to 2.9 $\mu g_{drug}/mg_{IOL}$ for diopter +21.0 D. This improvement in CIP loading can be attributed to the concurrent increase in the solubility of the drug (from 1.83 10^{-7} to 4.51 10^{-7} respectively) and polymer swelling due to CO_2 sorption [22]–[25]. With the addition of ethanol as co-solvent, the drug loadings were similar at 8 and 20 MPa. It is well known that co-solvent such as ethanol promotes the solubility of polar drugs in CO_2 by enhancing the overall polarity of the fluid phase. Furthermore, the CO_2 sorption and swelling/plasticizing can also increase with the addition of a co-solvent if polymer /CO_2/co-solvent interactions are favored [3], [17]. An absence of any further drug impregnation at higher pressure in the presence of ethanol could be either due to the saturation of IOLs or lack of improvement in polymer/drug interactions.

Interestingly, impregnation yields were comparable for samples processed with ethanol (CIP_III and CIP_IV) and only $scCO_2$ at 20 MPa (experiment CIP_II). Hence, CIP loading was performed without the use of co-solvent from hereon which is also preferable for the intended application.

In-vitro drug release from impregnated IOLs was conducted for 60 days for both diopters (+5.0 and +21.0 D). The release kinetics from CIP loaded IOLs is illustrated in Figure III. 24 and Figure III. 25. A continuous drug release of 20 days was obtained from IOLs impregnated at 8 MPa (CIP_I) without co-solvent in comparison to 40 days for samples prepared at 20

MPa (CIP_II) and with ethanol (CIP_III and IV). Drug release from lenses was sustained and without an initial burst (inset Figure III. 25.) which suggests in-depth (absence drug deposit on the surface) and homogeneous impregnation of the drug in IOLs.

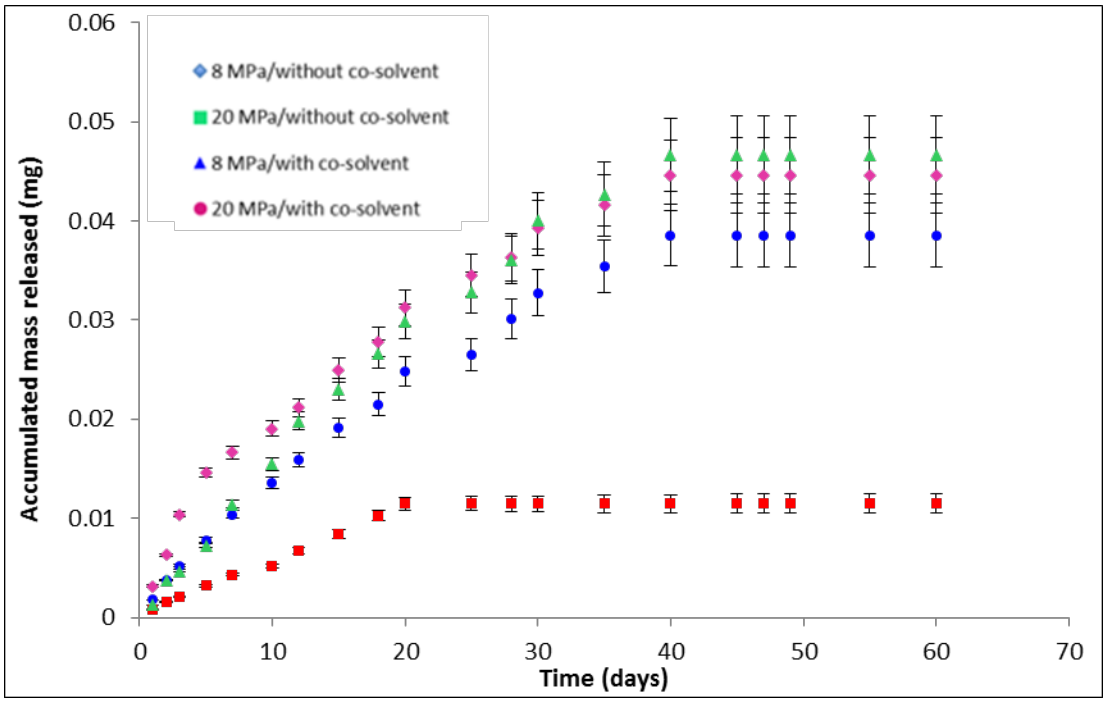

Figure III. 24 Accumulated drug release from IOLs (+5.0 D) impregnated at 308 K with the pressurization flow rate of 0.25 $kg.h^{-1}$, impregnation duration of 2 hours and depressurization rate of 0.2 $MPa.min^{-1}$.

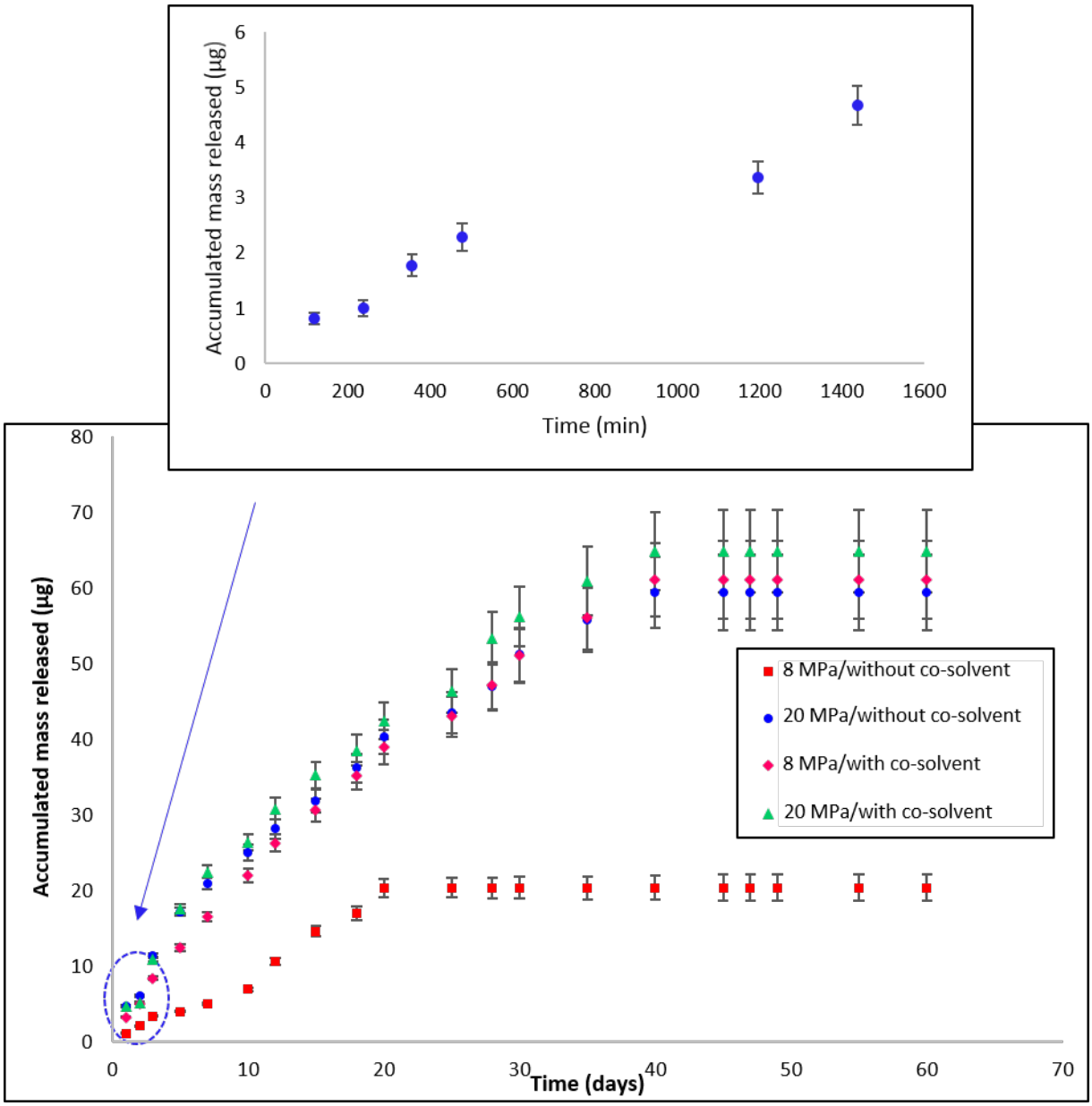

Figure III. 25 Accumulated drug release from IOLs (+21.0 D) impregnated at 308 K with the pressurization flow rate of 0.25 kg.h^{-1}, impregnation duration of 2 hours and depressurization rate of 0.2 MPa.min^{-1}.

Release profiles discussed above were fitted with equation Eq. (2) and the fitting parameters obtained for both diopters (+5.0 and +21.0 D) are summarized in Table III. 21.

Table III. 21 CIP release kinetic parameters obtained by fitting with Eq (2).

Experiments	Kinetics parameters					
	+5.0 D			+21.0 D		
	n	K	R^2	n	k	R^2
CIP_I	0.835	0.072	0.995	0.748	0.076	0.972
CIP_II	0.907	0.043	0.962	0.810	0.058	0.975
CIP_III	0.866	0.052	0.987	0.842	0.052	0.997
CIP_IV	0.884	0.050	0.994	0.794	0.065	0.965

For all the experiments, the exponent value (n) is ranging between 0.5 and 1.0 which suggests that the drug release occurred by an anomalous transport type (*i.e.* the superimposition of Fickian controlled and swelling controlled release) [12][11].

The release rate constant (k) decreased as the impregnation pressure increased or when a co-solvent was used. This indicates that the affinity between P-HEMA IOLs and CIP increases with the increase in pressure or the addition of a co-solvent [26]. A regression coefficient of higher than 96% indicates that the model currently used fits well with drug release profiles. Release exponents were similar for IOLs impregnated in different conditions for both diopters.

b. Experimental design

Following the results of the first series of experiments, it could be concluded that drug loadings were significantly influenced by the change in pressure in the absence of a co-solvent. Moreover, increase in pressure in the presence of co-solvent had no significant influence on the impregnation yield. Therefore, a response surface methodology based on experimental design was used to study the influence of operating conditions on the impregnation of CIP on +21. 0 D IOLs. Two entry values with 5 levels each were considered: pressure (8 to 20 MPa) and impregnation duration (30 to 240 min).

The operational conditions and results from these experiments are summarized in the Table III. 22. All impregnations were carried out at 308 K with a CO_2 flow rate (for pressurization) of 0.25 $kg.h^{-1}$ and a depressurization rate of 0.2 $MPa.min^{-1}$ without the use of co-solvent. The repeatability of the experiment in the middle of domain (CIP_ED_IX) was verified (Appendix B).

Table III. 22 Experimental design conditions for supercritical impregnation of IOLs (+21.0D).

N°	P	t_{imp}	m_{0IOL}	$m_{CIP\ imp}$	Y_{imp}	$t_{release}$
	MPa	min	mg±0.2	µg	$\mu g_{drug}/mg_{IOL}$	Days
CIP_ED*_I	10	60	19.0	**26 ± 0.2**	**1.4 ± 0.1**	≈ **18**
CIP_ED_II	10	210	18.6	**30 ± 0.3**	**1.6 ± 0.1**	≈ **40**
CIP_ED_III	18	60	18.9	**39 ± 0.3**	**2.1 ± 0.2**	≈ **30**
CIP_ED_IV	18	210	19.5	**53 ± 0.4**	**2.7 ± 0.2**	≈ **40**
CIP_ED_V	14	30	19.2	**22 ± 0.1**	**1.1 ± 0.1**	≈ **18**
CIP_ED_VI	14	240	20.0	**41 ± 0.3**	**2.0 ±0.1**	≈ **45**
CIP_ED_VII	8	135	19.1	**21 ± 0.2**	**1.1 ± 0.1**	≈ **10**
CIP_ED_VIII	20	135	19.5	**67 ± 0.4**	**3.4 ± 0.2**	≈ **45**
CIP_ED_IX	14	135	18.8	**35 ± 0.1**	**1.7 ±0.0**	≈ **20**
CIP_ED_IX**	14	135	18.8	**31 ± 0.1**	**1.6 ± 0.0**	≈ **20**

* ED: Experimental design.

** For this drug release experiment, a single sample was collected at the end of release to quantify the drug release.

For the different experimental conditions, impregnated amounts ranged between 21 - 67 µg which suggests that the studied factors have noteworthy an influence on the response surface. Figure III. 26 presents release kinetics of CIP impregnated samples prepared at different pressures and durations.

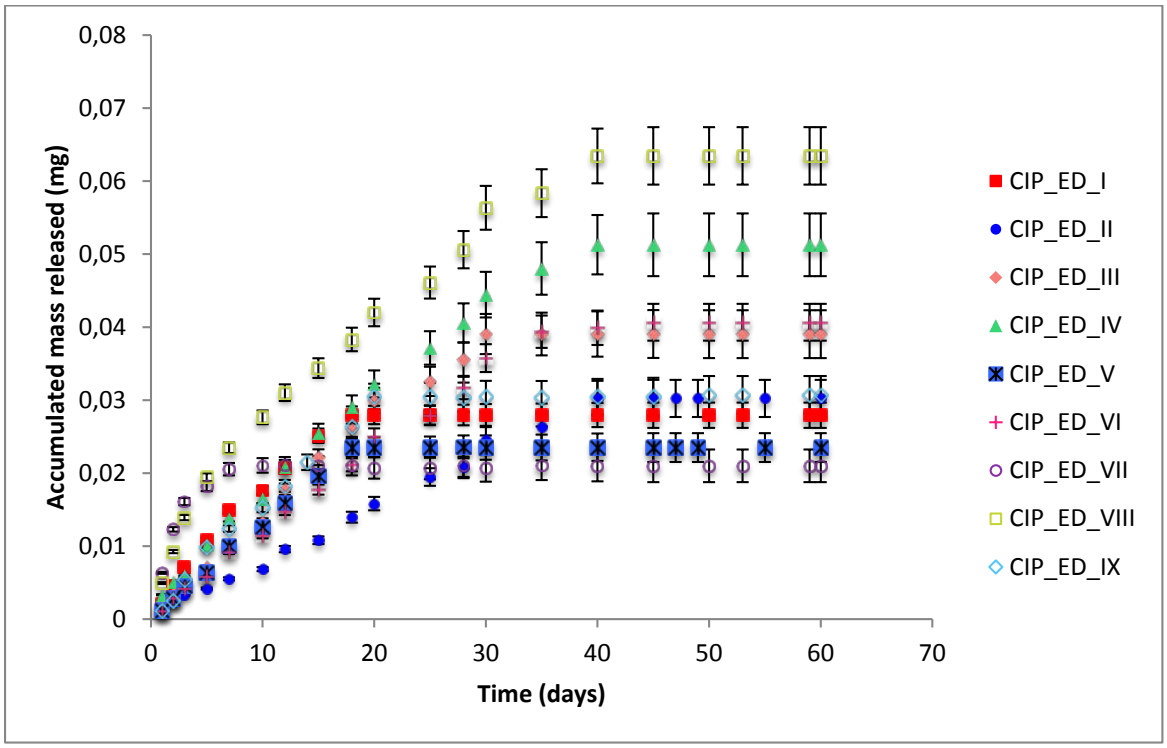

Figure III. 26 Accumulated drug release from IOLs (+21.0 D) impregnated, using experimental design, at 308 K, pressurization flow rate of 0.25 $kg.h^{-1}$, without co-solvent and depressurization rate of 0.2 $MPa.min^{-1}$.

The drug release duration was dependent on the mass of CIP impregnated in IOLs at various conditions. For example, a sustained release ranging from 10 - 30 days was obtained for CIP_ED_I, III, V, VII and IX. Whereas, samples with higher impregnation yields (CIP_ED_II, IV, VI and VIII) showed drug release for significantly longer durations (40-45 days).

Figure III. 27 presents examples of samples prepared at 14 and 18 MPa to explain the effect of impregnation duration on release kinetics. It is interesting to note that the drug release is always higher and extended for samples prepared with longer impregnation durations at a given pressure even when slopes do not appear significantly dissimilar. Therefore, it can be concluded that increasing the impregnation time allows a more in-depth diffusion of the drug facilitated by the improved swelling of the polymer.

a)

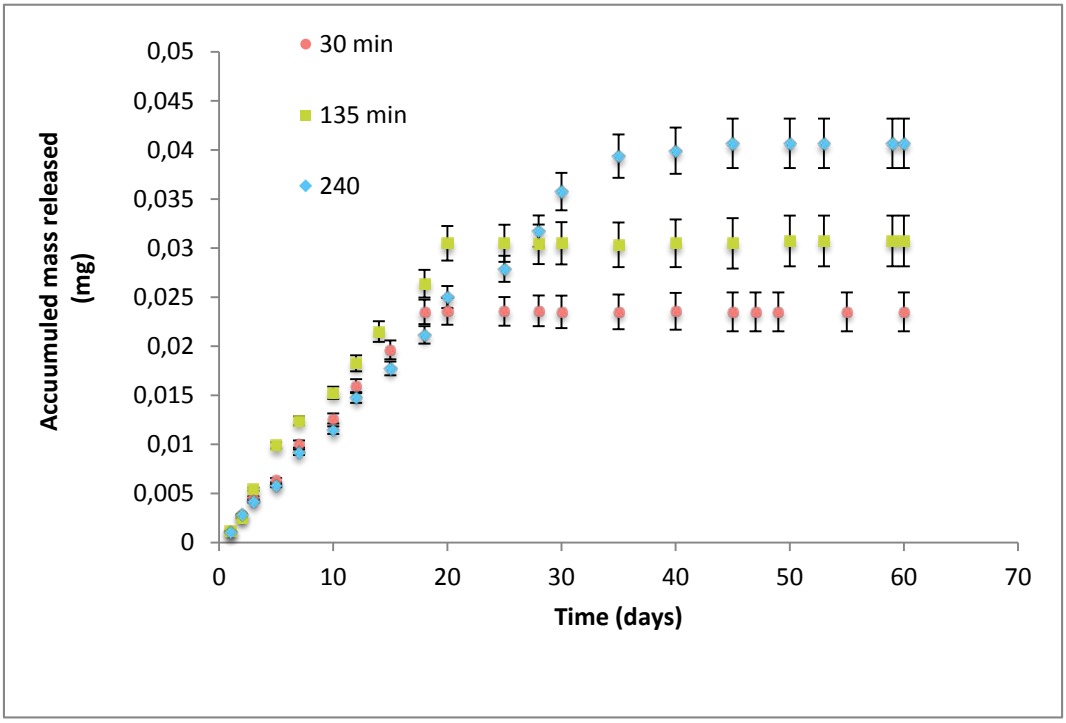

b)

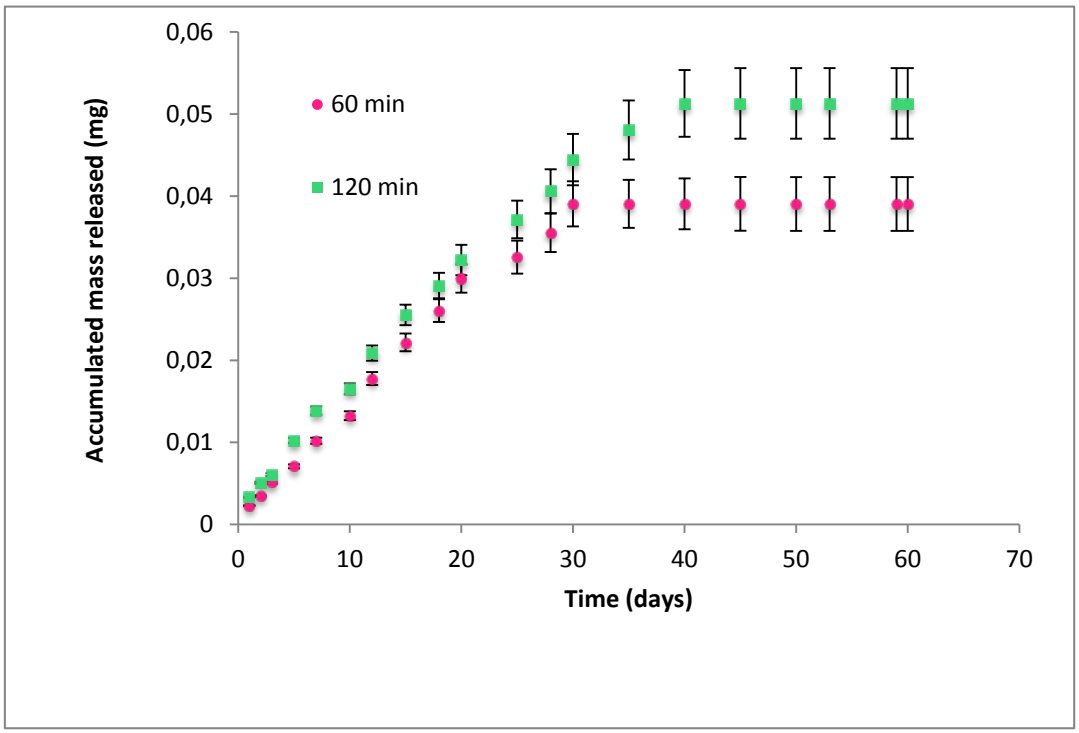

Figure III. 27 Accumulated drug release from IOLs (+21.0 D) impregnated, using experimental design, at a) 14 MPa (experiment CIP_ED_V, IX and VI), b) 18 MPa (experiments CIP_ED_III and IV).

Release profiles were fitted to equation Eq. (2) to obtain release exponents for impregnated IOLs similar to the preliminary experiments. The fitting parameters obtained for IOL samples are summarized in Table III. 23.

Table III. 23 CIP release kinetic parameters obtained by fitting with Eq (2).

	Kinetics parameters		
	+21.0 D		
Samples	n	k	R^2
CIP_I	0.555	0.133	0.977
CIP_II	0.837	0.039	0.987
CIP_III	0.685	0.090	0.981
CIP_IV	0.772	0.058	0.991
CIP_V	0.727	0.061	0.985
CIP_VI	0.982	0.031	0.991
CIP_VII	0.859	0.307	0.992
CIP_VIII	0.839	0.053	0.989
CIP_IX	0.894	0.123	0.972

Similar to preliminary experiments, release exponents ranging between 0.5 and 1 confirm drug release occurring following an anomalous transport type (i.e. the superimposition of Fickian controlled and swelling controlled release). The impregnated amounts obtained from release profiles were used to calculate an impregnation model by multilinear regression. The model coefficients are presented in the Eq. 4 and a regression coefficient (R^2) of 0.945 suggests that this model can be considered as reliable tool to predict changes in impregnated amounts within the studied operating conditions.

$$y = 0.032 + 0.012\,x_1 + 0.005\,x_2 + 0.006x_{11}^2 - 0.001x_{22}^2 + 0.002x_{12} \qquad Eq.4$$

Figure III. 28 shows the impregnated amount predicted by the RSM model in terms of pressure and impregnation duration.

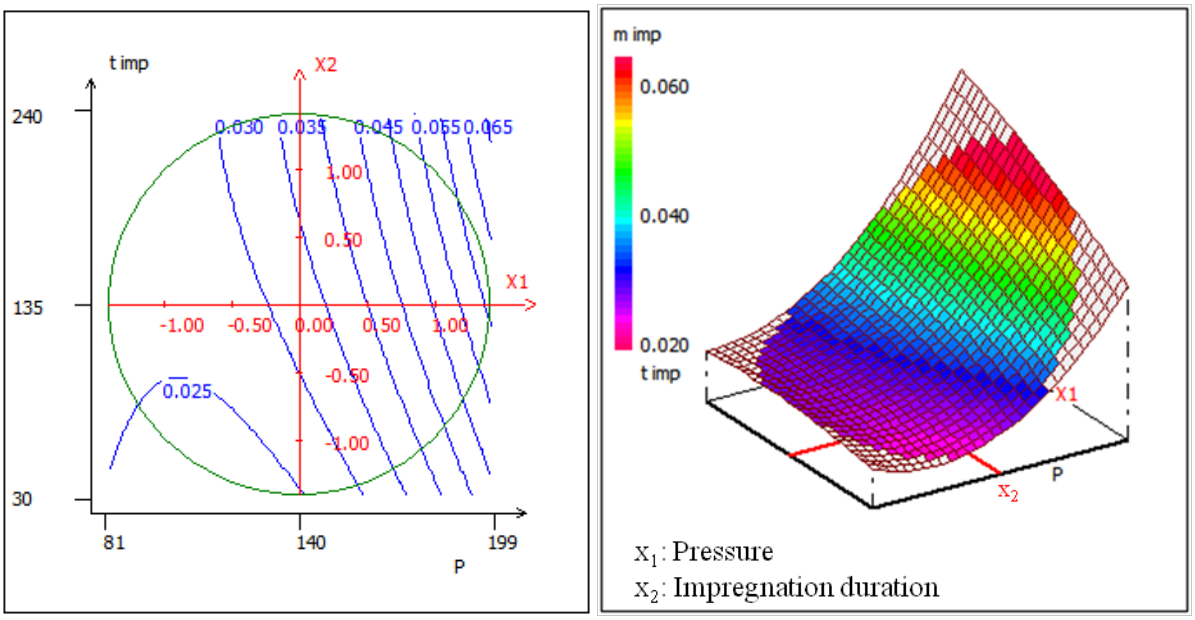

Figure III. 28 A two-dimensional contour plot and a three-dimensional response surface of impregnated mass (mg) illustrating optimal conditions for the supercritical impregnation of P-HEMA IOLs with CIP.

A high variation of response in terms of drug loading in IOLs with the pressure increase is evident in Figure III. 28. This is expected due to improved drug solubility and swelling/plasticization of polymers in $scCO_2$ at higher pressures [22]–[25], [27], [28]. The effect of impregnation duration is minimal at low pressures but significant at pressures above 14 MPa. A direct impact of increase in processing time on drug impregnation at higher pressures is apparent in Figure III. 28. This could also be attributed to higher CO_2 sorption resulting in polymer swelling and improved dissolution of CIP. In other words, it could be suggested that thermodynamic equilibrium was not reached at low impregnation durations.

The lowest drug loading of 21 µg was obtained on samples processed at 8 MPa for 135 minutes whilst highest drug loading (67 µg) was achieved at 20 MPa for the same duration. 8 and 20 MPa were the lowest and highest pressures studied in this work and response surface clearly shows high pressure as the key factor for efficient drug impregnation in IOLs.

III. 4. 3. Comparison between PMMA and P-HEMA IOLs impregnation

This work aimed to study the impregnation of two types of IOLs: rigid IOLs (PMMA) and foldable IOLs (P-HEMA) with two ophthalmic drugs: DXP and CIP. The influence of the

pressure and the presence of co-solvent for both kinds of IOLs and with both drugs was studied and discussed above.

As illustrated in Table III. 24, in absence of co-solvent and for both systems PMMA and P-HEMA/DXP, increasing pressure had no influence on the impregnation and interestingly, impregnation yields were comparable. Addition of co-solvent improves the impregnation for both systems at low pressure (8 MPa). However, the increase in pressure from 8 to 20 MPa in presence of co-solvent was unfavorable for impregnation of PMMA/DXP system and had no significant effect (but maintained the same impregnation yield) for the system P-HEMA DXP. One explanation could be a weaker affinity between PMMA/DXP compared to P-HEMA /DXP system which favors the partition coefficient towards the fluid phase at high pressure in the presence of co-solvent.

In the absence of co-solvent, the partition coefficient (K) decreases with an increase of pressure (from 8 to 20 MPa) for both types of IOLs, we explain this phenomenon by two factors, first an increase in CO_2 density results in increased solvent power of CO_2, and thus solubility of DXP in the fluid phase increases ($1.22\ 10^{-7}$ to $2.15\ 10^{-7}$ in molar fraction). At the same time, increasing the CO_2 density results in an increase of swelling of PMMA matrix. The partition coefficients for both IOLs loaded with DXP were quite similar in the absence of co-solvent ($5.\ 88\ 10^3$ and $5.\ 94\ 10^3$ at 8 MPa and $3.44\ 10^3$ and $3.61\ 10^3$ at 20 MPa) and this could be explained by a quite similar affinity between DXP and both IOLs (PMMA and P-HEMA) in these conditions.

Table III. 24 Impregnation of PMMA and P-HEMA IOLs with DXP.

	PMMA			P-HEMA		
Pressure	$m_{DXP\ imp}$	Y_{imp}	K	$m_{DXP\ imp}$	Y_{imp}	K
MPa	µg	µg $_{drug}$/mg $_{IOL}$	-	µg	µg $_{drug}$/mg $_{IOL}$	-
Without co-solvent						
8	159 ±24	8.4 ±1.3	$5.88\ 10^3$	165 ± 2.4	8.5 ± 1.3	$5.94\ 10^3$
20	165 ± 24	8.7 ± 1.3	$3.44\ 10^3$	182 ± 2.7	9.1 ± 1.4	$3.61\ 10^3$
With co-solvent						
8	240 ± 36	12.0 ± 1.8	-	247 ± 3.7	13.1 ± 2.0	-
20	99 ± 15	4.9 ± 0.7	-	270 ± 4.0	13.8 ± 2.1	-

Regarding the impregnation of CIP and as we can observe in the Table III. 25, in absence of co-solvent and for both loaded systems PMMA and P-HEMA/CIP, pressure increasing enhances impregnation. The addition of ethanol as a co-solvent in the procedure resulted in

significant increase in drug impregnation at lower pressure (8 MPa). Nevertheless, the increase in pressure from 8 to 20 MPa in presence of co-solvent had no significant effect (but maintains the same impregnation yields) for both IOLs.

In the absence of co-solvent, the partition coefficient (K) increases in the same way with an increase in pressure (from 8 to 20 MPa) for both types of IOLs. These results could be explained by two factors, first an increase in the CIP solubility in the fluid phase ($1.83\ 10^{-7}$ to $4.51\ 10^{-7}$) and a weak affinity between CIP and both kinds of IOLs.

In the absence of co-solvent, the partition coefficients for both IOLs loaded with CIP were quite comparable and this could be explained by a quite similar affinity between CIP and both IOLs (PMMA and P-HEMA).

Table III. 25 Impregnation of PMMA and P-HEMA IOLs with CIP.

	PMMA			P-HEMA		
Pressure	$m_{CIP\ imp}$	Y_{imp}	K	$m_{CIP\ imp}$	Y_{imp}	K
MPa	µg	µg $_{drug}$/mg $_{IOL}$	-	µg	µg $_{drug}$/mg $_{IOL}$	-
Without co-solvent						
8	16 ± 1	0.8 ± 0.1	$6.11\ 10^2$	20 ± 0.2	0.95 ± 0.1	$7.22\ 10^2$
20	48 ± 4	2.4 ± 0.2	$7.21\ 10^2$	59 ±0.5	2.86 ± 0.3	$8.44\ 10^2$
With co-solvent						
8	55 ± 5	2.8 ± 0.1	-	61 ± 0.5	2.98 ± 0.3	-
20	57 ± 5	2.8 ± 0.2	-	65 ± 0.5	3.20 ± 0.3	-

III. 4. Conclusions

IOLs have proven significance in the field of therapeutics and their development is an upcoming route for ocular drug delivery [29]. This work aimed to prepare drug impregnated rigid and foldable intraocular lenses (PMMA and P-HEMA) in order to combine cataract surgery and postoperative treatment in a single procedure. Two commonly used drugs, ciprofloxacin and dexamethasone 21-phosphate disodium to prevent cataract postoperative complications were studied in this work. The supercritical impregnation was carried out in a batch mode and the impregnated yields were determined by drug release studies for both types of IOLs.

Regarding the first part of this work, PMMA IOLs were loaded with DXP and CIP in various impregnation conditions. The pressurization flow rate has no influence on the visual aspect of IOLs. For PMMA/DXP system, supercritical impregnations were initially performed at different conditions of pressure, temperature, impregnation duration and presence/quantity of co-solvent. Drug loading improvement in presence of co-solvent was obtained at 8 MPa. While, an increase in pressure in presence of co-solvent leads to a decrease in impregnation yields. The increase in temperature and impregnation duration was unfavorable to impregnation.

Following the results of the preliminary experiments, a response surface methodology based on experimental designs was applied to study the influence of operating conditions on impregnation. Two input variables were considered: amount of co-solvent (1 to 10 %mol) and impregnation duration (30 to 240 min). DXP impregnation yields ranging between 5.64 and 18.35 μg/mg were obtained. The response surface indicated the impregnation duration to be the governing factor in impregnation where decrease in impregnation duration promoted drug loading. The variation in the amount of co-solvent, has a low but complex influence on impregnation. However, the higher impregnation amount was obtained at short impregnation duration (30 min) and low quantity of co-solvent (5.5 %mol).

The influence of pressure and presence of co-solvent was studied on the second system PMMA/CIP. Unlike DXP, in absence of co-solvent, increasing pressure enhances impregnation. However, in the presence of ethanol, the increase in pressure (from 8 to 20 MPa) did not affect the drug loading.

The highest impregnation yields for DXP and CIP in PMMA lenses were 18.3 and 2.9 $\mu g/mg_{IOL}$ respectively indicating higher affinity of DXP for PMMA IOLs than CIP and this result was confirmed by the values of partition coefficient.

The second part of this work concerns the impregnation of foldable P-HEMA IOLs with DXP and CIP. The importance of coupling slow pressurization and depressurization phases during supercritical treatment of IOLs was demonstrated in order to avoid the appearance of undesirable foaming. Coupling slow pressurization (flow rate of 0.25 $kg.h^{-1}$) and depressurization (at 0.2 $MPa.min^{-1}$) was necessary to maintain the clearness of P-HEMA IOLs.

A pretreatment step to remove the sorbed aqueous solution on P-HEMA lenses was carried out using two different methods: oven and $scCO_2$. DSC analyses of IOLs dried in an oven at 363 K and with $scCO_2$ at 313 K and 14 MPa for 135 min showed same Tg (394 K) confirming efficient removal of water.

The influence of different parameters on the impregnation with DXP and CIP was studied. For the system PMMA/DXP, the influence of pressure (8 and 20 MPa) and the use of a co-solvent was studied. The use of ethanol (5 %mol) as a co-solvent improves DXP impregnation in IOLs of both diopters (+21.0 and 32.0 D). The DXP loading involved addition of a washing step to ensure the removal of residual ethanol from P-HEMA IOLs.

For P-HEMA/CIP system, supercritical impregnations were initially carried out at pressures 8 and 20 MPa in the presence or absence of ethanol as a co-solvent for two diopters (+5.0 D and +21.0 D). Unlike DXP, drug loading enhancement with the pressure was observed in the absence of co-solvent for both diopters. Whereas, addition of co-solvent had no further improvement in the impregnation yield of CIP. Once again and following the results of the first series of experiments, a response surface methodology based on experimental designs was applied to study the influence of operating conditions on impregnation in the absence of a co-solvent. Two input variables were considered: pressure (8 to 20 MPa) and impregnation duration (30 to 240 min). The CIP impregnation ranging between 1.1 to 3.4 μg/mg was obtained from these experiments. The response surface indicated the pressure to be the governing factor in impregnation as an increase in pressure promoted drug loading. The effect of impregnation duration on CIP loading was only obvious at relatively high pressures (>14 MPa).

The highest impregnation yields for DXP and CIP in P-HEMA lenses were 14.53 and 4.12 $\mu g/mg_{IOL}$ respectively. This indicates higher affinity of DXP for P-HEMA IOLs than CIP and this result was confirmed by the values of partition coefficient. Despite the low solubility of drugs (DXP and CIP) in the fluid phase, we have successfully obtained a homogeneous and in depth impregnation of IOLs (PMMA and P-HEMA).

A prolonged drug delivery during 40 days was obtained for most impregnation experiments (both kinds of IOLs).

This study provides important information on the impregnation of two commonly used drugs in the complications related to cataract surgery on P-HEMA IOLs which could be used to carry out simultaneous loading of both drugs in the future.

NMR analyses were performed on drug (DXP and CIP) impregnated lenses (PMMA and P-HEMA) in the presence of a co-solvent and did not show presence of residual ethanol. These results showed that impregnated IOLs are suitable for ophthalmic application.

References

[1] J. . Aquavella and G. . Rao, “Contact lenses,” *J.B. Lippincot, Philadelphia*, pp. 47–225, 1987.

[2] R. M. Pellegrino, F. Segoloni, and C. Cagini, “Simultaneous determination of Ciprofloxacin and the active metabolite of Prulifloxacin in aqueous human humor by high-performance liquid chromatography.,” *J. Pharm. Biomed. Anal.*, vol. 47, no. 3, pp. 567–74, Jul. 2008.

[3] Y. Masmoudi, L. Ben Azzouk, O. Forzano, J.-M. Andre, and E. Badens, “Supercritical impregnation of intraocular lenses,” *J. Supercrit. Fluids*, vol. 60, pp. 98–105, Dec. 2011.

[4] D. Baş and İ. H. Boyacı, “Modeling and optimization I: Usability of response surface methodology,” *J. Food Eng.*, vol. 78, no. 3, pp. 836–845, Feb. 2007.

[5] J. Schaefer and E. O. Stejskal, “Carbon-13 nuclear magnetic resonance of polymers spinning at the magic angle,” *J. Am. Chem. Soc.*, vol. 98, no. 4, pp. 1031–1032, 1976.

[6] R. L. Cook, C. H. Langford, C. Tn, and C. M. Preston, “97/02437 A modified cross-polarization magic angle spinning 13C NMR procedure for the study of humic materials,” *Fuel Energy Abstr.*, vol. 38, no. 3, p. 193, 1997.

[7] O. B. Peersen, X. L. Wu, I. Kustanovich, and S. O. Smith, “Variable-Amplitude Cross-Polarization MAS NMR,” *J. Magn. Reson. Ser. A*, vol. 104, no. 3, pp. 334–339, Oct. 1993.

[8] G. Gerbaud, F. Ziarelli, and S. Caldarelli, “Increasing the robustness of heteronuclear decoupling in magic-angle sample spinning solid-state NMR,” *Chem. Phys. Lett.*, vol. 377, no. 1–2, pp. 1–5, Aug. 2003.

[9] W. I. Higuchi, “Diffusional Models Useful in Biopharmaceutics,” *J. Pharm. Sci.*, vol. 56, no. 3, pp. 315–324, 1967.

[10] I. Galdi and G. Lamberti, “Drug release from matrix systems: analysis by finite element methods,” *Heat Mass Transf.*, vol. 48, no. 3, pp. 519–528, 2012.

[11] P. L. Ritger and N. Peppas, “A simple equation for description of solute release I. Fickian and non-fickian release from non-swellable devices in the form of slabs, spheres, cylinders or discs,” *J. Control. Release*, vol. 5, no. 1, pp. 23–36, 1987.

[12] P. L. Ritger and N. a. Peppas, “A simple equation for description of solute release II. Fickian and anomalous release from swellable devices,” *J. Control. Release*, vol. 5, no. 1, pp. 37–42, 1987.

[13] C.-A. Lee, M. Tang, and Y.-P. Chen, “Measurement and correlation for the solubilities of cinnarizine, pentoxifylline, and piracetam in supercritical carbon dioxide,” *Fluid Phase Equilib.*, vol. 367, pp. 182–187, Apr. 2014.

[14] Y.-P. Chen, “Personal communication, National Taiwan University,” 2015.

[15] R. B. Chim, M. B. C. de Matos, M. E. M. Braga, a. M. a. Dias, and H. C. de Sousa, “Solubility of Dexamethasone in Supercritical Carbon Dioxide,” *J. Chem. Eng. Data*, vol. 57, no. 12, pp. 3756–3760, Dec. 2012.

[16] E. Reverchon and S. Cardea, “Production of controlled polymeric foams by

supercritical CO2," *J. Supercrit. Fluids*, vol. 40, no. 1, pp. 144–152, 2007.

[17] V. P. Costa, M. E. M. Braga, C. M. M. Duarte, C. Alvarez-Lorenzo, A. Concheiro, and H. C. Gil, Maria H.de Sousa, "Anti-glaucoma drug-loaded contact lenses prepared using supercritical solvent impregnation," *J. Supercrit. Fluids*, vol. 53, no. 1–3, pp. 165–173, Jun. 2010.

[18] S. Üzer, U. Akman, and Ö. Hortaçsu, "Polymer swelling and impregnation using supercritical CO2: A model-component study towards producing controlled-release drugs," *J. Supercrit. Fluids*, vol. 38, no. 1, pp. 119–128, Aug. 2006.

[19] S. G. Kazarian, *Supercritical Fluid Impregnation of Polymers for Drug Delivery, Supercritical Fluid Technology for Drug Product Development*, Marcel Dek. New York, 2004.

[20] S. K. Goel and E. J. Beckman, "Generation of Microcellular Polymeric Foams Using Supercritical Carbon Dioxide. I: Effect of Pressure and Temperature on," vol. 3, no. 74.

[21] Z. M. Xu, X. L. Jiang, T. Liu, G. H. Hu, L. Zhao, Z. N. Zhu, and W. K. Yuan, "Foaming of polypropylene with supercritical carbon dioxide," *J. Supercrit. Fluids*, vol. 41, no. 2, pp. 299–310, 2007.

[22] O. Guney and A. Akgerman, "Synthesis of controlled-release products in supercritical medium," *AIChE J.*, vol. 48, no. 4, pp. 856–866, 2002.

[23] M. E. M. Braga, H. S. R. C. Silva, M. H. Gil, M. T. V. Pato, E. I. Ferreira, C. M. M. Duarte, and H. C. de Sousa, "Supercritical solvent impregnation of ophthalmic drugs on chitosan derivatives," *J. Supercrit. Fluids*, vol. 44, no. 2, pp. 245–257, Mar. 2008.

[24] M. Champeau, J.-M. Thomassin, T. Tassaing, and C. Jerome, "Drug Loading of Sutures by Supercritical CO $_2$ Impregnation: Effect of Polymer/Drug Interactions and Thermal Transitions," *Macromol. Mater. Eng.*, vol. 300, no. 6, pp. 596–610, 2015.

[25] J. Yu, Y. Guan, S. Yao, and Z. Zhu, "Preparation of Roxithromycin-Loaded Poly (l - lactic Acid) Films with Supercritical Solution Impregnation," pp. 13813–13818, 2011.

[26] F. Yañez, L. Martikainen, M. E. M. Braga, C. Alvarez-Lorenzo, A. Concheiro, C. M. M. Duarte, M. H. Gil, and H. C. de Sousa, "Supercritical fluid-assisted preparation of imprinted contact lenses for drug delivery.," *Acta Biomater.*, vol. 7, no. 3, pp. 1019–1030, Mar. 2011.

[27] V. P. Costa, M. E. M. Braga, J. P. Guerra, A. R. C. Duarte, C. M. M. Duarte, E. O. B. Leite, M. H. Gil, and H. C. de Sousa, "Development of therapeutic contact lenses using a supercritical solvent impregnation method," *J. Supercrit. Fluids*, vol. 52, no. 3, pp. 306–316, Apr. 2010.

[28] M. Champeau, J.-M. Thomassin, T. Tassaing, and C. Jérôme, "Drug Loading of Polymer Implants by Supercritical CO2 Assisted Impregnation: a Review," *J. Control. Release*, vol. 209, pp. 248–259, 2015.

[29] M. Aqil and H. Gupta, "Contact lenses in ocular therapeutics," *Drug Discov. Today*, vol. 17, no. 9–10, pp. 522–527, May 2012.

CHAPTER IV
Impregnation of silica

Table contents

IV. 1. Introduction **160**
IV. 2. Materials **160**
IV. 2. 1. Silica **160**
IV. 2. 2. Fenofibrate **160**
IV. 2. 3. Solvent **161**
IV. 3. Methods **161**
IV. 3. 1. Impregnation procedures **161**
IV. 3. 1. 1. Impregnation via incipient wetness 161
IV. 3. 1. 2. Supercritical impregnation 162
IV. 3. 2. Characterization of silica **162**
IV. 3. 2. 1. Nitrogen adsorption **162**
IV. 3. 2. 2. Transmission electron microscopy (TEM) **162**
IV. 3. 2. 3. X-ray diffraction (XRD) **163**
IV. 3. 2. 4. Impregnation yields **163**
IV. 3. 2. 5. Differential scanning calorimetry (DSC) **163**
IV. 4. Results and discussions **163**
IV. 4. 1. Characterization of silica before impregnation **164**
IV. 4. 2. Impregnation using incipient wetness **165**
IV. 4. 3. Influence of supercritical treatment on silica structural properties **165**
IV. 4. 4 Supercritical impregnation **166**
IV. 5 Conclusion **170**
References **171**

IV. 1. Introduction

This part of PhD work is performed within the framework of a collaboration with Formac pharmaceuticals (Belgium) and aims to elaborate suitable dosage formulations for oral administration of poorly-water soluble drugs. Mesoporous silica was chosen as impregnation support because of its high porosity and hydrophilicity, which should improve the dissolution kinetics and/or the solubility of hydrophobic drugs. Fenofibrate was chosen as an example of a poorly water-soluble drug, representative of Class II drugs as defined by the biopharmaceutics classification system [1]. It is highly lipophilic and is used clinically to lower lipid levels in the body [2].

The objective of this work is to achieve a high loading of Fenofibrate with a low degree of crystallinity since the dissolution of an amorphous drug is more rapid than that of a crystalline form [1]. Supercritical impregnation was compared to conventional incipient wetness mode in terms of impregnation yield, duration as well as in terms of drug solid state form (degree of crystallinity of the impregnated drug).

IV. 2. Materials

The materials used for the impregnation of silica are presented in the following sections.

IV. 2. 1. Silica

The impregnation support used is an amorphous ordered mesoporous silica (OMS-7) provided by Formac Pharmaceuticals NV (Belgium).

IV. 2. 2. Fenofibrate

Fenofibrate, a model active pharmaceutical ingredient with poor water solubility, was selected for this study. Fenofibrate (propan-2-yl 2-{4-[(4-chlorophenyl) carbonyl] phenoxy}-2-methylpropanoate) was supplied by Formac Pharmaceuticals NV (Belgium). Its skeletal formula is presented in Figure IV. 1. It is solid under ambient conditions with a molar mass of 0.360 $kg.mol^{-1}$.

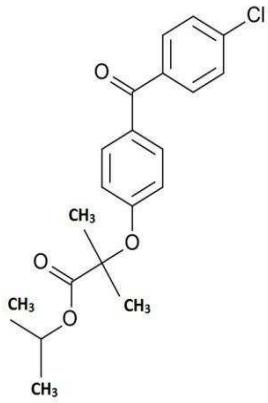

Figure IV. 1 Skeletal formula of Fenofibrate

IV. 2. 3. Solvent

The supercritical fluid used as impregnation solvent is carbon dioxide (CO_2, purity > 99.7%), which was supplied by Air Liquide (France).

IV. 3. Methods

IV. 3. 1. Impregnation procedures

Two methods of impregnation were carried out in this work: incipient wetness and supercritical impregnation.

IV. 3. 1. 1. Impregnation via incipient wetness

Samples were loaded into silica using the incipient wetness method. For that purpose, a loading solution of 100 $mg.mL^{-1}$ of Fenofibrate in Dichloromethane was prepared. 8.55 mL of this solution was then added to 2 g of silica in 3 fractions of 2.85 mL. Between each fraction, the mixture was stirred with a spatula for 5 min. Finally, the solvent is evaporated at 298 K for 55 min to remove the main part of the residual solvent and subsequently dried under reduced pressure (± 0.005 MPa) at 313 K for 24 hours.

Before and after impregnation, silica should be stored under a controlled atmosphere in order to avoid water adsorption. Indeed, because of the presence of a large number of free silanol groups on its surface structure, large amount of water can be adsorbed by forming hydrogen bonds [4].

IV. 3. 1. 2. Supercritical impregnation

The supercritical impregnation set-up used in the study is schematically represented and described in chapter III (Figure III.3). Supercritical impregnations were carried out in a batch mode, without using a co-solvent. For that purpose, a fixed amount of the ordered mesoporous silica (0.5 g of silica per experiment) and a known quantity of the API protected by a frit filter, to prevent any contamination of silica, were placed in the high pressure cell. The vessel was closed and heated to 308 K, and then filled with CO_2 using the high pressure pump until the desired operational pressure was reached. The temperature and the pressure were maintained for a pre-established impregnation duration under stirring to promote API solubilization and the supercritical fluid phase homogenization. The supercritical phase, containing the API, diffused within the porosity of silica. At the end of experiment, the cell was depressurized by venting out the CO_2 in isothermal conditions.

IV. 3. 2. Characterization of silica

IV. 3. 2. 1. Nitrogen adsorption

Nitrogen adsorption-desorption isotherms were recorded at 177 K using a Micromeritics TriStar II apparatus. API-free OMS-7 and API-loaded OMS-7 were pre-treated for 2 hours under nitrogen flow at 250 and 303 K respectively. Sample weights were normalized to mass of pure silica. The pore size distribution was calculated from the desorption branch of the isotherm using the Barrett–Joyner–Halenda (BJH) model. The total surface area was calculated via the Brunauer-Emmett-Teller (BET) model. The total pore volume was derived directly from the adsorption isotherm at $p/p_0 = 0.95$.

The influence of treatment with $scCO_2$ on the porous structure of the silica was also characterized by nitrogen sorption analysis.

IV. 3. 2. 2. Transmission electron microscopy (TEM)

TEM was performed on an FEI Tecnai G2 Spirit Twin operating at 120 kV. Samples were prepared on 50 nm 300-mesh carbon-coated copper grids. Scanning electron microscopy (SEM) images were obtained with a SEM Philips XL 30 FEG. Samples are prepared on carbon tape and coated with gold.

IV. 3. 2. 3. X-ray diffraction (XRD)

The crystallinity of silica was evaluated by powder XRD. Diffraction patterns were obtained using reflection geometry on an X'Pert Pro diffractometer equipped with a real-time X'Celerator detector (PanAlytical, Eindhoven, The Netherlands). Samples were flattened onto zero-background plate holders and analyzed at ambient temperature and relative humidity. Samples were scanned in a continuous mode from 4 ° to 40 ° θ (with a 2 θ step size of 0.0167 °). CuKα radiation (1.54 Å) was used with a generator voltage and current of 45 kV and 40 mA, respectively. The sample was rotated with a 4 s revolution time. The incident beam path was equipped with a 10 mm programmable anti-scatter slit, a 0.04 radian Soller slit and a 0.020 mm Nickel filter.

IV. 3. 2. 4. Impregnation yields

The impregnation yields for both impregnation methods: incipient wetness and supercritical impregnation, were determined by extraction of the API in the impregnated silica with methanol. 5 mg of impregnated silica was introduced into a flask of 5 mL and the volume was completed with methanol. The samples were sonicated for 30 min and left for an additional 90 min at room temperature and under regular manual agitation. The silica was then separated from the methanol by filtration. The API dissolved in methanol was quantified by HPLC-UV analysis.

HPLC experiments were carried out with a 20 µL sample loop. The chromatographic separation was performed using an analytical column (Lichrospher 60 RP-8 select B 5µm 125x4.6 mm) at 303 K. A mixture of 70/30 v/v% Acetonitrile/Ammonium acetate with a pH of 3.5 and a flow rate of 1.0 $mL.min^{-1}$, was applied as the mobile phase. The Fenofibrate was detected using a UV-Vis detector at a wavelength of 287 nm.

IV. 3. 2. 5. Differential scanning calorimetry (DSC)

Differential scanning calorimetry was carried out between 203 and 373 K at a heating rate of 10 K/min using a Mettler Toledo DSC. DSC analysis was performed in order to determine the degree of crystallinity of impregnated API in the silica support.

IV. 4. Results and discussions

In this work, we are interested to the impregnation of mesoporous silica with poorly water-soluble drug, Fenofibrate, using two impregnation methods: impregnation using incipient

witness and supercritical impregnation. The impregnation studies and some characterizations before and after the impregnation of silica are presented in the following sections.

IV. 4. 1. Characterization of silica before impregnation

The structural properties of silica material used in this study were determined by powder X-ray diffraction, scanning electron microscopy and by nitrogen adsorption.

The degree of crystallinity of silica was evaluated by powder X-ray diffraction. After silica calcination at 823 K, a wide peak was observed at a 2 θ angle in the range 15–30. The XRD pattern presented in Figure IV. 2 reveals that the silica material was amorphous.

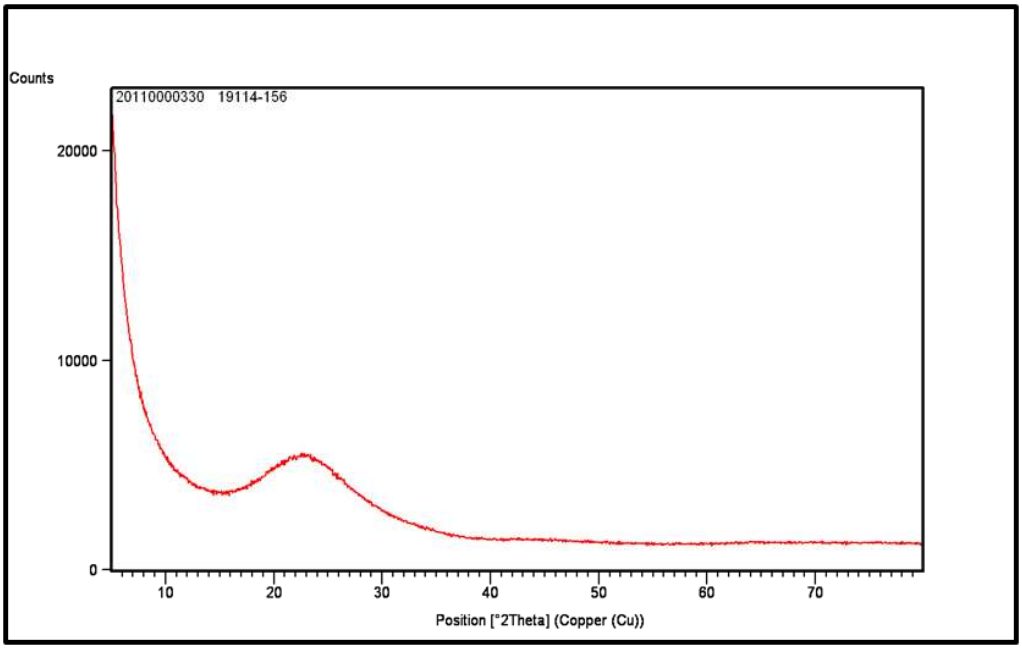

Figure IV. 2 XRD pattern of the calcined OMS-L-7.

Scanning electron microscopy provides information on the morphology and the microscopic scale structure of silica. The TEM observations of the calcined material reveal a hexagonal periodic arrangement of the channels, i.e. a honeycomb pattern. Figure IV. 3 displays TEM images of the calcined material.

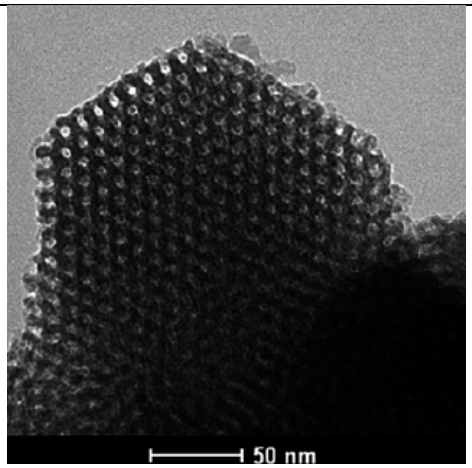

Figure IV. 3 TEM picture of the calcined material.

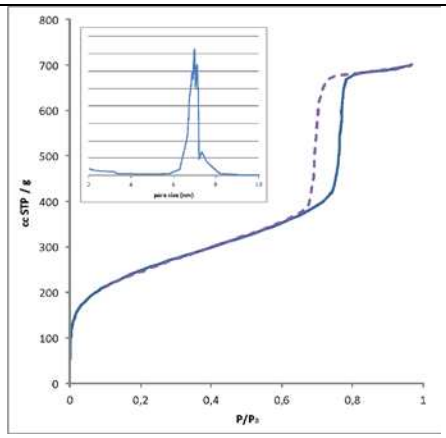

Figure IV. 4 N_2 physisorption of the calcined material.

The porosity of silica was determined by nitrogen sorption at 77 K (Figure IV. 4). The pore volume of these materials is around 0.9 to 1.1 $cm^3.g^{-1}$. The pore size distribution was calculated from the desorption branch of the isotherm indicating narrow mesopore size distribution ranging from 6 to 7.5 nm. The BET method was used to calculate a specific surface area varying between 450 and 600 $m^2.g^{-1}$ depending on the samples.

IV. 4. 2. Impregnation using incipient wetness

The impregnation of Fenofibrate in silica was reproducible; with an impregnation yield of 30 mg_{drug}/mg_{silica}. The degree of crystallinity obtained was very low (<1%).

IV. 4. 3. Influence of supercritical treatment on silica structural properties

Before performing supercritical impregnations, some preliminary studies were required in order to determine the influence of supercritical treatment on the structural properties of pure silica support under various depressurization conditions.

For that purpose, supercritical treatment was carried out at 20 MPa (the highest pressure used for impregnation) and 308 K in absence of Fenofibrate. A contact duration of 2 hours was maintained before depressurization. Three depressurization rates were considered corresponding to slow (0.07 $MPa.min^{-1}$), intermediate (0.5 $MPa.min^{-1}$) and fast (> 2 $MPa.min^{-1}$) depressurization conditions.

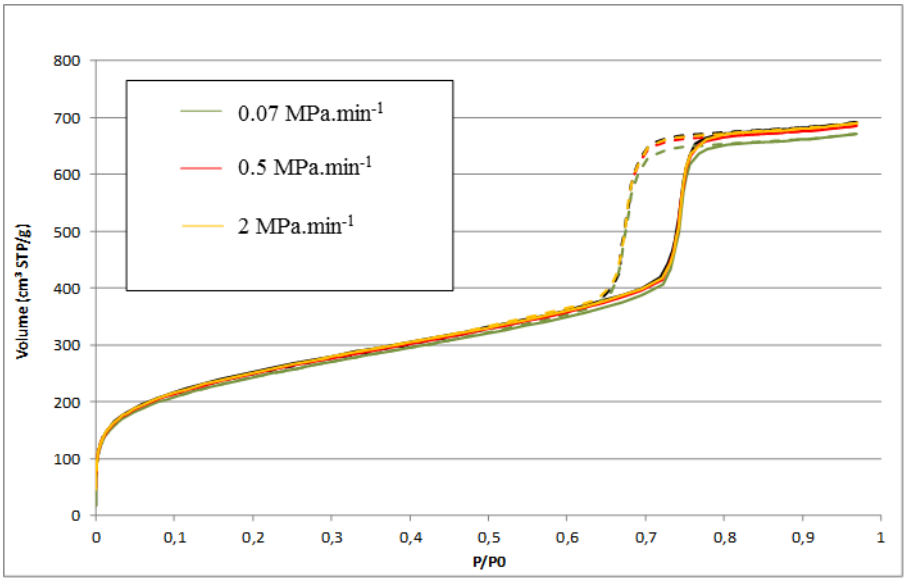

Figure IV. 5 N_2 sorption analysis of treated silica with $scCO_2$ and untreated silica.

N_2 sorption analyses were carried out on the treated samples with $scCO_2$ and were compared to that of untreated silica. Figure IV. 5 shows the nitrogen adsorption isotherms of the untreated silica reference and of samples subjected to the three different depressurization rates. All four isotherms almost overlap indicating that the depressurization protocol does not modify the structural properties of the silica considered here.

IV. 4. 4 Supercritical impregnation

The influence of different experimental conditions on supercritical impregnation efficiency was studied. The concentration of the drug in the fluid phase was varied. The phase behavior of the mixture of drug and $scCO_2$ is very important for the choice of experimental conditions of impregnation. The solubility of Fenofibrate in $scCO_2$ was reported in the literature [3] and is illustrated in Figure IV. 6, where $y_{Fenofibrate}$ represents the molar fraction of Fenofibrate in CO_2.

We have worked in saturated conditions or in under-saturated conditions (by changing the pressure and/or the mass of API introduced in the autoclave). Two contact durations between the $scCO_2$ and silica were tested (30 and 120 min). Furthermore, the depressurization phase was carried out in slow conditions (depressurization rate of 0.07 $MPa.min^{-1}$) and rapid conditions (> 2 $MPa.min^{-1}$).

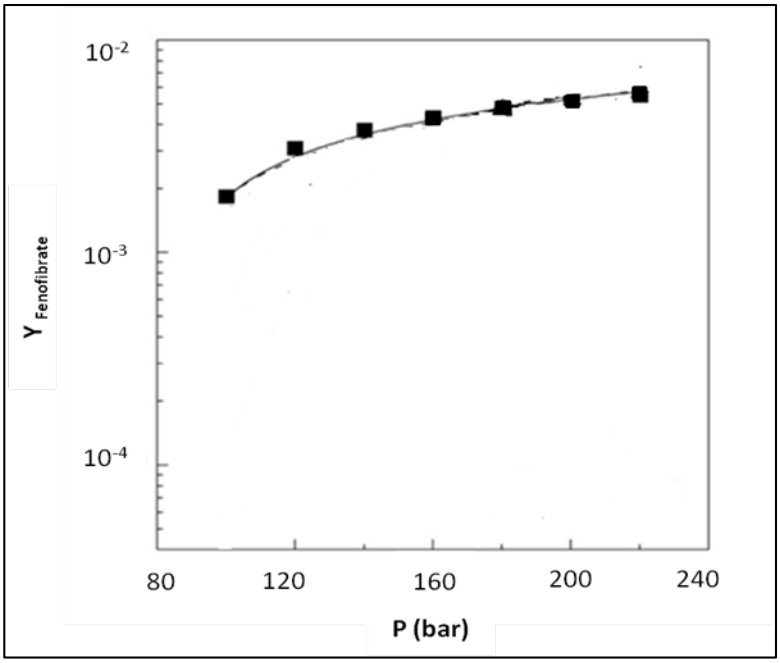

Figure IV. 6 Experimental solubility for Fenofibrate in $scCO_2$ at 308 K [3].

In order to study the influence of the drug concentration in the fluid phase on impregnation, the pressure was varied from 10 to 20 MPa at 308 K. The corresponding solubilities of Fenofibrate in $scCO_2$ and the densities of CO_2 in the experimental conditions tested in this work are summarized in Table IV. 1.

Table IV. 1 Solubility of Fenofibrate (molar fraction) in $scCO_2$ at 308 K.

P MPa	CO_2 density $kg.m^{-3}$	$y_{Fenofibrate}$
10	714.82	$1.83\ 10^{-3}$
16	828.10	$4.30\ 10^{-3}$
20	866.48	$5.28\ 10^{-3}$

The experimental conditions as well as the corresponding results in terms of impregnation yields (Y_{imp}) and degree of crystallinity of the impregnated API (X_{crys}) are reported in Table IV. 2.

Table IV. 2 Supercritical impregnation of Fenofibrate into silica at 308 K.

P MPa	$m_{saturation}$ g	$m_{fenofibrate}$ g	Duration min	Depressurization MPa.min^{-1}	Y_{imp} mg_{drug}/g_{silica}	X_{crys} %
10	1.4	2$^{(*)}$	30	Rapid	326 ± 9	1.3
10	1.4	2$^{(*)}$	30	0.07	324 ± 12	0.2
16	3.7	4 $^{(*)}$	120	0.07	-	-
16	3.7	1$^{(**)}$	120	0.07	485 ± 5	1.1
20	4.7	5.5$^{(*)}$	30	Rapid	659 ± 38	20.5
20	4.7	5.5$^{(*)}$	120	Rapid	623 ± 22	20.5
20	4.7	5.5$^{(*)}$	120	0.07	-	-
20	4.7	2$^{(**)}$	120	0.07	481 ± 1	0.5

$^{(*)}$ Saturated conditions; $^{(**)}$ Under-saturated conditions, (-) Nozzle plugging

Increasing the pressure from 10 to 20 MPa in rapid depressurization conditions improves the impregnation yields from 326 to 659 mg_{drug}/g_{silica} (experiments 1 and 5). Indeed, the solubility of Fenofibrate in CO_2 increases when the pressure increases and therefore the amount of drug transported within the porous silica increases. Varying the impregnation duration (30 or 120 min) at a pressure of 20 MPa leads to similar impregnation yields as well as degrees of crystallinity of the impregnated Fenofibrate (experiments 5 and 6). Therefore, a short contact duration of 30 min is sufficient for impregnation.

Although the impregnation yield achieved at 20 MPa is attractive (659 mg_{drug}/g_{silica}), a degree of crystallinity of impregnated Fenofibrate of 20.5 % (Figure IV. 7) can be considered as high and should be lowered in order to enhance drug dissolution kinetics. Indeed, the dissolution of an amorphous drug is more rapid than that of a crystalline form [1]. In order to limit loaded Fenofibrate crystallinity, and since all the samples that were depressurized in slow depressurization conditions exhibited low degree of drug crystallinity, supercritical impregnations were then carried out in slow depressurization conditions (0.07 MPa.min^{-1}).

At 10 MPa and in the case of rapid depressurization conditions, there is a small peak in the DSC thermogram around the drug's melting point (355 K) indicating that some of the drug was crystalline (Figure IV. 7). This peak is not significant under slow depressurization conditions. The corresponding degree of crystallinity of loaded Fenofibrate was decreased from 1.3 % to 0.2 % as the depressurization rate was reduced (respectively experiment 1 and

2). This may be due to higher supersaturations of Fenofibrate in the fluid phase during a rapid depressurization. Importantly, in these conditions, the depressurization rate did not appear to affect the impregnation yield at low pressure (10 MPa).

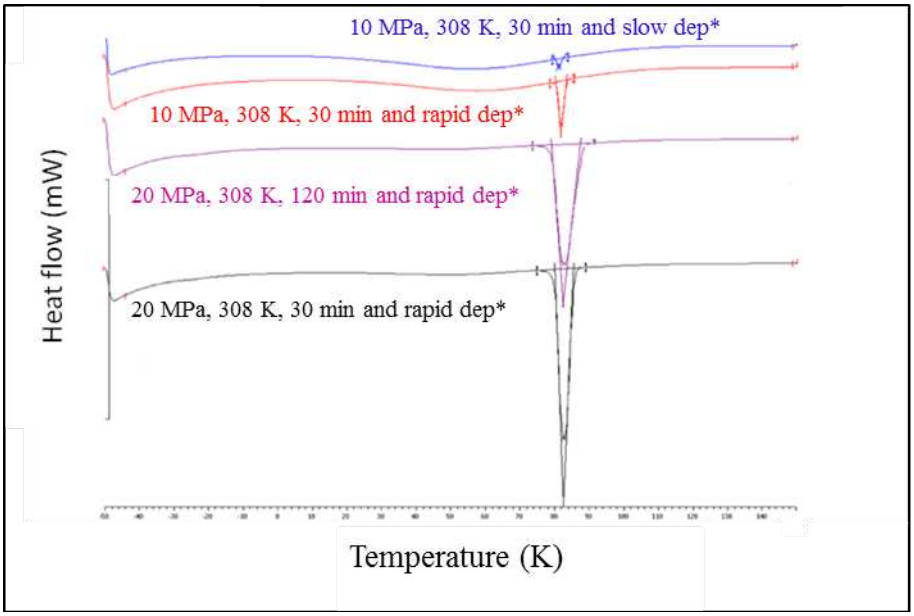

Figure IV. 7 DSC thermograms of impregnated silica**.**

*dep: Depressurization rate.

At higher pressures (16 and 20 MPa, experiments 3 and 7), when the impregnation was carried out using slow depressurization conditions, a plugging of the nozzles was observed. This was due to the high solubility of Fenofibrate in CO_2 at high pressures. During the depressurization step, CO_2 was supersaturated with Fenofibrate leading to its reprecipitation. Nozzle plugging was avoided by carrying out supercritical impregnation for the drug under saturation conditions of API.

In these conditions (experiments 4 and 8), a low degree of crystallinity was obtained (1.1 % at 16 MPa and 0.5 % and 20 MPa). At 20 MPa, by decreasing the depressurization rate and by working with an under-saturated fluid phase, the crystallinity degree was significantly reduced from 20.5 to 0.5 % (experiments 6 and 8). In these same conditions and even if the corresponding impregnation yield was reduced from 623 to 481 mg_{drug}/g_{silica} because of the lower concentrations of Fenofibrate in the fluid phase during impregnation, the yield was still in the range of expected values.

Under slow depressurization conditions, the impregnation yield increases as the pressure is incremented from 10 to 16 MPa in different drug saturation conditions of the fluid phase

(experiments 2 and 4). A further increase in pressure up to 20 MPa (experiment 8), does not improve the impregnation yields even if the mass and therefore the concentration of Fenofibrate in $scCO_2$ was increased.

The drug loading of the supercritical impregnation at high pressures (> 485 mg_{drug}/g_{silica} at 16 and 20 MPa) were improved compared to that obtained through the witness impregnation route (300 mg_{drug}/g_{silica}) while avoiding the use of organic solvent. By carrying out slow depressurization conditions, the degree of crystallinity of loaded Fenofibrate using supercritical impregnation was comparable (about 1 %) to that observed via the solvent method.

IV. 5 Conclusion

Our study aimed to improve the bioavailability of Fenofibrate by loading it in hydrophilic mesoporous silica. Supercritical impregnations were performed through a batch process at 308 K and pressure varying between 10 and 20 MPa. The impregnation using incipient wetness was carried out using dichloromethane as the liquid solvent.

Supercritical impregnation of silica with Fenofibrate led to high impregnation yields up to 485 mg_{drug}/g_{silica} with an intended low drug crystallinity (as low as 1 %). Those results are enhanced compared to those obtained using the incipient wetness (300 mg_{drug}/g_{silica}). Additionally, since no co-solvent was used, supercritical treatment does not leave any traces of solvent in the impregnated silica.

References

[1] R. J. Ahern, J. P. Hanrahan, J. M. Tobin, K. B. Ryan, and A. M. Crean, "European Journal of Pharmaceutical Sciences Comparison of fenofibrate – mesoporous silica drug-loading processes for enhanced drug delivery," *Eur. J. Pharm. Sci.*, vol. 50, no. 3–4, pp. 400–409, 2013.

[2] Z. Jia, P. Lin, Y. Xiang, X. Wang, J. Wang, X. Zhang, and Q. Zhang, "A novel nanomatrix system consisted of colloidal silica and pH-sensitive polymethylacrylate improves the oral bioavailability of fenofibrate," *Eur. J. Pharm. Biopharm.*, vol. 79, no. 1, pp. 126–134, 2011.

[3] Y.-M. Chen, P.-C. Lin, M. Tang, and Y.-P. Chen, "Solid solubility of antilipemic agents and micronization of gemfibrozil in supercritical carbon dioxide," *J. Supercrit. Fluids*, vol. 52, no. 2, pp. 175–182, Mar. 2010.

Conclusions and perspectives

A clean and environment friendly impregnation process using supercritical technology was used to elaborate two kinds of drug delivery systems based on medical devices (polymeric intraocular lenses) and dosages forms (mesoporous silica supports).

In a first part of this study, commercial intraocular lenses were impregnated with drug molecules in order to combine cataract surgery and postoperative treatment in a single procedure. For that purpose, supercritical impregnation process was carried out to load rigid and foldable intraocular lenses made respectively from derivatives of Poly (Methyl MethAcrylate) (PMMA) and poly Poly (2-HydroxyEthyl MethAcrylate) (P-HEMA) with two different ocular drugs, an anti-inflammatory drug (Dexamethasone 21 phosphate disodium designed as DXP) and an antibiotic (Ciprofloxacin, designed as CIP).

According to the state of the art described in Chapter II, a few studies on supercritical impregnation of therapeutic contact lenses with various classes of drugs were performed and an extended drug delivery was observed. To the best of our knowledge no therapeutic contact lenses have yet been approved or commercialized. As far as we know, this study is the first work dealing with supercritical impregnation of intraocular lenses and more practically on commercially available PMMA and P-HEMA IOLs, which makes its originality.

For both types of IOLs, supercritical impregnations were carried out in a batch mode and the impregnation yields were determined through drug release kinetics studies. A response surface methodology based on experimental designs was used to determine the influence of the operating conditions on supercritical impregnation. In order to determine the worth studying parameters and to delimit the experimental domain, preliminary experiments were carried out in a first step for each type of IOL.

Regarding the system PMMA/DXP, drug loading improvement in presence of co-solvent (Ethanol in this study) was obtained at low pressures (8 MPa), while pressure increase in presence of co-solvent leads to a decrease in impregnation yields. Interestingly, impregnation yields were improved at low pressure in the presence of co-solvent. Hence, all DXP loadings later in this work were performed at 8 MPa and in the presence of co-solvent. The increase in temperature and impregnation duration led to a decrease in drug loading.

Following the results of the preliminary experiments, a response surface methodology based on experimental designs was applied to study the influence of operating conditions on impregnation. Two input variables were considered: amount of co-solvent (1 to 10 %mol) and impregnation duration (30 to 240 min). The response surface indicated the impregnation

duration to be the governing factor in impregnation while decrease in impregnation duration promoted drug loading.

The influence of pressure and the use of a co-solvent was studied on the system PMMA/CIP. Unlike DXP, in absence of co-solvent, increasing pressure enhances drug loading. However, in the presence of co-solvent, the increase in pressure did not affect the drug loading.

Regarding the second kind of IOLs, P-HEMA, impregnations of DXP and CIP drugs were also performed. For the system P-HEMA/DXP, the use of ethanol (5 %mol) as a co-solvent improves DXP impregnation yield in IOLs. The DXP loading in presence of a co-solvent involved an extra washing step to ensure efficient removal of ethanol from P-HEMA IOLs.

For P-HEMA/CIP system and following the preliminary results of the first series of experiments, it could be concluded that drug loadings were significantly influenced by the change in pressure in the absence of a co-solvent. Moreover, increase in pressure in the presence of co-solvent had minimal influence on the impregnation yield. Therefore, a response surface methodology based on experimental design was used to study the influence of operating conditions, on the impregnation of CIP on +21. 0 D IOLs, in the absence of co-solvent according to the aimed application. Two entry values with 5 levels each were considered; pressure (8 to 20 MPa) and impregnation duration (30 to 240 min). The response surface indicated the pressure to be the governing factor in impregnation where increasing the pressure promoted drug loading.

The highest impregnation yields for DXP and CIP in PMMA IOLs were 18.3 and 2.8 $\mu g/mg_{IOL}$ respectively and the highest impregnation yields for DXP and CIP in P-HEMA IOLs were 14.5 and 4.1 $\mu g/mg_{IOL}$ respectively. Which indicates higher affinity of DXP for PMMA and P-HEMA IOLs than CIP, this result was confirmed by the values of partition coefficient. Despite the low solubility of drugs (DXP and CIP) in the fluid phase, we have successfully obtained a homogeneous and in depth impregnation of IOLs (PMMA and P-HEMA).

NMR analyzes performed on drug (DXP and CIP) impregnated IOLs (PMMA and P-HEMA) in the presence of a co-solvent did not show the presence of residual solvent if a washing step with $scCO_2$ is carried out. These results indicate that impregnated IOLs can be suitable for ophthalmic application even if ethanol is used as co-solvent.

A prolonged drug delivery during 40 days was obtained for most impregnation experiments (both kinds of IOLs).

FTIR-ATR analyses were carried out on the non treated and impregnated IOLs (PMMA and P-HEMA) with both drugs within a collaboration with the University of Greenwich (Dr. John Tetteh, University of Greenwich). FTIR-ATR spectrum (non shown in this manuscript) of a non treated IOL as well as that of impregnated IOLs in different conditions with DXP and CIP do not reveal differences. Supercritical impregnation does not induce any change in the characteristic IOLs structural peaks. In addition, by comparison with the spectrum of pure drugs, that of impregnated IOLs did not indicate the presence of drug peak. This result can be due to a molecular dispersion of the drugs in the matrix at a molecular level.

The second part of this work thesis aimed to improve the bioavailability of Fenofibrate by loading it in mesoporous silica. Supercritical impregnations were performed through a batch process at pressures varying between 10 and 20 MPa and without using any co-solvent. The incipient wetness method was carried out using dichloromethane as an organic solvent. While the incipient wetness impregnation led to a Fenofibrate loading up to 300 mg_{drug}/g_{silica} in 48 h of impregnation, the supercritical impregnation method yielded loading up to 485 mg_{drug}/g_{silica} in 120 min of impregnation duration, at 16 MPa and 308 K, with a low degree of crystallinity (about 1 %) comparable to that observed via the incipient wetness method. In addition to the enhancement of impregnation efficiency in significantly shorter impregnation durations, the supercritical route provides a solvent-free alternative for impregnation.

Concerning IOLs impregnation, based on the obtained results within this PhD study, future work might be performed to further investigate the influence of operating conditions on supercritical impregnation such as the influence of temperature and impregnation duration in the absence of co-solvent on PMMA IOLs and the influence of long impregnation duration in the absence of co-solvent on P-HEMA IOLs.

To facilitate the understanding of the impregnation results, a study on the swelling and the evolution of the $scCO_2$ diffusion front within each type of polymer (PMMA and P-HEMA) at different conditions of pressures and temperatures is required. Furthermore, the measurements of the solubilities (study in progress in collaboration with Pr. Yan-Ping Chen, National Taiwan University) of both drugs (DXP and CIP) should be performed in the same conditions of impregnation in order to determine the partition coefficients of the drug between the fluid phase and the polymeric support.

Optical properties measurements are in progress in the framework of a collaboration with a Laure Siozade, Aix-Marseille Université. The first results are encouraging since results within the tolerance range of international standards were obtained.

Impregnation experiments using soaking into liquid are of interest in order to compare impregnation efficiency with those obtained within this PhD work. Some tests performed in our laboratory show that the impregnation yields obtained by supercritical impregnation are significantly higher than those obtained by the soaking into liquid process following the methods described by (Aiache *et al*, *2008*).

Following this Ph.D. work, the *In-vivo* drug release and clinical tests will be key milestones of this study and may be expected in the framework of a collaboration with a private partner that has already started.

The use of magnetic suspension balance would be of great interest, in order to follow the evolution of impregnation in time and to better understand the impregnation process.

Finally, this study on IOLs impregnation provides important information on the feasibility of supercritical impregnation with two commonly used drugs in complications related to cataract surgery and can be extended to other drugs (as for the prevention of posterior capsular opacification, for glaucoma or also diabetes treatments). The developed method can also be applied to any kind of implants or prosthesis. Simultaneous loading of several drugs in the future is possible and is worth studying.

Appendix A

UV-Visible measurements

UV-Visible (Jenway 6715) was used to determine the absorption wavelength of both drugs (DXP and CIP) used in our work.

A. 1. Dexamethsaone 21-phosphat disodium (DXP)

The absorption wavelength of DXP was determined by spectral analysis (using Jenway 6715 UV/Vis) of solution simulating the aqueous humor (5 ml) containing 4 mg of DXP. A maximum wavelength of 248 nm has been found for DXP.

The calibration curve, describing the absorbance versus the concentration of DXP in the solution simulating the aqueous humor, was determined spectrophometrically at 248 nm by analyzing a solution at 0.2 mg / ml successively diluted. Figure A. 1 illustrates the evolution of absorbance versus the concentration of DXP in the solution simulating the aqueous humor, the BEER Lambert relationship is applicable in the linear domain.

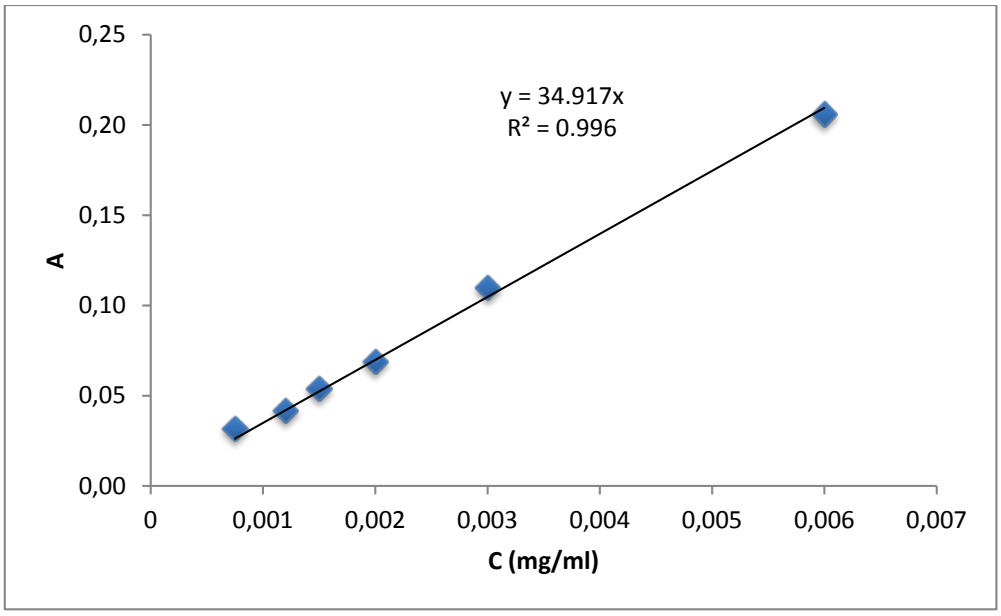

Figure A. 1 calibration curve of DXP in solution simulating the aqueous humor.

A. 2. Ciprofloxacin (CIP)

The absorption wavelength of CIP was determined by spectral analysis (using Jenway 6715 UV/Vis) of solution simulating the aqueous humor (5 ml) containing 4 mg of CIP. A maximum wavelength of 277 nm has been found for CIP.

The calibration curve, describing the absorbance versus the concentration of CIP in the solution simulating the aqueous humor, was determined spectrophometrically at 277 nm by analyzing a solution at 0.2 mg/ml successively diluted. Figure A. 2 illustrates the evolution of absorbance versus the concentration of CIP in the solution simulating the aqueous humor, the BEER Lambert relationship is applicable in the linear domain.

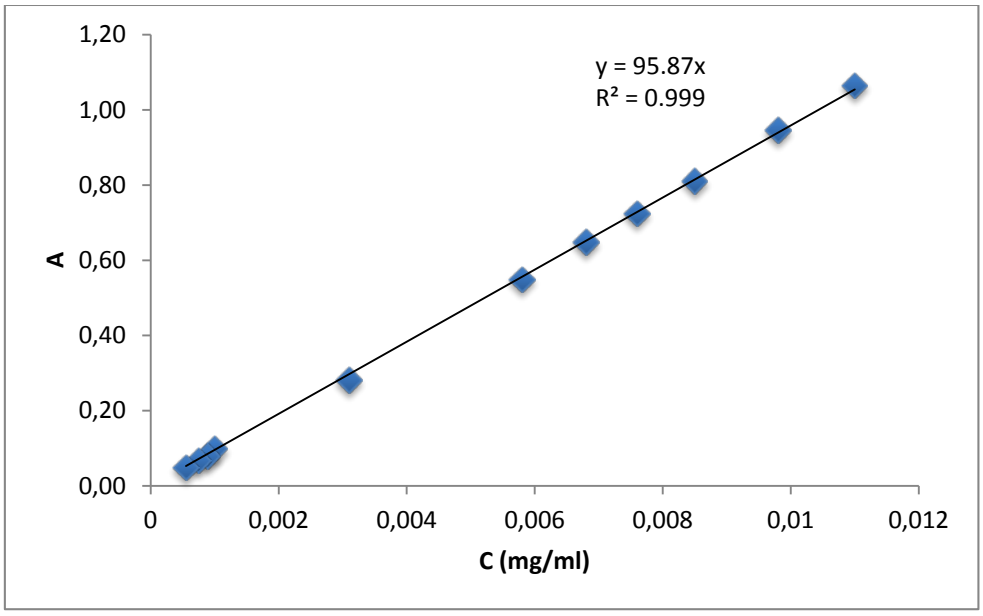

Figure A. 2 calibration curve of CIP in solution simulating the aqueous humor.

Appendix B

Reproducibility of impregnation results

In this work, the supercritical impregnations of two kinds of IOLs (PMMA and P-HEMA) with DXP and CIP were carried out. The experiments were repeated three or four time to check the reproducibility of our results.

B. 1. PMMA/ DXP

As we can observe in the Table B. 1, repeatability of results obtained by the preliminary impregnation experiments for the system PMMA/DXP was verified.

Table B. 1 Repeatability of results obtained by the preliminary impregnation experiments for the system PMMA/DXP.

N°	m_{0IOL} (*)	Pressure	$m_{DXP\ imp}$	y_{imp}	$t_{release}$
	mg±0.2	bar	µg	$\mu g_{drug}/mg_{IOL}$	days
Without co-solvent					
DXP_1(1)	18.9	80	159±24	8.4±1.3	40
DXP_1(2)	19.1	80	157±30	8.2±1.4	41
DXP_2(1)	19.0	200	165±24	8.9±1.3	40
DXP_2(2)	19.1	200	170±36	8.9±1.5	42

Regarding the experimental design for the system PMMA/DXP, the experiment in the middle of the experimental domain (DXP_ED_9) was repeated three times to verify the validity of the stated model. The results are reproducible.

Table B. 2 Repeatability of results for supercritical impregnation in DXP_ED_9.

N°	m_{0IOL}	Amount of co-solvent	t_{imp}	$m_{DXP\ imp}$	y_{imp}	$t_{release}$
	mg±0.2	%mol	min	μg	$\mu g_{drug}/mg_{IOL}$	days
DXP_ED_9(1)	19.0	5.5	135	184 ± 19	9.44 ± 1.00	41
DXP_ED_9(2)	20.1	5.5	135	215±22	10.68±1.14	40
DXP_ED_9(3)	19.7	5.5	135	191±19	9.68±1.04	43

B. 2. P-HEMA/ CIP

Regarding the experimental design for the system P-HEMA/CIP, the experiment in the middle of domain (CIP_ED_IX) was repeated three time to verify the validity of the stated model. The results are reproducible.

Table B. 3 Repeatability of results for supercritical impregnation in CIP_ED_IX.

N°	P	t_{imp}	m_{0IOL}	$m_{CIP\ imp}$	y_{imp}	$t_{release}$
	bar	min	mg±0.2	μg	$\mu g_{drug}/mg_{IOL}$	Days
CIP_ED_IX (1)	140	135	18.8	35 ± 0.1	1.86 ± 0.05	20
CIP_ED_IX (2)	140	135	19.0	33 ± 0.2	1.75 ± 0.12	20
CIP_ED_IX (3)	140	135	18.8	32 ± 0.2	1.70 ± 0.11	22

Appendix C
Experimental design

A response surface methodology based on experimental designs was used in our work to determine the influence of the operating conditions on supercritical impregnation for both systems (PMMA/DXP and P-HEMMA/CIP). For this, an empirical mathematical model is used. For validation of this model suitability, several techniques were used *i.e.* residual analysis, ANOVA (ANalysis Of VAriance) and prediction error sum of squares residuals (especially the coefficient of determination, R^2). The model, once validated, was used to predict the response in the whole experimental domain with good precision.

C. 1. Results of the experimental design for the system PMMA/DXP

Analyze of variance: response m imp

Source of variation	Sum of squares	Degrees of freedom	Mean square	ratio	Signif
Regression	0.0431	5	0.0086	7.8753	0.303 **
Residues	0.0438	10	0.0044		
Validity	0.0383	5	0.0077	7.0025	2.61 *
Error	0.0055	5	0.0011		
Total	0.0869	15			

Estimates and statistics of coefficients: m imp

Standard Error of the response	0.0331
R2	0.496
R2A	0.244
Nbre ddl	5

Nam	Coefficient	F.Inflation	Standard Deviation	t.exp.	Signif. %
b0	0.2035		0.0167	12.19	< 0.01 ***
b1	-0.0508	1.06	0.0104	-4.89	0.450 **
b2	0.0110	1.04	0.0094	1.17	29.5
b1-1	0.0108	1.22	0.0119	0.91	40.6
b2-2	-0.0159	1.20	0.0113	-1.41	21.9
b1-2	0.0399	1.05	0.0150	2.67	4.46 *

Study of residues of the response

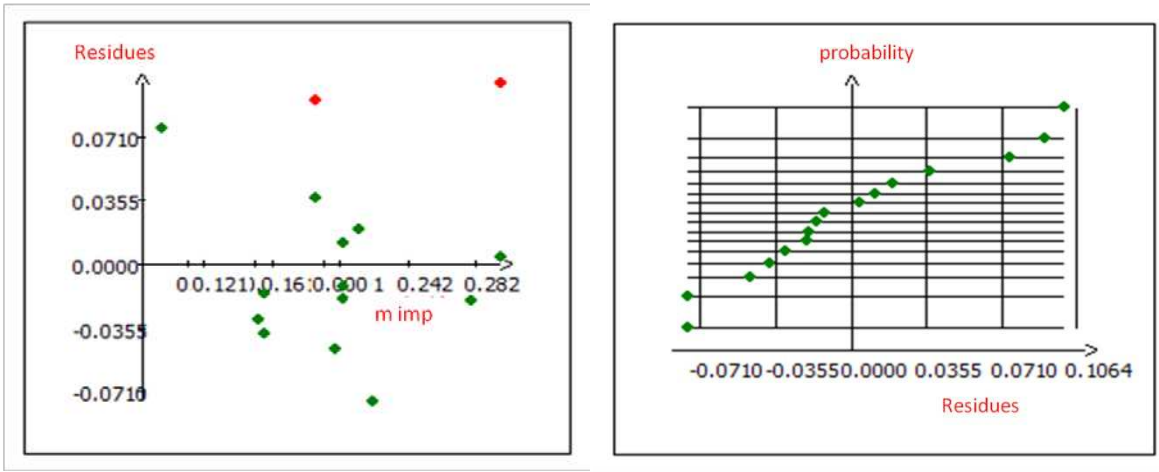

C. 2. Results of the experimental design for the system P-HEMA/CIP

Analyze of variance : response m imp

Source of variation	Sum of squares	Degrees of freedom	Mean square	ratio	Signif
Regression	$2.87434\ 10^{-3}$	5	$5.74868\ 10^{-4}$	160.9632	< 0.01 ***
Residues	$1.66095\ 10^{-4}$	10	1.66095E-0005		
Validity	$1.41095\ 10^{-4}$	3	$4.70317\ 10^{-5}$	13.1689	0.289 **
Error	$2.50000\ 10^{-5}$	7	$3.57143\ 10^{-6}$		
Total	$3.04044\ 10^{-3}$	15			

Estimates and statistics of coefficients: m imp

Standard Error of the response	0.002
R2	0.945
R2A	0.918
Nbre ddl	7

Nam	Coefficient	F.Inflation	Standard Error	t.exp.	Signif. %
b0	0.032		0.001	34.41	< 0.01 ***
b1	0.012	1.06	0.001	20.94	< 0.01 ***
b2	0.005	1.06	0.001	8.09	< 0.01 ***
b1-1	0.006	1.18	0.001	8.63	< 0.01 ***
b2-2	-0.001	1.18	0.001	-1.06	32.5
b1-2	0.003	1.01	0.001	3.11	1.71 *

Study of residues of the response

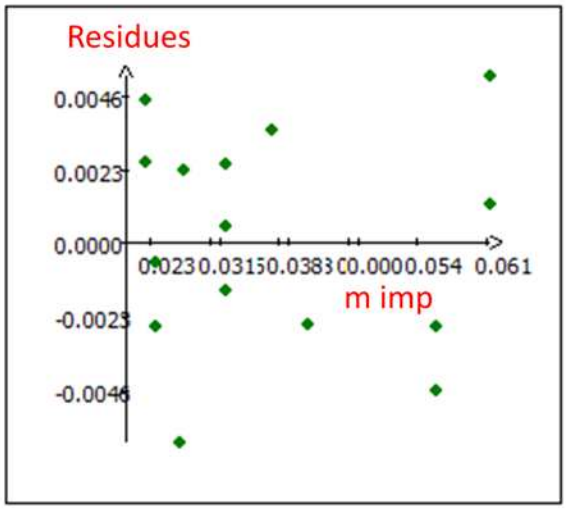

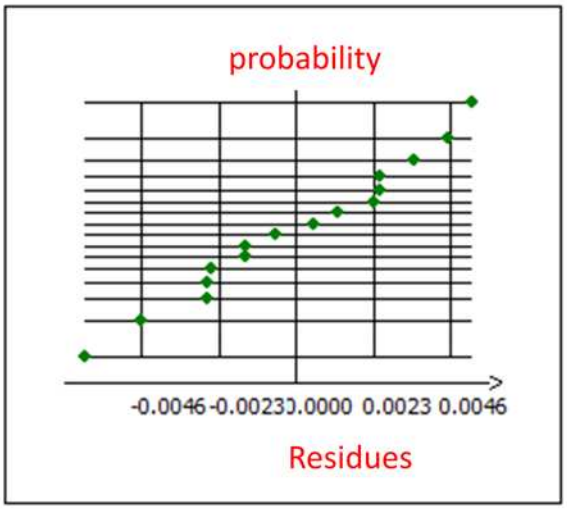

SUPERCRITICAL FLUID IMPREGNATION FOR THE ELABORATION OF CONTROLLED DRUG DELIVERY SYSTEMS

Abstract

Supercritical impregnation is an attractive "clean" alternative to conventional impregnation processes using generally liquid organic solvents. Among other applications, the impregnation process can be used for the development of controlled drug delivery systems applied to the pharmaceutical and medical fields. This work focuses on the preparation of controlled drug delivery systems using supercritical impregnation of drugs in two kinds of impregnation supports: polymeric matrices (intraocular lenses) and porous supports (mesoporous silica). Firstly, the supercritical impregnation of polymeric intraocular lenses (IOLs), used in cataract surgery, by an anti-inflammatory drug (Dexamethasone 21-phosphate disodium: DXP) and an antibiotic (Ciprofloxacin: CIP), is studied. More particularly, two polymeric IOLs were tested: rigid intraocular lenses made from derivative of PMMA and foldable intraocular lenses made from derivative of P-HEMA. Supercritical impregnations were carried out in a batch mode and the impregnation yields were determined through drug release kinetics studies in a solution simulating the aqueous humor. The influence of operating conditions on impregnation was studied by performing preliminary impregnation experiments followed by experimental designs. Transparent IOLs presenting an effective impregnation were obtained. The highest impregnation yields for DXP and CIP in PMMA IOLs were 18.3 and 2.8 $\mu g_{drug}/mg_{IOL}$ respectively and the highest impregnation yields for DXP and CIP in P-HEMA IOLs were 14.5 and 4.1 $\mu g_{drug}/mg_{IOL}$ respectively. Those results indicate higher affinity of DXP for PMMA and P-HEMA IOLs than CIP, which was confirmed by the values of partition coefficients. Despite the low solubility of each drug in the fluid phase, homogeneous and in-depth impregnations were successfully obtained. A prolonged drug delivery during 40 days was obtained for most impregnation experiments (for both kinds of IOLs). The second part of this work deals with the loading of a poorly water-soluble drug (Fenofibrate) in a mesoporous silica for improving drug dissolution kinetics. Supercritical impregnations were carried out with pure CO_2 at different pressures (10 to 20 MPa) and depressurization conditions (rapid and slow). Supercritical impregnation method yielded loading up to 485 $\mu g_{drug}/mg_{silica}$ in 120 min of impregnation duration, while incipient wetness method led to a Fenofibrate loading up to 300 $\mu g_{drug}/mg_{silica}$ in 48 hours of impregnation. A low degree of crystallinity (about 1%) comparable for both impregnations methods was obtained.

Keywords: controlled drug delivery systems, supercritical impregnation, intraocular lenses, mesoporous silica.

IMPRÉGNATION SUPERCRITIQUE POUR L'ÉLABORATION DE SYSTÈMES DE DÉLIVRANCE DE MÉDICAMENTS

Résumé

Le procédé d'imprégnation en milieu supercritique est une alternative « propre » à l'imprégnation par voie liquide. Entre autres applications, les procédés d'imprégnation peuvent être utilisés pour l'élaboration de systèmes de délivrance de médicaments appliqués aux domaines pharmaceutique et médical. Cette étude porte sur l'élaboration de systèmes de délivrance de médicaments en utilisant l'imprégnation supercritique des principes actifs sur deux types de supports : des matrices polymériques (lentilles intraoculaires) et des matrices poreuses (silice mésoporeuse). Dans le premier cas, des lentilles polymériques intraoculaires (IOLs), utilisées pour la chirurgie de la cataracte, ont été imprégnées par un anti-inflammatoire (Dexaméthasone 21-phosphate disodium: DXP) et un antibiotique (Ciprofloxacine: CIP). Plus particulièrement, deux types de lentilles ont été étudiés : des IOLs rigides à base de PMMA et des IOLs souples à base de P-HEMA. Les expériences d'imprégnation supercritique ont été effectuées en mode batch et les taux d'imprégnation ont été déterminés par des études de cinétique de relargage des principes actifs dans une solution simulant l'humeur aqueuse. L'influence des conditions opératoires sur l'efficacité de l'imprégnation a été étudiée en réalisant des expériences d'imprégnation préliminaires suivies par des plans d'expériences. Des lentilles transparentes présentant une imprégnation effective ont été obtenues. Les taux d'imprégnation les plus élevés obtenus pour l'imprégnation du DXP et CIP dans le PMMA sont de 18,3 et 2,8 $\mu g_{drug}/mg_{IOL}$ respectivement et les taux d'imprégnation les plus élevés obtenus pour l'imprégnation du DXP et CIP avec le P-HEMA sont de 14,5 et 4,1 $\mu g_{drug}/mg_{IOL}$ respectivement. Ces résultats indiquent une plus grande affinité du DXP pour les PMMA et P-HEMA IOLs que pour la CIP, ce qui a été confirmé par les valeurs du coefficient de partage obtenus. En dépit de la faible solubilité de chaque principe actif dans la phase fluide, une imprégnation homogène et en profondeur dans les IOLs (PMMA et P-HEMA). Un relargage prolongé dans le temps durant 40 jours a été obtenu pour la plupart des expériences d'imprégnation (pour les deux types d'IOLs). Dans le second cas, une silice mésoporeuse a été utilisée comme support d'imprégnation pour un médicament faiblement hydrosoluble (Fénofibrate), afin d'augmenter sa cinétique de dissolution. L'imprégnation supercritique a été effectuée avec le CO_2 pur en faisant varier la pression entre 10 et 20 MPa et les conditions de dépressurisation (rapide et lente). Tandis que l'imprégnation supercritique a permis d'obtenir des taux d'imprégnation pouvant atteindre 485 $\mu g_{drug}/mg_{IOL}$ durant 120 min d'imprégnation, l'imprégnation conventionnelle a permis d'obtenir des taux de 300 $\mu g_{drug}/mg_{silica}$ après une imprégnation de 48 heures. Un faible degré de cristallinité (de l'ordre de 1%) comparable pour les deux techniques d'imprégnation a été obtenu.

Mots-clés: systèmes de délivrance de médicament, imprégnation supercritique, lentilles intraoculaires, silice mésoporeuse.

Discipline : **GÉNIE DES PROCÉDÉS**

Laboratoire de Mécanique, Modélisation et procédés propres
Université Aix-Marseille, UMR CNRS 7340
Europôle de l'Arbois, bâtiments Laennec, hall C
13545 Aix-en-Provence cedex 4